CHAPTER VII

PRESENTATION, ANALYSIS AND DISCUSSION OF EXPERIMENTAL RESULTS

7.1. Presentation of Results

Experimental schedule prepared as given in Table 5.1 has been followed for the investigation of the influence of various factors on the consolidation characteristics of clays. It is proposed to present the data, observations and results according to the following scheme. The details of the materials tested, equipments employed amd laboratory observations from consolidation tests are given as Appendix in Volume No. II. A detailed index of the above appendix is prepared and presented below to serve as guide to all experimental data.

These experimental observations are proposed to be analysed and discussed from fundamental considerations. It is proposed to compare these experimental results with those

Table 7.1. Properties of Material Tested

Material / Property	Kaolinite	Reference	Bentonite	Reference	Illite	Reference
Predominant Mineral	Kaolinite	Fig.C 7	Montmorillo-nite	Fig. C 8	Illite	Fig.C 9
Specific Gravity	2.55	Table C.1	2.34	Table 2	2.6	Table C.3
Clay content	43%	Fig. C 4	72%	Fig. C 6	49%	Fig. C.5
Liquid Limit	67.8%	Fig. C 1	365%	Fig. C 2	46.4%	Fig. C.3
Plasticity Index	36.6%	Table C 4 (Vol.II)	301.42	Table C 5 (Vol.II)	21.4	Table C 6 (Vol.II)
Activity	0.85	Table C 4	4.18	Table C 5	0.437	Table C 6
Source	Saurashtra, Gujarat India	-	Saurashtra Gujarat India	-	Fithion Illinoice U.S.A.	-

Table No. 7.2. Index for Experimental Results as given in Appendix H

CLAY MINERAL

PLOT	Kaolinite				Bentonite				Illite			
	Casa	Oedo	Rowe	Oedo	Casa	Oedo	Rowe	oedo	Casa	Oedo	Rowe	Oedc
Settlement - D.G. vs Time	1 - 6		22,24,26,18		7 -		30,32,34, 36,38		12 - 18		40,41,43, 45	
$\frac{U_m}{\Delta\sigma}$ vs Time	-		23,25,27,29		-		31,33,35,37 39		-		42,44	
Void Ratio vs Log Pressure	19		47		20		48		21		49	

DEGREE OF SATURATION

PLOT	Kaolinite			Bentonite		
	+ OMC	OMC	- OMC	+ OMC	OMC	-OMC
Settlement - D.G. vs Time	55 - 60	50 - 54	61 - 62	71 - 74	63 - 66	67 - 70
Void Ratio vs Log Pressure	75	75	75	76	76	76

FABRIC STRUCTURE

PLOT	Kaolinite				Bentonite			
	Flocc	Dispr	Flocc	Dispr	Flocc	Dispr	Flocc	Dispr
	Casa-Oedo		Rowe-Oedo		Casa-Oedo		Rowe-Oedo	
Settlement - D.G. vs Time	77-83	84-89	107,109, 111,113	117,119 121,123	90-94	96-102	125,126, 128	130,132, 134,136
$\frac{U_{m\%}}{\Delta\sigma}$ vs Time	-	-	108,110, 112,114	116,118, 120,122 124	-	-	127,129,	131,133, 135,137
Void-Ratio vs Log Pressure	103	104	138	139	105	106	140	141

DRAINAGE PATH

PLOT	Kaolinite		
	Vertical	Horizontal	Inclined
Settlement - D.G. vs Time	142 - 146	152 - 156	147 - 151
Void Ratio vs Log Pressure	157	157	157

	H = 0.25"	H = 0.5"	H = 1"	H = 2"
Settlement - D.G. vs Time	257 - 263	264 - 269	270 - 275	276 - 281
Void Ratio vs Log Pressure	282	283	284	285

STRESS HISTORY

PLOT	Kaolinite (Casa - Oedo)			
	Set I	Set II	Set III	Set IV
Settlement D.G. vs Time	158 - 169	170 - 181	182 - 198	199 - 210
Void Ratio vs Log Pressure	211	211	212	212

PLOT	Kaolinite						Bentonite	
	Casa Oedo	Rowe Oedo	Casa Oedo	Rowe Oedo	Casa Oedo	Casa Oedo	Rowe Oedo	Rowe Oedo
	P/P= 1		P/P=2		P/P=4	P/P=8	P/P=1	P/P=2
Settlement D.G. vs Time	213-217	229,231, 233,235	218-221	237, 239, 241, 243	222-225	226-228	245,247, 249	251
$\frac{U_{m\%}}{\Delta\sigma}$ vs Time	-	230,232, 234,236	-	238,240 242,244	-	-	246,248, 250	252
Void Ratio vs Log Pressure	19	253	228	254	228	228	255	256

from theory discussed in Chapter IV. The theoretical values computed are presented in Volume II as Appendix G.

7.2. Determination of Parameters

7.2.1. Co-efficient of Consolidation

In the present work the Naylor-Doran (1948) curve fitting method is employed to determine the coefficient of consolidation, C_v. The method is based on the theory of distribution of errors to evaluate the correct value fitting with the experimental curve. It is known that square root method (Taylor 1942) cannot take into account the final reading while the log time method (Casagrande 1936) is unable to mark initial reading leading to errors in the general curve. A stepwise procedure for the determination of co-efficient of consolidation is explained in terms of an actual example as given in Table 7.3.

(i) Note initial δ_i' and final δ_f' dial gauge readings from root time curve (Fig. 7.1) and log time curve (Fig. 7.2) respectively. In this example $\delta_i' = 1112$ and $\delta_f' = 690$.

(ii) Plot log(1 - U') against time in minutes as shown in Fig. 7.3.

(iii) Set up one tangent at (1 - U') = 0.4 and another one at (1 - U') = 0.2. Measure ordinates corresponding to zero time and any other convenient time. In the example, the values are $(1 - U')_{0.2}^{t=0} = 0.63$, $(1 - U')_{0.4}^{t=0} = 0.78$ and $(1 - U')_{0.2}^{t=20} = 0.212$, $(1 - U')_{0.4}^{t=20} = 0.195$. Put the values obtained on the chart

Table 7.3. Determination of Co-efficient of Consolidation by Naylor-Doran (1948)method.

Sample : Ill-Sat-Casa Load Intensity : 0.8 kg/cm^2

Clock Time	Time (Mnts)	Diag Gauge Reading X 10^{-4}inch.	Δh	δ'_i=1112 $\delta - \delta'_\delta$	δ'_f=660 $1-U' = \frac{\delta - \delta'_\delta}{\delta'_i - \delta_f}$	δ'_i=112 $\delta - \delta_f$	δ_f=690 $1-U' = \frac{\delta - \delta_f}{\delta'_i - \delta_f}$
10am.	0	1129	0	452	1.0	432	1.0
	1/4	1065	64	405	0.896	375	0.867
	1	1040	89	380	0.752	350	0.81
	2¼	975	154	315	0.697	285	0.66
	4	929	200	269	0.594	239	0.554
	6¼	883	246	223	0.492	193	0.447
	9	944	285	184	0.407	154	0.349
	12¼	808	320	148	0.328	118	0.274
	16	784	345	124	0.274	94	0.217
	20¼	756	373	96	0.212	66	0.152
	25	734	395	74	0.163	44	0.102
	36	700	429	40	0.088	10	0.023
	49	682	447	22	-	-	-
	66	670	459	10	-	-	-
	90	657	471	-	-	-	-
12-40pm	157	646	483	-	-	-	-
1-30	207	641	488	-	-	-	-
2-30	267	637	492	-	-	-	-
5-00	417	631	498	-	-	-	-
6-15	492	627	501	-	-	-	-
7-30	567	626	503	-	-	-	-
10am.	24 hours	617	514	-	-	-	-

h_o= .7543 ϵ = - 0.075

h =-.0690 η = + 0.01

h_1= .6853 $C_v = \frac{0.567}{27.5} d_{80}^2$

$h_{av} = \frac{1.4396}{2}$ $= 0.0206 d_{80}^2$

= .7198 = 0.0024 in^2/Mnt

d_{av}= .3599 h_o = .7543

h_{80} =-.0725

d_{av}= .1295 h_{80} = .6818 d_{80}^2= .1162

$$\delta_f = \frac{\delta'_f - \epsilon \delta'_i}{1 - \epsilon} = \frac{660 + 0.075 \times 111}{1.075}$$

$$= 690$$

$$i = \frac{\delta'_i + \eta \delta_f}{1 + \eta} = \frac{112 + 0.01 \times 690}{1 + 0.01}$$

$$= 1108$$

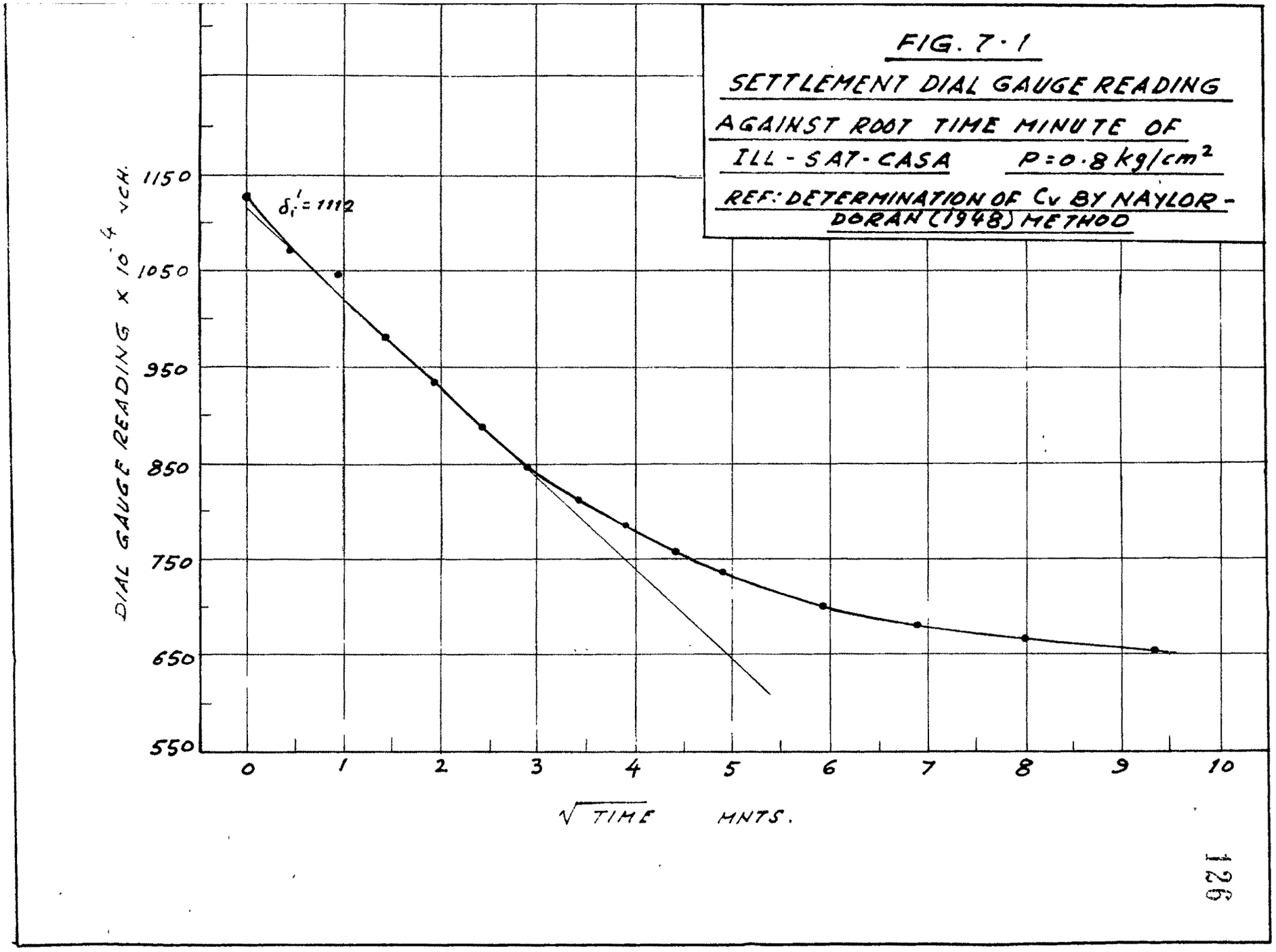
FIG. 7·1
SETTLEMENT DIAL GAUGE READING
AGAINST ROOT TIME MINUTE OF
ILL - SAT - CASA P = 0·8 kg/cm²
REF: DETERMINATION OF Cv BY NAYLOR - DORAN (1948) METHOD
DIAL GAUGE READING x 10⁻⁴ VCH.
1150
1050
950
850
750
650
550
δ₁' = 1112
0
1
2
3
4
5
6
7
8
9
10
√ TIME MNTS.

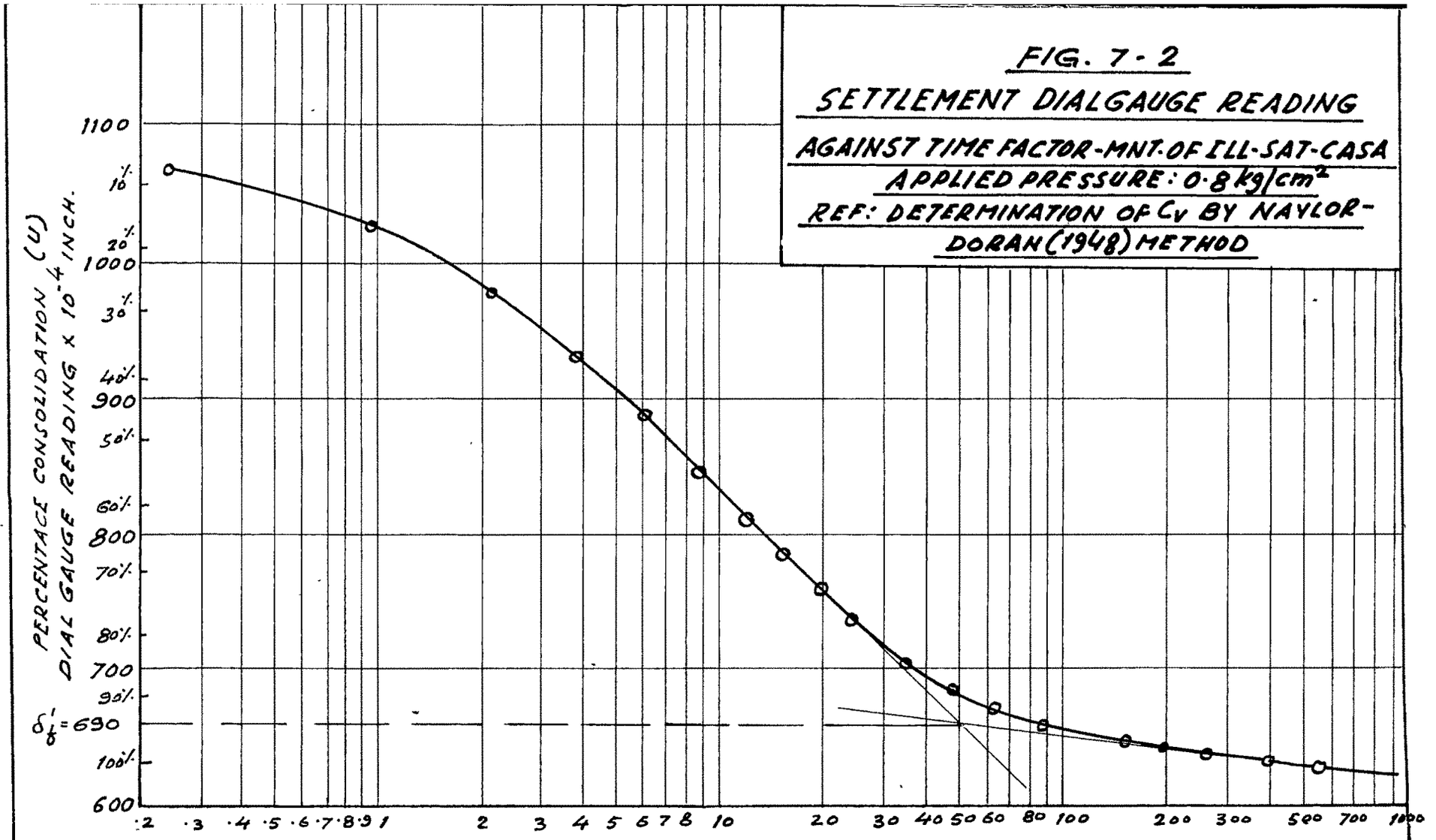
FIG. 7-2
SETTLEMENT DIALGAUGE READING
AGAINST TIME FACTOR-MNT. OF ILL-SAT-CASA
APPLIED PRESSURE: 0·8 kg/cm²
REF: DETERMINATION OF Cv BY NAYLOR-DORAN (1948) METHOD
PERCENTAGE CONSOLIDATION (U)
DIAL GAUGE READING x 10⁻⁴ INCH.
1100
10%
20%
1000
30%
40%
900
50%
60%
800
70%
80%
700
90%
δ'f = 690
100%
600
·2 ·3 ·4 ·5 ·6 ·7 ·8 ·9 1 2 3 4 5 6 7 8 10 20 30 40 50 60 80 100 200 300 500 700 1000
TIME - MNTS.

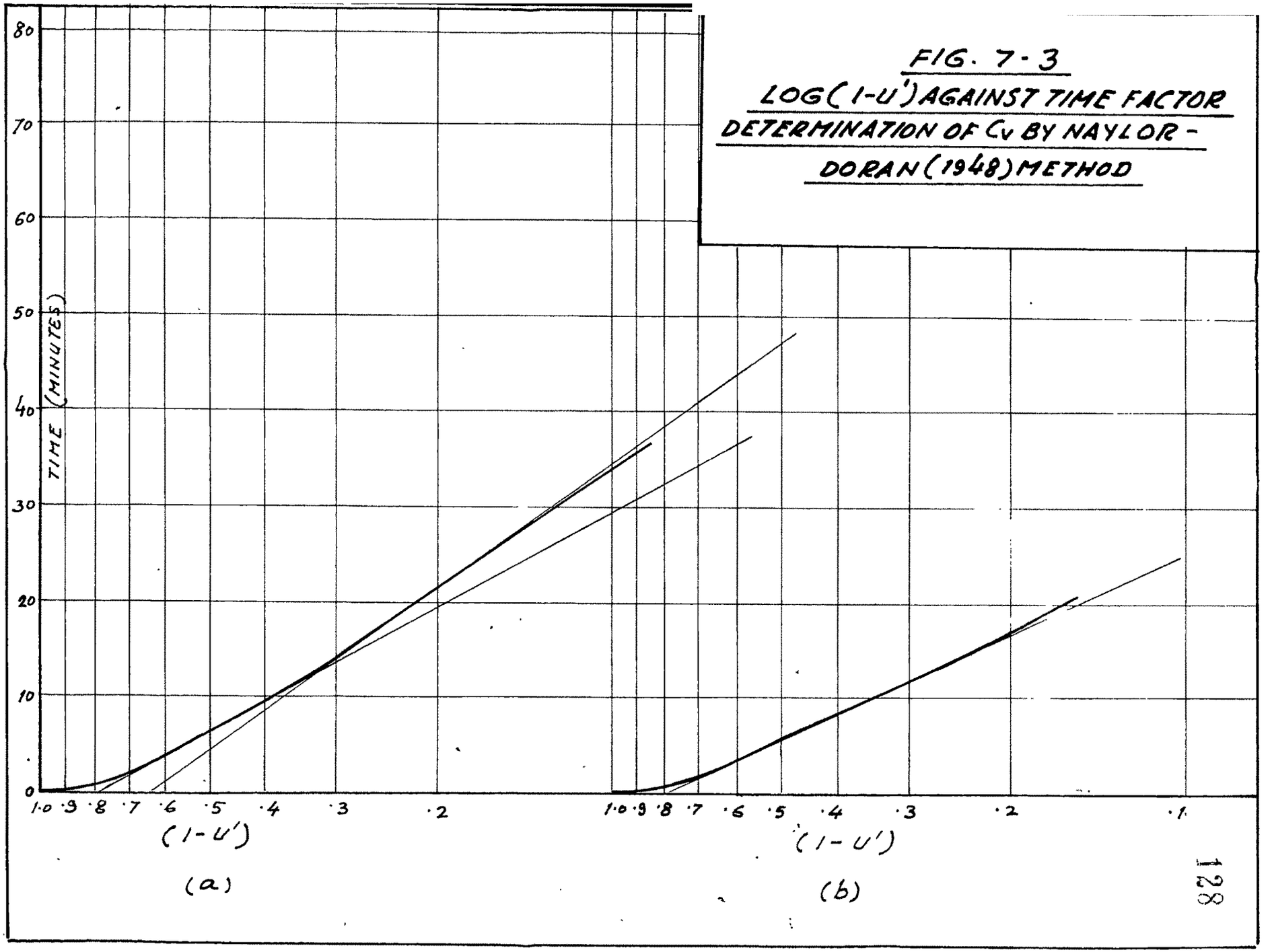

FIG. 7-3

LOG(1-U') AGAINST TIME FACTOR

DETERMINATION OF C_v BY NAYLOR-DORAN (1948) METHOD

(Fig. 7.4) and draw diagonals between these points whose intersection determines the value ϵ on the absicca of the chart. In this example value of $\epsilon = -0.075$. Find the correct value of the final reading by the formula :

$$\delta_f = \frac{\delta_f' - \epsilon \delta_i'}{1 - \epsilon} \quad \text{In this case } \delta_f = 690$$

(iv) Now replot log (1 - U') using the correct value, δ_f against time as shown in Fig. 7.3. Extend the straight portion backwards to read off the intercept on (1 - U') axis. In this example the value is 0.81. Using this value of intercept determin the value of η from the chart (Fig. 7.5). In this particular example, $\eta = +.01$. Find the correct value of the initial reading by the formula :

$$\delta_i = \frac{\delta_i + \eta \delta_f}{1 + \eta}$$

Here in the example δ_i works out to be 1108.

(v) Measure the time for 80% cohsolidation from log time curve (Fig. 7.2). In this example, t_{80} = 27.5 minutes.

(vi) Determine the coefficient of consolidation c_v by the following relation :

$$c_v = \frac{T_{80} d_{80}^2}{t_{80}}$$

where T_{80} is the theoretical time factor. In this example, T_{80} for Terzaghi theory (P = 0) is 0.567 and d_{80} = .3404 inch. Thus, c_v for fitting with Terzaghi theory is .0024 $in^2/Mt.$

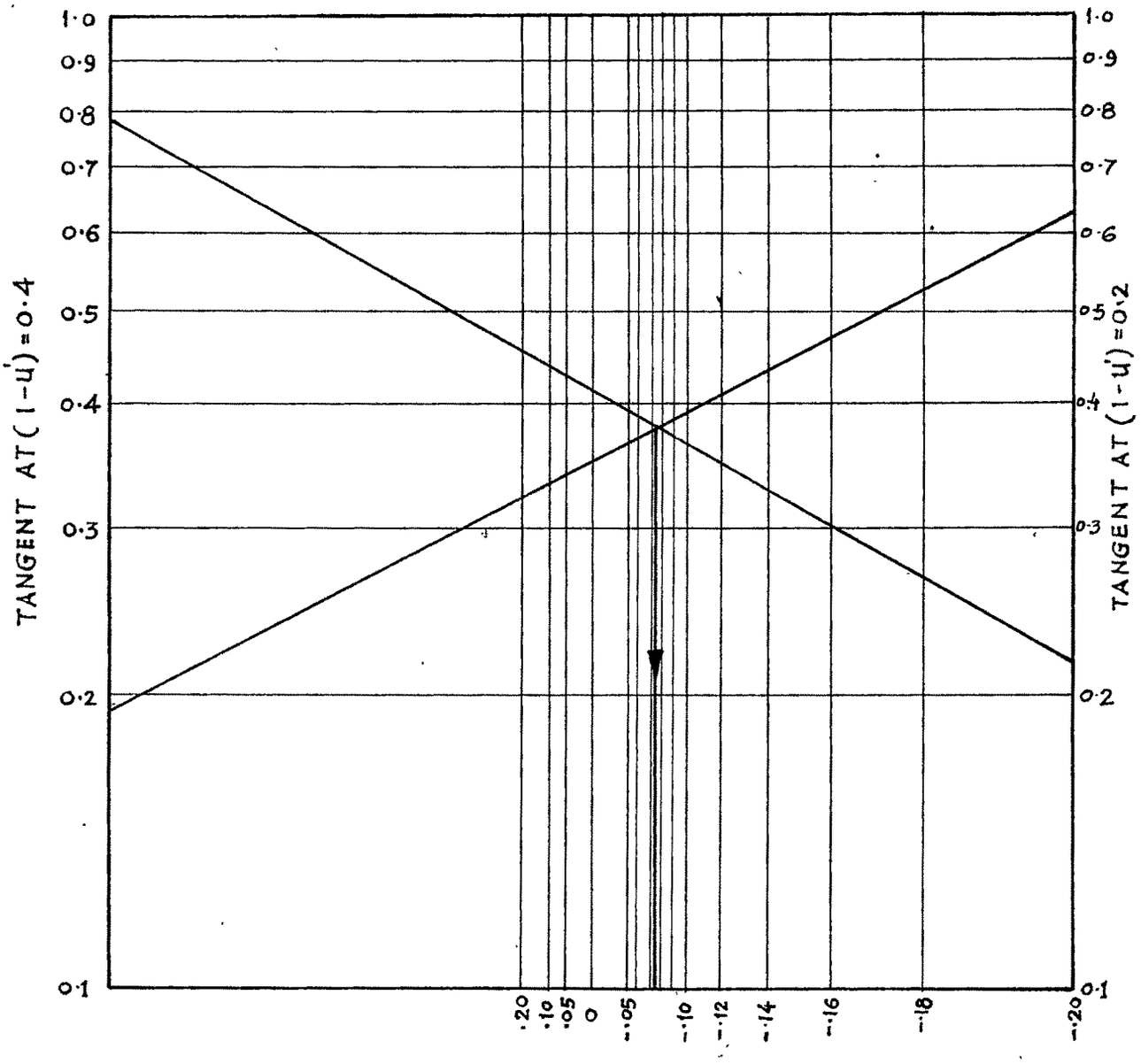

FIG.7·4 CHART OF DETERMINATION OF ε

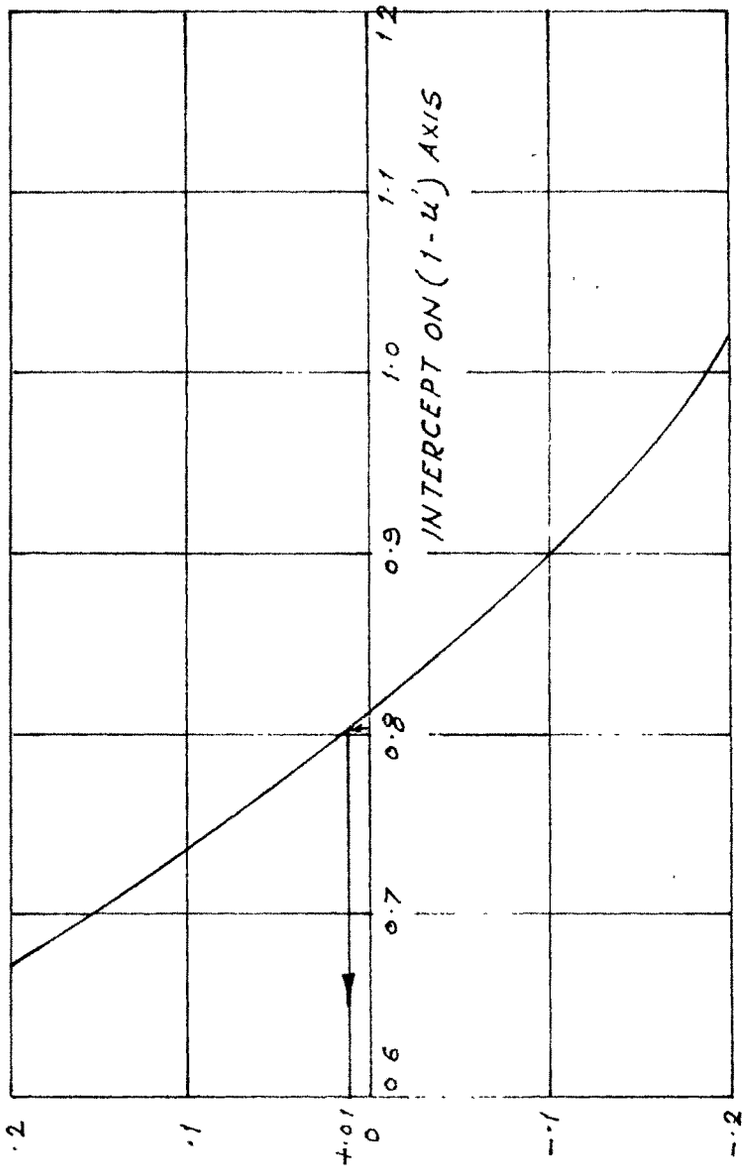

FIG. 7.5 CHART OF DETERMINATION OF η

Similarly, c_v is determined for other values of P.

7.2.2. Compression Index

The classical definition of the compression index, Cc, is the slope of the straight line portion of a virgin compression curve. In the present work the definition is same except that the slope has been worked out at various intervals of pressure and void ratio taking the portion under consideration as straight line. Example illustrated by the Table 7.4 presents the method of determination. Fig. 7.6 represents the void ratio-effective stress plot for the sample illustrated.

7.2.3. Degree of Secondary Compression

In order to measure the influence of various physico-chemical factors which cause a time lag other than the hydrodynamic lag, a parameter giving the percentage of secondary compression in a total consolidation designated as degree of secondary compression is used. The value of this parameter, is determined by separating the value of secondary compression as per Naylor-Doran method (1948). The evaluation of this parameter is illustrated by an example given in Table 7.6. Fig. 7.7 represents the dial gauge reading versus log time plot for the sample used in the example.

7.2.4. Parameter 'P'

'P' is a lumped parameter which accounts for the physico-chemical and mechanical factors in terms of deformability.

Table 7.4. Determination of Compression Index

Load Intensity kg/cm^2	$\bar{P}$ = Average Load Intensity	$\text{Log}(\frac{P_2}{P_1}) = A$	Δe	$C_c = \frac{\Delta e}{A}$
0.1				
	0.15		1.02	3.39
0.2				
	0.3		1.75	5.82
0.4				
	0.6	0.301	1.9	6.315
0.8				
	1.2		1.2	3.99
1.6				
	2.4		0.9	2.99
3.2				
	4.8		1.0	3.32
6.4				

Table 7.5. Determination of Percentage Secondary Compression

Load Intensity Kg/cm^2	Δh	δ_i	δ_f	$\Delta h' = \delta_i - \delta_f$	$\lambda = \frac{\Delta h'}{\Delta h} X100$ (Percentage primary consolidation)	(100-λ) Percentage secondary compression
0.2	1094	2310	1252	1058	65.0	35.0
0.8	1248	2193	1208	885	74.4	25.6
1.6	911	1558	665	893	81.0	19.0
3.2	883	1567	840	727	82.8	17.2
6.4	670	1284	672	612	90.2	9.8

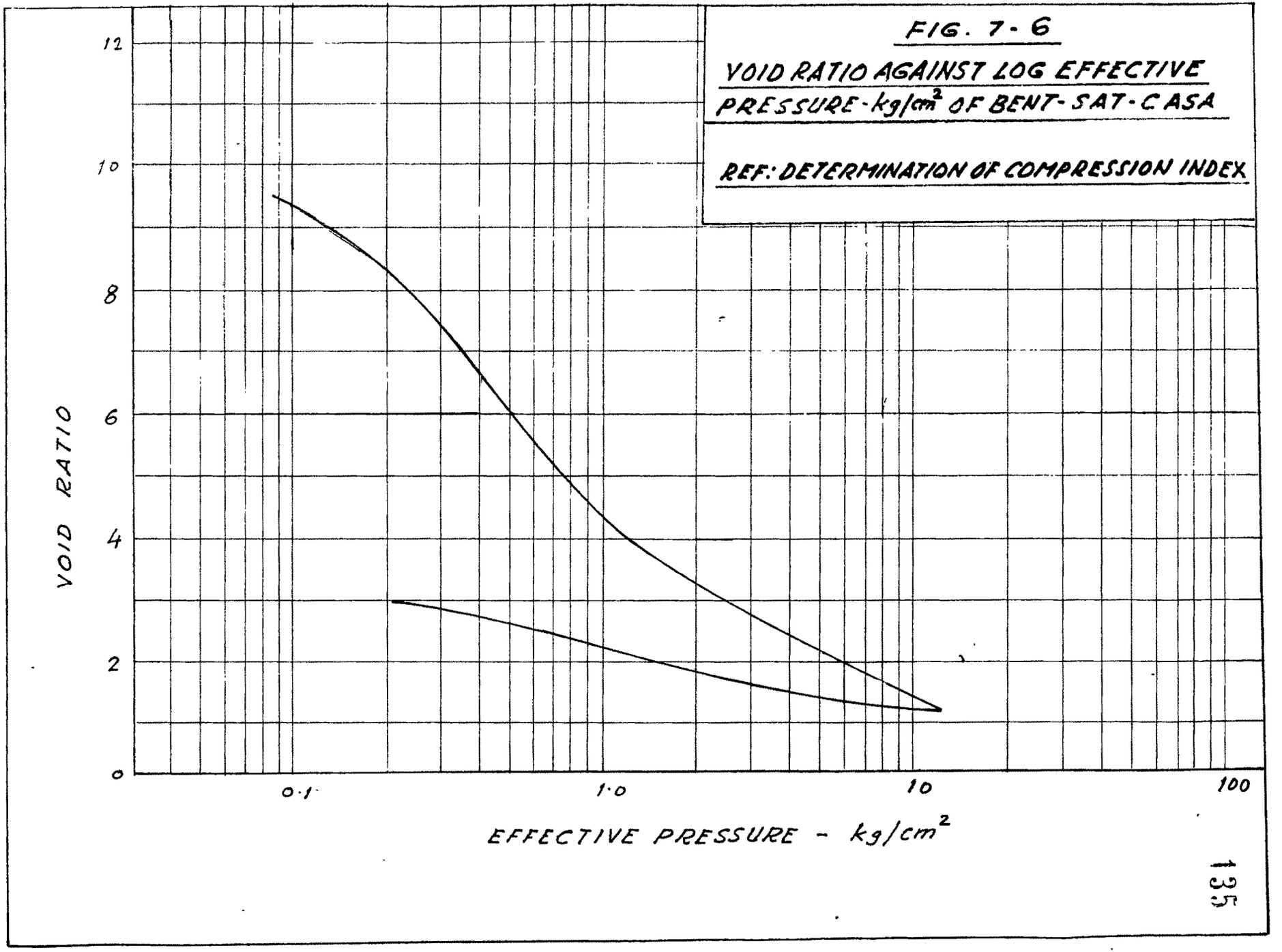
FIG. 7-6
VOID RATIO AGAINST LOG EFFECTIVE PRESSURE - kg/cm² OF BENT-SAT-CASA
REF: DETERMINATION OF COMPRESSION INDEX
VOID RATIO
12
10
8
6
4
2
0
0·1
1·0
10
100
EFFECTIVE PRESSURE - kg/cm²

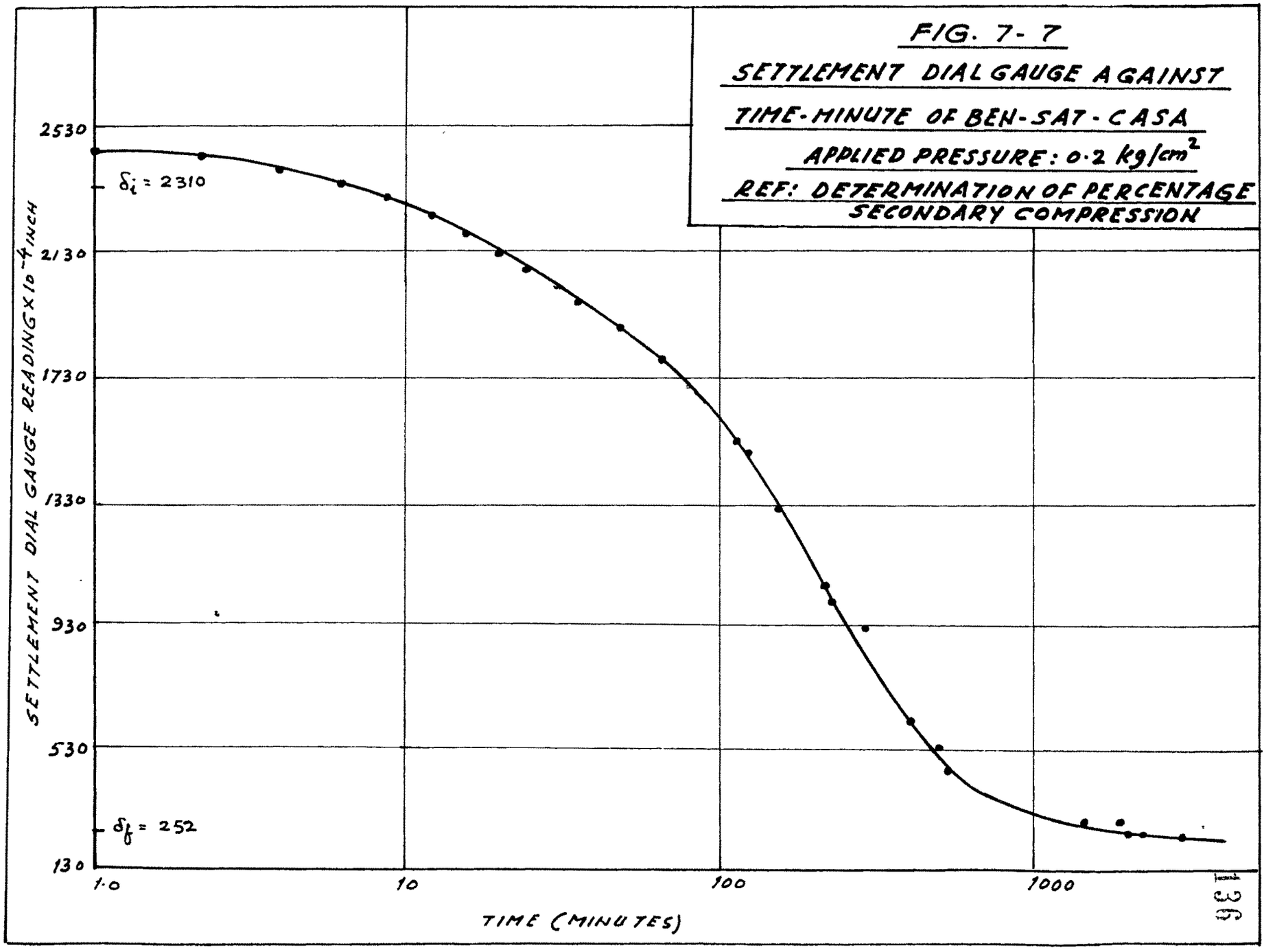
FIG. 7-7
SETTLEMENT DIAL GAUGE AGAINST
TIME-MINUTE OF BEN-SAT-CASA
APPLIED PRESSURE: 0·2 kg/cm²
REF: DETERMINATION OF PERCENTAGE
SECONDARY COMPRESSION
SETTLEMENT DIAL GAUGE READING X 10⁻⁴ INCH
2530
2130
1730
1330
930
530
130
δi = 2310
δf = 252
1·0
10
100
1000
TIME (MINUTES)
136

P = 0 represents a Terzaghi classical case which ignores the influence of the characteristics of constituents of soil material. The object behind introducing this parameter is to evaluate the influence of the various factors on the consolidation characteristics of soil. In the present work, parameter 'P' has been regarded as a constant and is determined by comparing experimental curve with the theoretical curve.

7.2.5. Tangent Modulus, Secant Modulus and Hysteresis Modulus

Tangent modulus(E_i) is an initial slope of e v/s logp curve determined by drawing a tangent to the convex portion of the curv Secant modulus is the average slope of e v/s logp curve at any po Hysteresis modulus is a mean slope of the loop. Fig. 7.8 illustra the meanings of the above terms.

7.3. Analysis and Discussion

7.3.1. Clay Mineral

Refer Figures 7.9 to 7.30 which are derived from the parent plots of Figures H - 1 to H - 49 reported in Appendix H of Vol.II

Analysis :

(i) Co-efficient of consolidation against percentage degree of consolidation. (Figures 7.9 to 7.13).

In case of kaolinite and illite unlike Bentonite the value almost remains constant throughout the process of consolidation. The general characteristics of Bentonite is similar for all loads but show constancy at higher loads. Upto 40% consolidation a slow increase is seen after which it decreases which is observed to be rapid at lighter loads.

(ii) Co-efficient of consolidation against applied effective pressure. (Figures 7,14 to 7.16).

The general characteristics of non-expanding mineral kaolinite and illite are similar while the expanding mineral

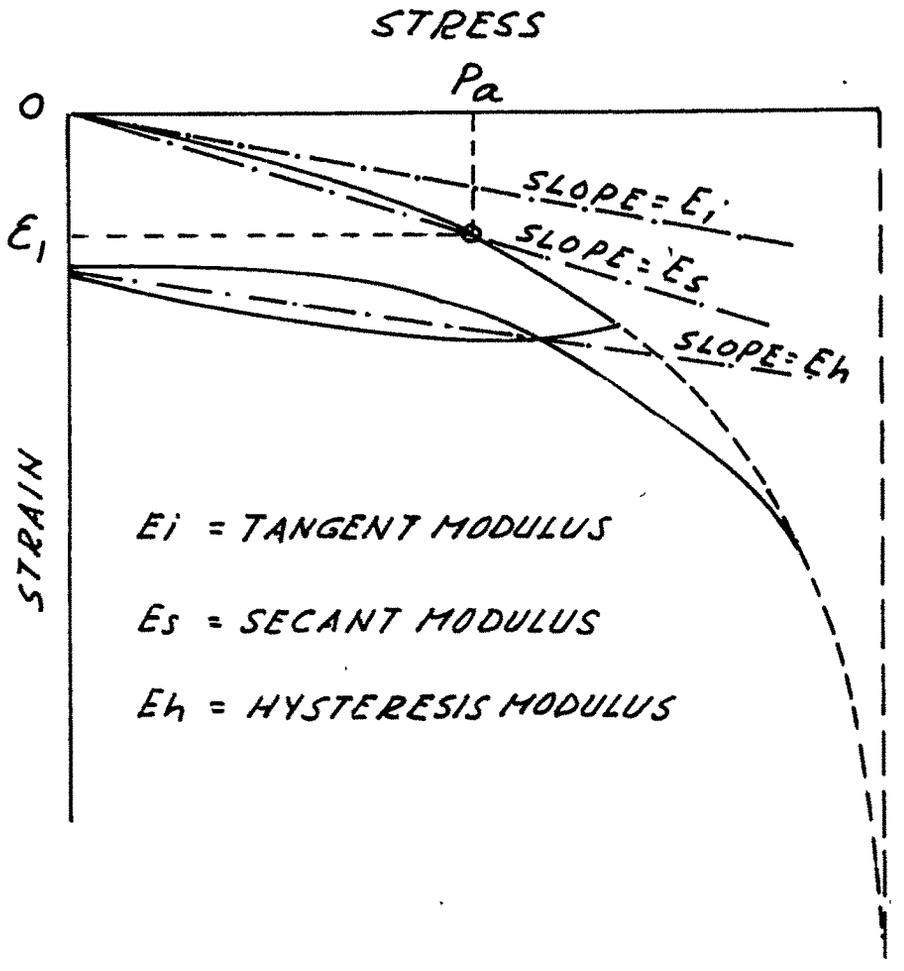

FIG. 7·8 INITIAL TANGENT MODULUS, SECANT MODULUS AND HYSTERESIS MODULUS IN STRESS-STRAIN DIAGRAM FOR CLAY

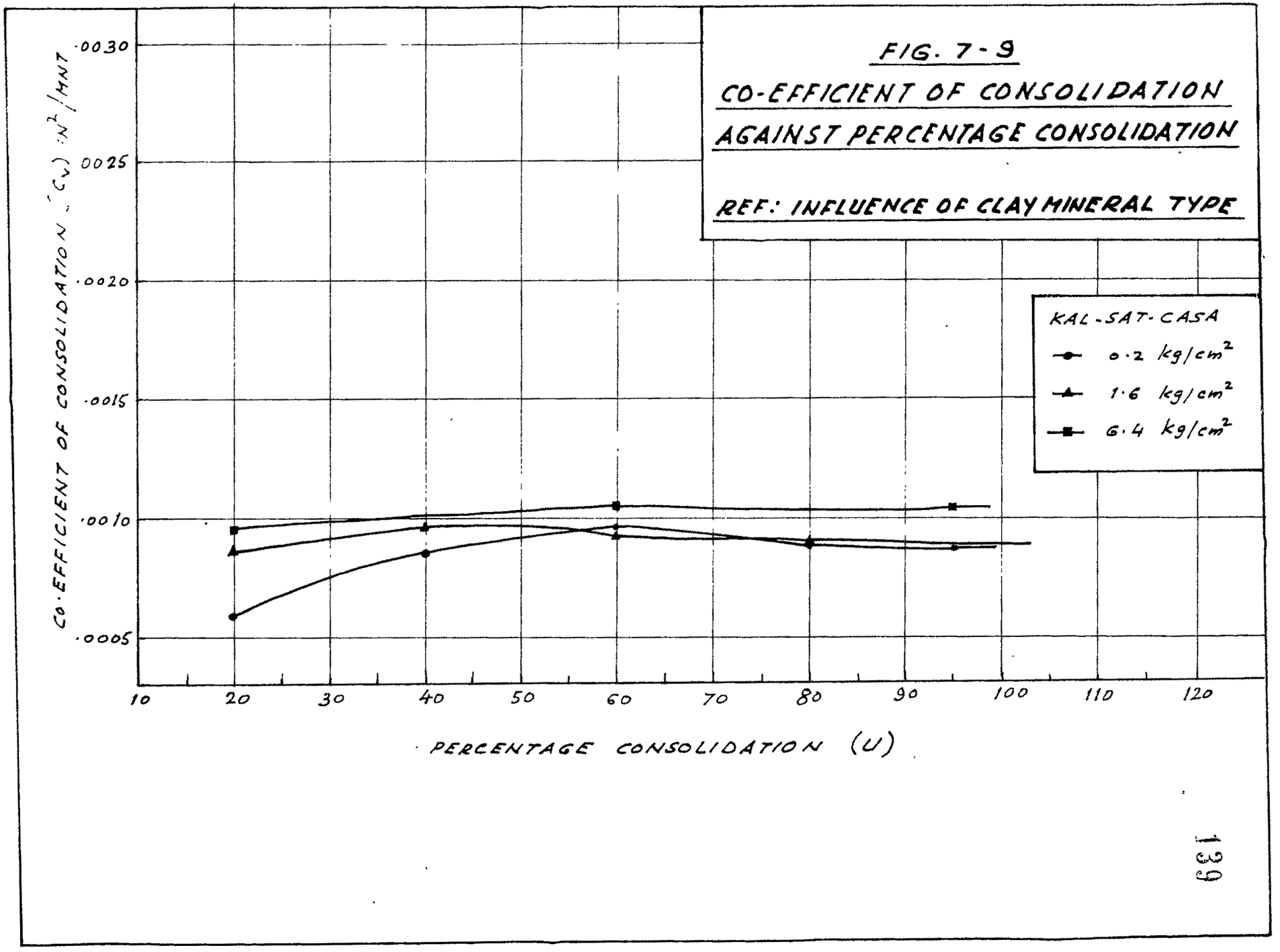
FIG. 7-9
CO-EFFICIENT OF CONSOLIDATION
AGAINST PERCENTAGE CONSOLIDATION
REF.: INFLUENCE OF CLAY MINERAL TYPE
KAL-SAT-CASA
0·2 kg/cm²
1·6 kg/cm²
6·4 kg/cm²
CO-EFFICIENT OF CONSOLIDATION (Cv) :N²/MNT
·0030
·0025
·0020
·0015
·0010
·0005
10
20
30
40
50
60
70
80
90
100
110
120
PERCENTAGE CONSOLIDATION (U)

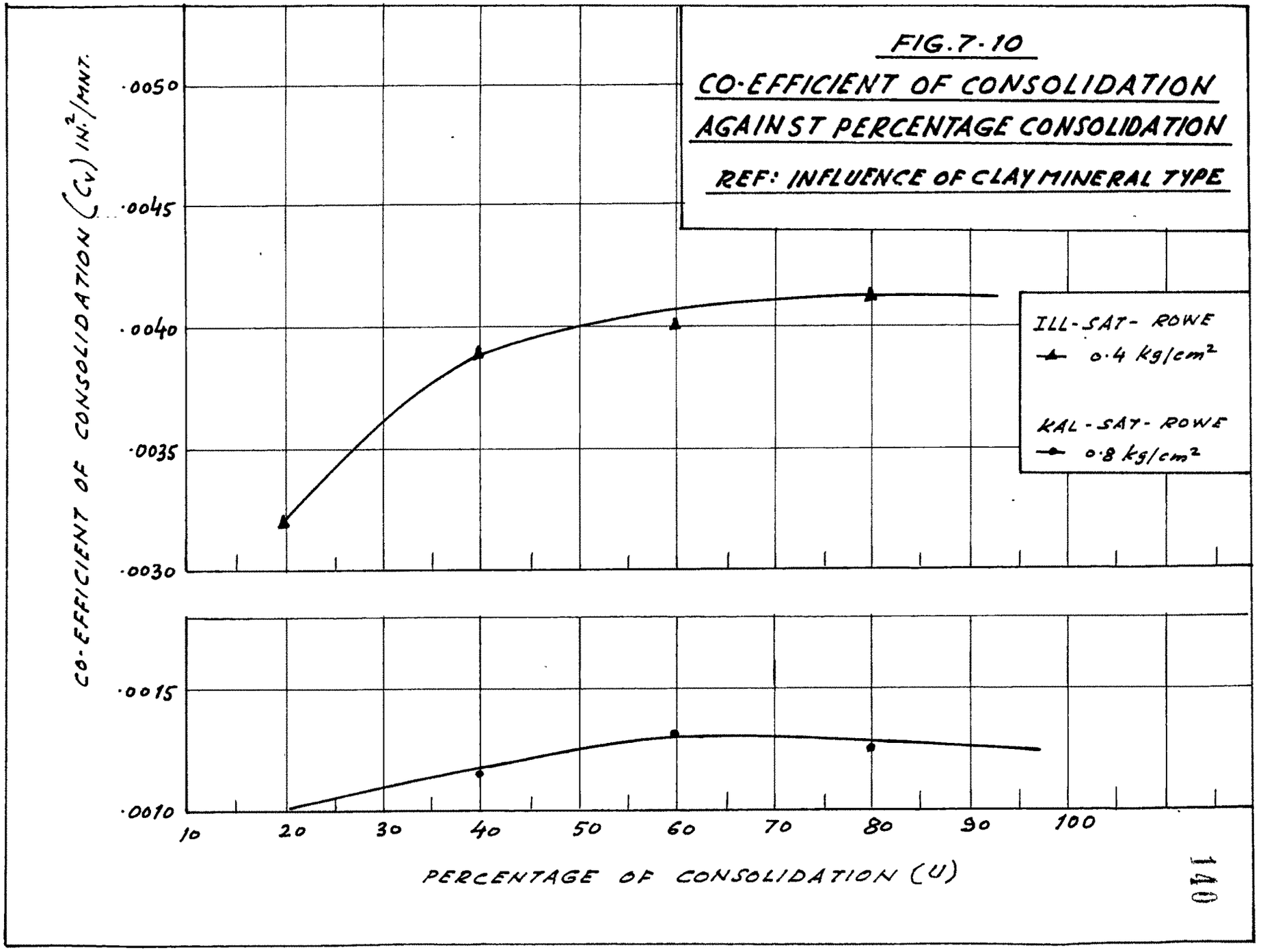
FIG.7·10
CO·EFFICIENT OF CONSOLIDATION
AGAINST PERCENTAGE CONSOLIDATION
REF: INFLUENCE OF CLAY MINERAL TYPE
ILL-SAT- ROWE
0·4 kg/cm²
KAL-SAT- ROWE
0·8 kg/cm²
CO-EFFICIENT OF CONSOLIDATION (Cv) IN.²/MNT.
·0050
·0045
·0040
·0035
·0030
·0015
·0010
10
20
30
40
50
60
70
80
90
100
PERCENTAGE OF CONSOLIDATION (U)

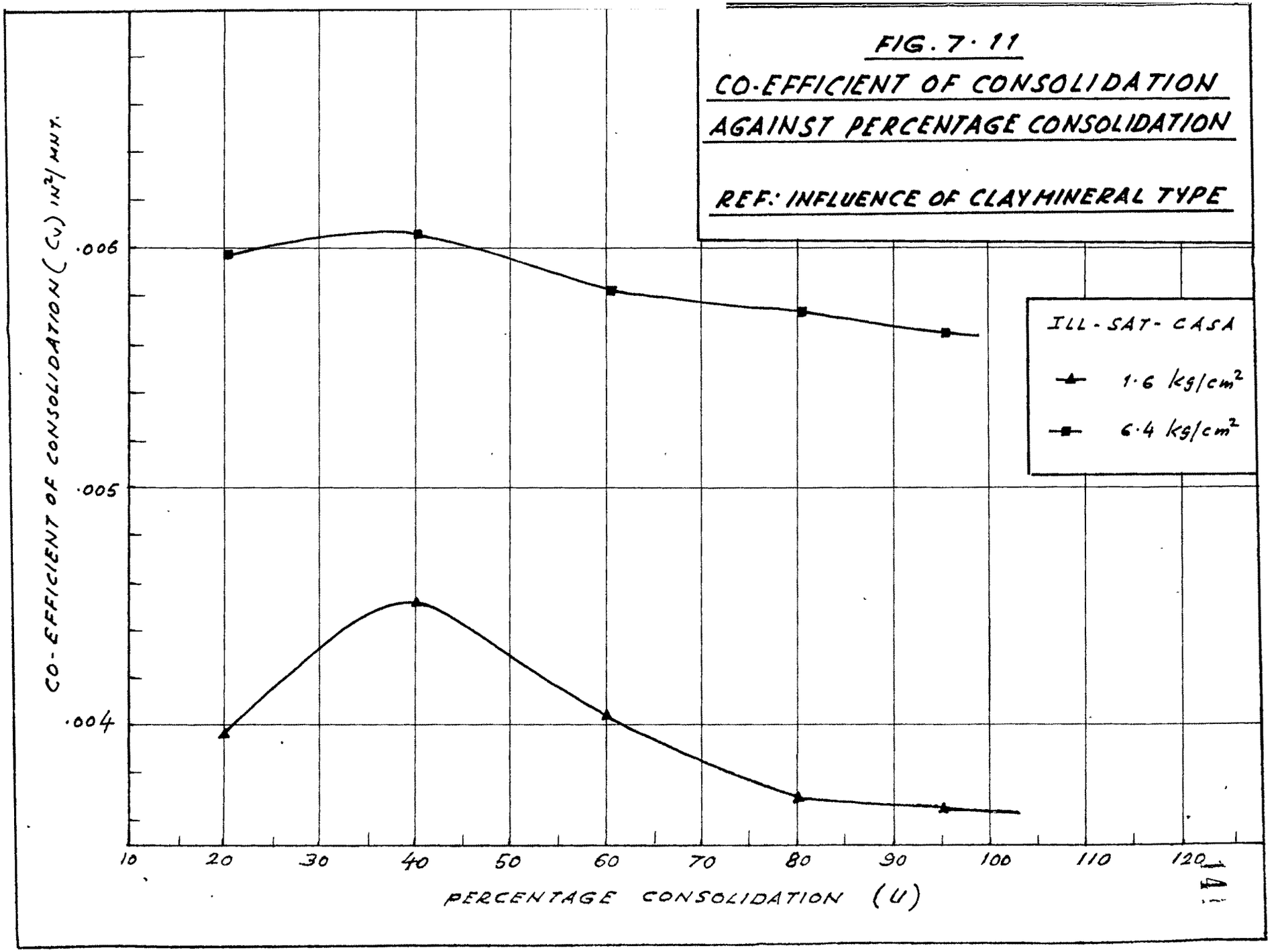
FIG. 7·11
CO-EFFICIENT OF CONSOLIDATION AGAINST PERCENTAGE CONSOLIDATION
REF: INFLUENCE OF CLAY MINERAL TYPE
ILL-SAT-CASA
1·6 kg/cm²
6·4 kg/cm²
CO-EFFICIENT OF CONSOLIDATION (Cv) in²/MNT.
.006
.005
.004
10
20
30
40
50
60
70
80
90
100
110
120
PERCENTAGE CONSOLIDATION (U)

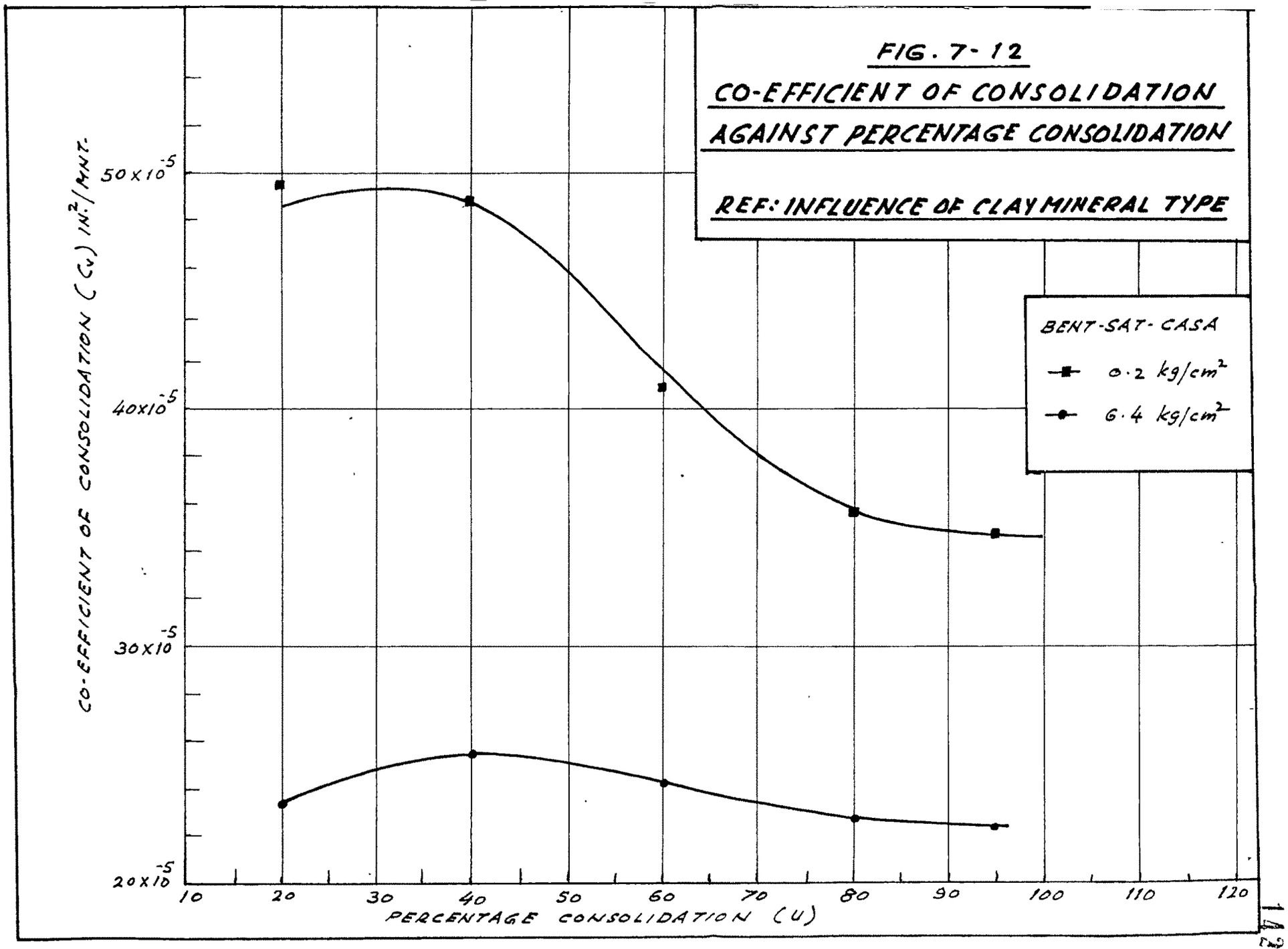
FIG. 7-12
CO-EFFICIENT OF CONSOLIDATION AGAINST PERCENTAGE CONSOLIDATION
REF: INFLUENCE OF CLAY MINERAL TYPE
BENT-SAT-CASA
0·2 kg/cm²
6·4 kg/cm²
CO-EFFICIENT OF CONSOLIDATION (Cv) IN.²/MNT.
50X10⁻⁵
40X10⁻⁵
30X10⁻⁵
20X10⁻⁵
10
20
30
40
50
60
70
80
90
100
110
120
PERCENTAGE CONSOLIDATION (U)

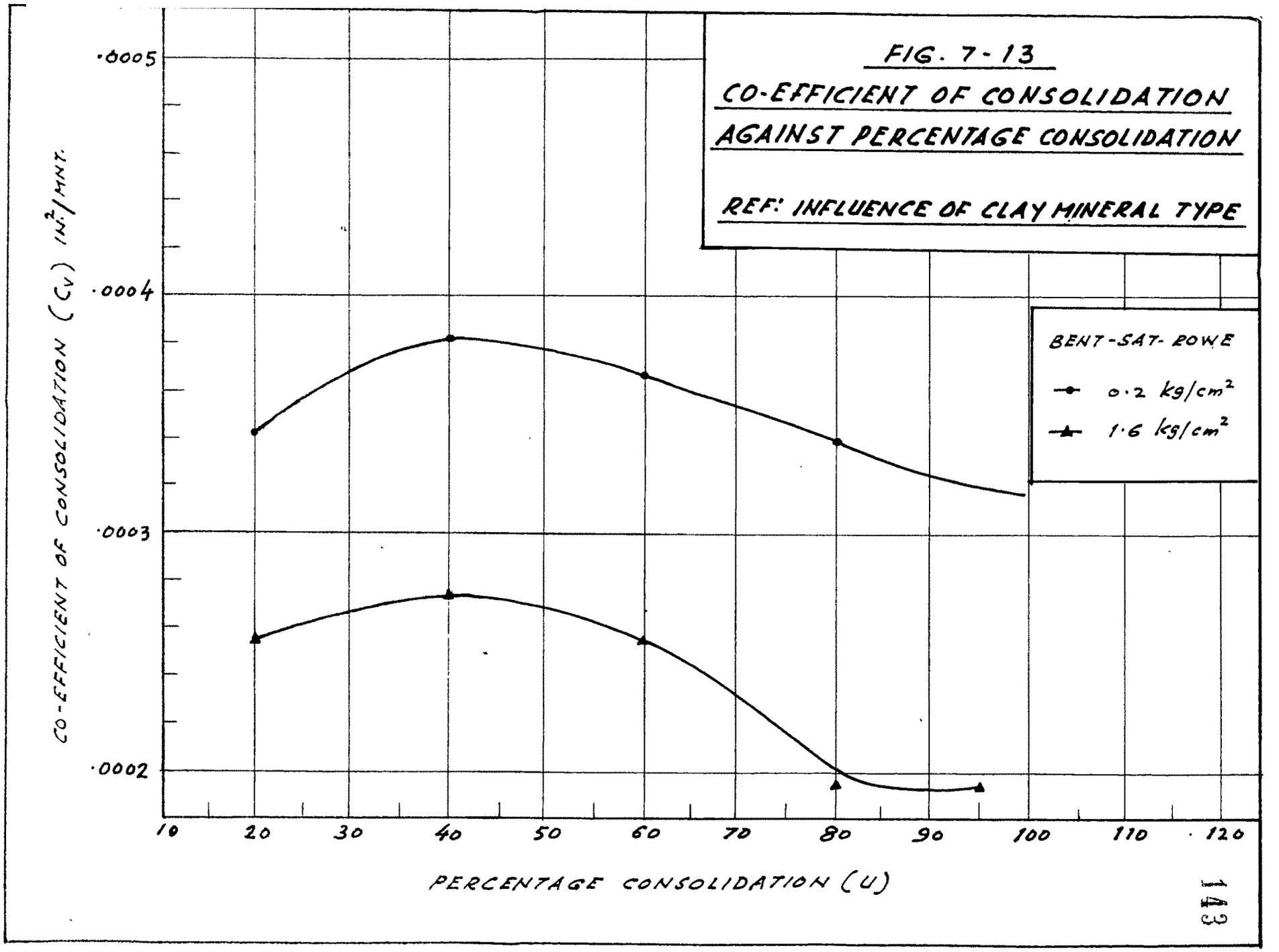
FIG. 7-13
CO-EFFICIENT OF CONSOLIDATION AGAINST PERCENTAGE CONSOLIDATION
REF: INFLUENCE OF CLAY MINERAL TYPE
BENT-SAT-POWE
0·2 kg/cm²
1·6 kg/cm²
CO-EFFICIENT OF CONSOLIDATION (Cv) IN.²/MNT.
·0005
·0004
·0003
·0002
10
20
30
40
50
60
70
80
90
100
110
120
PERCENTAGE CONSOLIDATION (U)

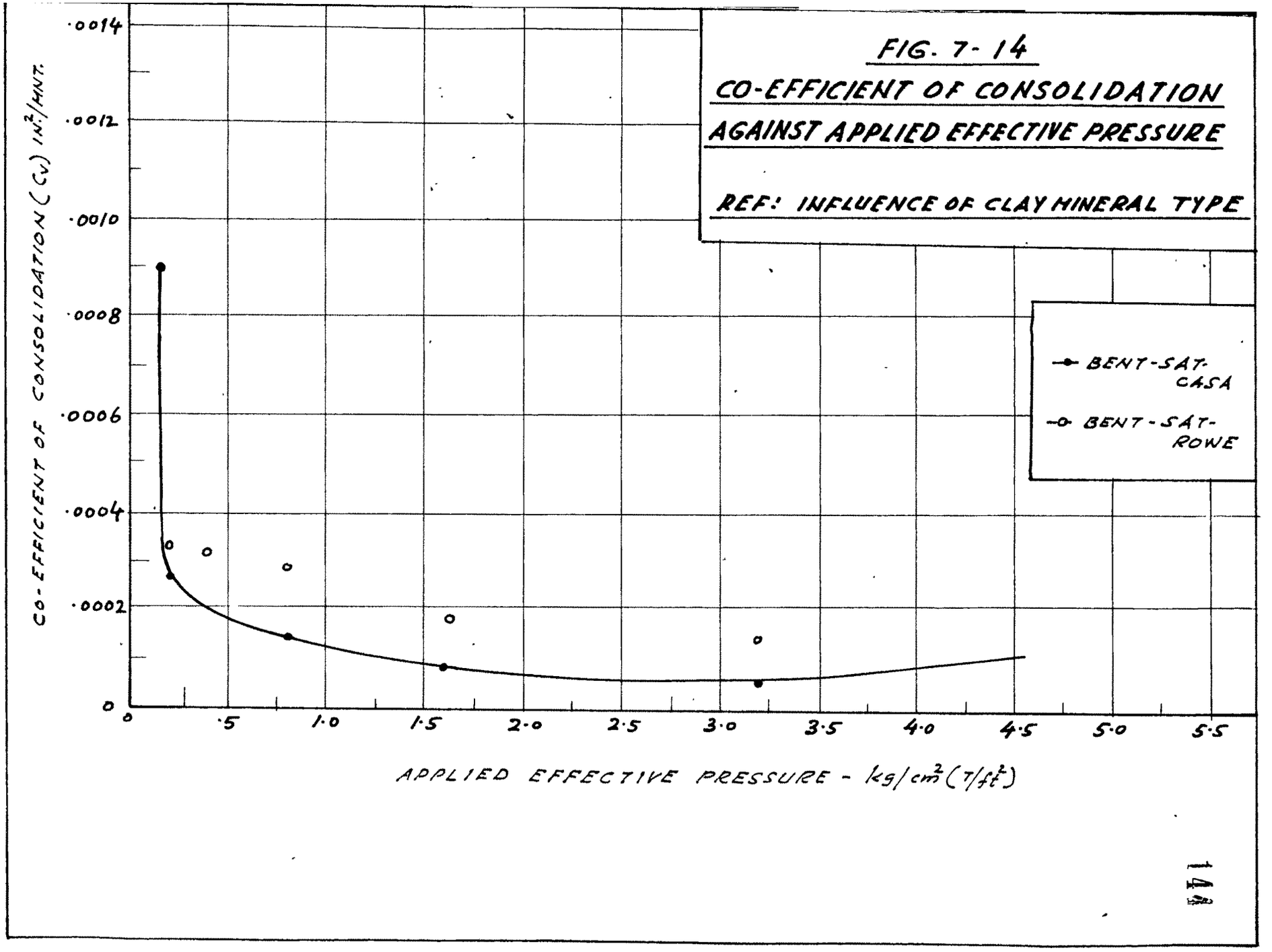
FIG. 7-14
CO-EFFICIENT OF CONSOLIDATION AGAINST APPLIED EFFECTIVE PRESSURE
REF: INFLUENCE OF CLAY MINERAL TYPE
BENT-SAT-CASA
BENT-SAT-ROWE
CO-EFFICIENT OF CONSOLIDATION (Cv) IN.²/MNT.
·0014
·0012
·0010
·0008
·0006
·0004
·0002
0
0
·5
1·0
1·5
2·0
2·5
3·0
3·5
4·0
4·5
5·0
5·5
APPLIED EFFECTIVE PRESSURE - kg/cm² (T/ft²)

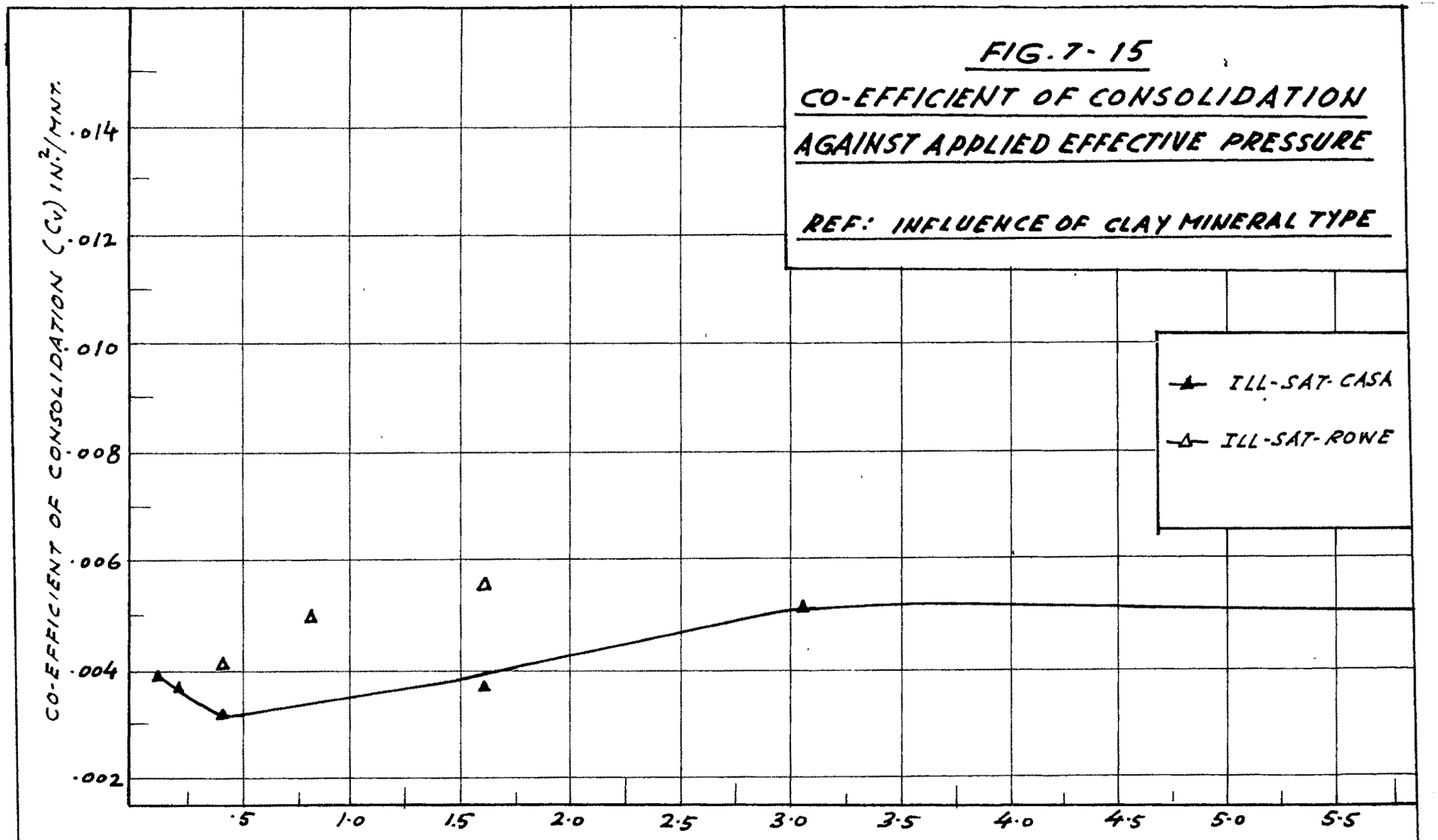
FIG. 7-15
CO-EFFICIENT OF CONSOLIDATION AGAINST APPLIED EFFECTIVE PRESSURE
REF: INFLUENCE OF CLAY MINERAL TYPE
ILL-SAT-CASA
ILL-SAT-ROWE
CO-EFFICIENT OF CONSOLIDATION (Cv) IN.²/MNT.
.014
.012
.010
.008
.006
.004
.002
.5
1.0
1.5
2.0
2.5
3.0
3.5
4.0
4.5
5.0
5.5
APPLIED EFFECTIVE PRESSURE - kg/cm² (T/ft²)

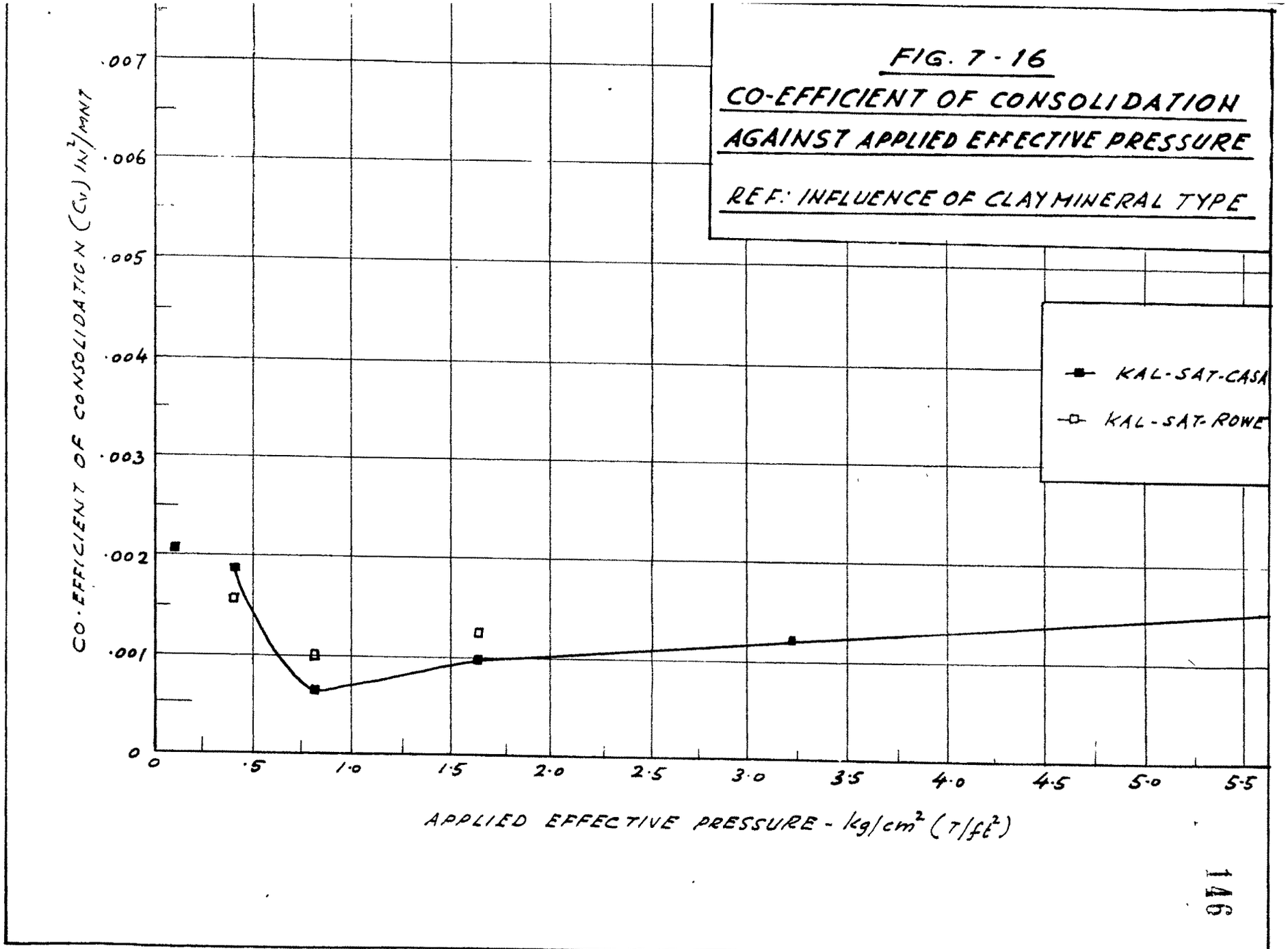
FIG. 7-16
CO-EFFICIENT OF CONSOLIDATION AGAINST APPLIED EFFECTIVE PRESSURE
REF: INFLUENCE OF CLAY MINERAL TYPE
KAL-SAT-CASA
KAL-SAT-ROWE
CO-EFFICIENT OF CONSOLIDATION (Cv) IN²/MNT
.007
.006
.005
.004
.003
.002
.001
0
0
.5
1.0
1.5
2.0
2.5
3.0
3.5
4.0
4.5
5.0
5.5
APPLIED EFFECTIVE PRESSURE - kg/cm² (T/ft²)

montmorillonite indicates different characteristics. The non-expanding group shows decrease in C_v value at lighter loads but with higher loads it tends to increase approximately to a constant value around a pressure value beyond about 6 kg/cm^2. On the other hand expanding group exhibits a rapid decrease in value at lighter loads which is approaching a constant value without showing increase even at higher load. The value of C_v is seen to decrease in order of kaolinite, illite and montmorillanite at all loads.

(iii) Compression index against applied average effective pressure. (Fig. 717).

It is evident both from the parent void ratio - effective pressure plots and also from compression index - effective pressure plots that there is a marked distinction between the characteristics of montmorillonitic clay and illitic clay and also with kaolinitic clay. The Bentonite clay shows a characteristic hump which is more or less absent in other two types of clays. In montmorillonite there is a large reduction in volume at low applied pressures and further application of pressure causes relatively small reductions in volume. For the kaolinite and illite, the amount of compression not only is less but there is relatively small decrease in volume with increasing pressures. It can be noted that Bentonite has much higher value of initial void ratio and indicates also higher compression index compared to illite and kaolinite.

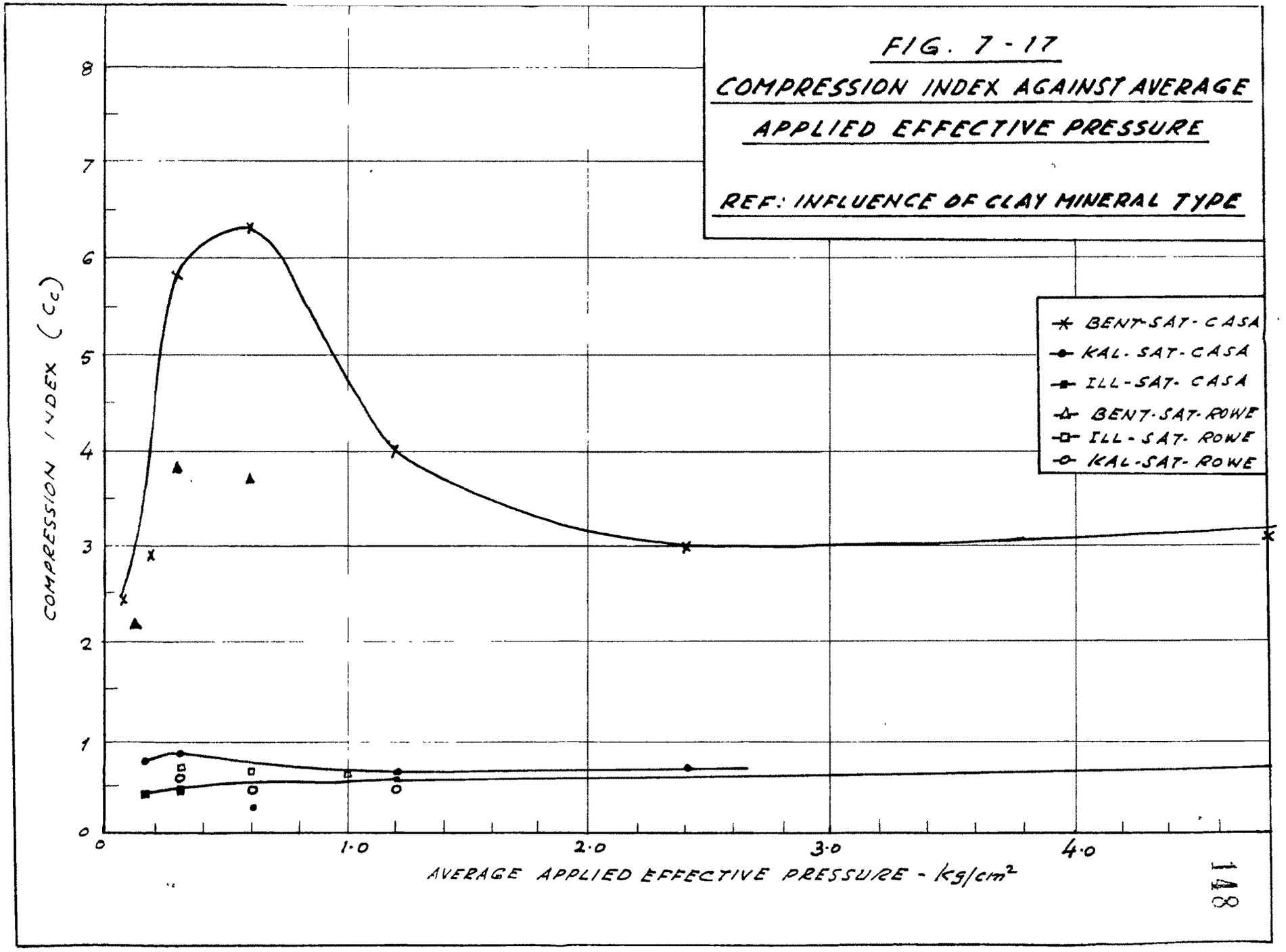
FIG. 7-17
COMPRESSION INDEX AGAINST AVERAGE APPLIED EFFECTIVE PRESSURE
REF: INFLUENCE OF CLAY MINERAL TYPE
BENT-SAT-CASA
KAL-SAT-CASA
ILL-SAT-CASA
BENT-SAT-ROWE
ILL-SAT-ROWE
KAL-SAT-ROWE
COMPRESSION INDEX (C_c)
AVERAGE APPLIED EFFECTIVE PRESSURE - kg/cm²
0
1
2
3
4
5
6
7
8
1·0
2·0
3·0
4·0
148

(iv) Degree of secondary compression against effective applied pressure. (Fig. 7.18)

The degree of secondary compression decreases rapidly at low pressures, slowly becoming insignificant at high loads. Bentonite reveals higher degree of secondary compression compared to the other two types.

(v) Parameter P against applied effective pressure (Figure 7.19 and Fig. 7.20 to Fig. 7.30).

From comparison with theoretical values with experimental observations it is clear that while kaolinite and illite fit closer to the Terzaghi curve montmorillonite deviates the most. Montmorillonite and illite values fall below Terzaghi with a deviation of about 5% and 3% respectively. Kaolinite shows 1.5% deviation at light loads and at higher loads it tends to fit with the classical theory. The experimental plots are also derived from mid plane pore pressure readings which agree well with the theory.

Discussion :

The most striking observation is that the consolidation characteristics of montmorillonite are markedly distinct from that of the other two minerals illite and kaolinite. The behaviour can be explained from basic differences in the nature of their lattice structure and prevalent intermolecular forces during the interaction in clay water system. The principal feature of montmorillonite mineral is that it has an expanding lattice structure, clay flocs are of highly dispersive nature,

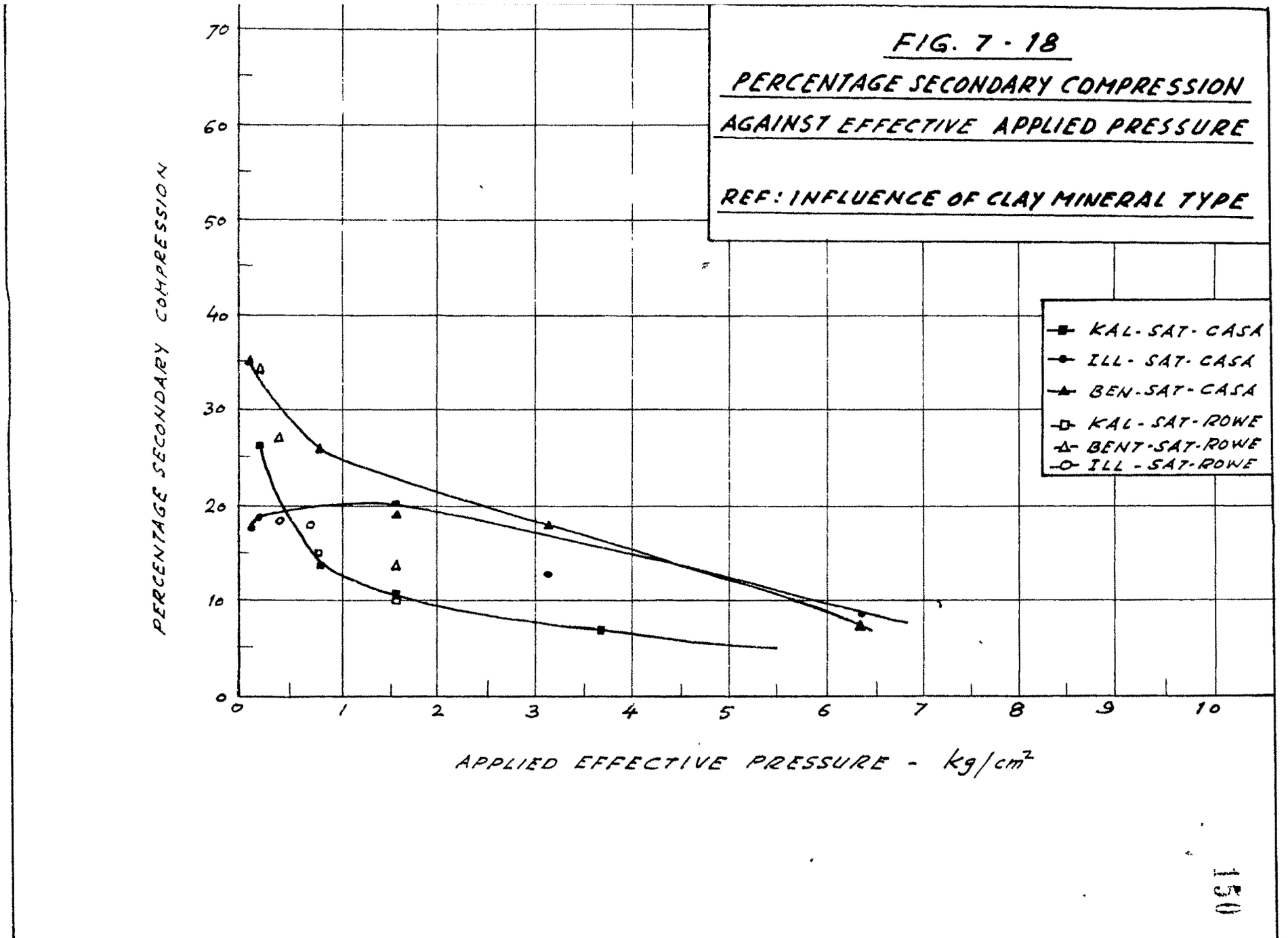
FIG. 7 - 18
PERCENTAGE SECONDARY COMPRESSION AGAINST EFFECTIVE APPLIED PRESSURE
REF: INFLUENCE OF CLAY MINERAL TYPE
KAL - SAT - CASA
ILL - SAT - CASA
BEN - SAT - CASA
KAL - SAT - ROWE
BENT - SAT - ROWE
ILL - SAT - ROWE
PERCENTAGE SECONDARY COMPRESSION
APPLIED EFFECTIVE PRESSURE - kg/cm²
0
10
20
30
40
50
60
70
0
1
2
3
4
5
6
7
8
9
10

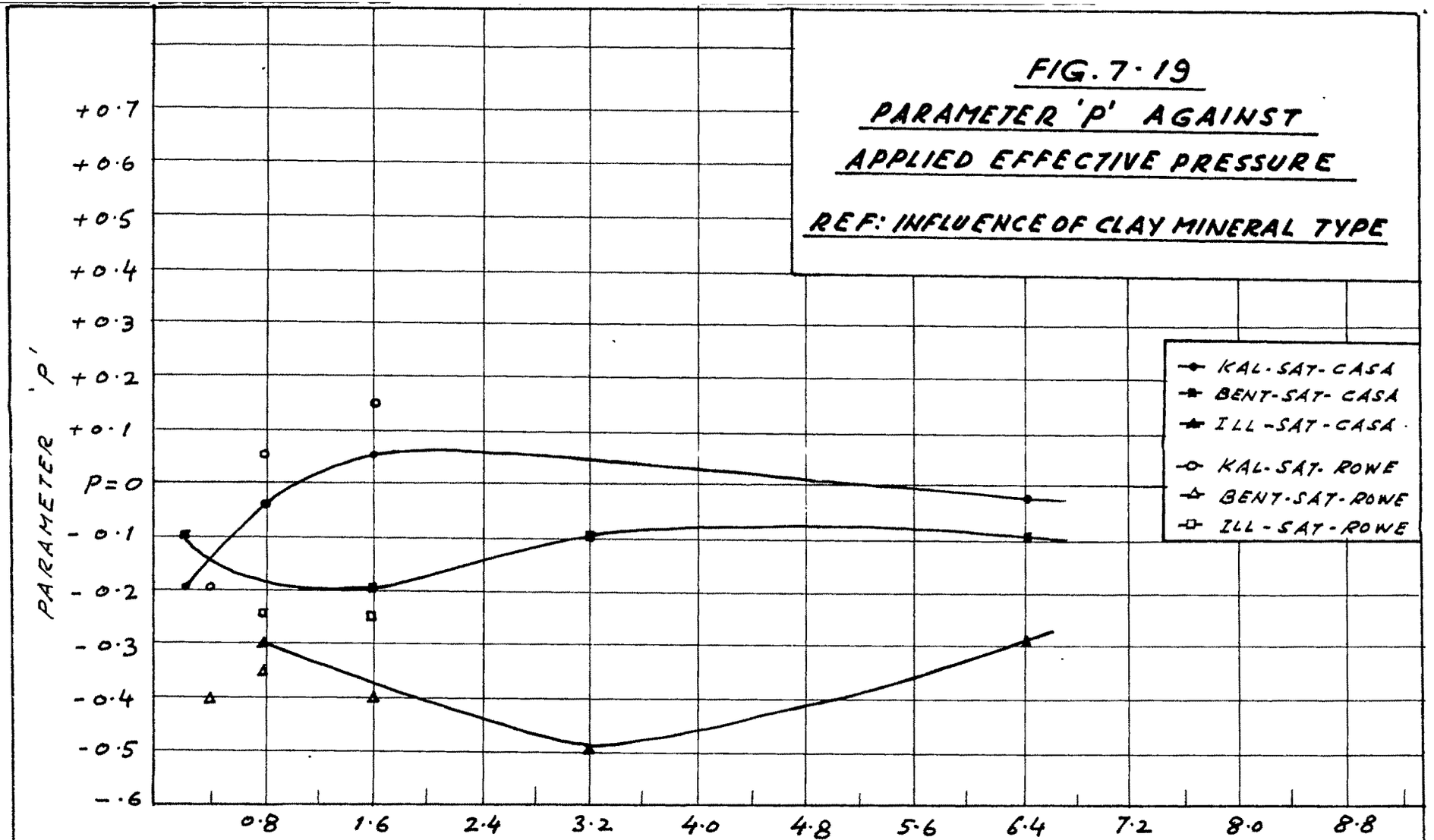

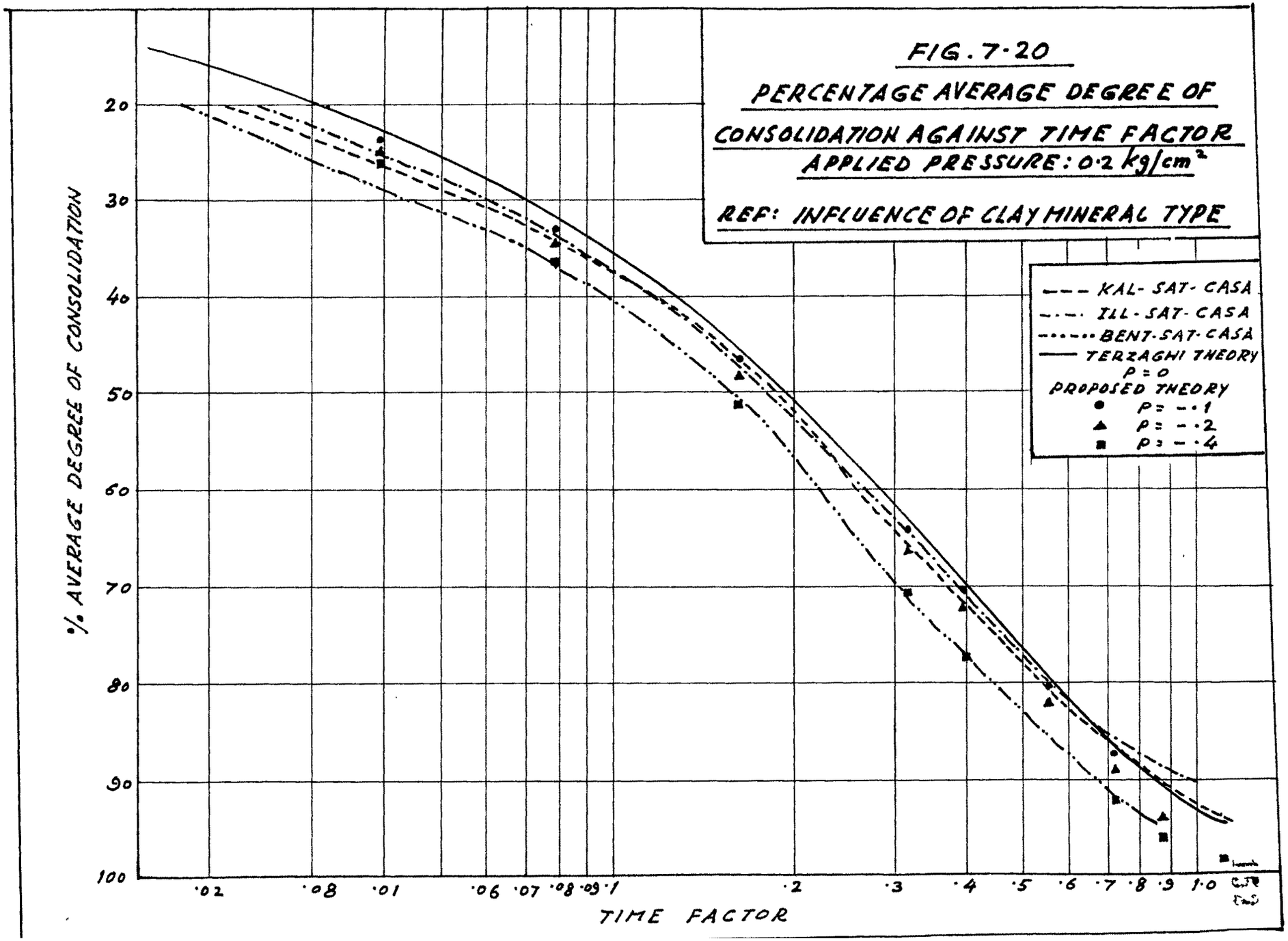
FIG. 7·20
PERCENTAGE AVERAGE DEGREE OF CONSOLIDATION AGAINST TIME FACTOR
APPLIED PRESSURE: 0·2 kg/cm²
REF: INFLUENCE OF CLAY MINERAL TYPE
KAL-SAT-CASA
ILL-SAT-CASA
BENT-SAT-CASA
TERZAGHI THEORY
P = 0
PROPOSED THEORY
P = -·1
P = -·2
P = -·4
% AVERAGE DEGREE OF CONSOLIDATION
20
30
40
50
60
70
80
90
100
·02
·08
·01
·06
·07
·08
·09
·1
·2
·3
·4
·5
·6
·7
·8
·9
1·0
TIME FACTOR

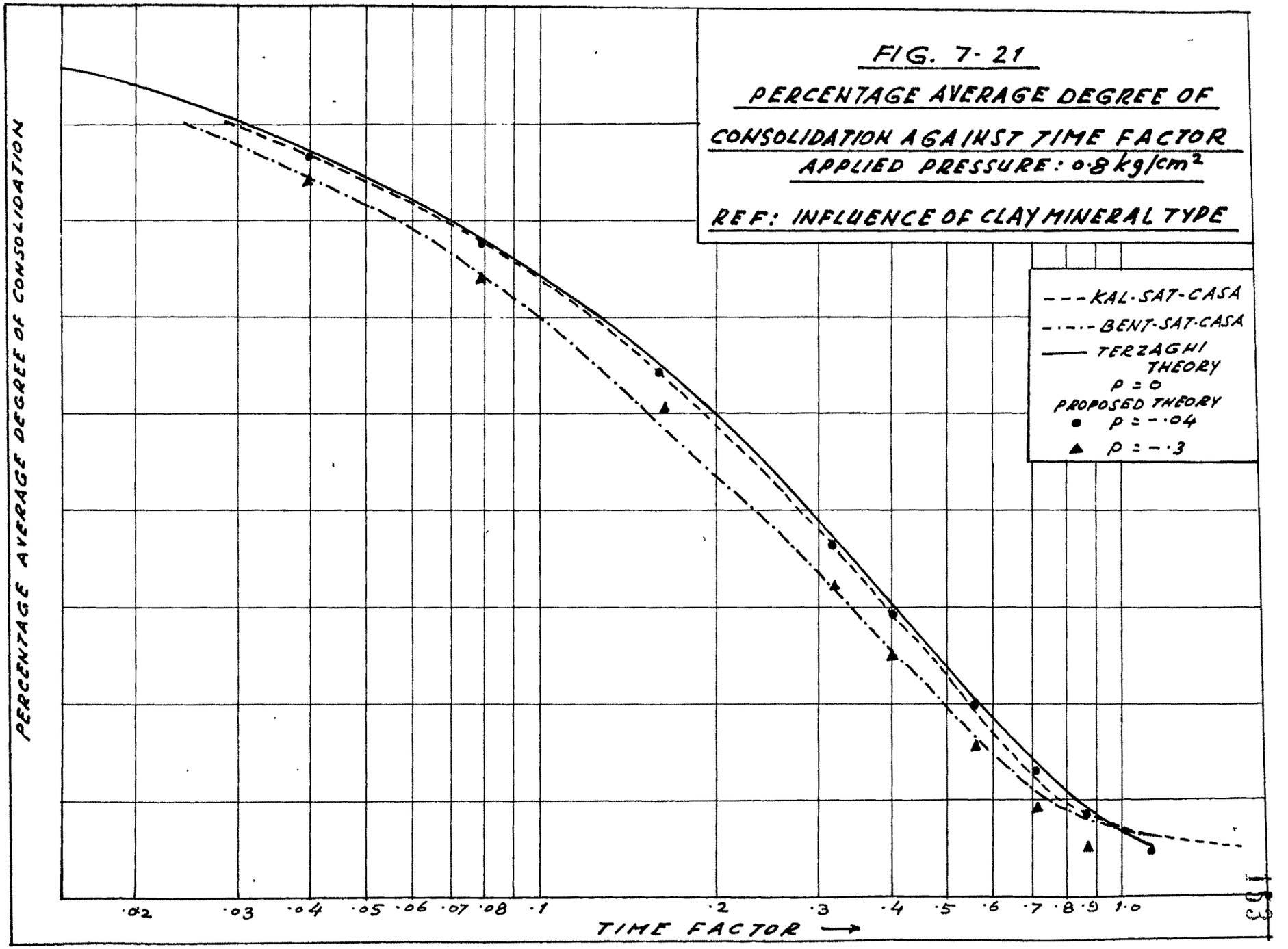
FIG. 7-21
PERCENTAGE AVERAGE DEGREE OF CONSOLIDATION AGAINST TIME FACTOR
APPLIED PRESSURE: 0·8 kg/cm²
REF: INFLUENCE OF CLAY MINERAL TYPE
KAL-SAT-CASA
BENT-SAT-CASA
TERZAGHI THEORY
PROPOSED THEORY
p = 0
p = -·04
p = -·3
PERCENTAGE AVERAGE DEGREE OF CONSOLIDATION
·02 ·03 ·04 ·05 ·06 ·07 ·08 ·1 ·2 ·3 ·4 ·5 ·6 ·7 ·8 ·9 1·0
TIME FACTOR →

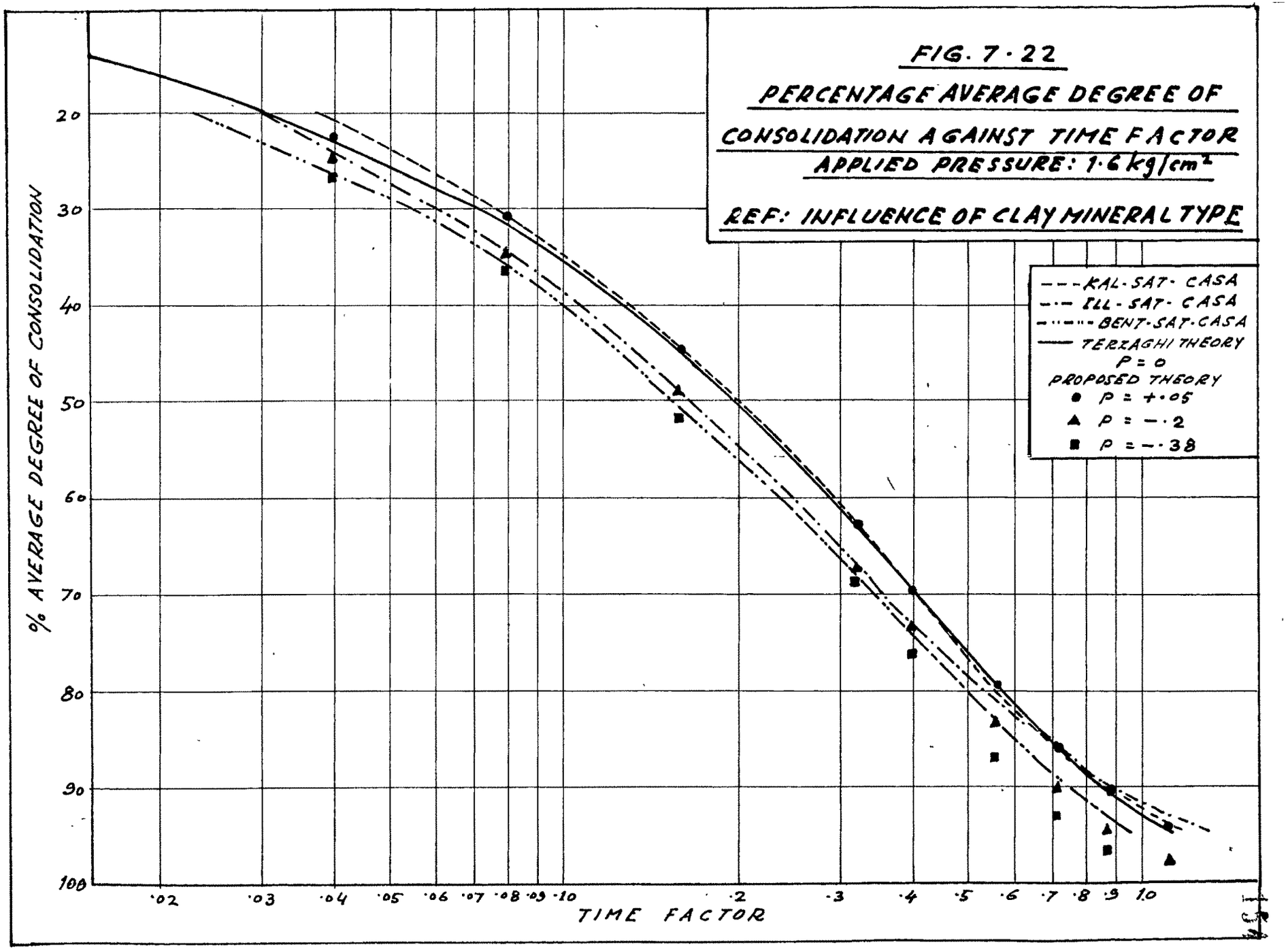
FIG. 7·22
PERCENTAGE AVERAGE DEGREE OF CONSOLIDATION AGAINST TIME FACTOR
APPLIED PRESSURE: 1·6 kg/cm²
REF: INFLUENCE OF CLAY MINERAL TYPE
KAL-SAT-CASA
ILL-SAT-CASA
BENT-SAT-CASA
TERZAGHI THEORY
P = 0
PROPOSED THEORY
P = +·05
P = −·2
P = −·38
% AVERAGE DEGREE OF CONSOLIDATION
20
30
40
50
60
70
80
90
100
·02
·03
·04
·05
·06
·07
·08
·09
·10
·2
·3
·4
·5
·6
·7
·8
·9
1.0
TIME FACTOR

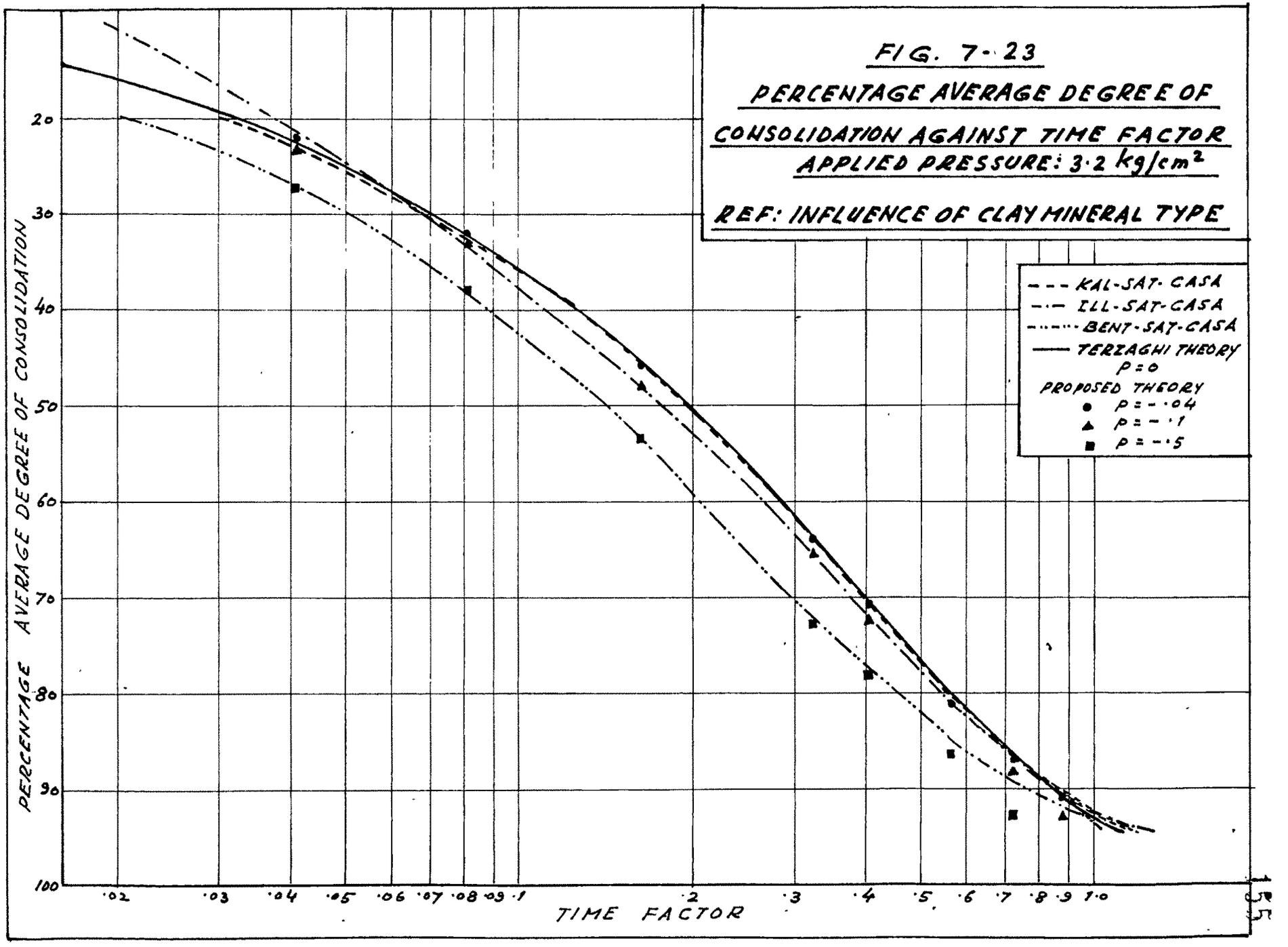
FIG. 7·23
PERCENTAGE AVERAGE DEGREE OF CONSOLIDATION AGAINST TIME FACTOR
APPLIED PRESSURE: 3·2 kg/cm²
REF: INFLUENCE OF CLAY MINERAL TYPE
KAL-SAT-CASA
ILL-SAT-CASA
BENT-SAT-CASA
TERZAGHI THEORY
P=0
PROPOSED THEORY
P=-·04
P=-·1
P=-·5
PERCENTAGE AVERAGE DEGREE OF CONSOLIDATION
20
30
40
50
60
70
80
90
100
·02
·03
·04
·05
·06
·07
·08
·09
·1
·2
·3
·4
·5
·6
·7
·8
·9
1·0
TIME FACTOR

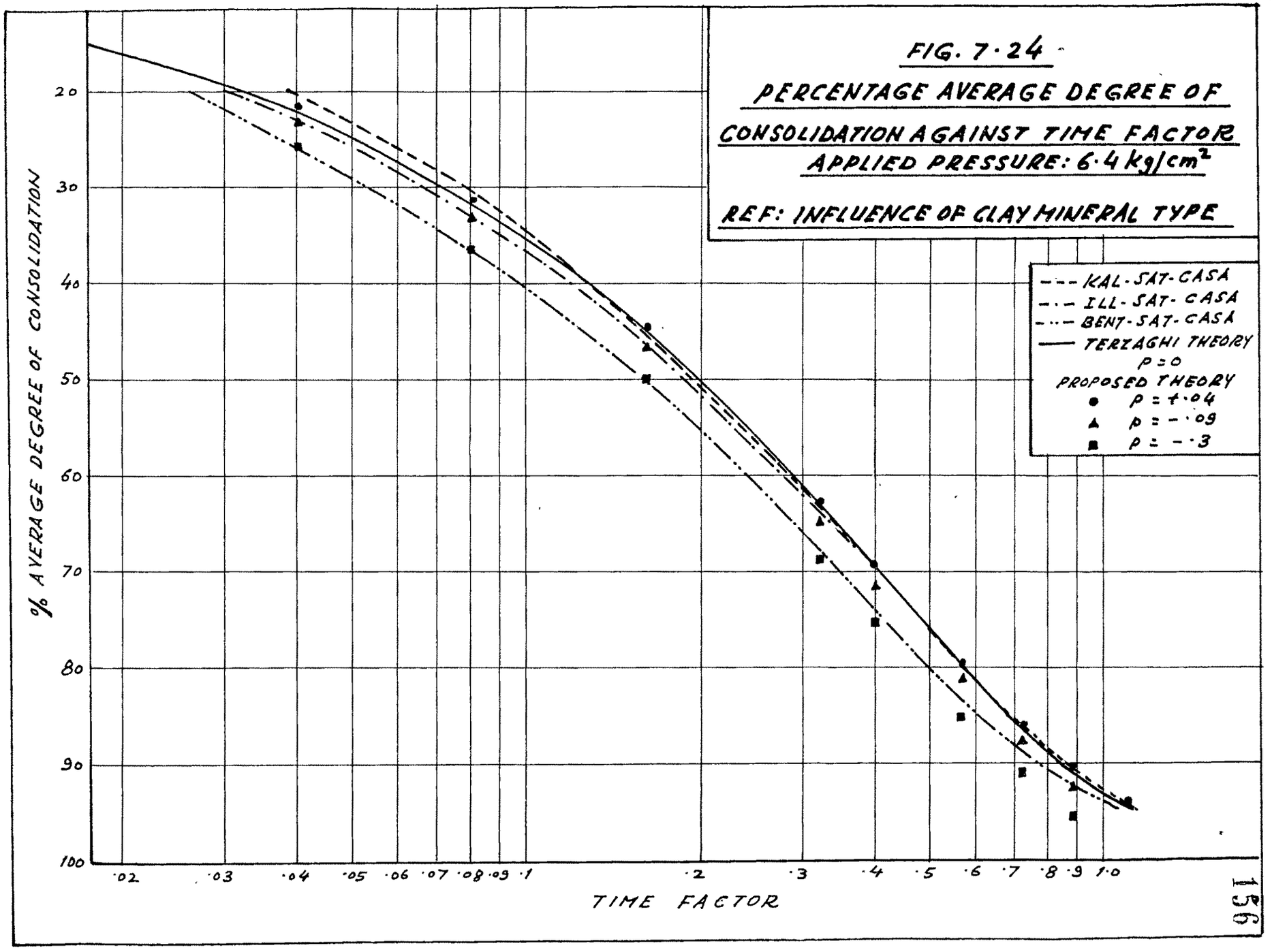
FIG. 7·24
PERCENTAGE AVERAGE DEGREE OF CONSOLIDATION AGAINST TIME FACTOR
APPLIED PRESSURE: 6·4 kg/cm²
REF: INFLUENCE OF CLAY MINERAL TYPE
KAL-SAT-CASA
ILL-SAT-CASA
BENT-SAT-CASA
TERZAGHI THEORY
p=0
PROPOSED THEORY
p = +·04
p = −·09
p = −·3
% AVERAGE DEGREE OF CONSOLIDATION
20
30
40
50
60
70
80
90
100
·02
·03
·04
·05
·06
·07
·08
·09
·1
·2
·3
·4
·5
·6
·7
·8
·9
1·0
TIME FACTOR

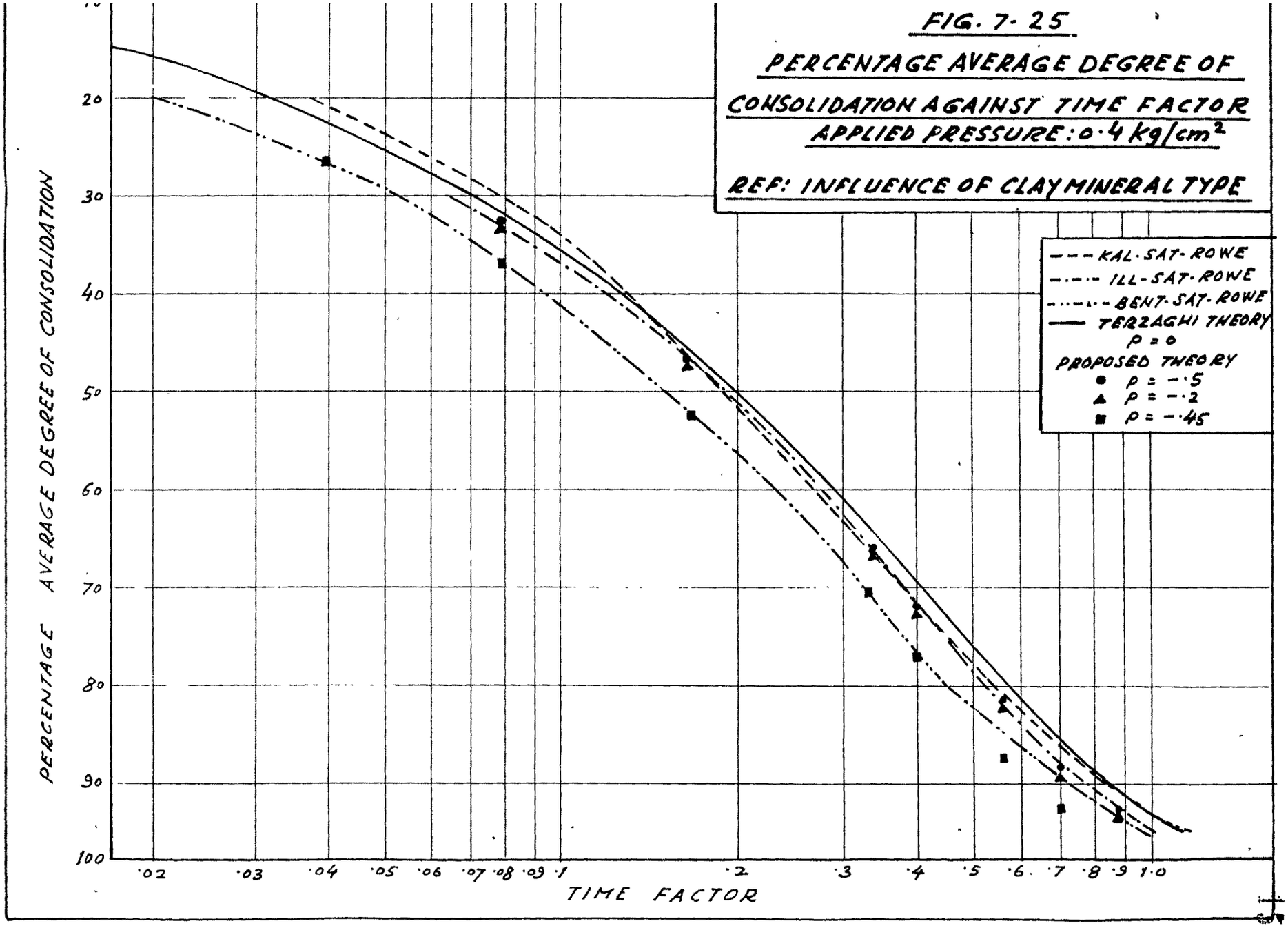
FIG. 7-25
PERCENTAGE AVERAGE DEGREE OF CONSOLIDATION AGAINST TIME FACTOR
APPLIED PRESSURE: 0·4 kg/cm²
REF: INFLUENCE OF CLAY MINERAL TYPE
KAL-SAT-ROWE
ILL-SAT-ROWE
BENT-SAT-ROWE
TERZAGHI THEORY
p = 0
PROPOSED THEORY
p = -·5
p = -·2
p = -·45
PERCENTAGE AVERAGE DEGREE OF CONSOLIDATION
20
30
40
50
60
70
80
90
100
·02
·03
·04
·05
·06
·07
·08
·09
·1
·2
·3
·4
·5
·6
·7
·8
·9
1·0
TIME FACTOR

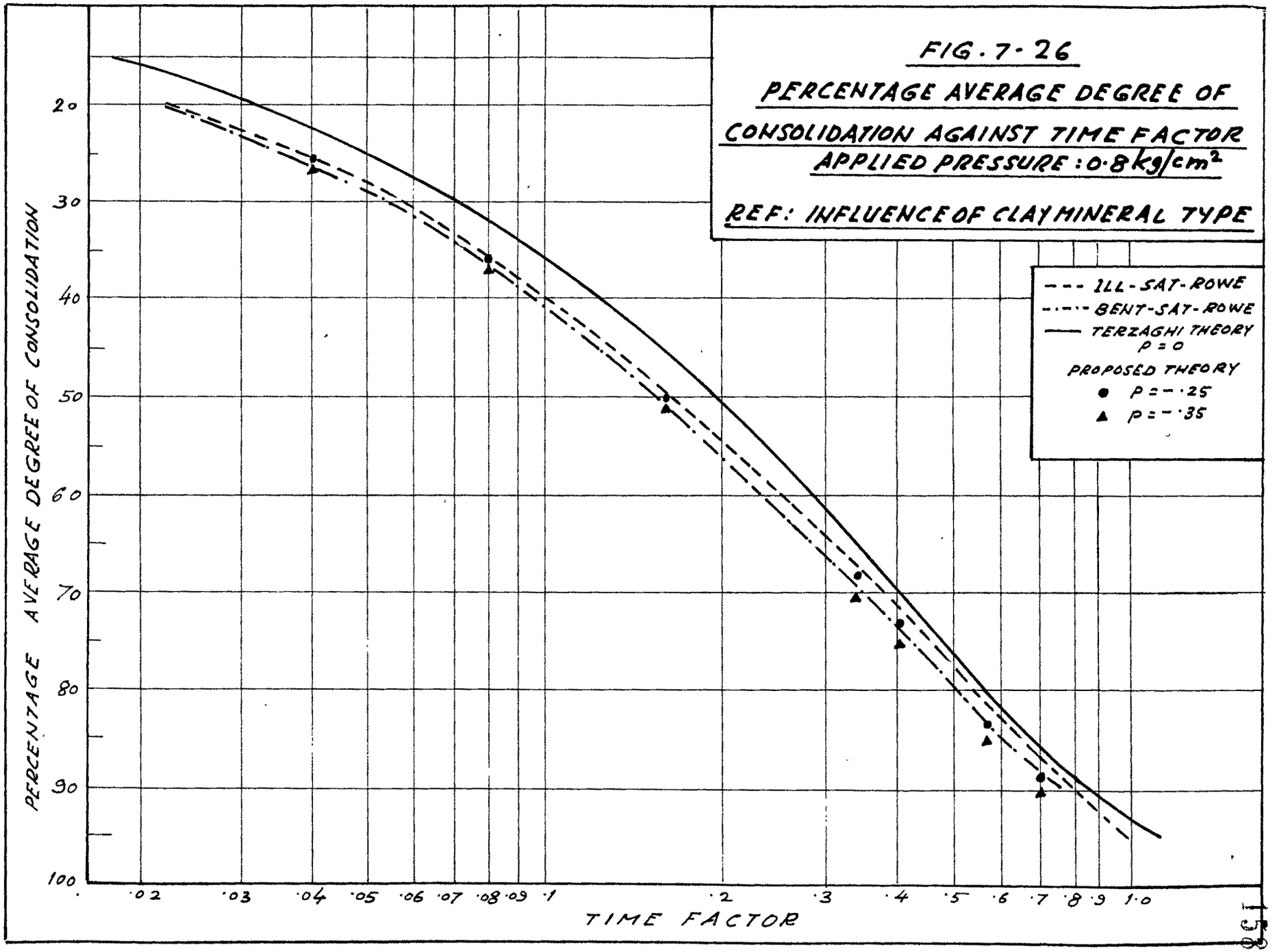
FIG. 7·26
PERCENTAGE AVERAGE DEGREE OF CONSOLIDATION AGAINST TIME FACTOR
APPLIED PRESSURE : 0·8 kg/cm²
REF: INFLUENCE OF CLAY MINERAL TYPE
--- ILL-SAT-ROWE
-·-·- BENT-SAT-ROWE
—— TERZAGHI THEORY p = 0
PROPOSED THEORY
● p = -·25
▲ p = -·35
PERCENTAGE AVERAGE DEGREE OF CONSOLIDATION
20
30
40
50
60
70
80
90
100
·02 ·03 ·04 ·05 ·06 ·07 ·08 ·09 ·1 ·2 ·3 ·4 ·5 ·6 ·7 ·8 ·9 1·0
TIME FACTOR

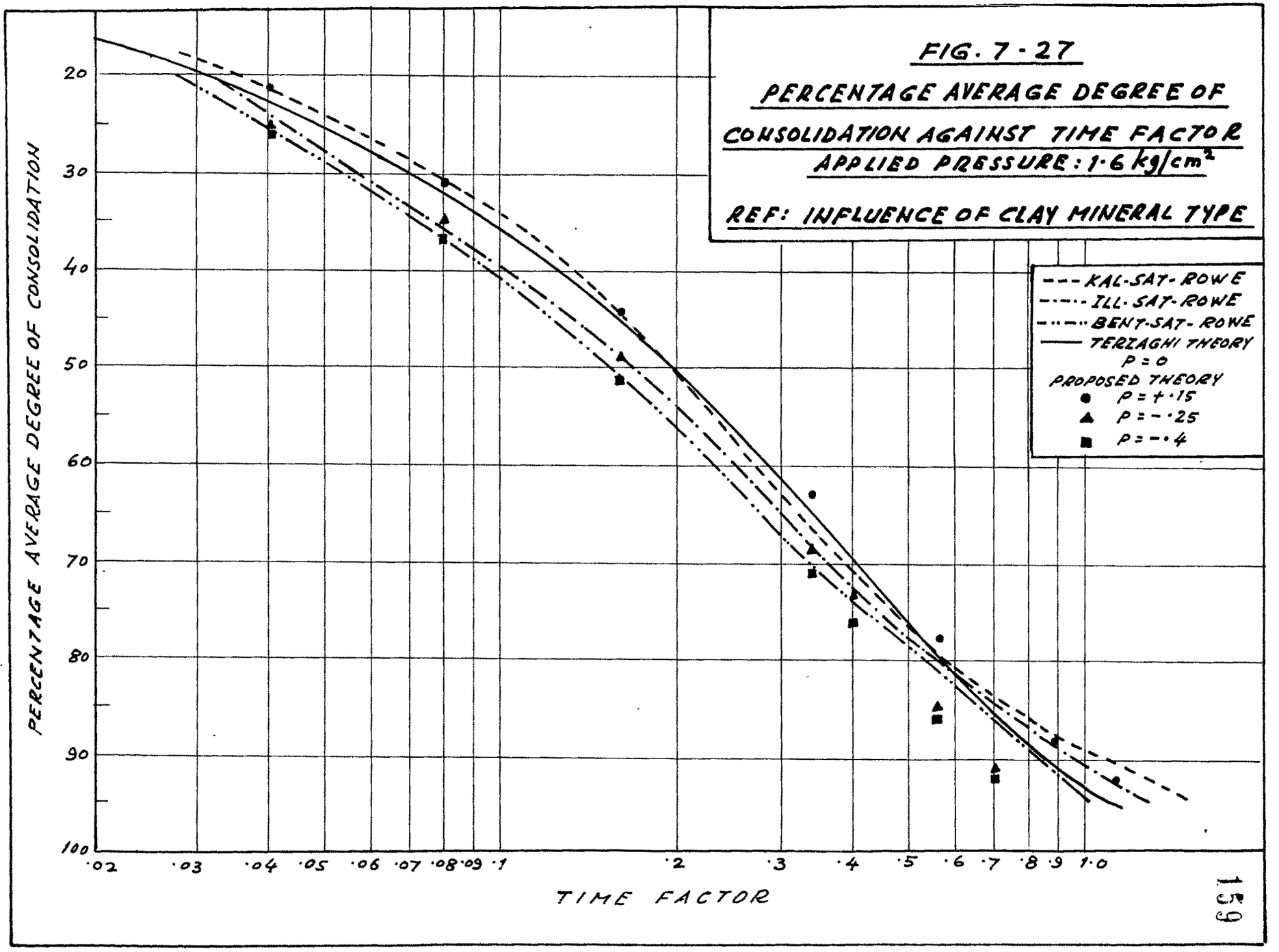
FIG. 7-27
PERCENTAGE AVERAGE DEGREE OF CONSOLIDATION AGAINST TIME FACTOR
APPLIED PRESSURE : 1·6 kg/cm²
REF: INFLUENCE OF CLAY MINERAL TYPE
KAL-SAT-ROWE
ILL-SAT-ROWE
BENT-SAT-ROWE
TERZAGHI THEORY
P = 0
PROPOSED THEORY
P = +·15
P = −·25
P = −·4
PERCENTAGE AVERAGE DEGREE OF CONSOLIDATION
20
30
40
50
60
70
80
90
100
·02
·03
·04
·05
·06
·07
·08
·09
·1
·2
·3
·4
·5
·6
·7
·8
·9
1·0
TIME FACTOR

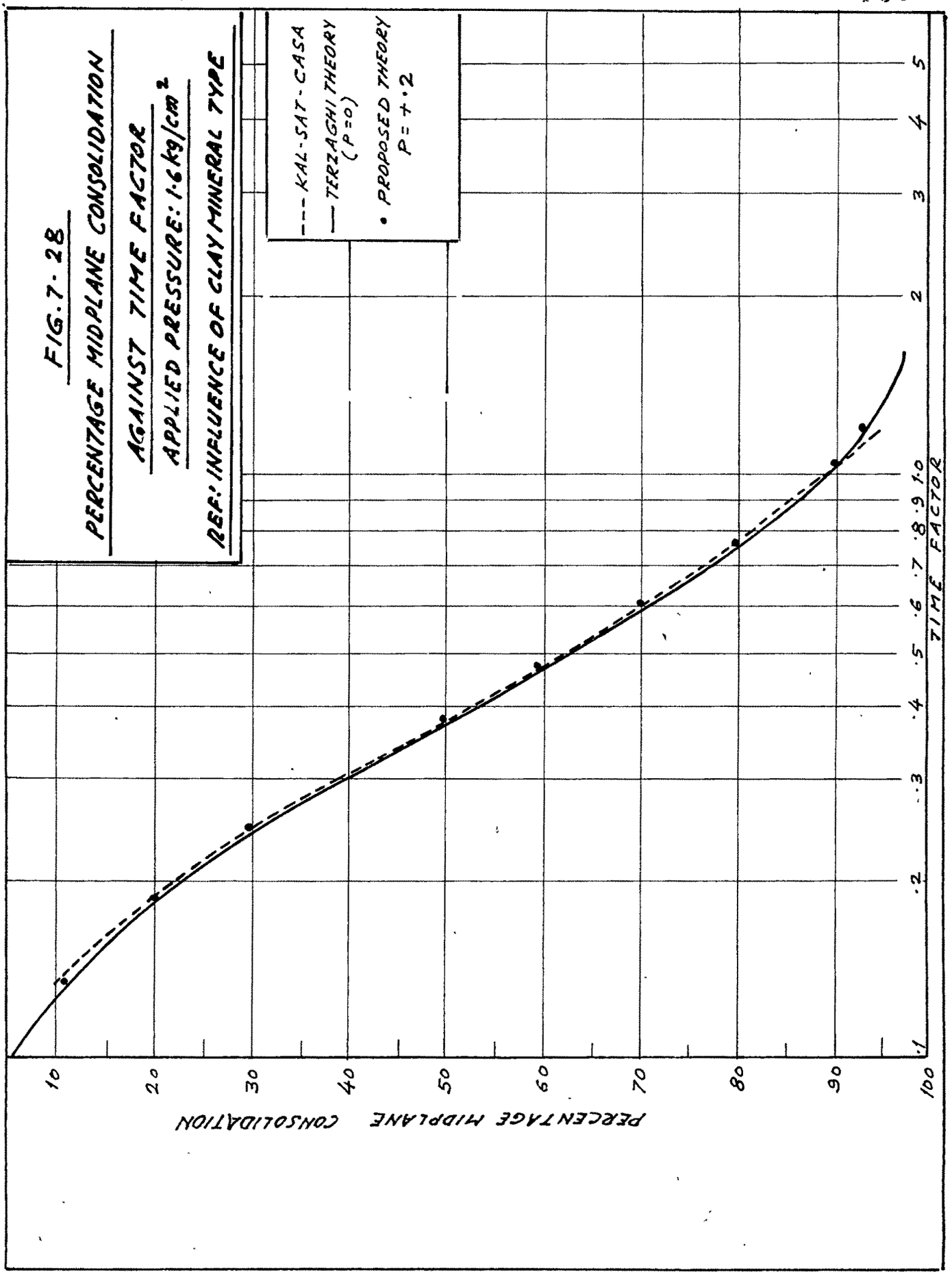
FIG. 7·28
PERCENTAGE MIDPLANE CONSOLIDATION AGAINST TIME FACTOR
APPLIED PRESSURE: 1·6 kg/cm²
REF: INFLUENCE OF CLAY MINERAL TYPE
--- KAL-SAT-CASA
— TERZAGHI THEORY (P=0)
• PROPOSED THEORY P=+·2
PERCENTAGE MIDPLANE CONSOLIDATION
10
20
30
40
50
60
70
80
90
100
TIME FACTOR
·1
·2
·3
·4
·5
·6
·7
·8
·9
1·0
2
3
4
5

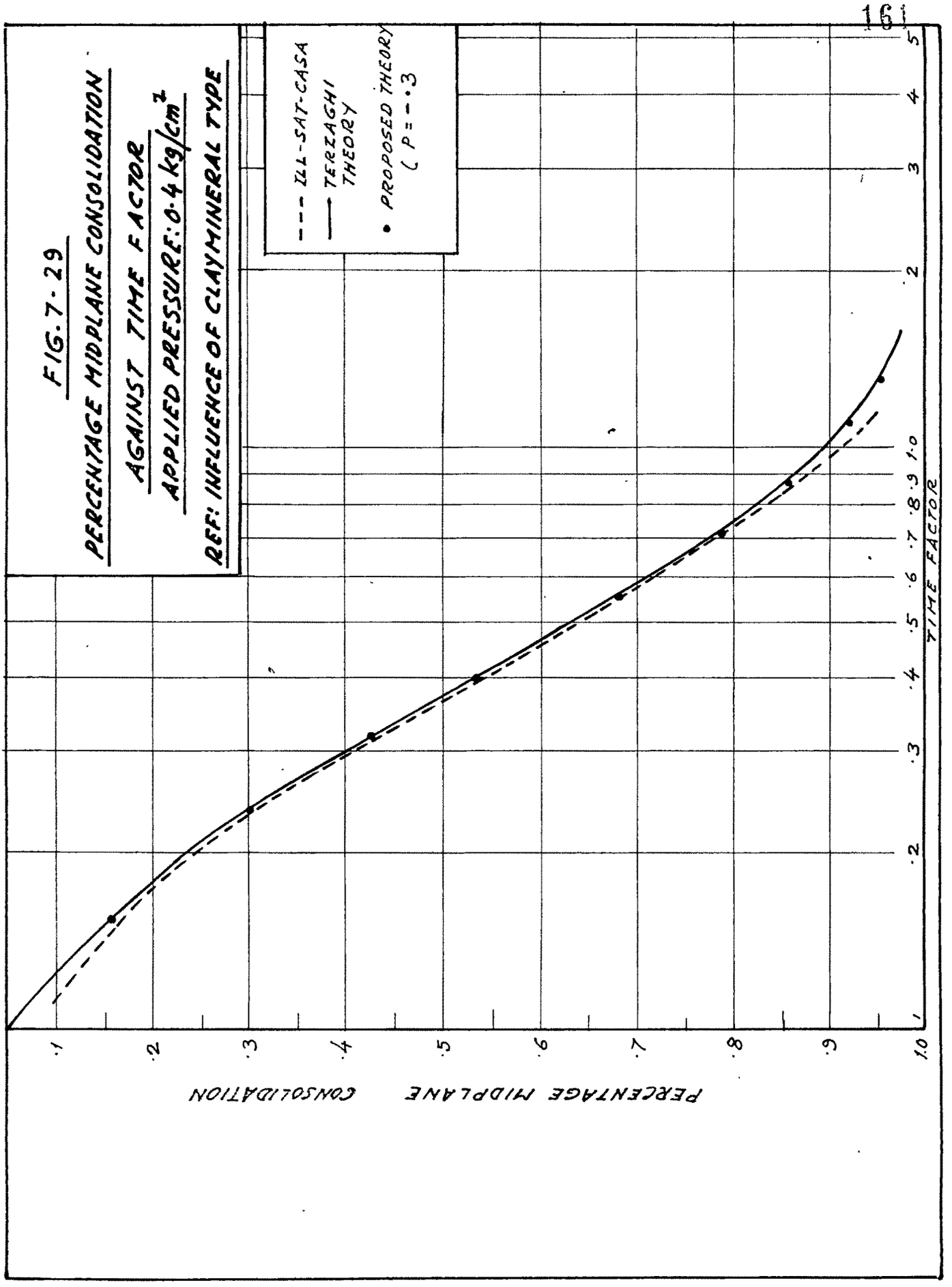
FIG. 7-29
PERCENTAGE MIDPLANE CONSOLIDATION AGAINST TIME FACTOR
APPLIED PRESSURE: 0·4 kg/cm²
REF: INFLUENCE OF CLAYMINERAL TYPE
--- ILL-SAT-CASA
—— TERZAGHI THEORY
• PROPOSED THEORY (P = -·3
PERCENTAGE MIDPLANE CONSOLIDATION
TIME FACTOR
·1 ·2 ·3 ·4 ·5 ·6 ·7 ·8 ·9 1·0
1 ·2 ·3 ·4 ·5 ·6 ·7 ·8 ·9 1·0 2 3 4 5

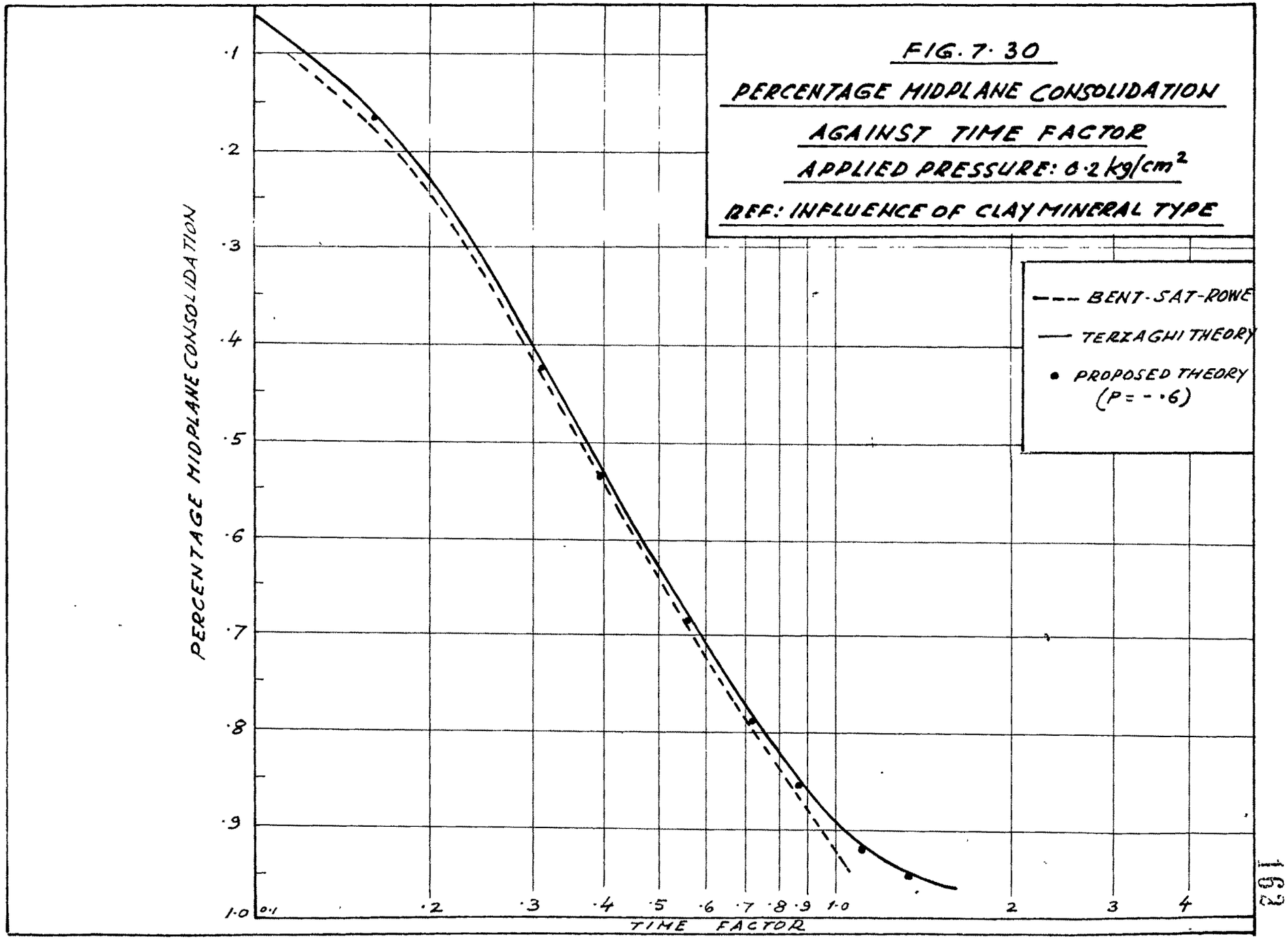
FIG. 7·30
PERCENTAGE MIDPLANE CONSOLIDATION
AGAINST TIME FACTOR
APPLIED PRESSURE: 0·2 kg/cm²
REF: INFLUENCE OF CLAY MINERAL TYPE
--- BENT-SAT-ROWE
— TERZAGHI THEORY
• PROPOSED THEORY (P = - ·6)
PERCENTAGE MIDPLANE CONSOLIDATION
·1
·2
·3
·4
·5
·6
·7
·8
·9
1·0
0·1
·2
·3
·4
·5
·6
·7
·8
·9
1·0
2
3
4
TIME FACTOR

and it possesses higher extent of potential surface which has perfectly oriented water of rigid nature. The observed slow initial rate of consolidation in montmorillonite can be attributed to the slowness with which the rigid oriented water breaks up under the applied load. In case of non-expanding group of minerals viz. kaolinite and illite the adsorbed water is comparatively less perfectly oriented. As a consequence the water would be more easily removed under the application of load.

The explanation for the consolidation behaviour from the point of view of intermolecular forces prevailing during the interaction in a clay water system can be derived from the Freundlich concept (1935). The swelling nature of the montmotillonite clay suggests that the net repulsive potential between two particles is predominant before the application of load. In the initial stages, the applied load potential is not sufficient enough to overcome those repulsive forces showing the sustanance of applied load but after some time the load potential predominates the decreasing repulsive forces. As a result, there occurs decrease in interparticle spacing causing expulsion of water after this initial hold up. On the other hand kaolinite has comparatively lesser net repulsive forces which are easily overcome by the applied load potential thereby reducing the interparticle spacing almost instantaneously.

Illite also behaves similar to kaolinite due to the presence of natural potassium which prevents the development of higher repulsive forces as in case of montmorillonite.

The observation of higher initial void ratio, higher compression index and nonlinear void ratio and effective pressure relationship with a initial convex curvature in montmorillonite can also be attributed to dominating repulsive forces. In kaolinite and illite these characteristics are not reflected because of lower repulsive forces except that under lighter loads at initial stages a slight resistance to the repulsive forces can be seen.

The peculiar characteristics of montmorillonitic clays over kaolinite and illite clays are also clearly reflected in the non-dimensional plot of degree of consolidation against the time factor. The curve of Bentonite deviates most from the Terzaghi curve which is essentially termed as ' Primary consolidation theory' derived on the consolidation of hydro-dynamic time lag only ignoring the time lag due to plastic resistance known as 'secondary compression.' Experimental results of Bentonite reveal notable secondary compression. This particular consolidation behaviour of Bentonite can be attributed to the rigid plastic nature of the oriented water which sustains the applied load in the beginning but with time the load potential predominates these forces permitting the

expulsion of free water although the plastic resistance is continuous throughout the process of consolidation. The variation in C_v value suggests that it may be time dependent co-efficient for expanding type clay mineral soil and similarly parameter P can also be a function of time.

7.3.2. Fabric Structure

Refer Figures 7.31 to 7. 62 which are derived from the parent plots of Figures H.77 to H.157 reported in Appendix H of Volume II.

Analysis :

(i) Co-efficient of consolidation against percentage degree of consolidation. (Refer Figures 7.31 to 7.38).

In both flocculated kaolinite and Bentonite C_v value shows a slow decrease during the consolidation under lighter loading, while at higher loading it tends to indicate constant value of C_v . In case of dispersed kaolinite and Bentonite initially the former shows decrease in C_v value under 0.2 kg/cm^2 but at the same loading the latter indicates a slight increase in the C_v value. As the consolidation proceeds the value tends to approach a constant value. At higher loads also the C_v value seems to remain more or less same.

(ii) Co-efficient of consolidation against applied effective pressure. (Figures 7.39 and 7.40).

Kaolinite and Bentonite do not exhibit similar characteris tics but the behaviour of flocculated and dispersed structure

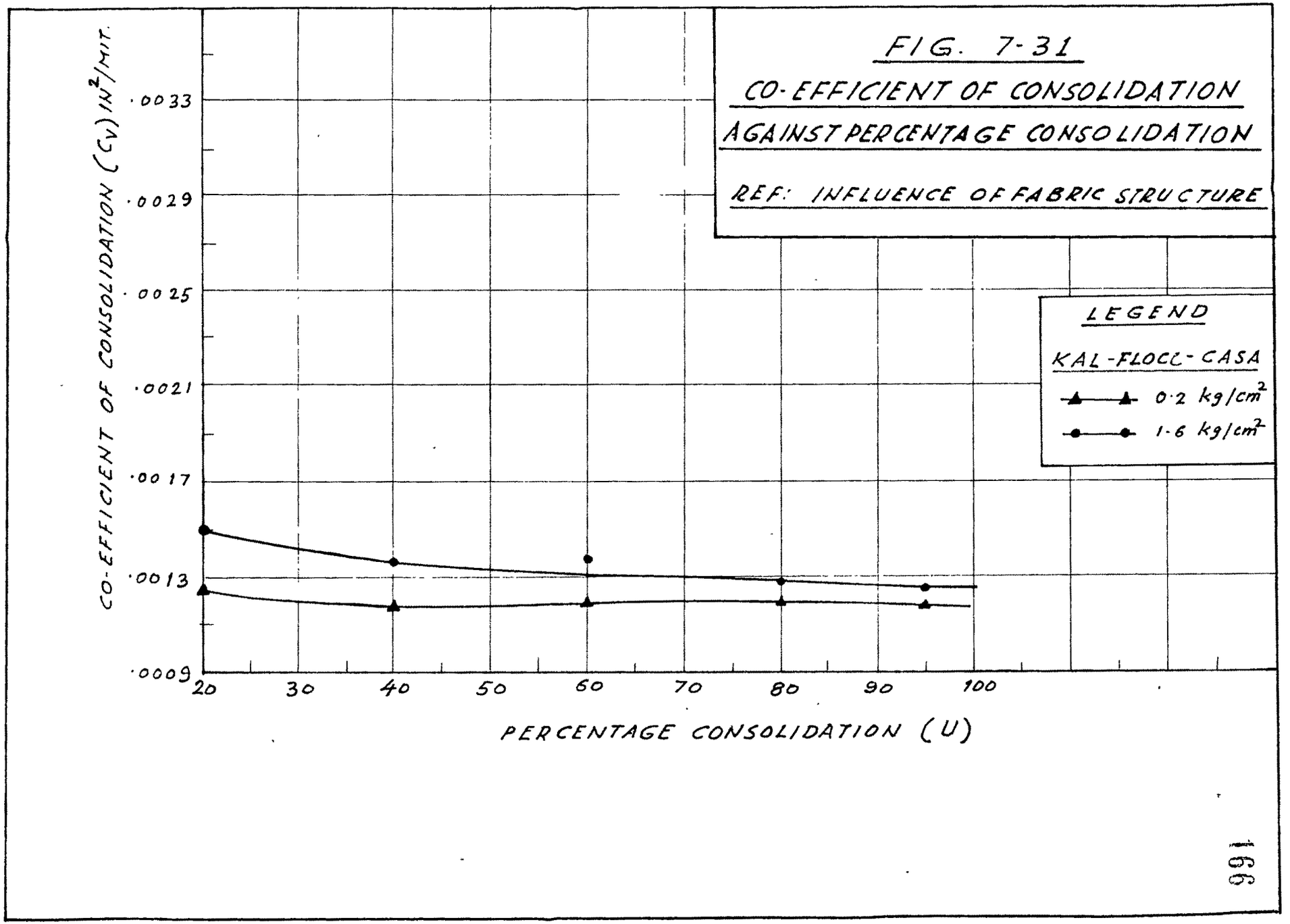
FIG. 7-31
CO-EFFICIENT OF CONSOLIDATION
AGAINST PERCENTAGE CONSOLIDATION
REF: INFLUENCE OF FABRIC STRUCTURE
LEGEND
KAL-FLOCC-CASA
0·2 kg/cm²
1·6 kg/cm²
CO-EFFICIENT OF CONSOLIDATION (Cv) IN²/MIT.
·0033
·0029
·0025
·0021
·0017
·0013
·0009
20
30
40
50
60
70
80
90
100
PERCENTAGE CONSOLIDATION (U)

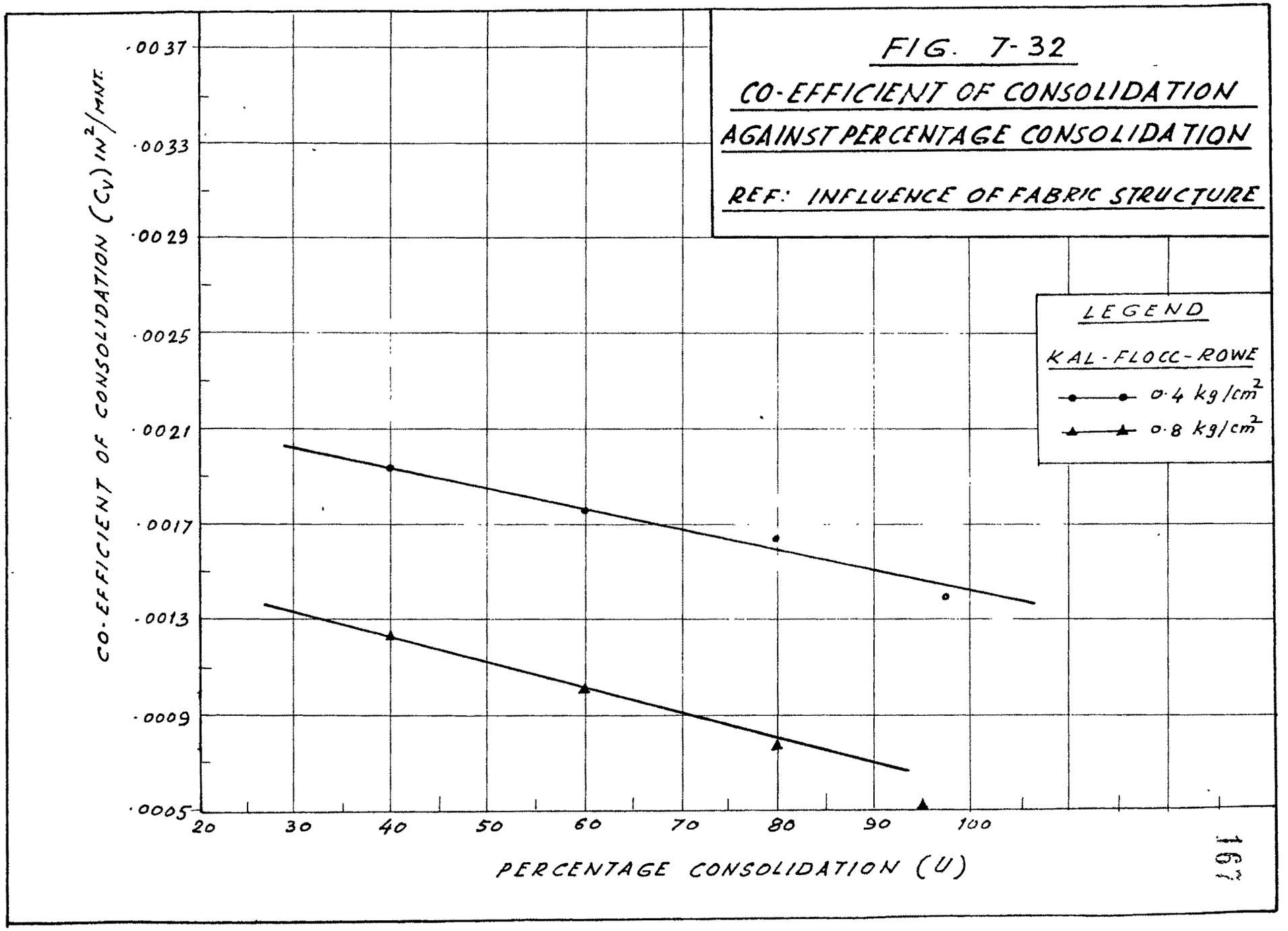
FIG. 7-32
CO-EFFICIENT OF CONSOLIDATION
AGAINST PERCENTAGE CONSOLIDATION
REF: INFLUENCE OF FABRIC STRUCTURE
LEGEND
KAL-FLOCC-ROWE
0·4 kg/cm²
0·8 kg/cm²
CO-EFFICIENT OF CONSOLIDATION (Cv) IN²/MNT.
·0037
·0033
·0029
·0025
·0021
·0017
·0013
·0009
·0005
20
30
40
50
60
70
80
90
100
PERCENTAGE CONSOLIDATION (U)

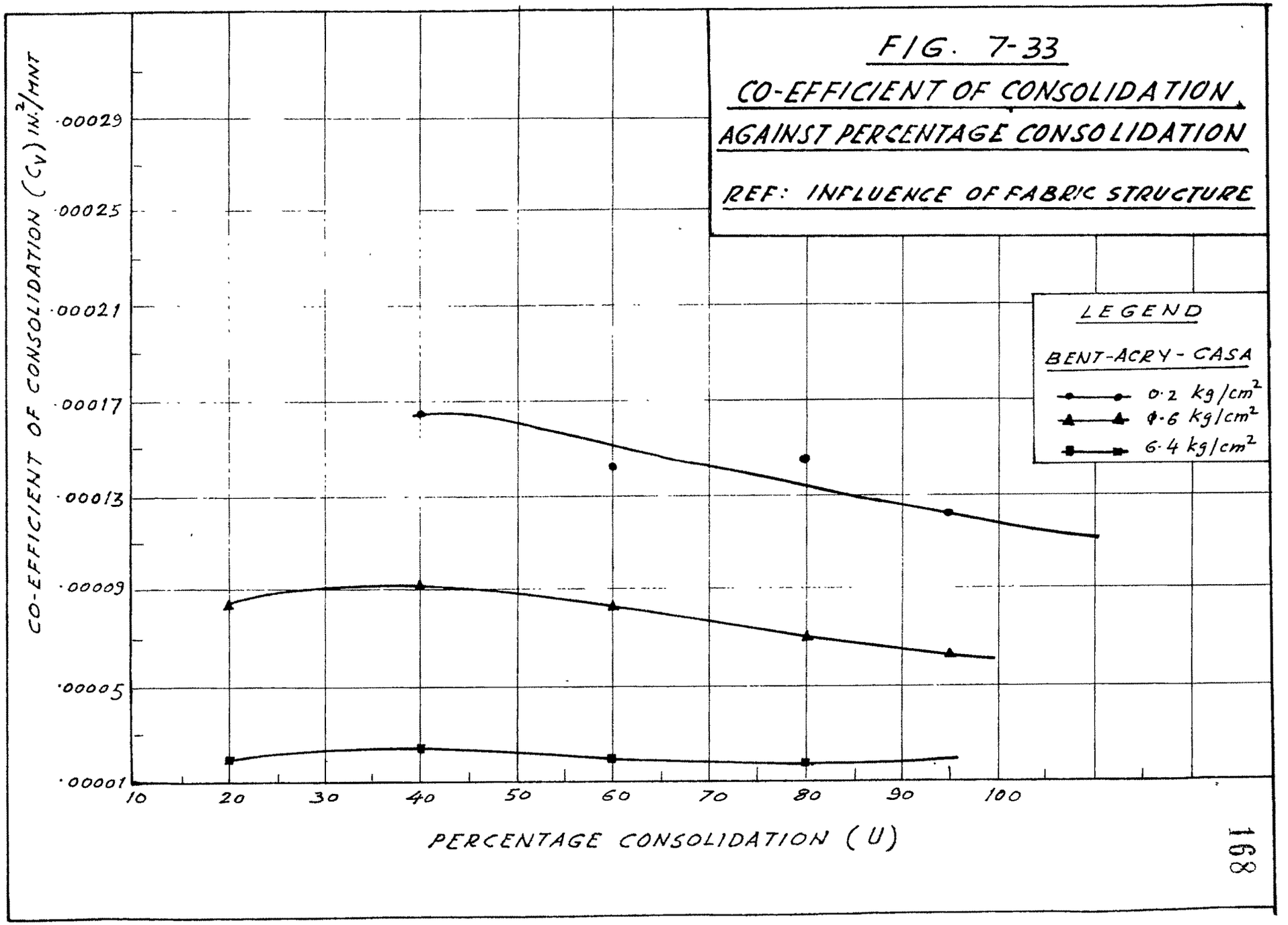
FIG. 7-33
CO-EFFICIENT OF CONSOLIDATION AGAINST PERCENTAGE CONSOLIDATION
REF: INFLUENCE OF FABRIC STRUCTURE
LEGEND
BENT-ACRY - CASA
0·2 kg/cm²
0·6 kg/cm²
6·4 kg/cm²
CO-EFFICIENT OF CONSOLIDATION (Cv) IN.²/MNT
·00029
·00025
·00021
·00017
·00013
·00009
·00005
·00001
10
20
30
40
50
60
70
80
90
100
PERCENTAGE CONSOLIDATION (U)

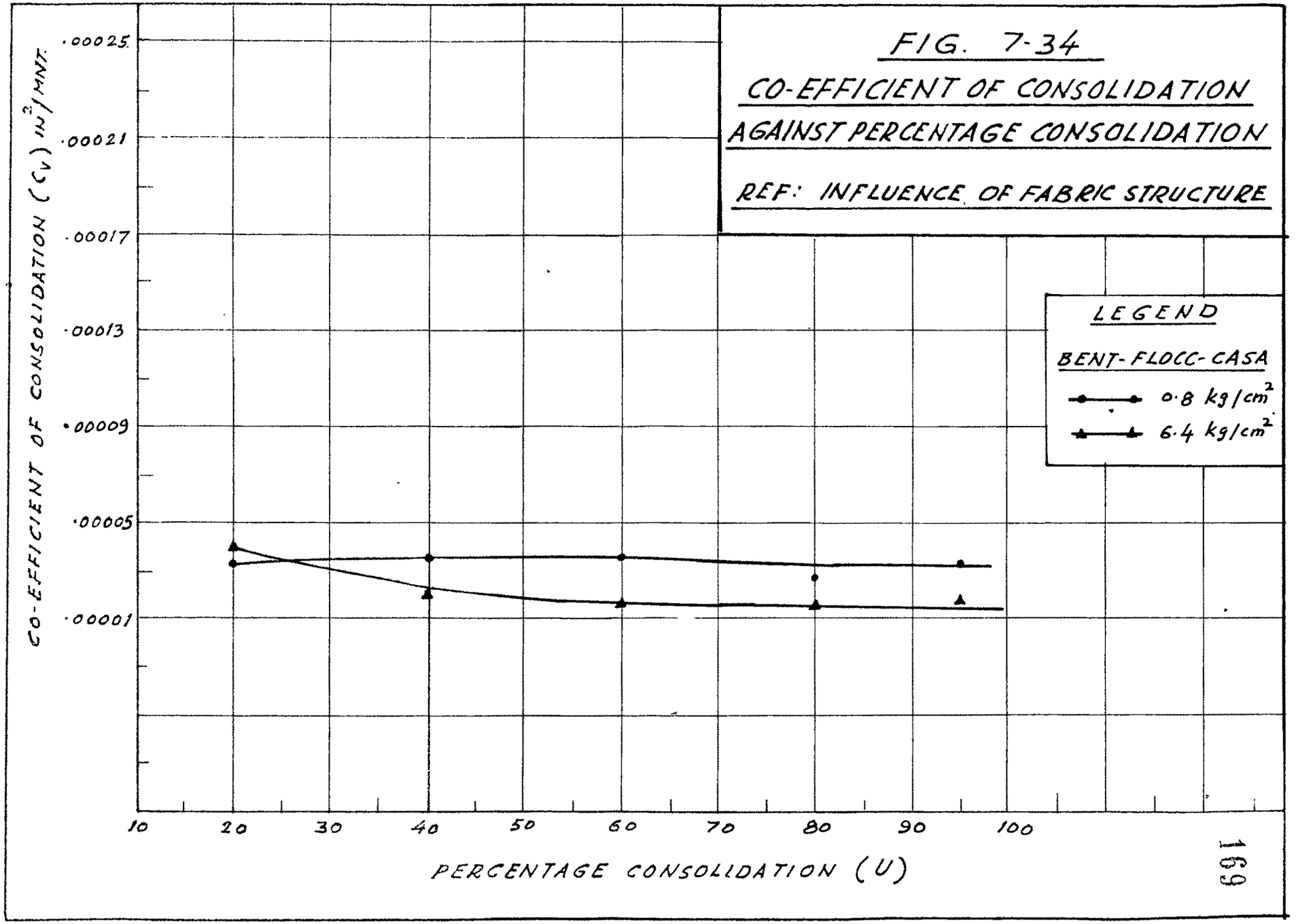
FIG. 7-34
CO-EFFICIENT OF CONSOLIDATION
AGAINST PERCENTAGE CONSOLIDATION
REF: INFLUENCE OF FABRIC STRUCTURE
LEGEND
BENT-FLOCC-CASA
0·8 kg/cm²
6·4 kg/cm²
CO-EFFICIENT OF CONSOLIDATION (Cv) in²/MNT.
·00025
·00021
·00017
·00013
·00009
·00005
·00001
10
20
30
40
50
60
70
80
90
100
PERCENTAGE CONSOLIDATION (U)

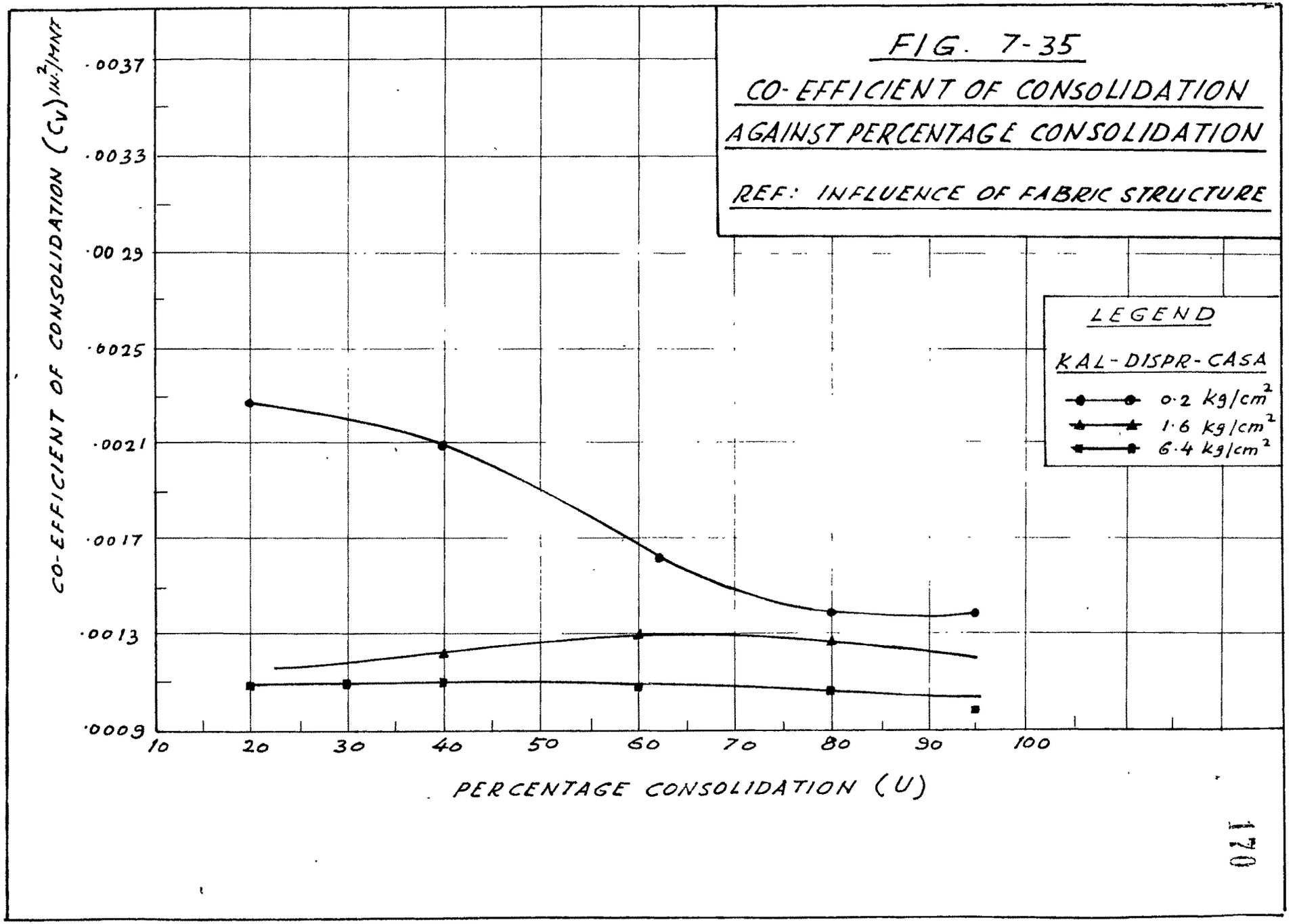
FIG. 7-35
CO-EFFICIENT OF CONSOLIDATION
AGAINST PERCENTAGE CONSOLIDATION
REF: INFLUENCE OF FABRIC STRUCTURE
LEGEND
KAL-DISPR-CASA
0·2 kg/cm²
1·6 kg/cm²
6·4 kg/cm²
CO-EFFICIENT OF CONSOLIDATION (Cv) in²/MNT
·0037
·0033
·0029
·0025
·0021
·0017
·0013
·0009
10
20
30
40
50
60
70
80
90
100
PERCENTAGE CONSOLIDATION (U)

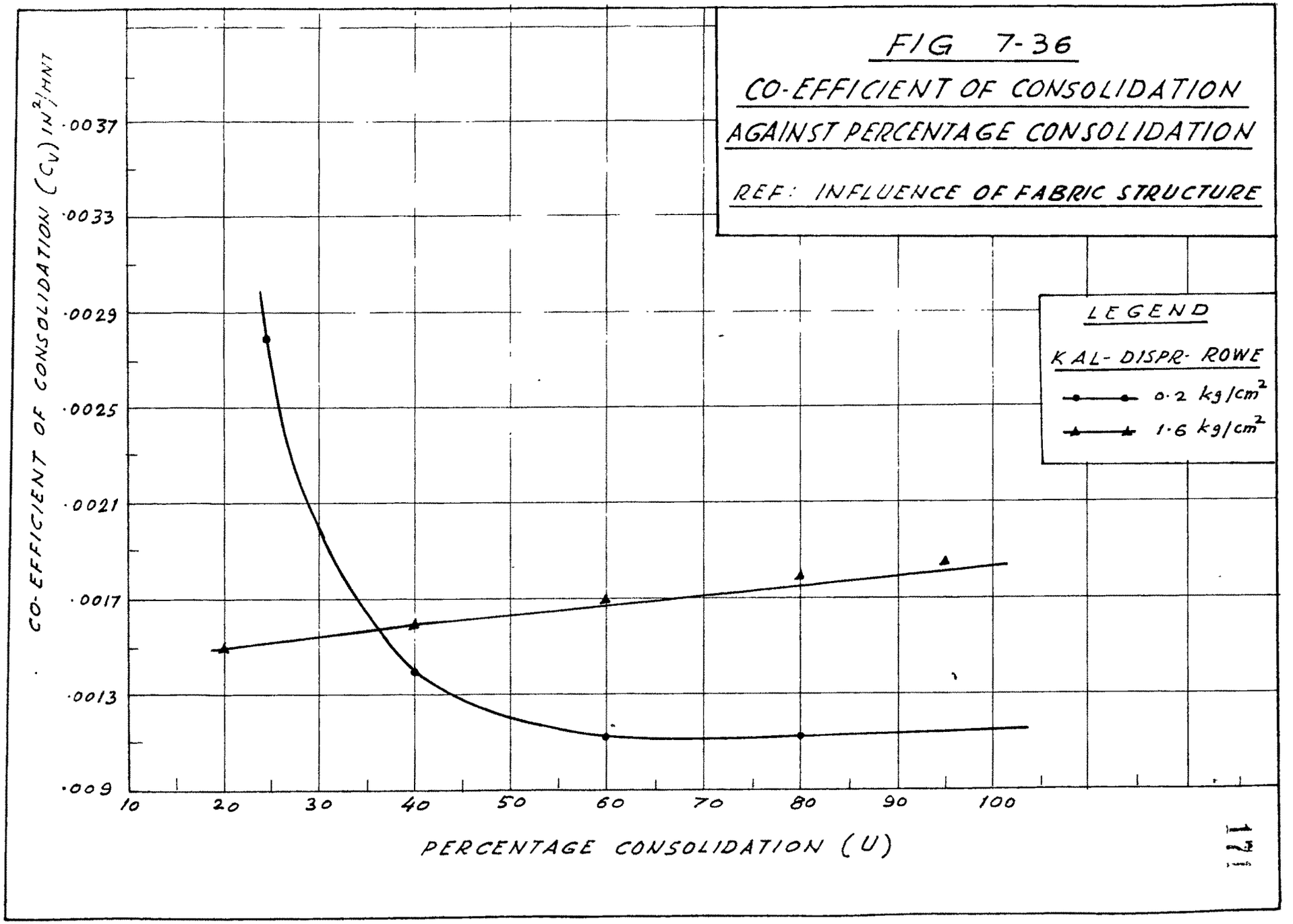
FIG 7-36
CO-EFFICIENT OF CONSOLIDATION
AGAINST PERCENTAGE CONSOLIDATION
REF: INFLUENCE OF FABRIC STRUCTURE
LEGEND
KAL-DISPR-ROWE
0·2 kg/cm²
1·6 kg/cm²
CO-EFFICIENT OF CONSOLIDATION (Cv) IN²/MNT
·0037
·0033
·0029
·0025
·0021
·0017
·0013
·009
10
20
30
40
50
60
70
80
90
100
PERCENTAGE CONSOLIDATION (U)

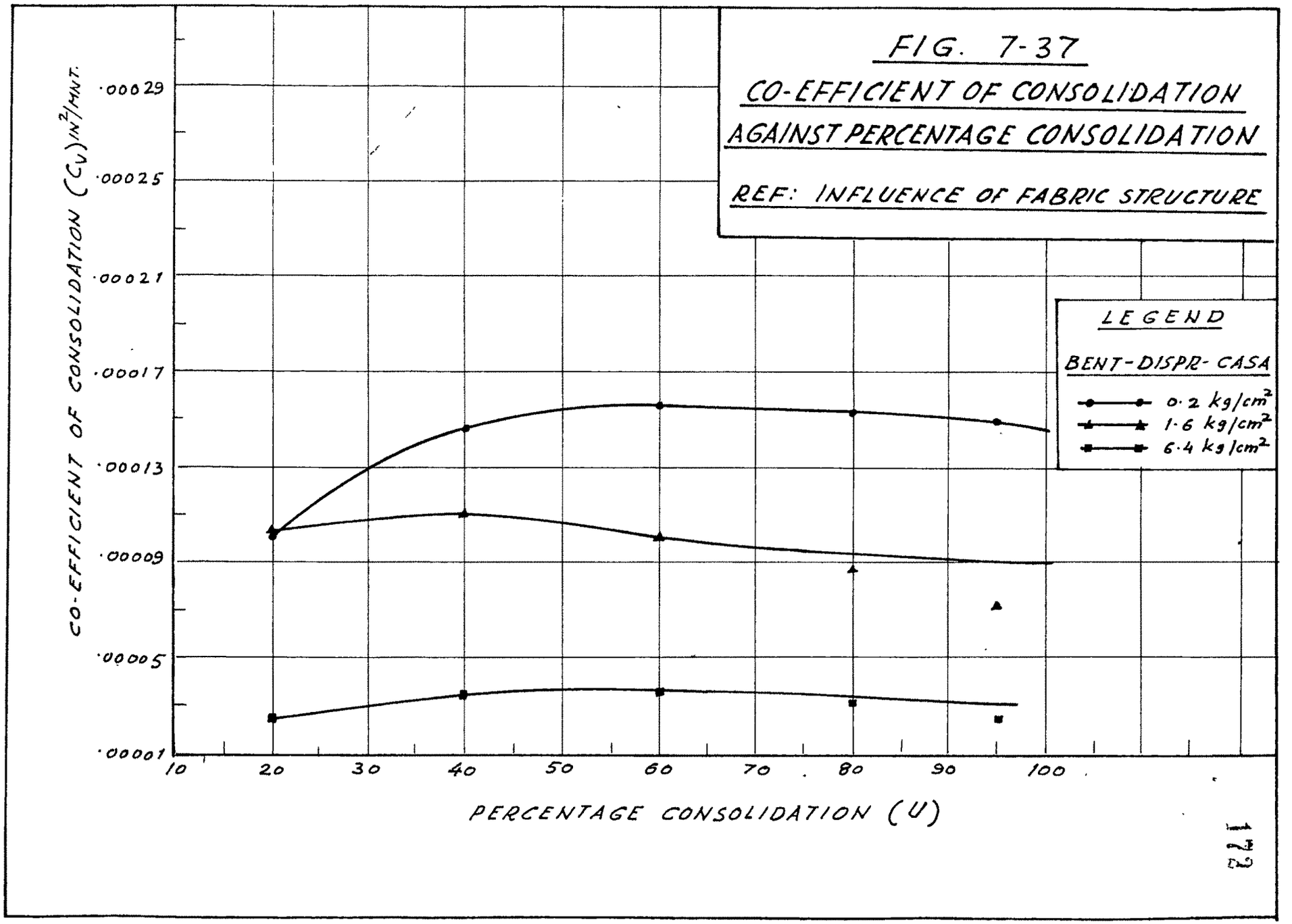
FIG. 7-37
CO-EFFICIENT OF CONSOLIDATION AGAINST PERCENTAGE CONSOLIDATION
REF: INFLUENCE OF FABRIC STRUCTURE
LEGEND
BENT-DISPR-CASA
0·2 kg/cm²
1·6 kg/cm²
6·4 kg/cm²
CO-EFFICIENT OF CONSOLIDATION (Cv) IN²/MNT.
·00029
·00025
·00021
·00017
·00013
·00009
·00005
·00001
10
20
30
40
50
60
70
80
90
100
PERCENTAGE CONSOLIDATION (U)

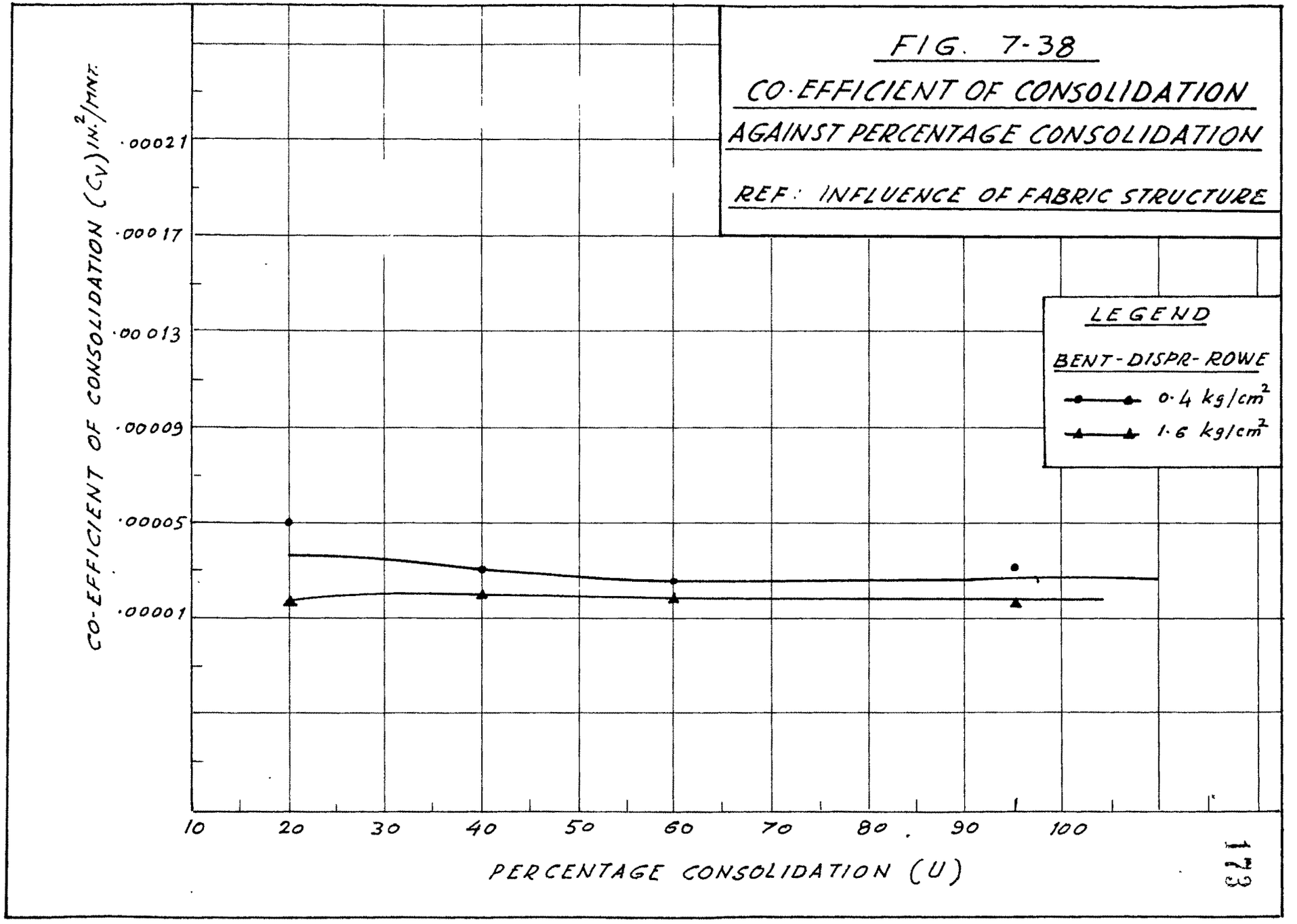
FIG. 7-38
CO-EFFICIENT OF CONSOLIDATION
AGAINST PERCENTAGE CONSOLIDATION
REF: INFLUENCE OF FABRIC STRUCTURE
LEGEND
BENT-DISPR-ROWE
0·4 kg/cm²
1·6 kg/cm²
CO-EFFICIENT OF CONSOLIDATION (Cv) IN.²/MNT.
·00021
·00017
·00013
·00009
·00005
·00001
10
20
30
40
50
60
70
80
90
100
PERCENTAGE CONSOLIDATION (U)

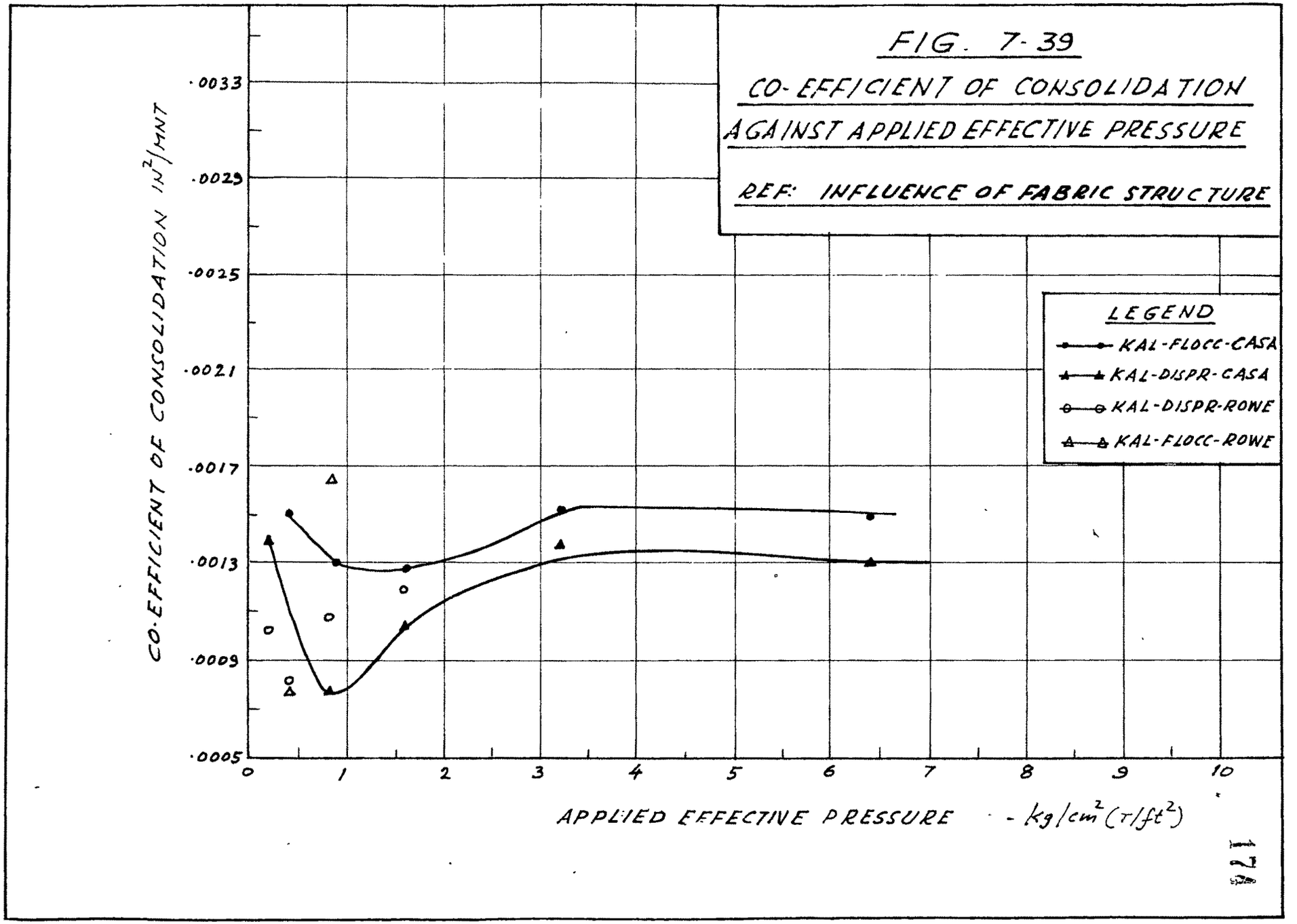
FIG. 7-39
CO-EFFICIENT OF CONSOLIDATION
AGAINST APPLIED EFFECTIVE PRESSURE
REF: INFLUENCE OF FABRIC STRUCTURE
LEGEND
KAL-FLOCC-CASA
KAL-DISPR-CASA
KAL-DISPR-ROWE
KAL-FLOCC-ROWE
CO-EFFICIENT OF CONSOLIDATION in²/MNT
.0033
.0029
.0025
.0021
.0017
.0013
.0009
.0005
0
1
2
3
4
5
6
7
8
9
10
APPLIED EFFECTIVE PRESSURE - kg/cm² (T/ft²)

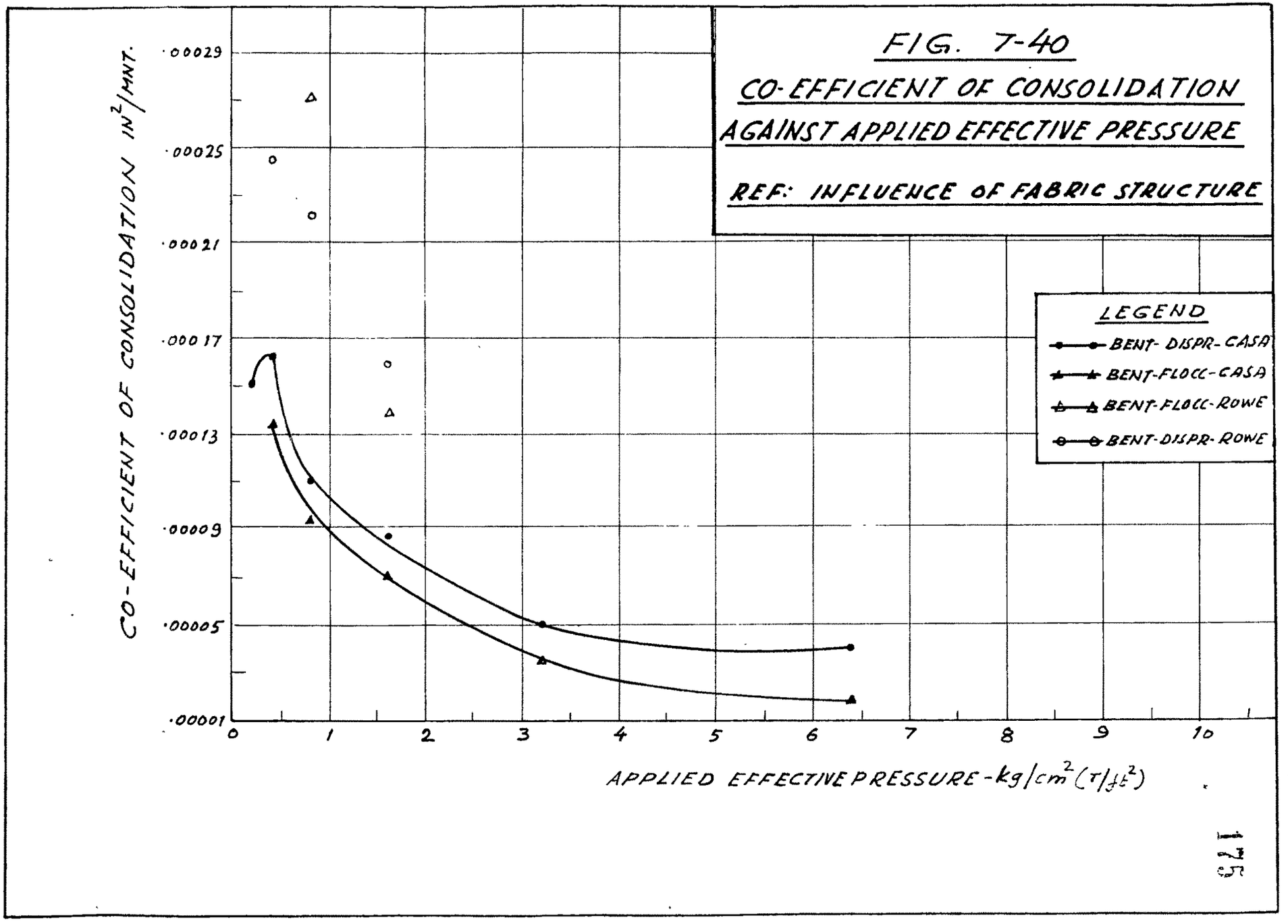
FIG. 7-40
CO-EFFICIENT OF CONSOLIDATION AGAINST APPLIED EFFECTIVE PRESSURE
REF: INFLUENCE OF FABRIC STRUCTURE
LEGEND
BENT- DISPR- CASA
BENT-FLOCC-CASA
BENT-FLOCC-ROWE
BENT-DISPR-ROWE
CO-EFFICIENT OF CONSOLIDATION IN²/MNT.
·00029
·00025
·00021
·00017
·00013
·00009
·00005
·00001
0
1
2
3
4
5
6
7
8
9
10
APPLIED EFFECTIVE PRESSURE - kg/cm² (T/ft²)

clays are almost similar. In kaolinite there is a decrease at light loadings and then an increase approaching a constant value at higher loadings. Whereas Bentonite shows a slight increase at 0.2 kg/cm^2 after which a rapid decrease is seen upto 3.2 kg/cm^2; from thereon the value remains unchanged.

(iii) Compression Index against applied average effective pressure. (Figures 7.41 and 7.42).

General trends of flocculated kaolinite and Bentonite show a hump which is distinct in case of Bentonite. At higher loads the tendency of the curve is to flatten out. For dispersed kaolinite and Bentonite samples, the curve descends initially and then becomes horizontal.

(iv) Percentage degree of secondary compression against applied effective pressure. (Figures 7.43 and 7.44).

Higher degree of secondary compression is observed in flocculated clays compared to dispersed clays. For dispersed clays, the amount of secondary compression is more under lighter loads which decreases rapidly and then remains more or less constant. It could be inferred that it is possible to reach 100% consolidation much earlier in case of initially dispersed structure than would be the case for an initially flocculated structure. In general the Bentonite samples show higher secondary compression than kaolinite.

(v) Parameter P against applied effective pressure (Figure 7.45 and 7.46 to 7.62).

A comparison of the experimental curve with the theoretica

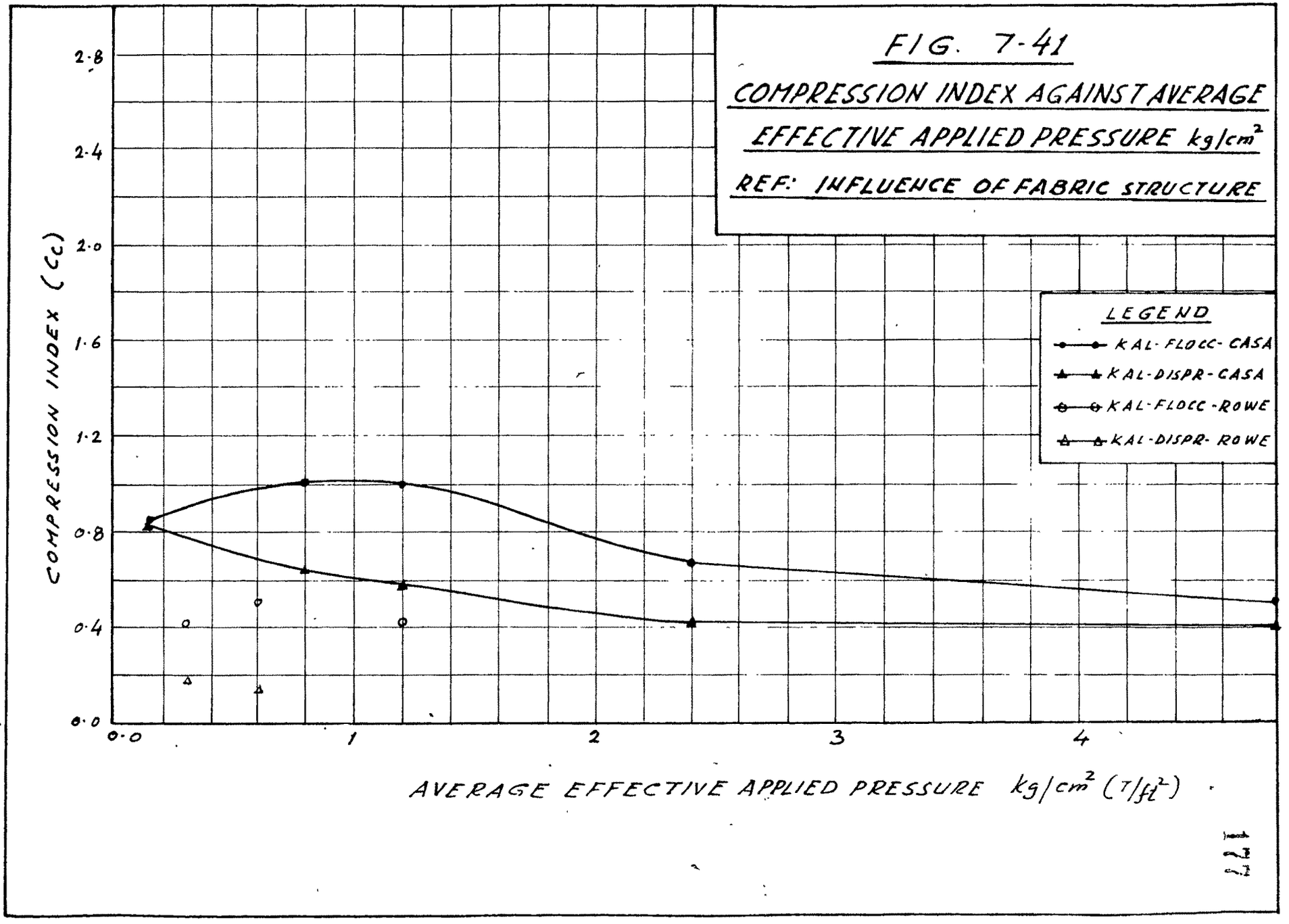
FIG. 7-41
COMPRESSION INDEX AGAINST AVERAGE EFFECTIVE APPLIED PRESSURE kg/cm²
REF: INFLUENCE OF FABRIC STRUCTURE
LEGEND
KAL-FLOCC-CASA
KAL-DISPR-CASA
KAL-FLOCC-ROWE
KAL-DISPR-ROWE
COMPRESSION INDEX (Cc)
2·8
2·4
2·0
1·6
1·2
0·8
0·4
0·0
0·0
1
2
3
4
AVERAGE EFFECTIVE APPLIED PRESSURE kg/cm² (T/ft²)

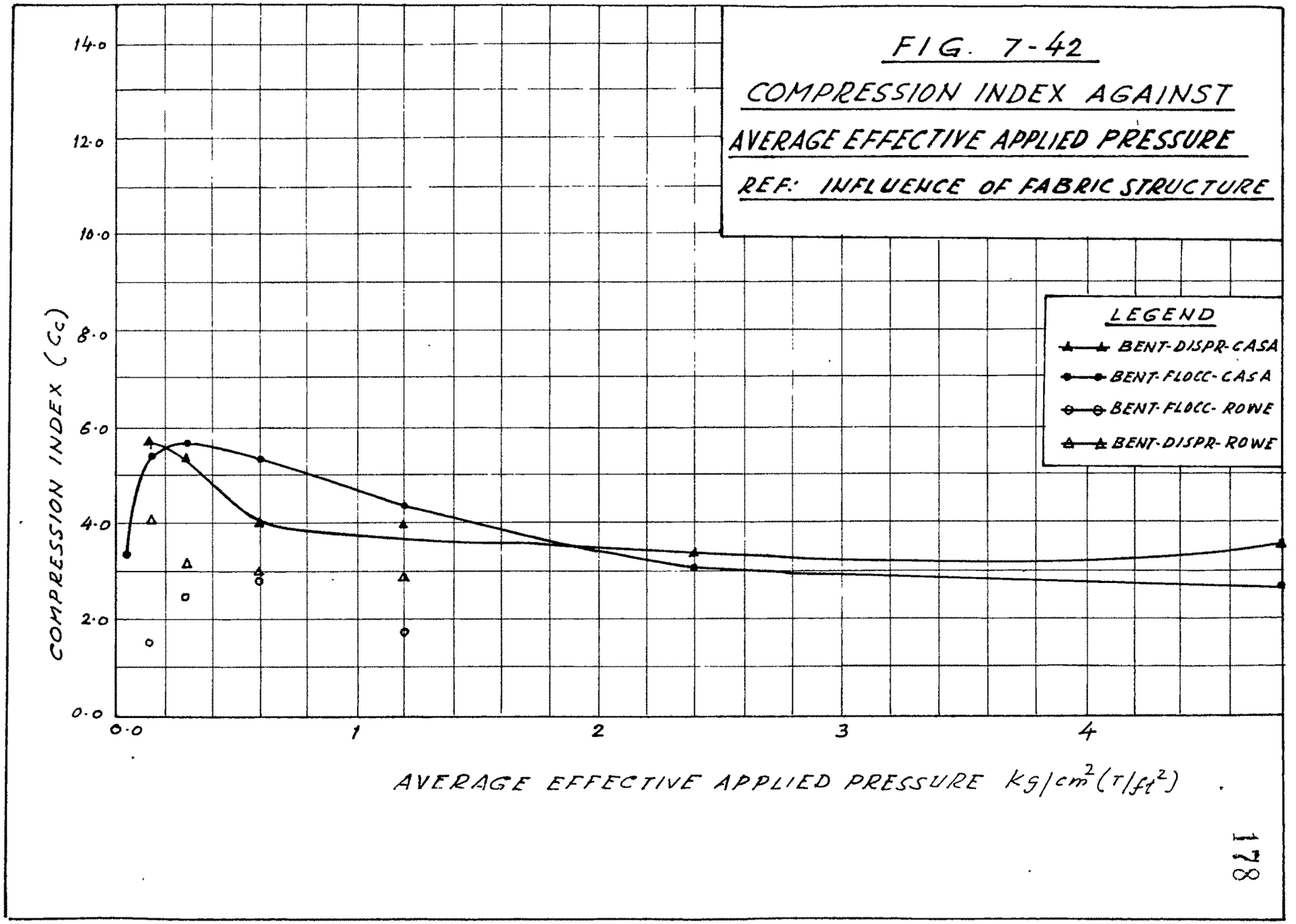
FIG. 7-42
COMPRESSION INDEX AGAINST
AVERAGE EFFECTIVE APPLIED PRESSURE
REF: INFLUENCE OF FABRIC STRUCTURE
LEGEND
BENT-DISPR-CASA
BENT-FLOCC-CASA
BENT-FLOCC-ROWE
BENT-DISPR-ROWE
COMPRESSION INDEX (Cc)
14·0
12·0
10·0
8·0
6·0
4·0
2·0
0·0
0·0
1
2
3
4
AVERAGE EFFECTIVE APPLIED PRESSURE kg/cm² (T/ft²)

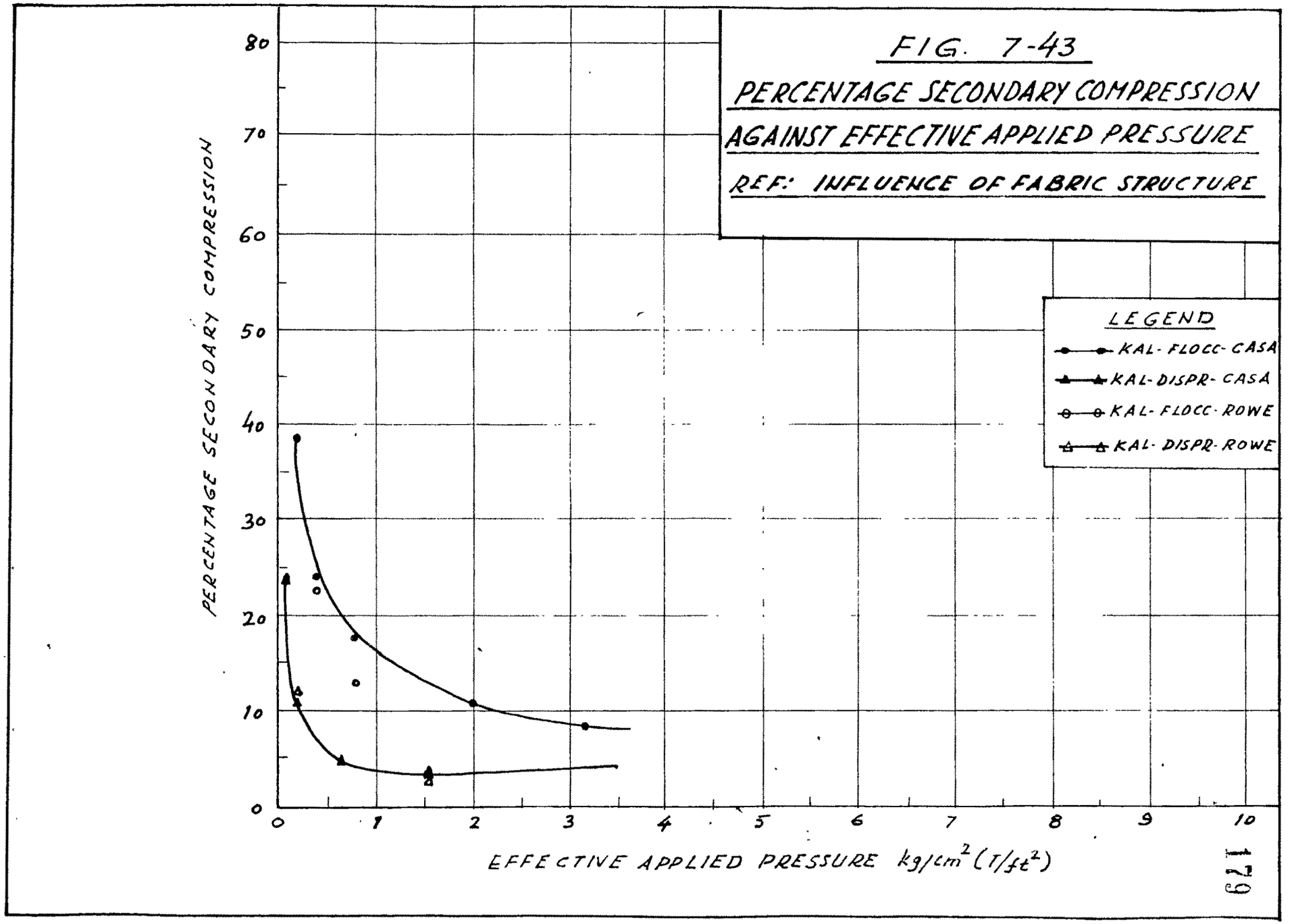
FIG. 7-43
PERCENTAGE SECONDARY COMPRESSION AGAINST EFFECTIVE APPLIED PRESSURE
REF: INFLUENCE OF FABRIC STRUCTURE
LEGEND
KAL-FLOCC-CASA
KAL-DISPR-CASA
KAL-FLOCC-ROWE
KAL-DISPR-ROWE
PERCENTAGE SECONDARY COMPRESSION
EFFECTIVE APPLIED PRESSURE kg/cm² (T/ft²)
0
10
20
30
40
50
60
70
80
0
1
2
3
4
5
6
7
8
9
10

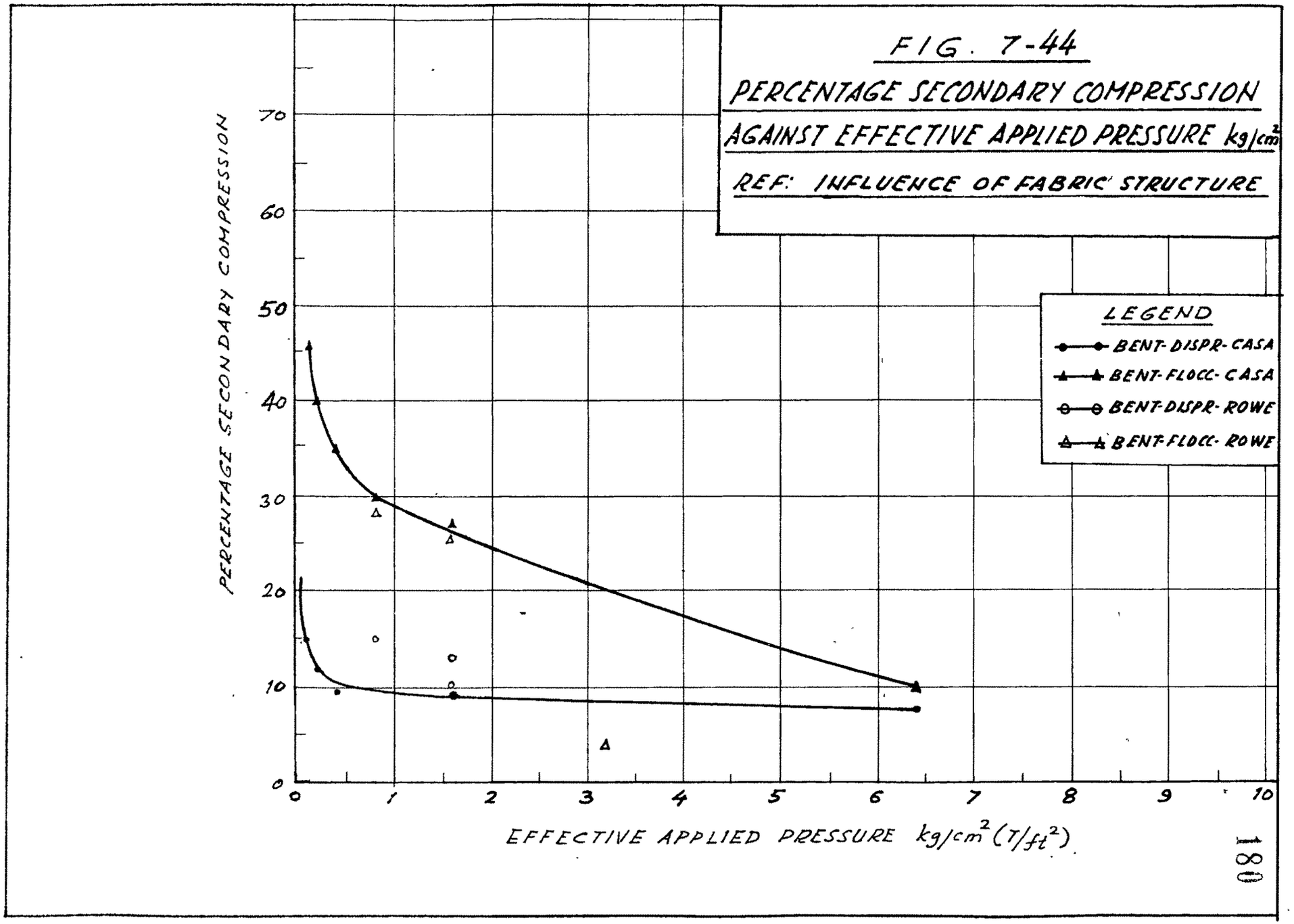
FIG. 7-44
PERCENTAGE SECONDARY COMPRESSION
AGAINST EFFECTIVE APPLIED PRESSURE kg/cm²
REF: INFLUENCE OF FABRIC STRUCTURE
LEGEND
BENT-DISPR-CASA
BENT-FLOCC-CASA
BENT-DISPR-ROWE
BENT-FLOCC-ROWE
PERCENTAGE SECONDARY COMPRESSION
0
10
20
30
40
50
60
70
0
1
2
3
4
5
6
7
8
9
10
EFFECTIVE APPLIED PRESSURE kg/cm² (T/ft²)

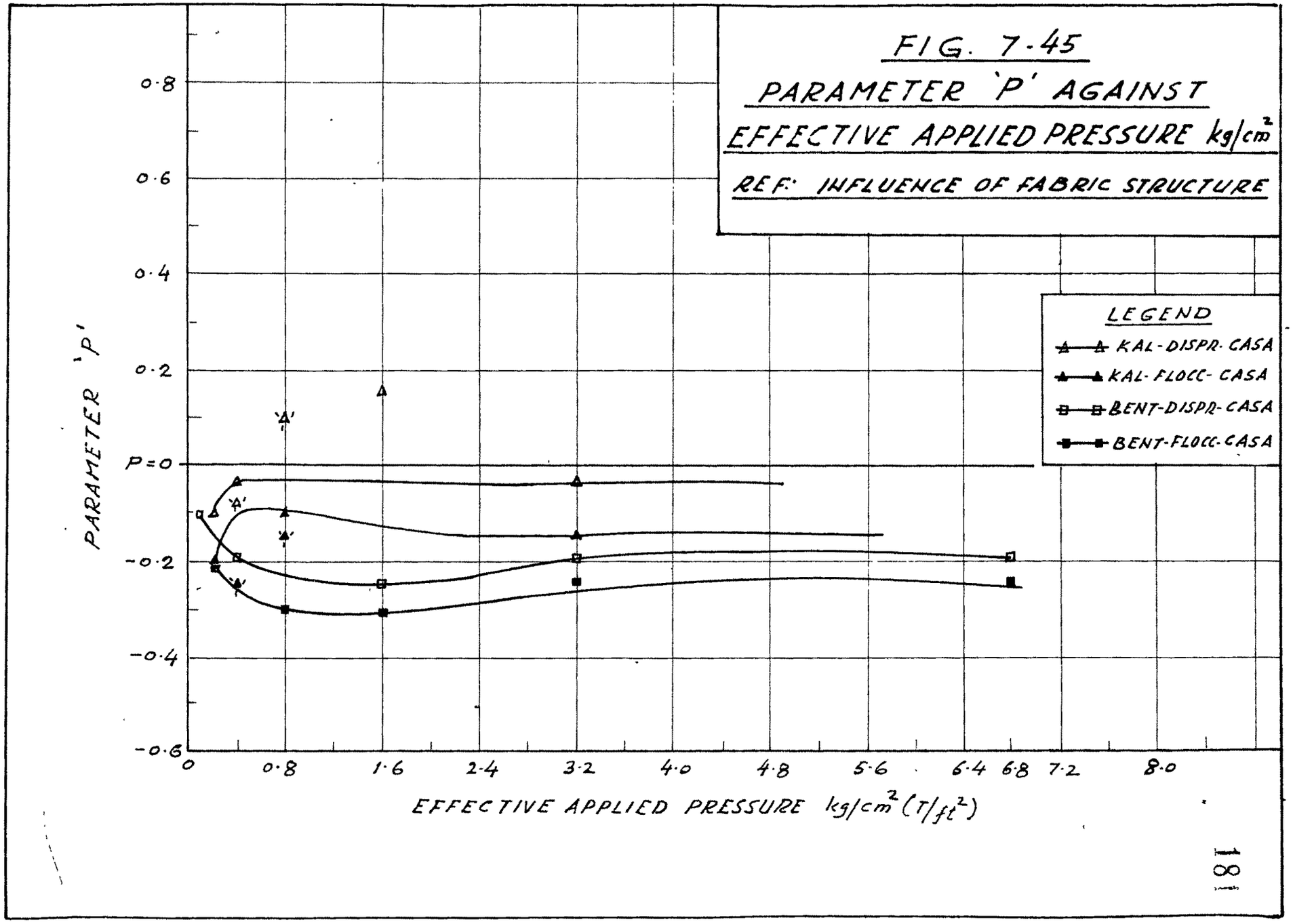
FIG. 7·45
PARAMETER 'P' AGAINST
EFFECTIVE APPLIED PRESSURE kg/cm²
REF: INFLUENCE OF FABRIC STRUCTURE
LEGEND
KAL-DISPR-CASA
KAL-FLOCC-CASA
BENT-DISPR-CASA
BENT-FLOCC-CASA
PARAMETER 'P'
0·8
0·6
0·4
0·2
P=0
-0·2
-0·4
-0·6
0
0·8
1·6
2·4
3·2
4·0
4·8
5·6
6·4
6·8
7·2
8·0
EFFECTIVE APPLIED PRESSURE kg/cm² (T/ft²)

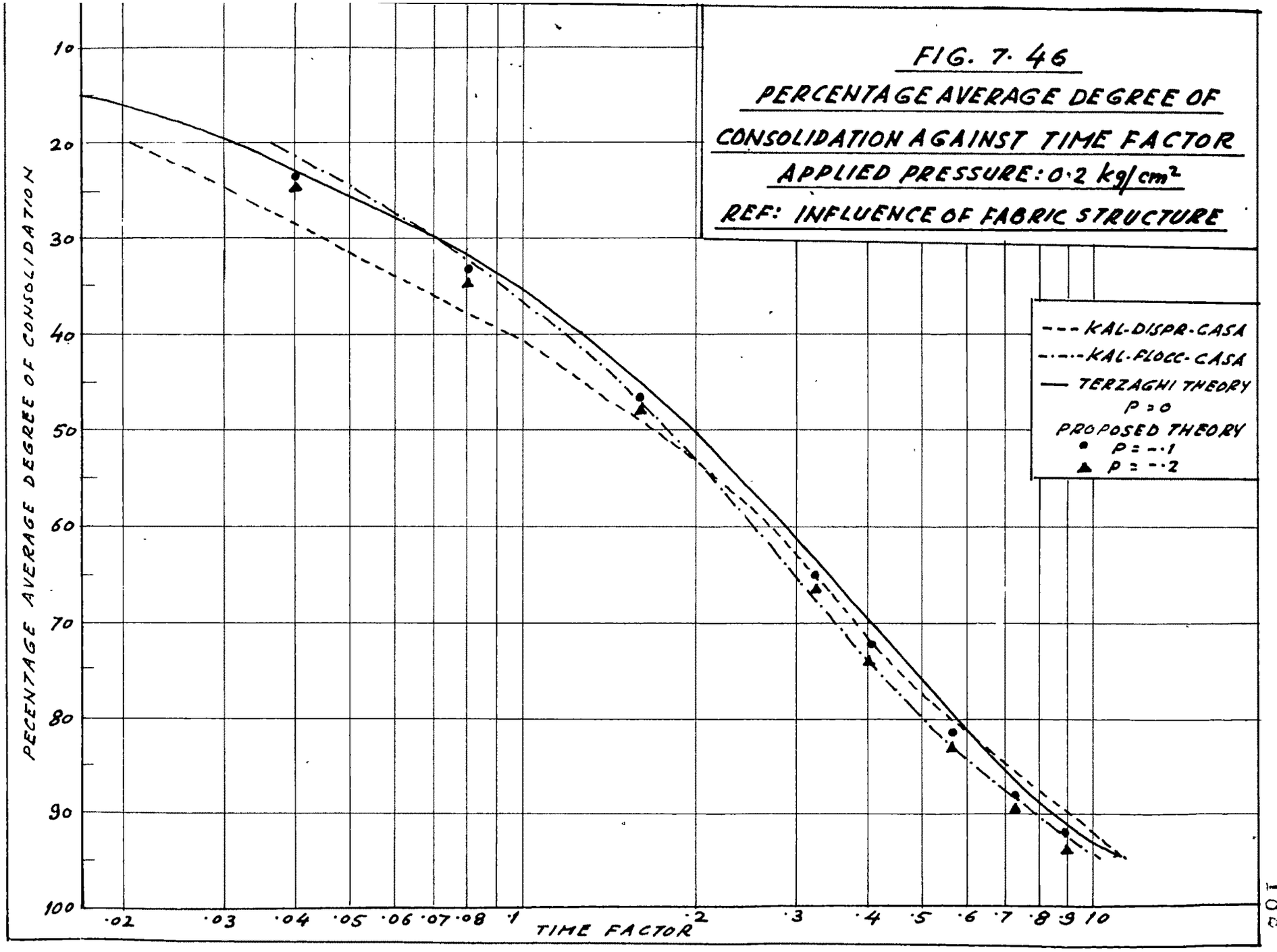
FIG. 7·46
PERCENTAGE AVERAGE DEGREE OF CONSOLIDATION AGAINST TIME FACTOR
APPLIED PRESSURE: 0·2 kg/cm²
REF: INFLUENCE OF FABRIC STRUCTURE
--- KAL-DISPR-CASA
-·-·- KAL-FLOCC-CASA
— TERZAGHI THEORY P = 0
PROPOSED THEORY
● P = -·1
▲ P = -·2
PECENTAGE AVERAGE DEGREE OF CONSOLIDATION
10
20
30
40
50
60
70
80
90
100
·02 ·03 ·04 ·05 ·06 ·07 ·08 ·1 ·2 ·3 ·4 ·5 ·6 ·7 ·8 ·9 10
TIME FACTOR

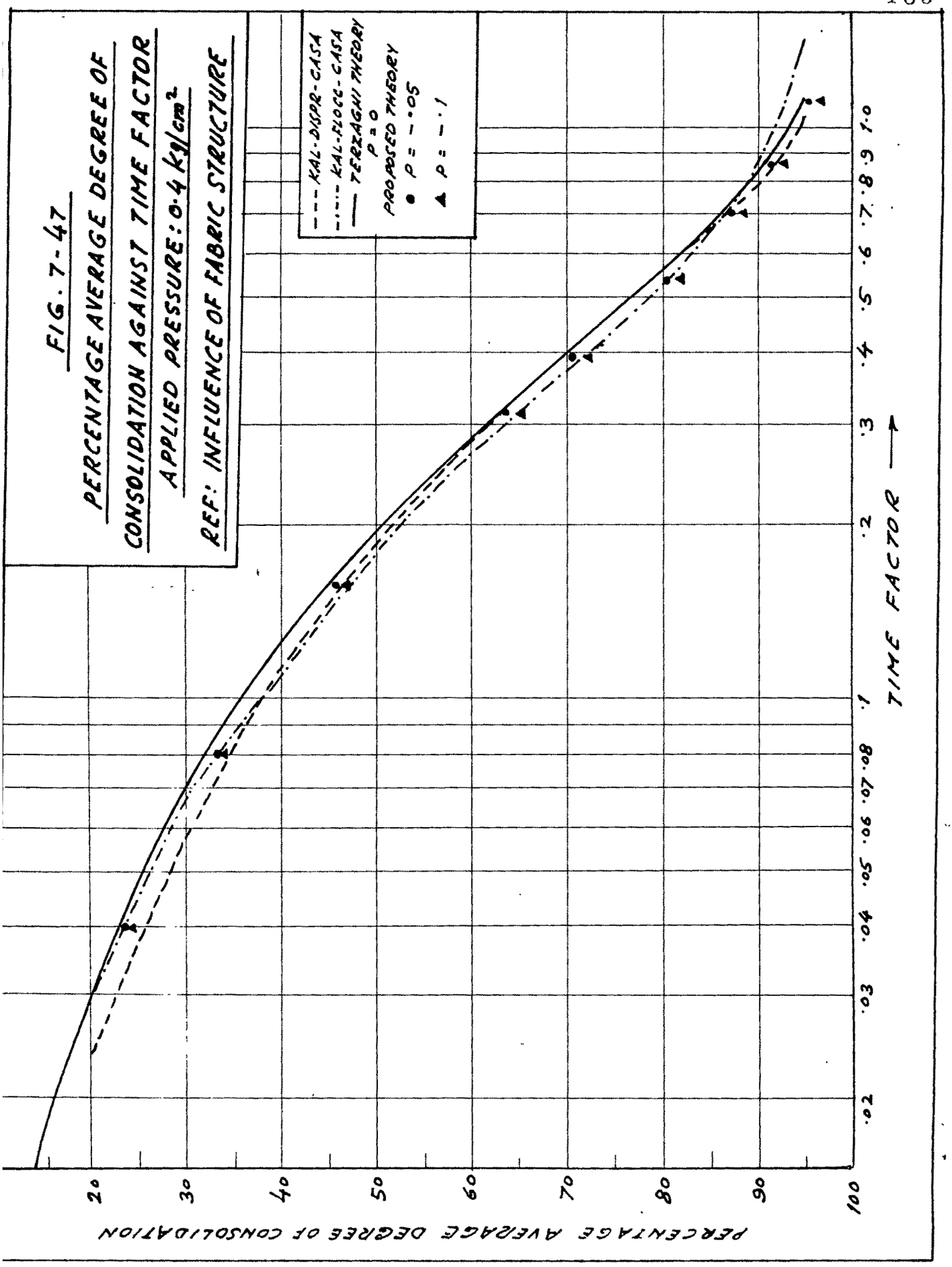
FIG. 7-47
PERCENTAGE AVERAGE DEGREE OF CONSOLIDATION AGAINST TIME FACTOR
APPLIED PRESSURE: 0·4 kg/cm²
REF: INFLUENCE OF FABRIC STRUCTURE
--- KAL-DISPR-CASA
-·-·- KAL-FLOCC-CASA
—— TERZAGHI THEORY
ρ = 0
PROPOSED THEORY
● ρ = -·05
▲ ρ = -·1
PERCENTAGE AVERAGE DEGREE OF CONSOLIDATION
20 30 40 50 60 70 80 90 100
TIME FACTOR →
·02 ·03 ·04 ·05 ·06 ·07 ·08 ·1 ·2 ·3 ·4 ·5 ·6 ·7 ·8 ·9 1·0

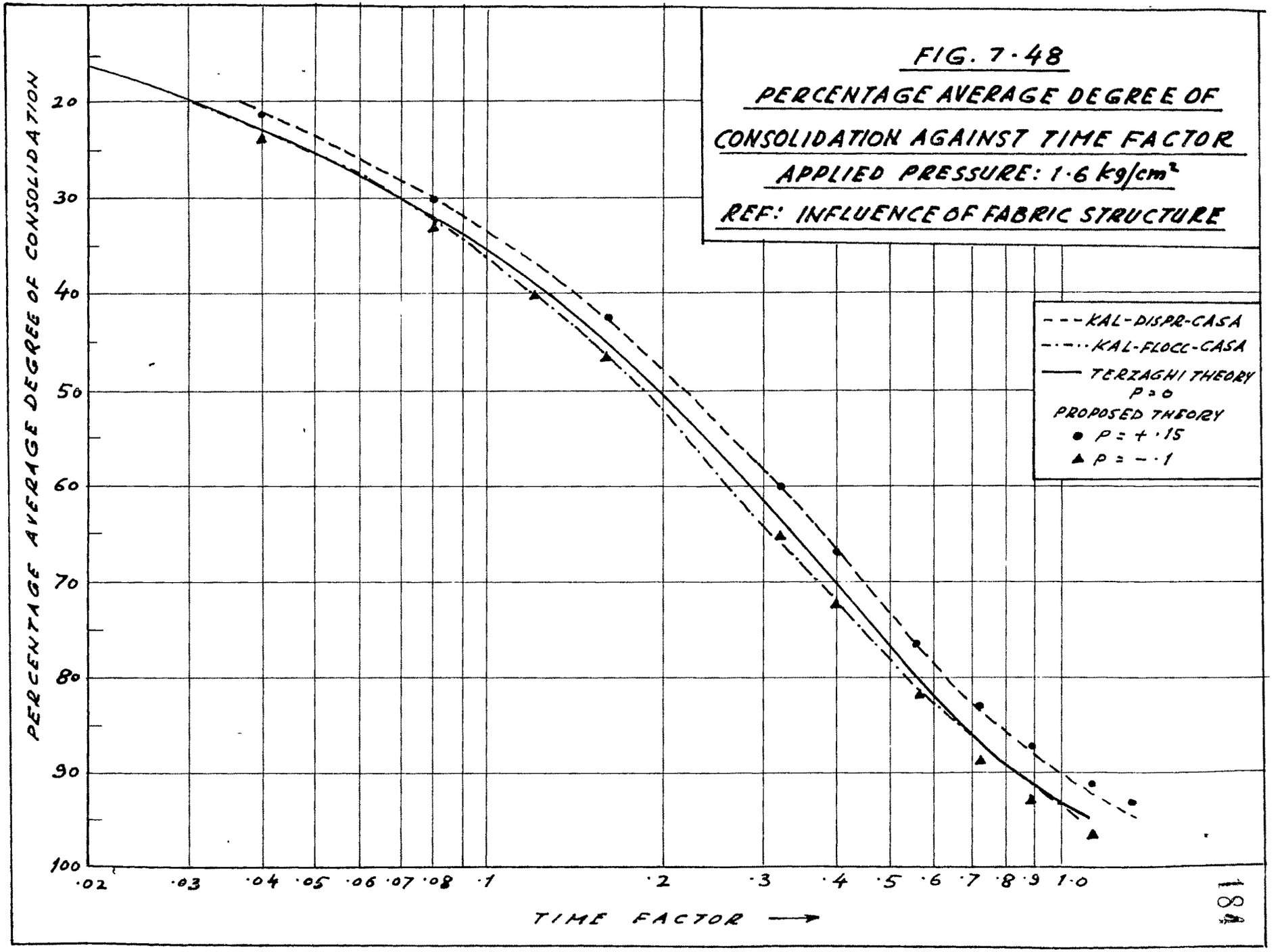
FIG. 7·48
PERCENTAGE AVERAGE DEGREE OF CONSOLIDATION AGAINST TIME FACTOR
APPLIED PRESSURE: 1·6 kg/cm²
REF: INFLUENCE OF FABRIC STRUCTURE
KAL-DISPR-CASA
KAL-FLOCC-CASA
TERZAGHI THEORY P=0
PROPOSED THEORY
P = +·15
P = −·1
PERCENTAGE AVERAGE DEGREE OF CONSOLIDATION
20
30
40
50
60
70
80
90
100
·02
·03
·04
·05
·06
·07
·08
·1
·2
·3
·4
·5
·6
·7
·8
·9
1·0
TIME FACTOR ⟶

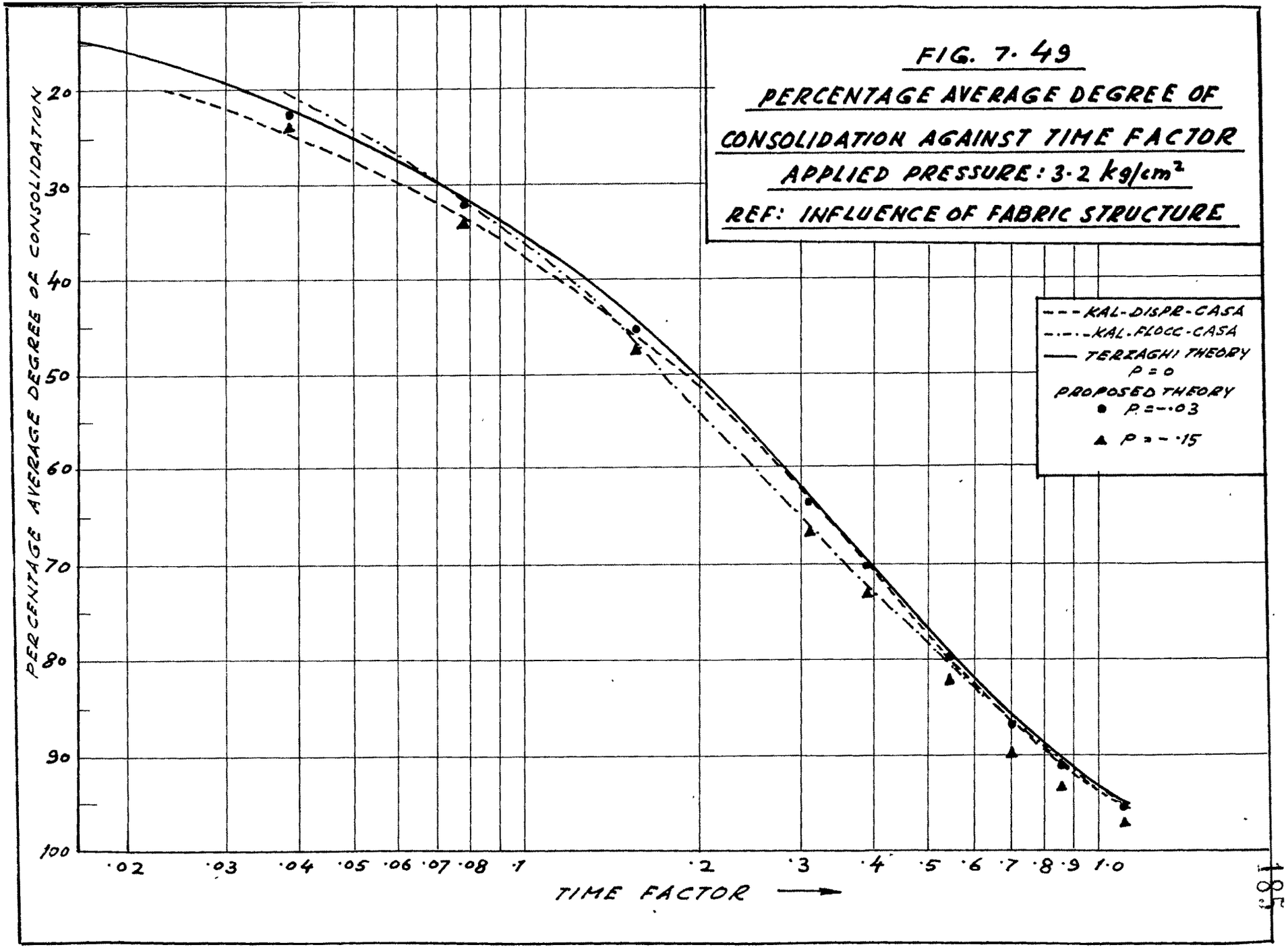
FIG. 7·49
PERCENTAGE AVERAGE DEGREE OF CONSOLIDATION AGAINST TIME FACTOR
APPLIED PRESSURE : 3·2 kg/cm²
REF: INFLUENCE OF FABRIC STRUCTURE
KAL-DISPR-CASA
KAL-FLOCC-CASA
TERZAGHI THEORY P = 0
PROPOSED THEORY
P = -·03
P = -·15
PERCENTAGE AVERAGE DEGREE OF CONSOLIDATION
20
30
40
50
60
70
80
90
100
·02 ·03 ·04 ·05 ·06 ·07 ·08 ·1 ·2 ·3 ·4 ·5 ·6 ·7 ·8 ·9 1·0
TIME FACTOR

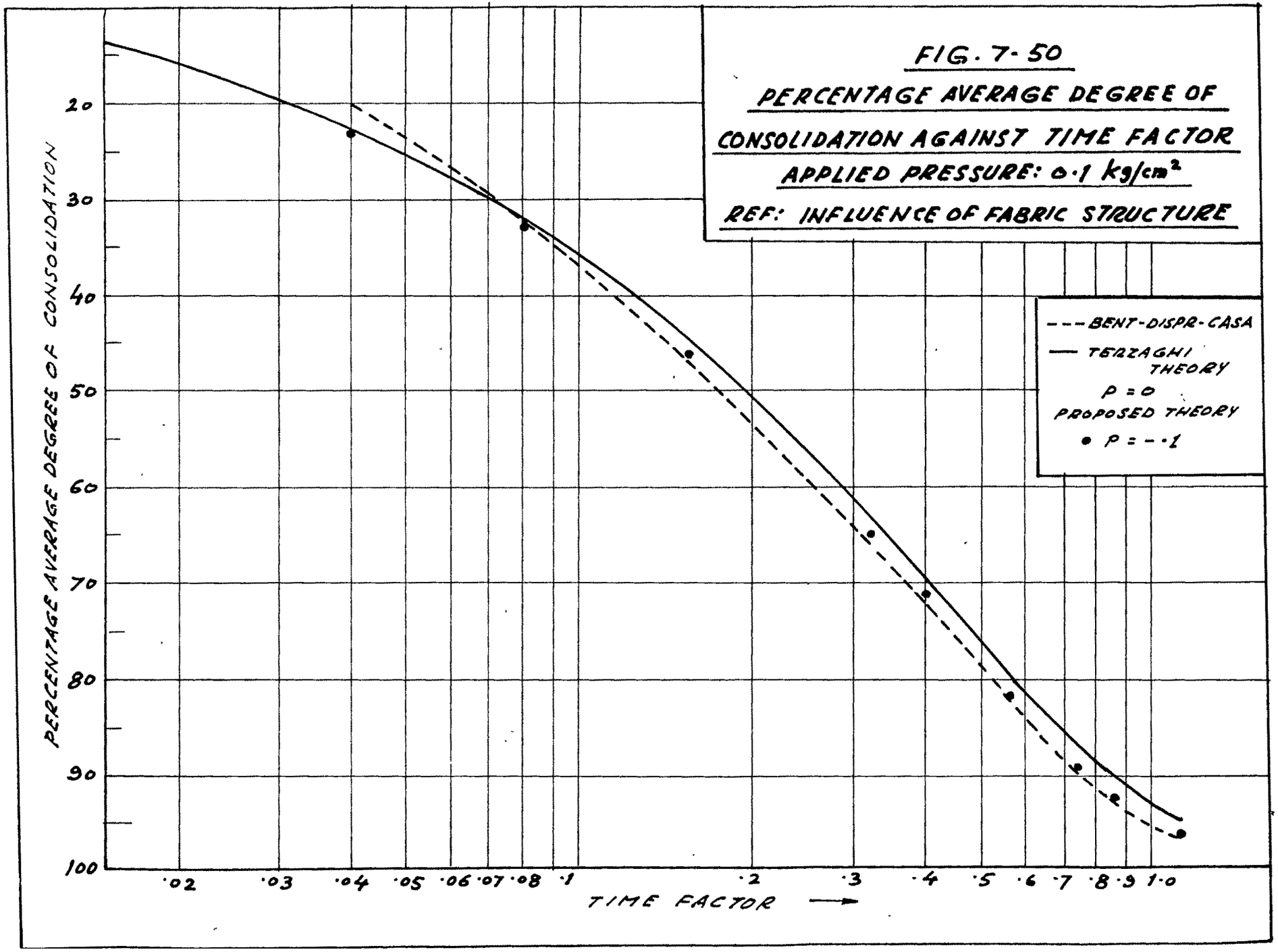
FIG. 7-50
PERCENTAGE AVERAGE DEGREE OF CONSOLIDATION AGAINST TIME FACTOR
APPLIED PRESSURE: 0·1 kg/cm²
REF: INFLUENCE OF FABRIC STRUCTURE
---BENT-DISPR-CASA
— TERZAGHI THEORY
P = 0
PROPOSED THEORY
• P = -·1
PERCENTAGE AVERAGE DEGREE OF CONSOLIDATION
20
30
40
50
60
70
80
90
100
·02 ·03 ·04 ·05 ·06 ·07 ·08 ·1 ·2 ·3 ·4 ·5 ·6 ·7 ·8 ·9 1·0
TIME FACTOR ⟶

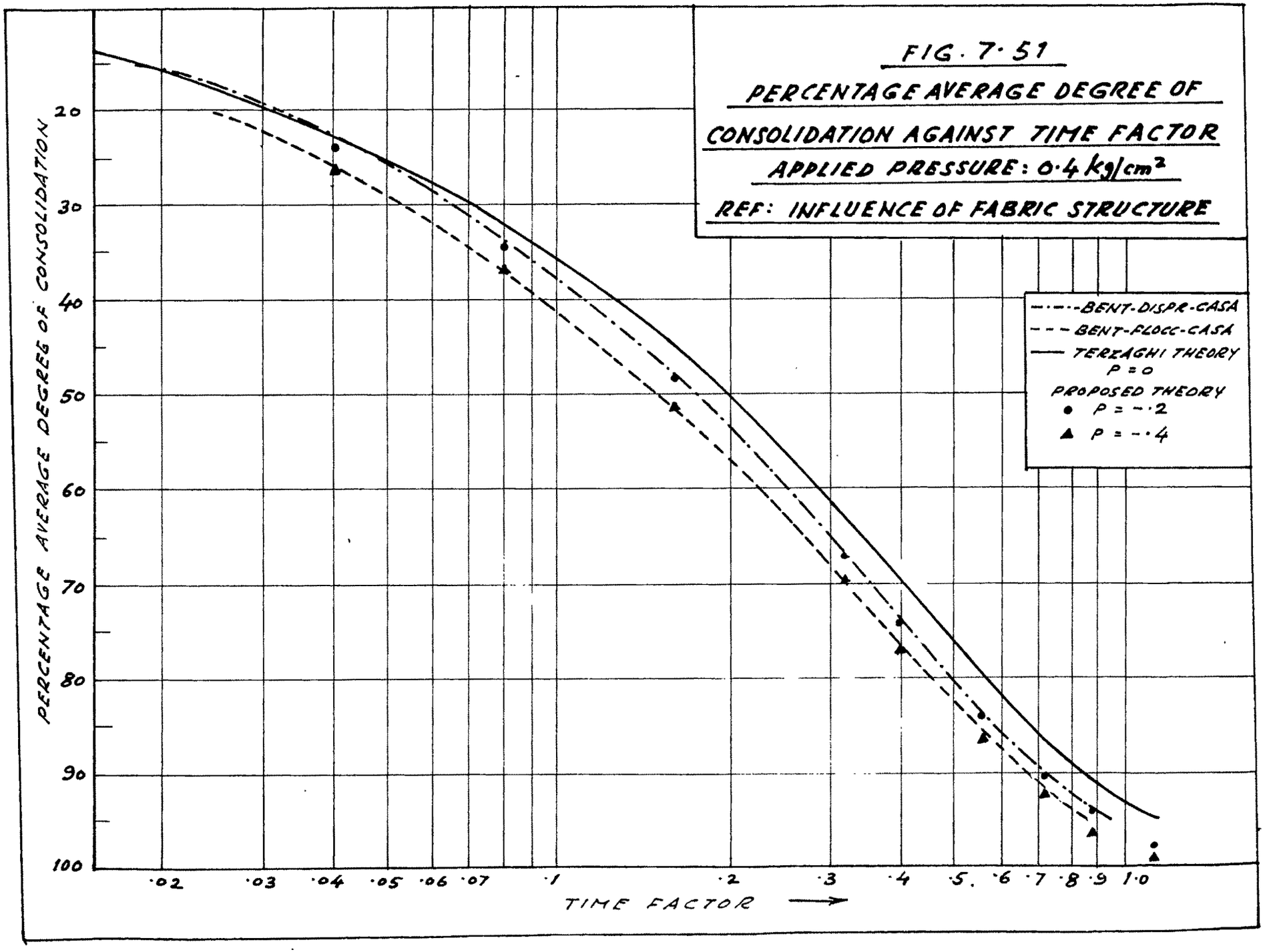
FIG. 7·51
PERCENTAGE AVERAGE DEGREE OF CONSOLIDATION AGAINST TIME FACTOR
APPLIED PRESSURE: 0·4 kg/cm²
REF: INFLUENCE OF FABRIC STRUCTURE
BENT-DISPR-CASA
BENT-FLOCC-CASA
TERZAGHI THEORY P=0
PROPOSED THEORY
P = -·2
P = -·4
PERCENTAGE AVERAGE DEGREE OF CONSOLIDATION
20
30
40
50
60
70
80
90
100
·02
·03
·04
·05
·06
·07
·1
·2
·3
·4
·5
·6
·7
·8
·9
1·0
TIME FACTOR

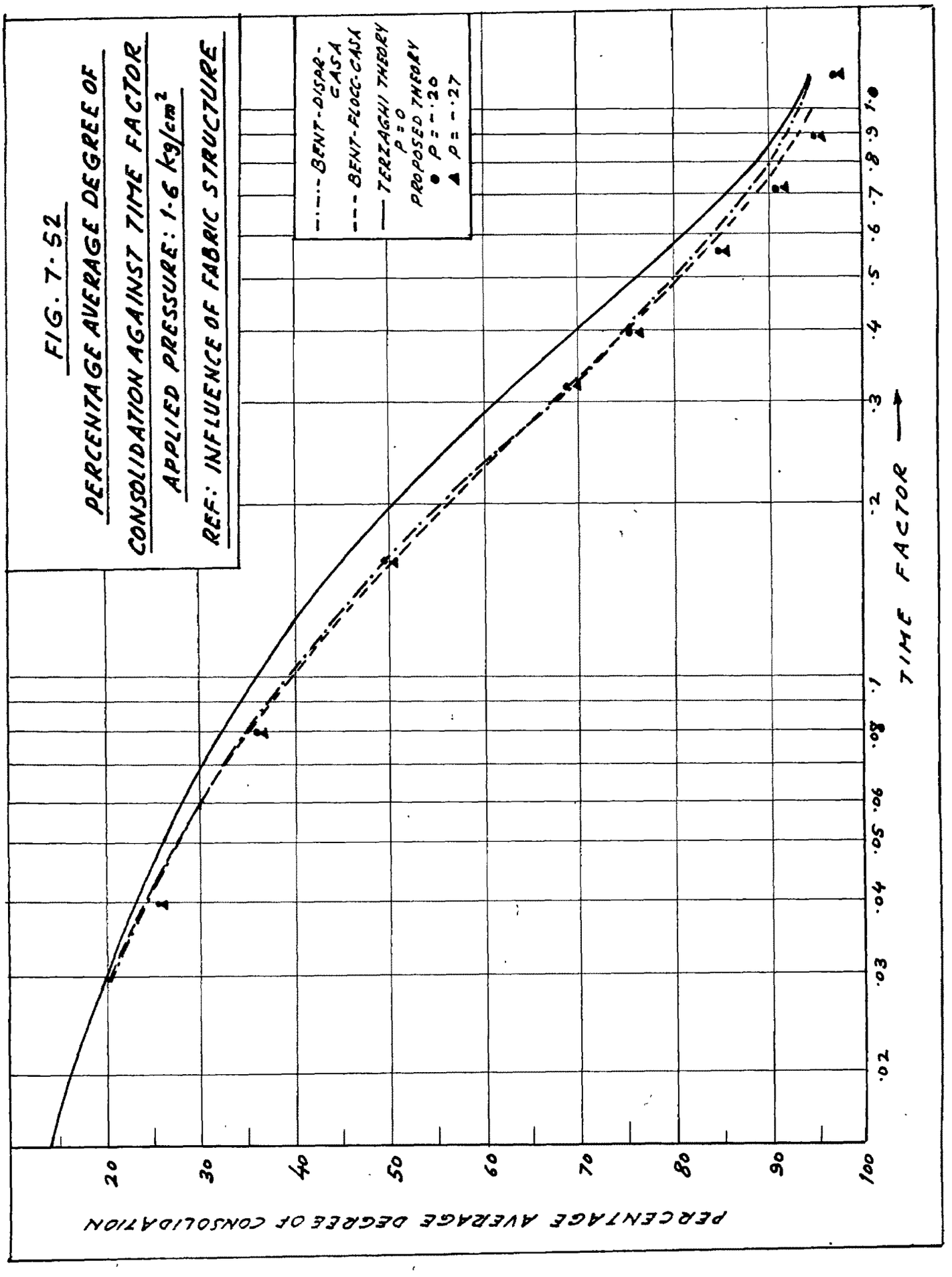
FIG. 7·52
PERCENTAGE AVERAGE DEGREE OF CONSOLIDATION AGAINST TIME FACTOR
APPLIED PRESSURE: 1·6 kg/cm²
REF: INFLUENCE OF FABRIC STRUCTURE
-·-·- BENT-DISPR-CASA
--- BENT-FLOCC-CASA
— TERZAGHI THEORY
ρ = 0
PROPOSED THEORY
● ρ = -·20
▲ ρ = -·27
PERCENTAGE AVERAGE DEGREE OF CONSOLIDATION
20
30
40
50
60
70
80
90
100
TIME FACTOR
·02
·03
·04
·05
·06
·08
·1
·2
·3
·4
·5
·6
·7
·8
·9
1·0

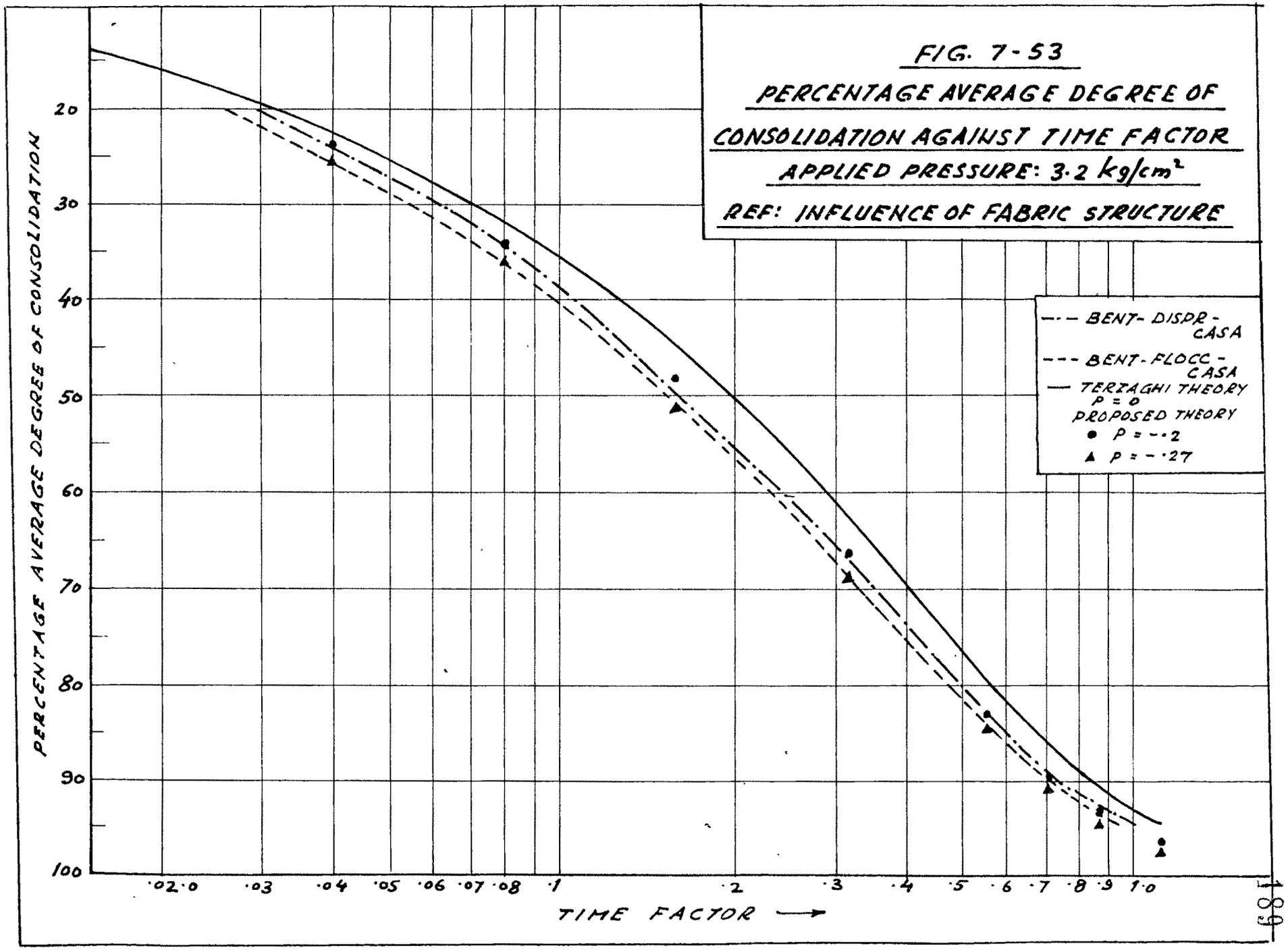
FIG. 7-53
PERCENTAGE AVERAGE DEGREE OF CONSOLIDATION AGAINST TIME FACTOR
APPLIED PRESSURE: 3·2 kg/cm²
REF: INFLUENCE OF FABRIC STRUCTURE
BENT- DISPR - CASA
BENT - FLOCC - CASA
TERZAGHI THEORY
P = 0
PROPOSED THEORY
P = -·2
P = -·27
PERCENTAGE AVERAGE DEGREE OF CONSOLIDATION
20
30
40
50
60
70
80
90
100
·02 ·0
·03
·04
·05
·06
·07
·08
·1
·2
·3
·4
·5
·6
·7
·8
·9
1·0
TIME FACTOR →

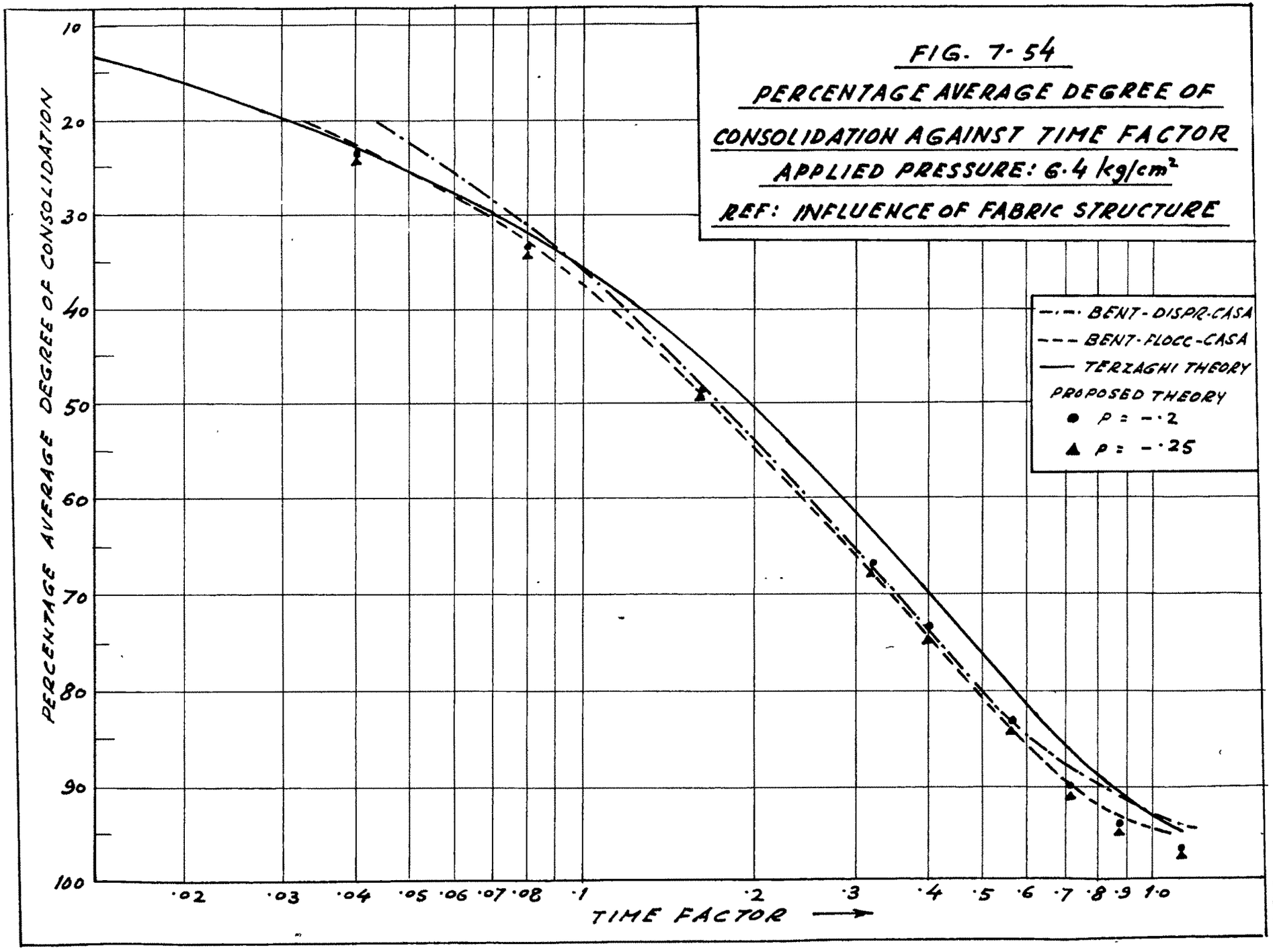
FIG. 7·54
PERCENTAGE AVERAGE DEGREE OF CONSOLIDATION AGAINST TIME FACTOR
APPLIED PRESSURE: 6·4 kg/cm²
REF: INFLUENCE OF FABRIC STRUCTURE
BENT-DISPR-CASA
BENT-FLOCC-CASA
TERZAGHI THEORY
PROPOSED THEORY
p = -·2
p = -·25
PERCENTAGE AVERAGE DEGREE OF CONSOLIDATION
10
20
30
40
50
60
70
80
90
100
·02 ·03 ·04 ·05 ·06 ·07 ·08 ·1 ·2 ·3 ·4 ·5 ·6 ·7 ·8 ·9 1·0
TIME FACTOR

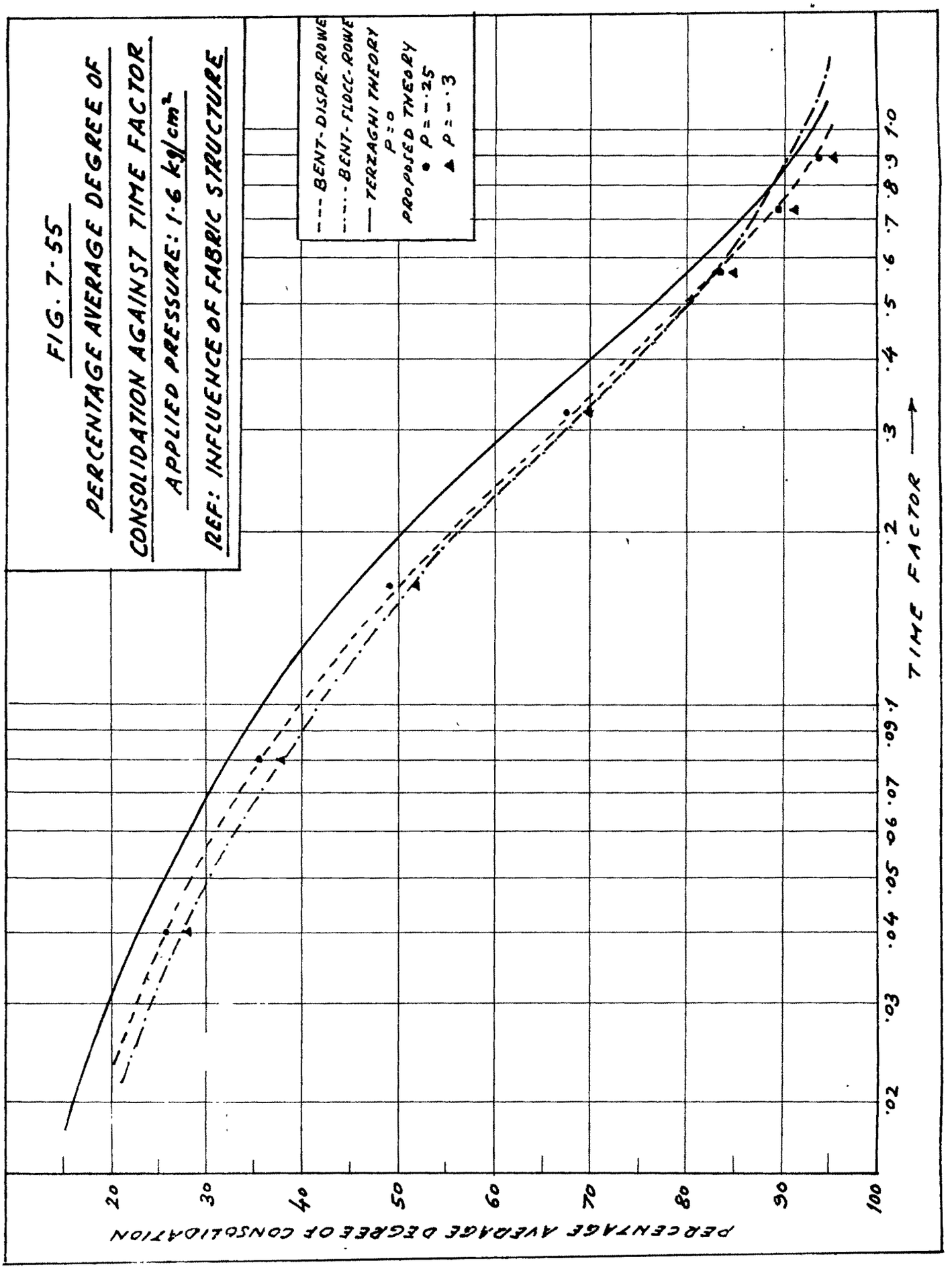
FIG. 7·55
PERCENTAGE AVERAGE DEGREE OF CONSOLIDATION AGAINST TIME FACTOR
APPLIED PRESSURE: 1·6 kg/cm²
REF: INFLUENCE OF FABRIC STRUCTURE
--- BENT-DISPR-ROWE
-·-·- BENT-FLOCC-ROWE
— TERZAGHI THEORY
P = 0
PROPOSED THEORY
• P = -·25
▲ P = -·3
PERCENTAGE AVERAGE DEGREE OF CONSOLIDATION
20
30
40
50
60
70
80
90
100
TIME FACTOR
·02
·03
·04
·05
·06
·07
·09
·1
·2
·3
·4
·5
·6
·7
·8
·9
1·0

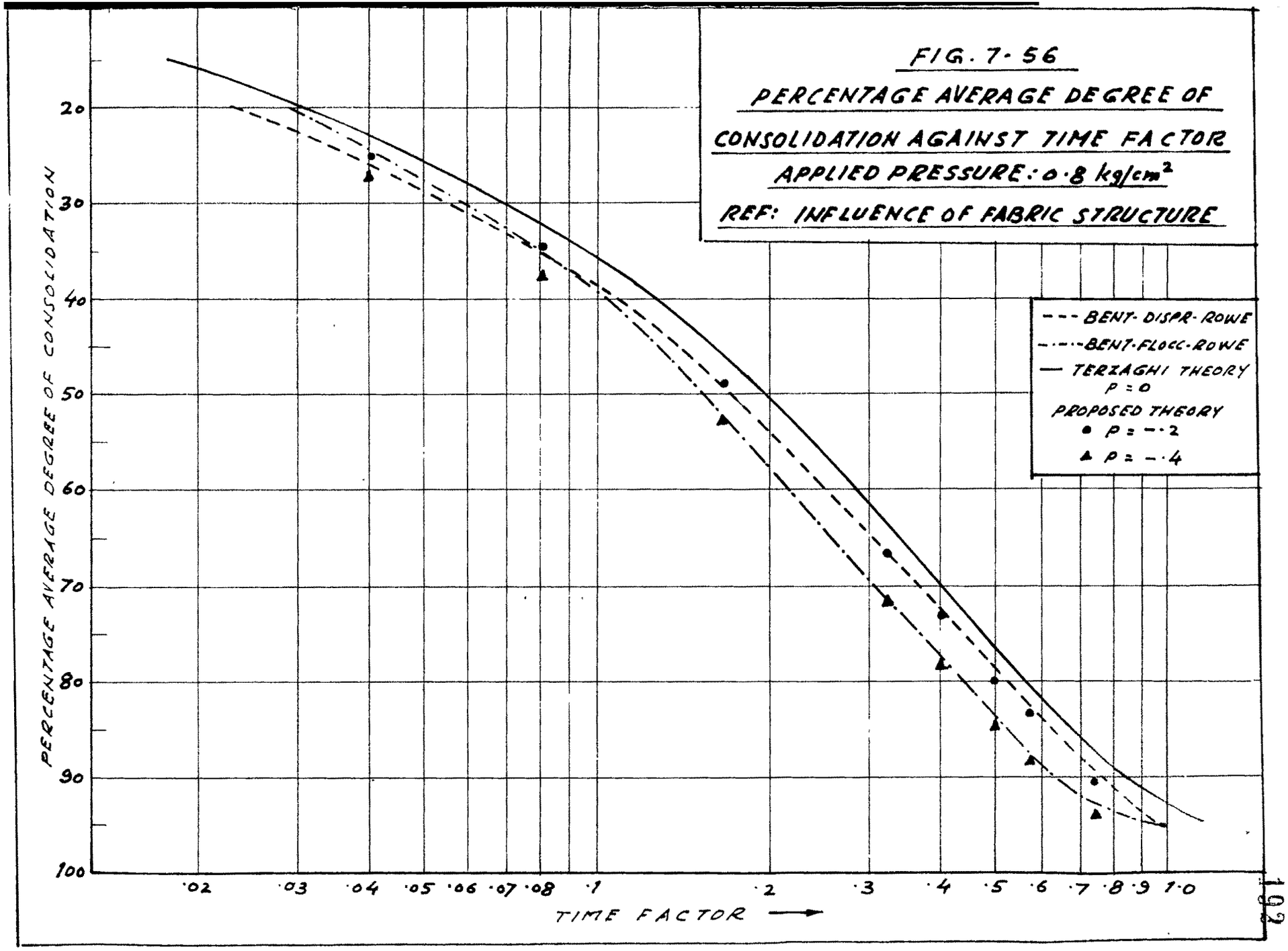
FIG. 7·56
PERCENTAGE AVERAGE DEGREE OF CONSOLIDATION AGAINST TIME FACTOR
APPLIED PRESSURE: 0·8 kg/cm²
REF: INFLUENCE OF FABRIC STRUCTURE
--- BENT-DISPR-ROWE
-·-·- BENT-FLOCC-ROWE
— TERZAGHI THEORY P = 0
PROPOSED THEORY
● P = -·2
▲ P = -·4
PERCENTAGE AVERAGE DEGREE OF CONSOLIDATION
20
30
40
50
60
70
80
90
100
·02 ·03 ·04 ·05 ·06 ·07 ·08 ·1 ·2 ·3 ·4 ·5 ·6 ·7 ·8 ·9 1·0
TIME FACTOR ⟶

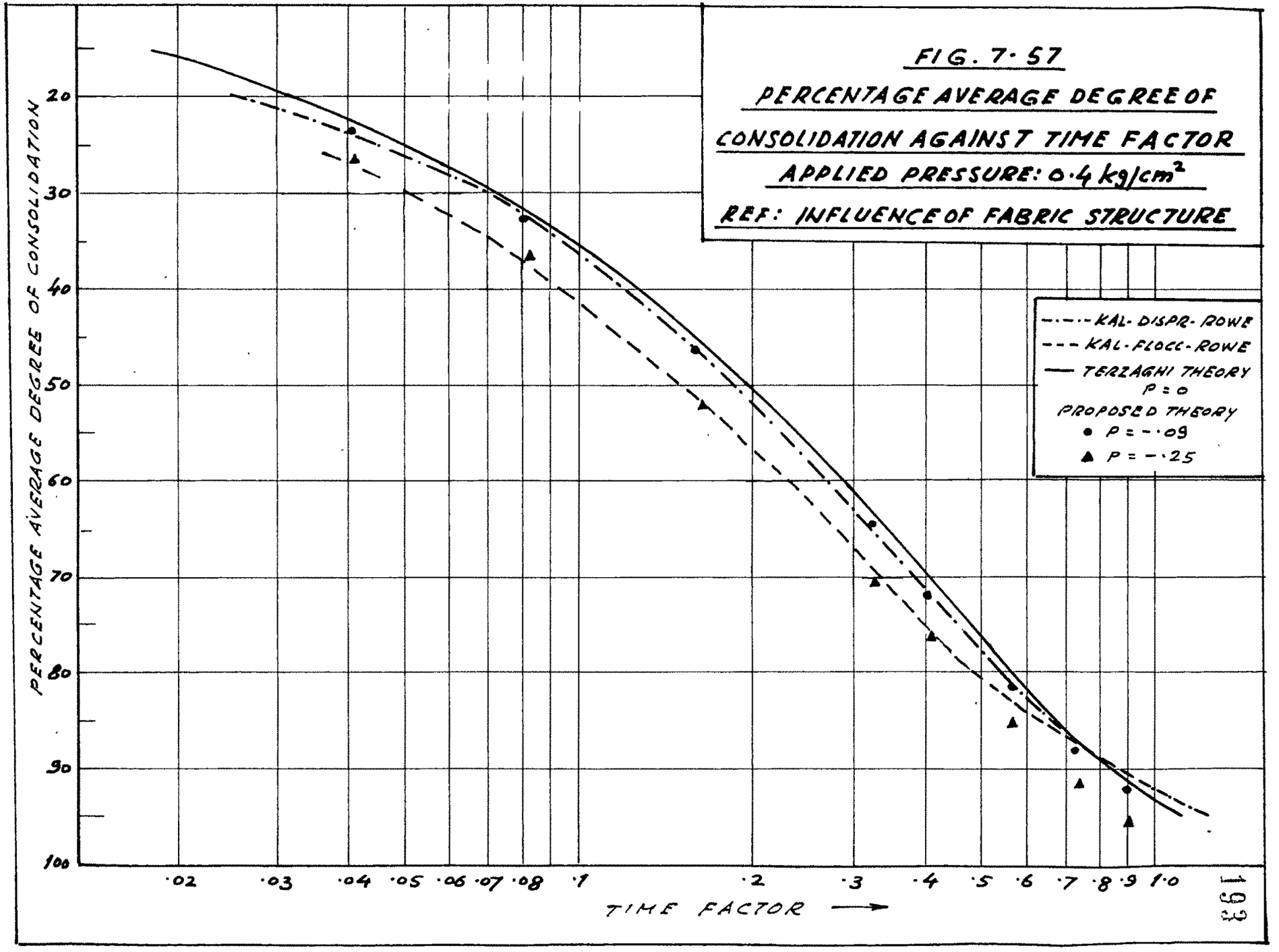
FIG. 7·57
PERCENTAGE AVERAGE DEGREE OF CONSOLIDATION AGAINST TIME FACTOR
APPLIED PRESSURE: 0·4 kg/cm²
REF: INFLUENCE OF FABRIC STRUCTURE
KAL-DISPR-ROWE
KAL-FLOCC-ROWE
TERZAGHI THEORY P = 0
PROPOSED THEORY
P = -·09
P = -·25
PERCENTAGE AVERAGE DEGREE OF CONSOLIDATION
20
30
40
50
60
70
80
90
100
·02 ·03 ·04 ·05 ·06 ·07 ·08 ·1 ·2 ·3 ·4 ·5 ·6 ·7 ·8 ·9 1·0
TIME FACTOR
196

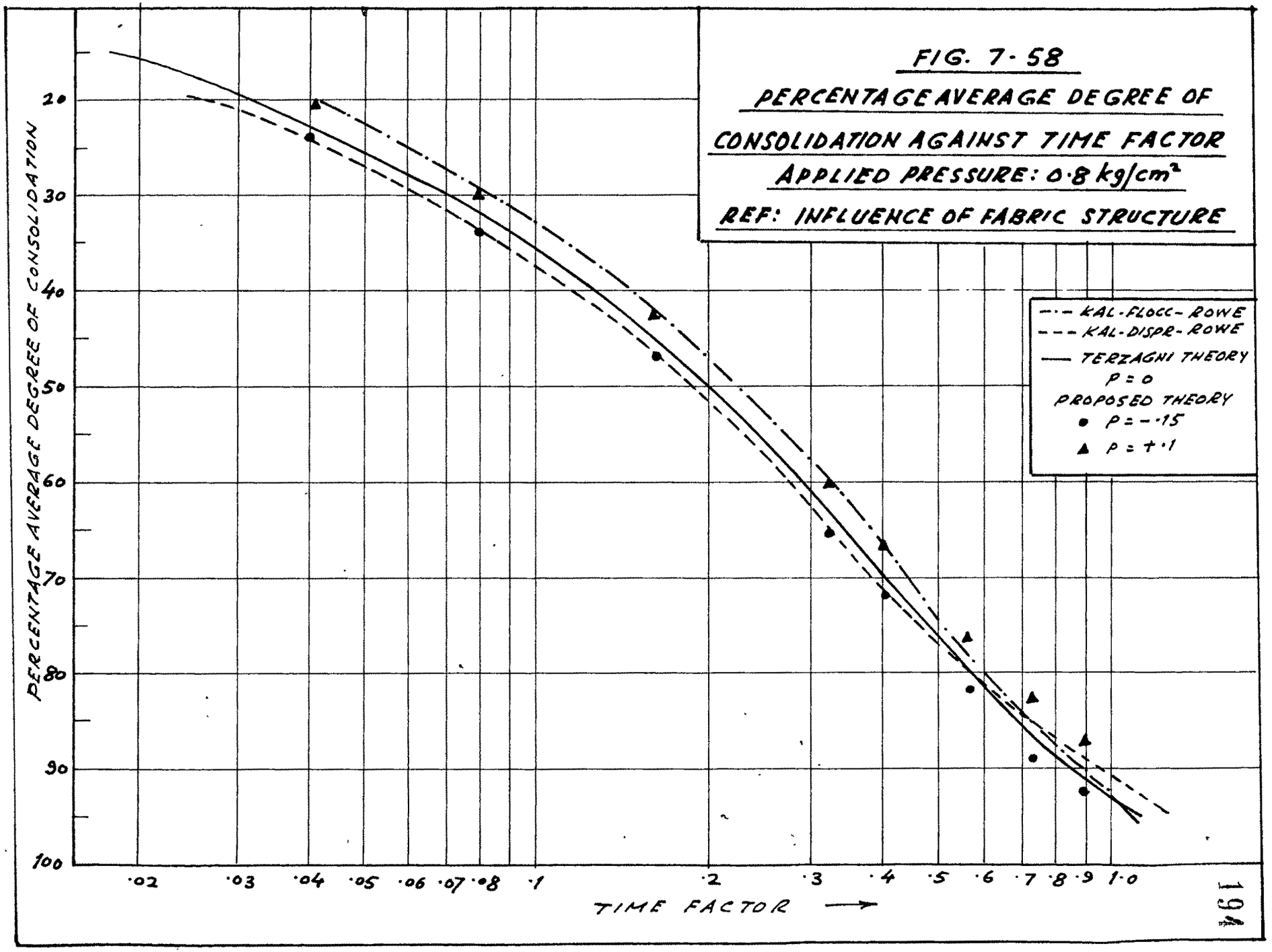
FIG. 7·58
PERCENTAGE AVERAGE DEGREE OF CONSOLIDATION AGAINST TIME FACTOR
APPLIED PRESSURE: 0·8 kg/cm²
REF: INFLUENCE OF FABRIC STRUCTURE
KAL-FLOCC-ROWE
KAL-DISPR-ROWE
TERZAGNI THEORY
P = 0
PROPOSED THEORY
P = −·15
P = +·1
PERCENTAGE AVERAGE DEGREE OF CONSOLIDATION
20
30
40
50
60
70
80
90
100
·02
·03
·04
·05
·06
·07
·08
·1
·2
·3
·4
·5
·6
·7
·8
·9
1·0
TIME FACTOR →

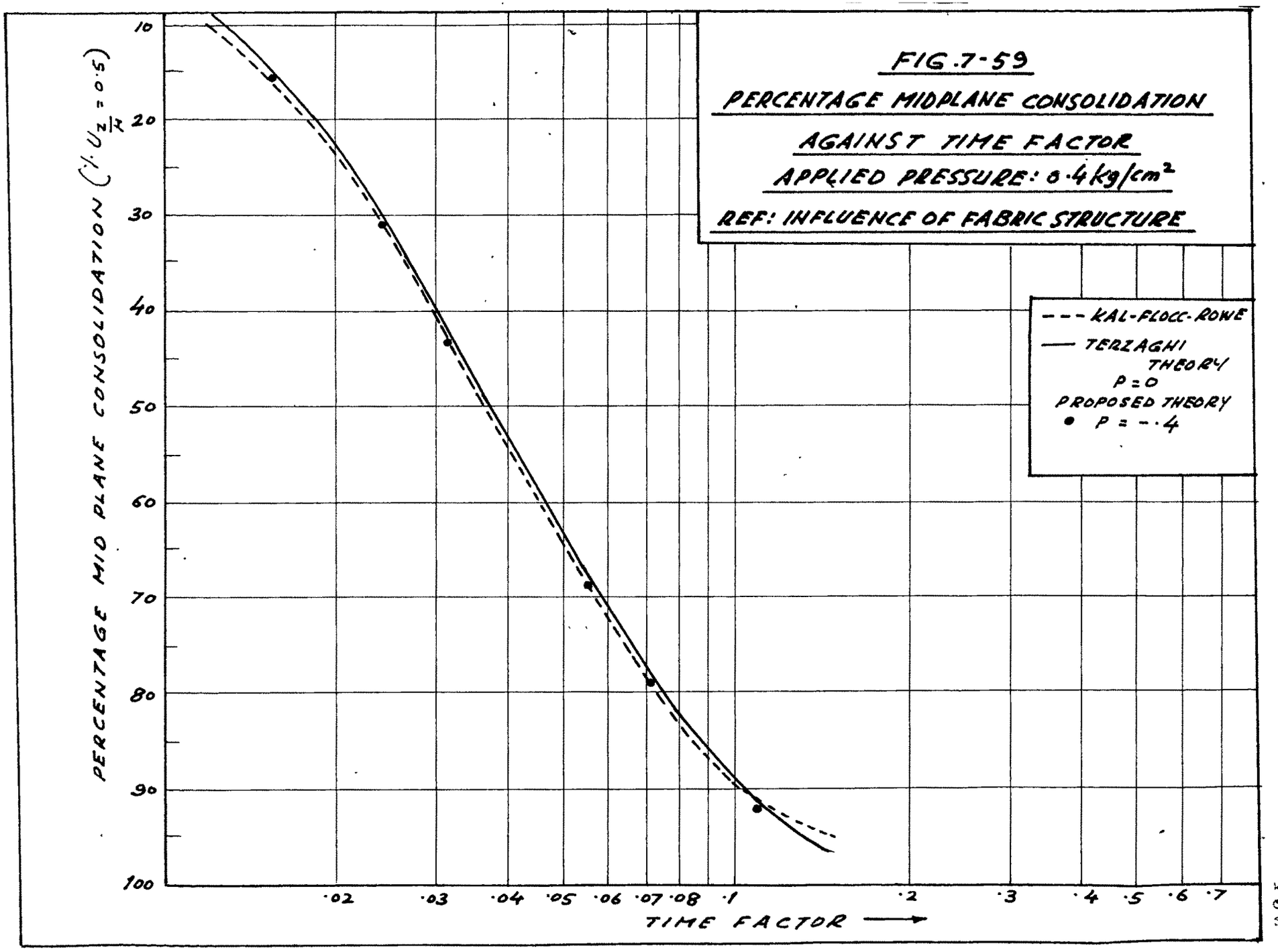
FIG.7-59
PERCENTAGE MIDPLANE CONSOLIDATION
AGAINST TIME FACTOR
APPLIED PRESSURE: 0·4 kg/cm²
REF: INFLUENCE OF FABRIC STRUCTURE
--- KAL-FLOCC-ROWE
— TERZAGHI THEORY
P = 0
PROPOSED THEORY
● P = -·4
PERCENTAGE MID PLANE CONSOLIDATION (% $U_{z/2}$ = 0·5)
10
20
30
40
50
60
70
80
90
100
·02
·03
·04
·05
·06
·07
·08
·1
·2
·3
·4
·5
·6
·7
TIME FACTOR

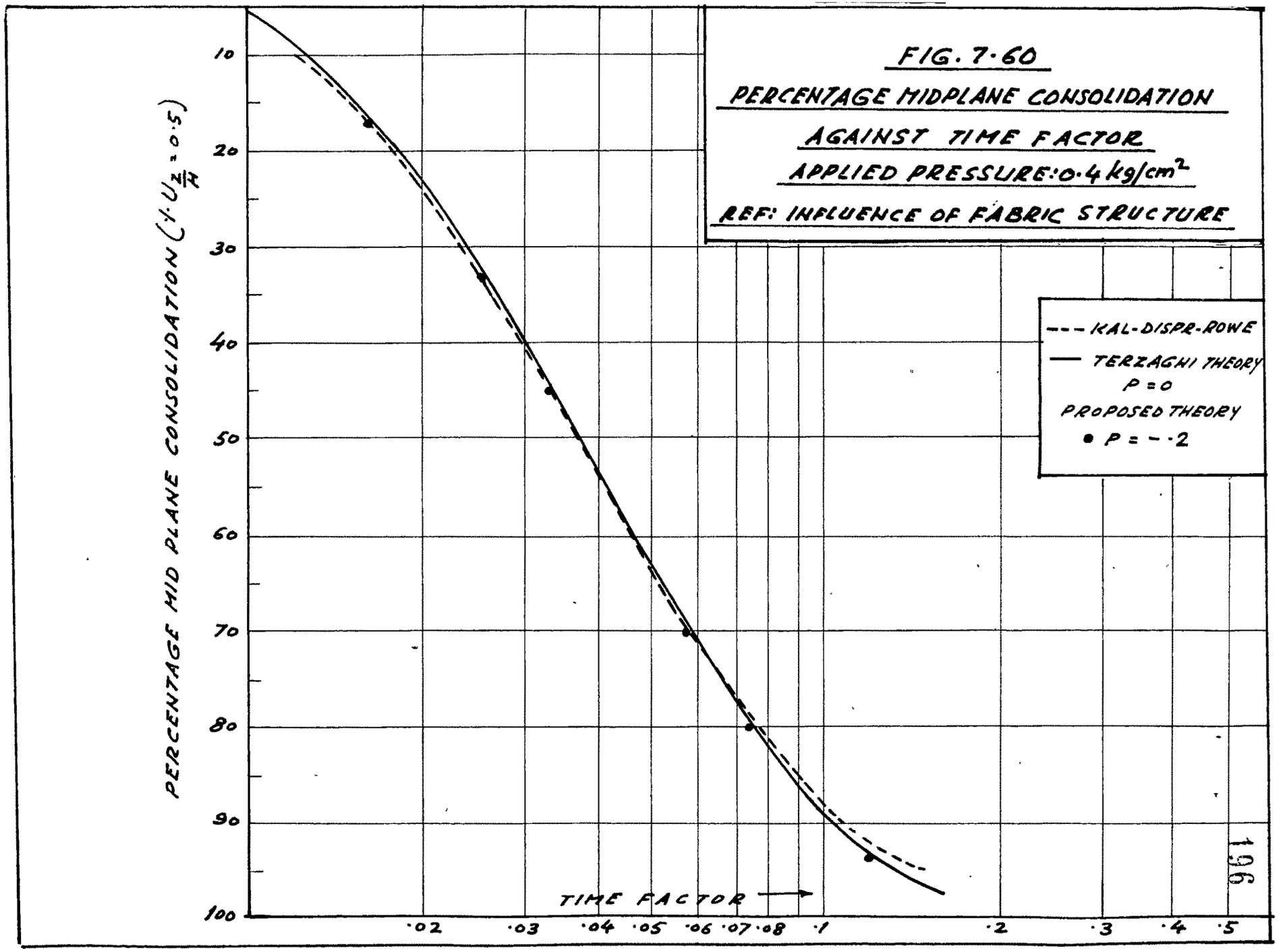
FIG. 7·60
PERCENTAGE MIDPLANE CONSOLIDATION
AGAINST TIME FACTOR
APPLIED PRESSURE: 0·4 kg/cm²
REF: INFLUENCE OF FABRIC STRUCTURE
--- KAL-DISPR-ROWE
— TERZAGHI THEORY
P = 0
PROPOSED THEORY
● P = −·2
PERCENTAGE MID PLANE CONSOLIDATION (% $U_{\frac{z}{H}=0.5}$)
10
20
30
40
50
60
70
80
90
100
TIME FACTOR →
·02
·03
·04
·05
·06
·07
·08
·1
·2
·3
·4
·5

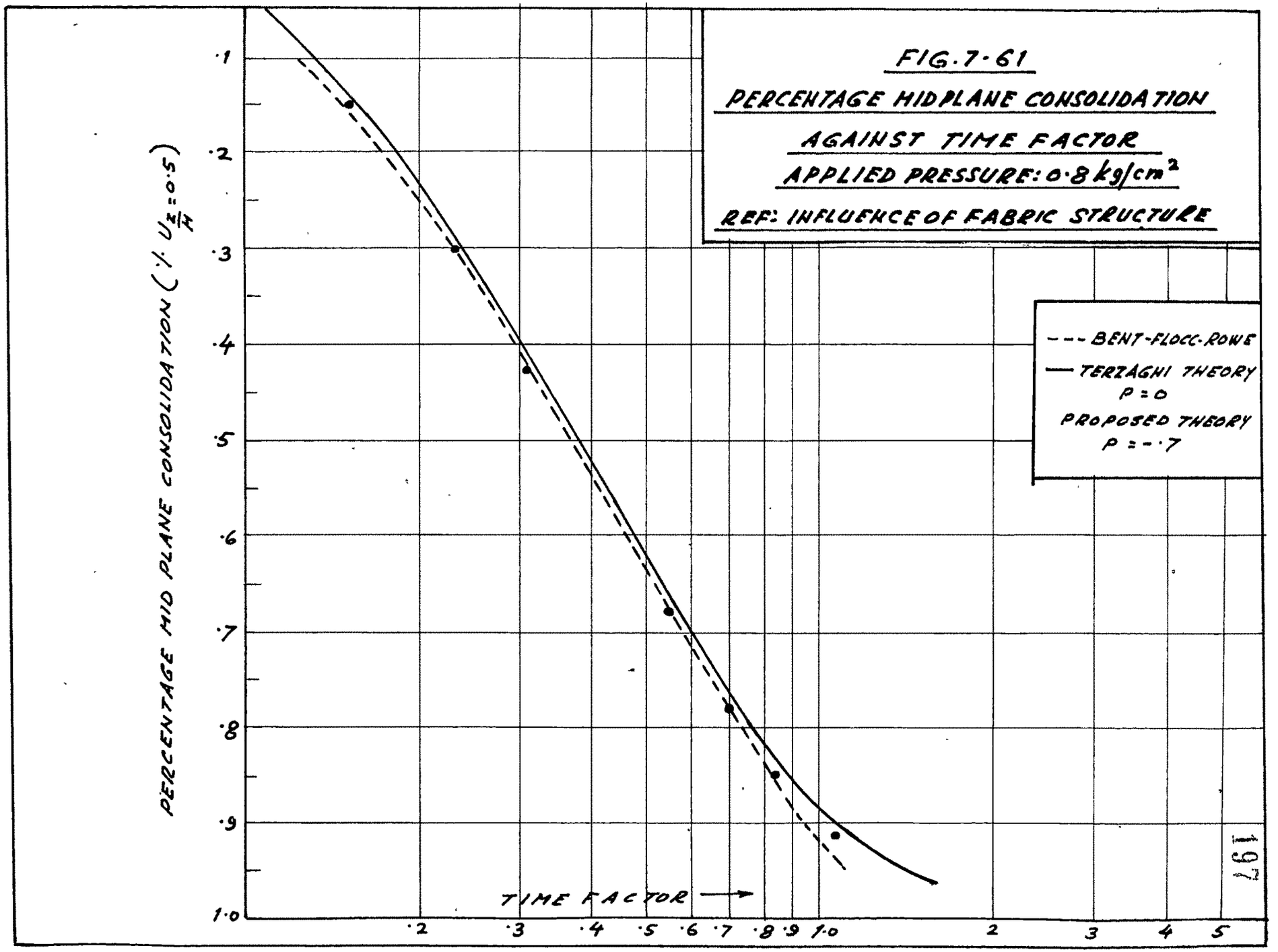
FIG. 7·61
PERCENTAGE MIDPLANE CONSOLIDATION
AGAINST TIME FACTOR
APPLIED PRESSURE: 0·8 kg/cm²
REF: INFLUENCE OF FABRIC STRUCTURE
--- BENT-FLOCC-ROWE
— TERZAGHI THEORY
P = 0
PROPOSED THEORY
P = -·7
PERCENTAGE MID PLANE CONSOLIDATION (% $U_{\frac{z}{H}=0.5}$)
·1
·2
·3
·4
·5
·6
·7
·8
·9
1·0
TIME FACTOR →
·2
·3
·4
·5
·6
·7
·8
·9
1·0
2
3
4
5

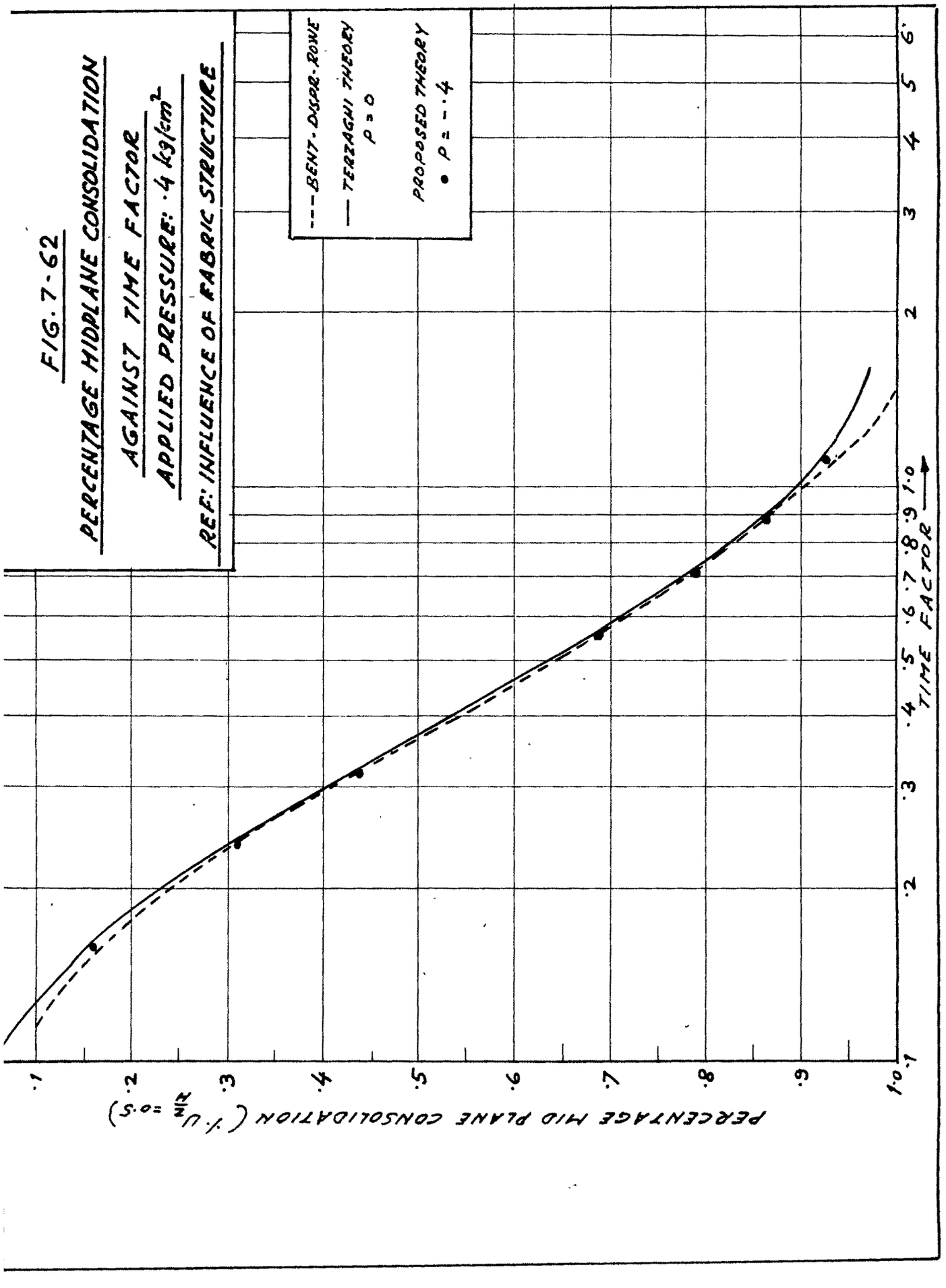
FIG. 7-62
PERCENTAGE HIDPLANE CONSOLIDATION
AGAINST TIME FACTOR
APPLIED PRESSURE: ·4 kg/cm²
REF: INFLUENCE OF FABRIC STRUCTURE
---BENT-DISPE-RONE
— TERZAGHI THEORY
ρ = 0
PROPOSED THEORY
• ρ = -·4
PERCENTAGE MID PLANE CONSOLIDATION (% U_MP = 0·5)
TIME FACTOR
·1
·2
·3
·4
·5
·6
·7
·8
·9
1·0
1·1
2
3
4
5
6

curve indicates that for dispersed clays it lies nearer to the classical curve, while for flocculated clays it falls a little farther away from it. The overall effect of either the dispersing agent or the flocculating agent is not seen to be prominent. The deviations for flocculated kaolinite and Bentonite are 2.2% and 4.5% respectively whereas for dispersed kaolinite and Bentonite the deviations are 1% and 5.5%. At higher loads the trend is to move towards the Terzaghi classical curve. Experimental plots based on mid plane pore pressure measurement show very little deviation with the Terzaghi theory and fit exactly with relevant P values.

Discussion :

The explanation to the various observed characteristics as a result of flocculation and dispersion in clays can be derived from link bond considerations. In developed flocculated structure 'edge to surface'or 'edge to edge', the proximity of link bonds is more prominent. When a load is applied over this structure, some resistance is offered by this link bonds and load has to overcome the edge to face or edge to edge attraction to alter the packing geometry. During this resistanc deformation can be regarded in the stage of 'Microcompressibility' and specific deformation can be expressed as a slow decay. As soon as local breakdown commences, the initial

resistance to compression diminishes and the rate of consolidation will increase to some extent. Progressive deformation can be visualised as 'Macrocompressibility' in which the deformation is caused by sliding and lifting of plate shaped particles with the further breaking up of link bonds and pressing out of the pore water. At these stage it reaches a semioriented equilibrium position altering the initial packing geometry, which loosens the 'interfacial grip' of adsorbed water at links of plate-shaped particle. This 'Microcompressibility' and 'interfacial grip' at links of plate shaped clay particles have no relevance under high engineering stresses thereby exhibiting very little initial resistance to compression. In a initially dispersed developed structure sample at liquid limit has a random oriented structure with semiparallel alignment of plate-shaped particles, but not in close proximity. Hence under light loading some resistance to compression is mobilized from both the structural matrix and the interaction of forces due to 'interfacial tension' between adsorbed and free pore water as described by Rosenquist (1959). Further application of load will cause a decrease in the particle spacing accompanied by some reorientation of particles reaching a state of more or less 'face to face' configuration. Therefore, under higher applied loads, it has little effect on

rate of consolidation. It can be inferred that 'Micro-compressibility' is decreasing from flocculent to dispersed structure. Its effect on rate of consolidation is also reducing from lighter loads to higher loads.

In flocculated Bentonite clay, due to the somewhat stronger link bond sometime for breakdown is required than for flocculated kaolinite clay which gives relatively much lower values of c_v at any percentage of consolidation. The high order of floc units in random orientation of Bentonite at liquid limit makes dispersing chemical not much effective, though c_v value is seen to increase upto some percentage of consolidation after which c_v either remains constant or decreases. It can be argued that dispersing agent is effective only in changing the random arrangement of particles in individual floc to semioriented arrangement leading to a decrease in the value of c_v with the increase in the pressure.

The resistance during microcompressibility occuring under light loads in flocculated clays is clearly reflected in the void ratio-effective pressure relationship and compression index against average effective pressure curve. The distinct characteristic revealed in flocculated Bentonite clay is the evidence of pronounced resistance. An almost contrary behaviour in dispersed clays is due to practically no resistance, the deformation being thus of only

microcompressibility nature. The higher degree of secondary compression in flocculated clays under lighter loads can be expected as there can be a possibility of further orientation of the structure as the compression proceeds. On the other hand in a dispersed structure the nonflocculated orientation does not have strong bonds as expected in flocculated structure. It is, therefore, possible to reach 100% consolidation much earlier than would be the case for initially flocculated structure. On the same background it can be argued that the dispersing agent tones down the effect of the physico-chemical forces while flocculating agent activates these forces. This offers the explanation to the observation that the behaviour of the remoulded samples in which structure is expected to be dispersed fits well with the Terzaghi theory while the larger deviation in flocculated clays is due to activation of physico-chemical forces ignored in the classical theory.

7.3.3. Degree of Saturation

Refer Figures 7.63 to 7.80 which are produced from the parent plots of Figures H.55 to H.76 reported in Appendix H of Volume II.

Analysis :

(i) Co-efficient of consolidation against percentage degree of consolidation.
(Figures 7.63 to 7.67)

In the kaolinite and Bentonite samples compacted either at

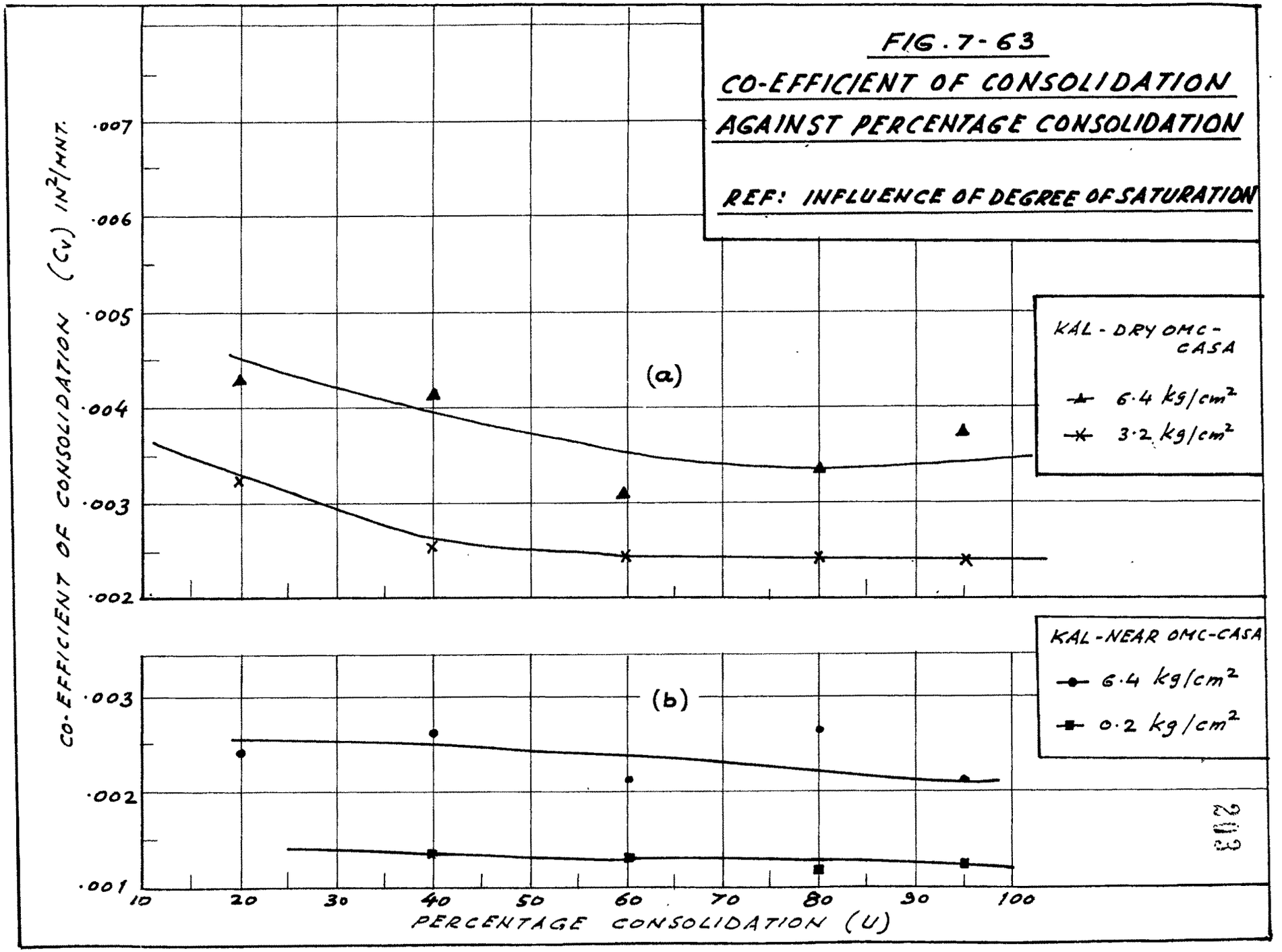
FIG. 7-63
CO-EFFICIENT OF CONSOLIDATION AGAINST PERCENTAGE CONSOLIDATION
REF: INFLUENCE OF DEGREE OF SATURATION
CO-EFFICIENT OF CONSOLIDATION (Cv) IN²/MNT.
.007
.006
.005
.004
.003
.002
(a)
KAL - DRY OMC - CASA
6·4 kg/cm²
3·2 kg/cm²
.003
.002
.001
(b)
KAL - NEAR OMC-CASA
6·4 kg/cm²
0·2 kg/cm²
10
20
30
40
50
60
70
80
90
100
PERCENTAGE CONSOLIDATION (U)
2112

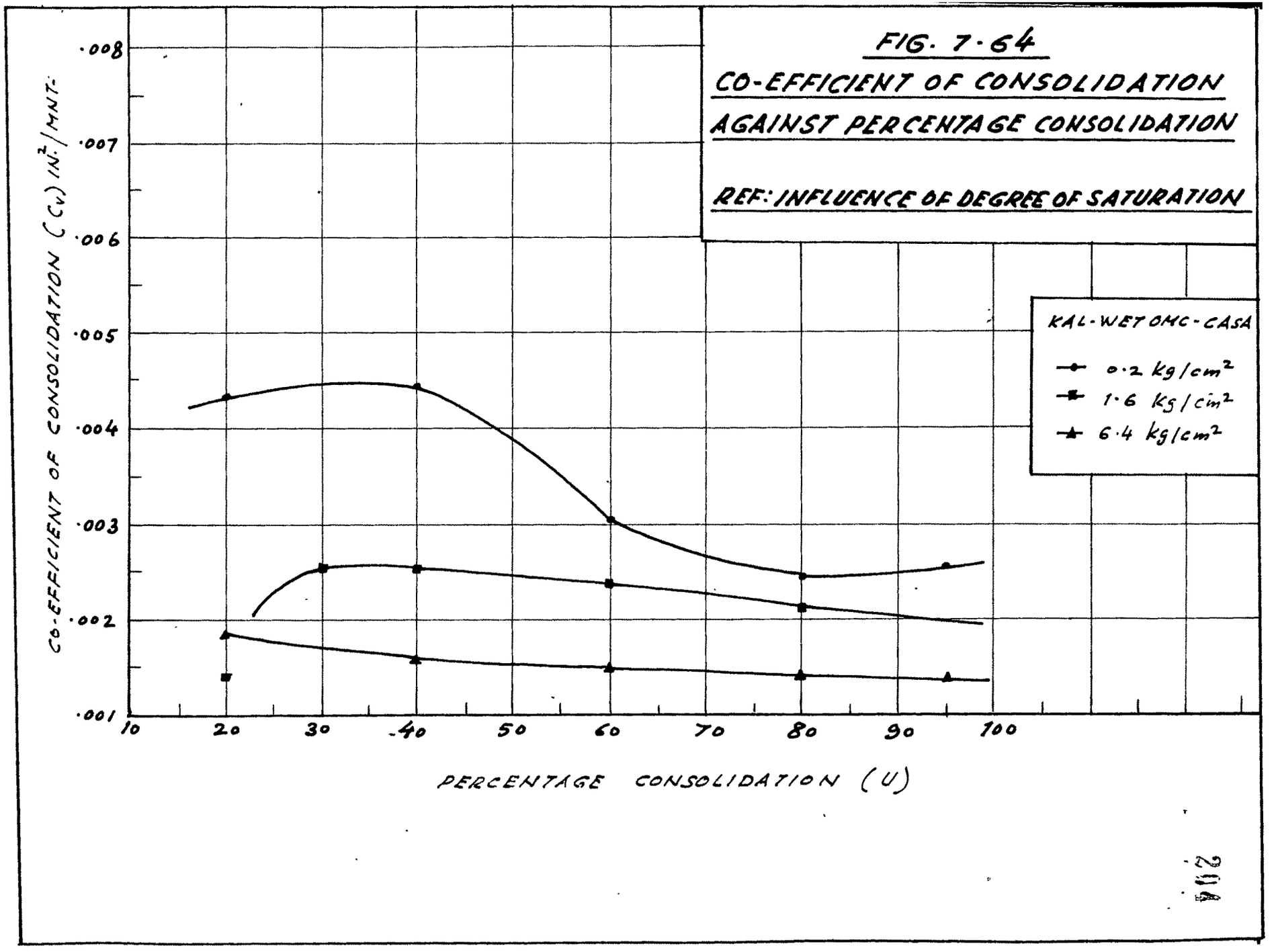
FIG. 7·64
CO-EFFICIENT OF CONSOLIDATION AGAINST PERCENTAGE CONSOLIDATION
REF: INFLUENCE OF DEGREE OF SATURATION
KAL-WET OMC-CASA
0·2 kg/cm²
1·6 kg/cm²
6·4 kg/cm²
CO-EFFICIENT OF CONSOLIDATION (Cv) IN.²/MNT.
·008
·007
·006
·005
·004
·003
·002
·001
10
20
30
40
50
60
70
80
90
100
PERCENTAGE CONSOLIDATION (U)

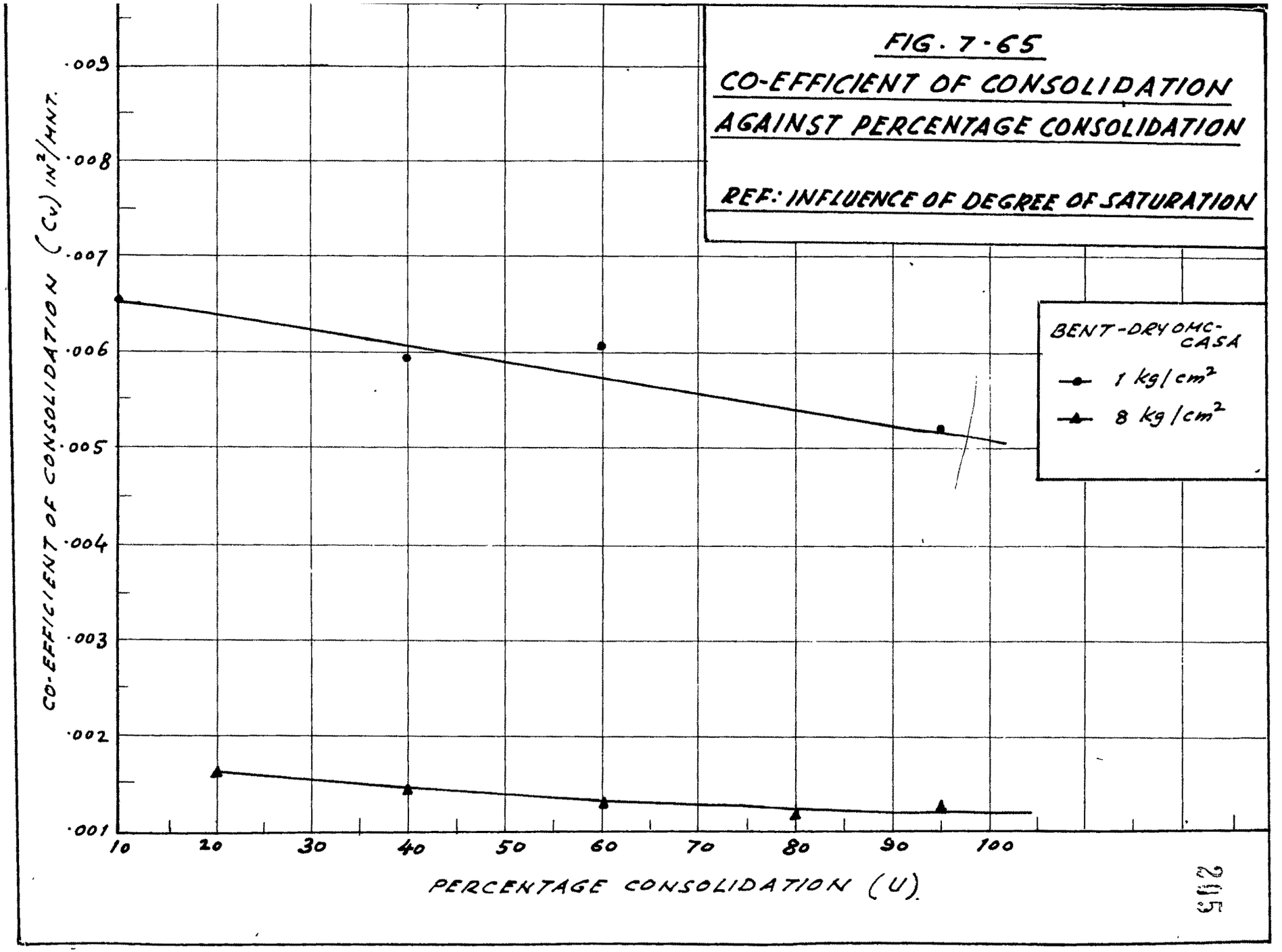
FIG. 7-65
CO-EFFICIENT OF CONSOLIDATION AGAINST PERCENTAGE CONSOLIDATION
REF: INFLUENCE OF DEGREE OF SATURATION
BENT-DRY OMC-CASA
1 kg/cm²
8 kg/cm²
CO-EFFICIENT OF CONSOLIDATION (Cv) IN²/MNT.
.009
.008
.007
.006
.005
.004
.003
.002
.001
10
20
30
40
50
60
70
80
90
100
PERCENTAGE CONSOLIDATION (U)
5112

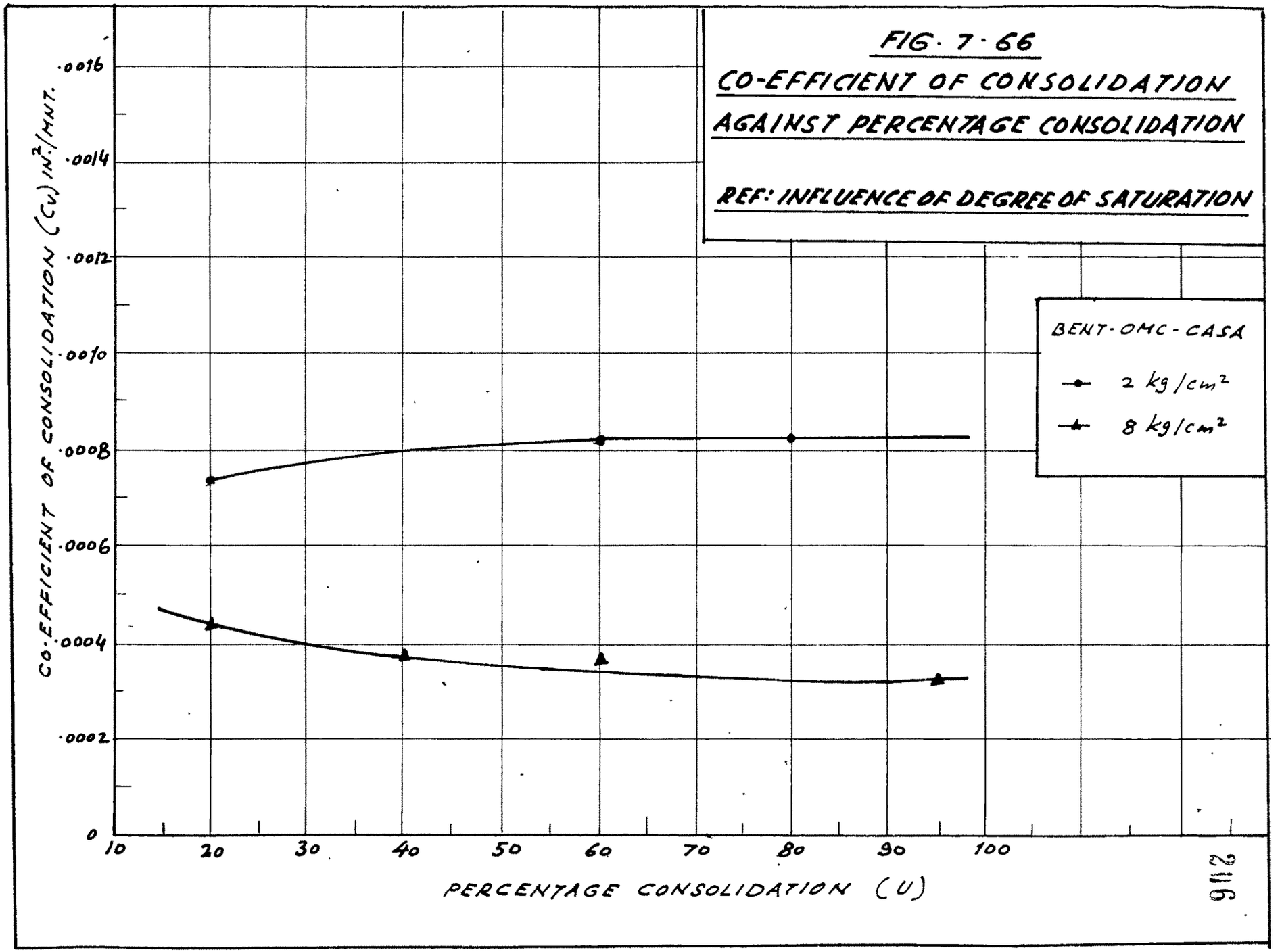
FIG. 7.66
CO-EFFICIENT OF CONSOLIDATION
AGAINST PERCENTAGE CONSOLIDATION
REF: INFLUENCE OF DEGREE OF SATURATION
BENT-OMC-CASA
2 kg/cm²
8 kg/cm²
CO-EFFICIENT OF CONSOLIDATION (Cv) IN.²/MNT.
.0016
.0014
.0012
.0010
.0008
.0006
.0004
.0002
0
10
20
30
40
50
60
70
80
90
100
PERCENTAGE CONSOLIDATION (U)
9112

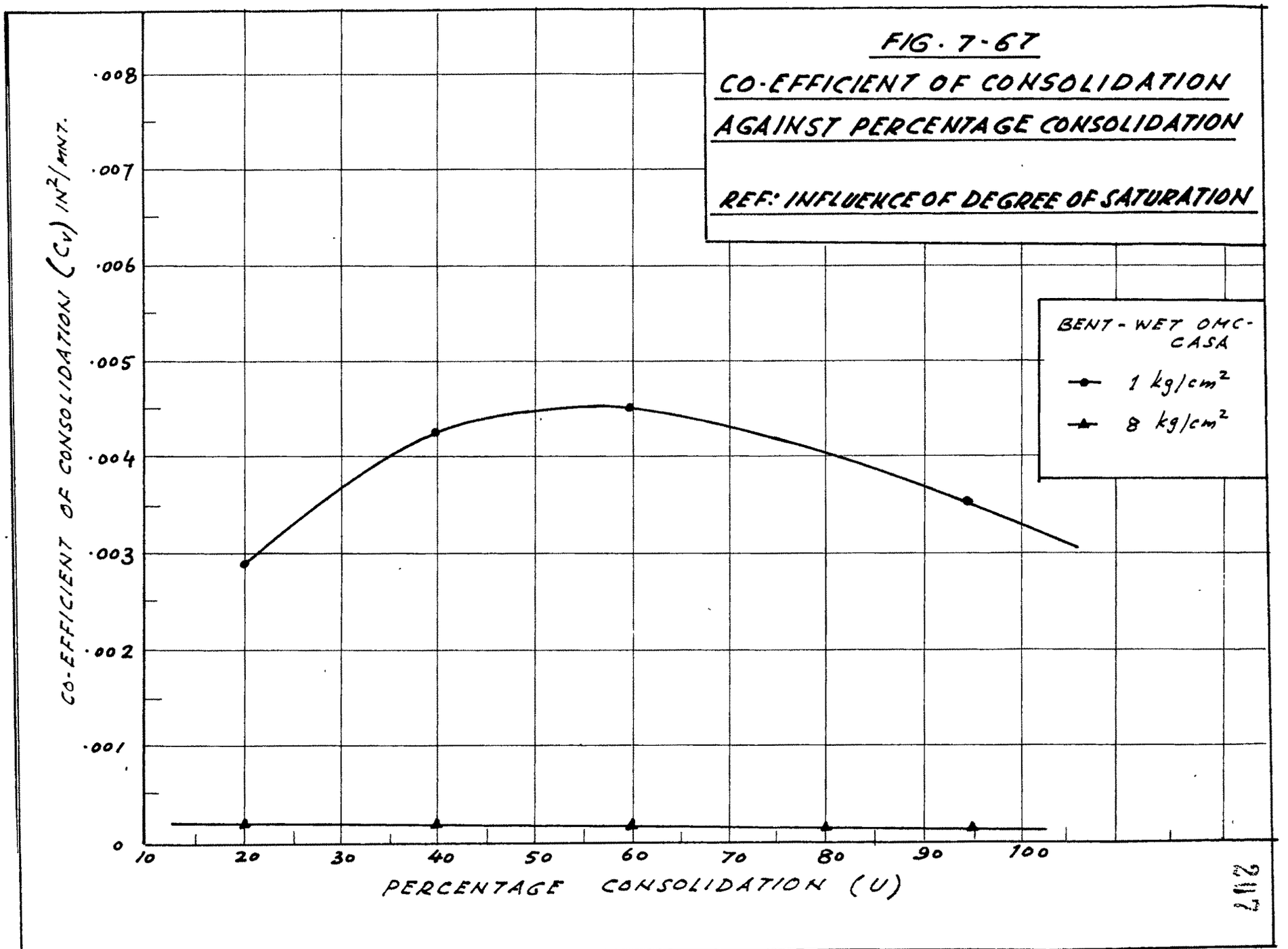
FIG. 7-67
CO-EFFICIENT OF CONSOLIDATION
AGAINST PERCENTAGE CONSOLIDATION
REF: INFLUENCE OF DEGREE OF SATURATION
BENT - WET OMC - CASA
1 kg/cm²
8 kg/cm²
CO-EFFICIENT OF CONSOLIDATION (Cv) IN²/MNT.
·008
·007
·006
·005
·004
·003
·002
·001
0
10
20
30
40
50
60
70
80
90
100
PERCENTAGE CONSOLIDATION (U)
2112

near OMC or at dry side of OMC the rate of consolidation is seen to be slightly decreasing eventually flattening to a constant value. No consolidation is noticed upto 1.6 kg/cm^2 for samples compacted at dry side of OMC. The characteristics of kaolinite and Bentonite compacted at wetside of OMC are similar showing initially an increase and then a decrease in the rate of consolidation tailing out to a constant value under light loads. The rate of consolidation at higher loads remains constant throughout the process of consolidation.

(ii) Co-efficient of consolidation against applied effective pressure.
(Figures 7.68 to 7.69).

Kaolinite sample shows a slight increase in the value of co-efficient of consolidation whereas Bentonite sample shows a continuous decrease irrespective of the moulding water content. The rate of consolidation increases in the order of samples compacted at wetside of OMC, at near OMC and at dry side of OMC.

(iii) Compression index against applied average effective pressure.
(Figure 7.70 and 7.71).

It is evident from the experimental curve that both kaolinite and Bentonite clays represent a same family, the former depicting a flatter curves while the later steeper curves. At higher average effective pressure both show a

FIG. 7-68

CO-EFFICIENT OF CONSOLIDATION AGAINST APPLIED EFFECTIVE PRESSURE

REF: INFLUENCE OF DEGREE OF SATURATION

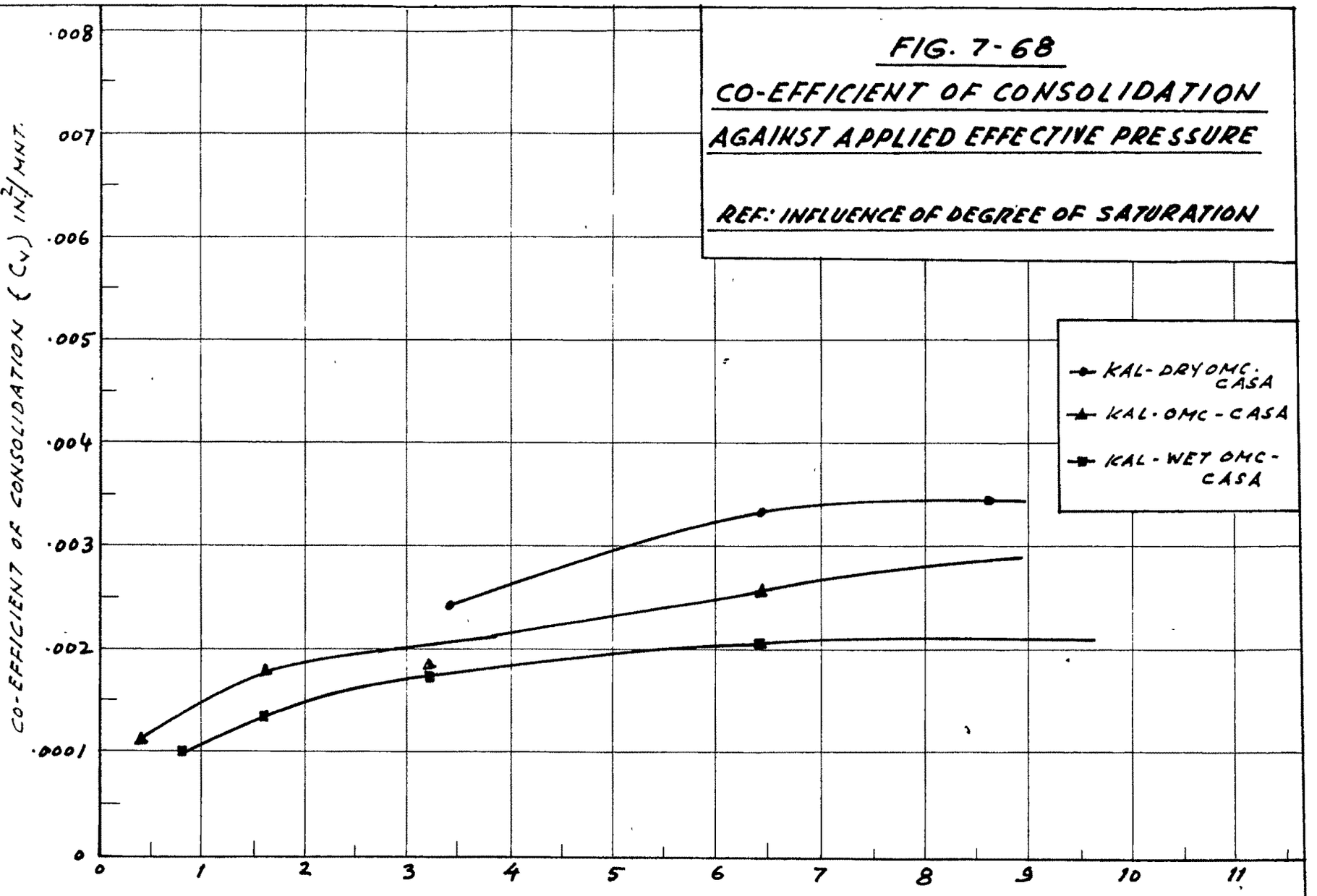

6112

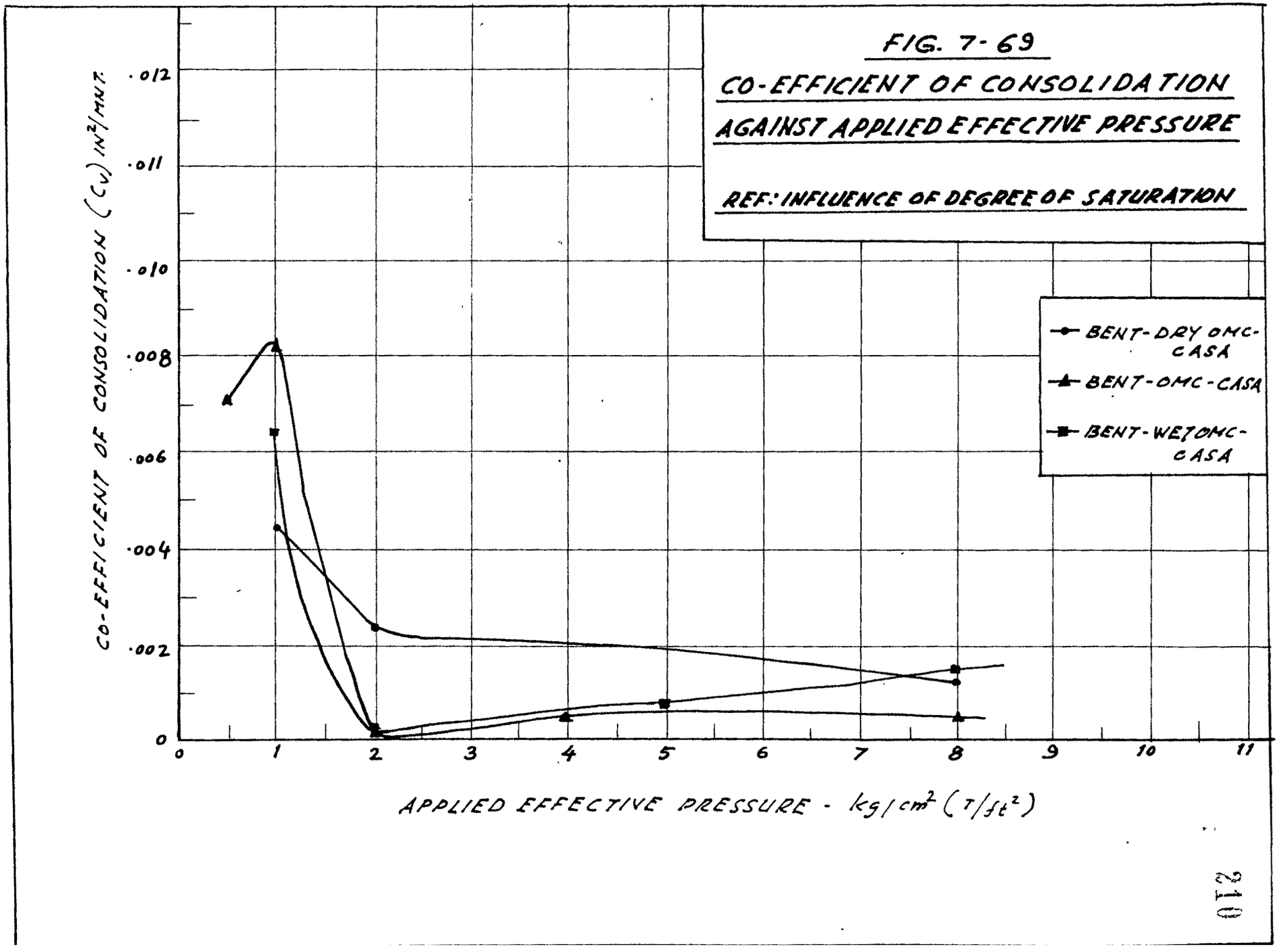
FIG. 7-69
CO-EFFICIENT OF CONSOLIDATION AGAINST APPLIED EFFECTIVE PRESSURE
REF: INFLUENCE OF DEGREE OF SATURATION
BENT-DRY OMC-CASA
BENT-OMC-CASA
BENT-WET OMC-CASA
CO-EFFICIENT OF CONSOLIDATION (C_v) IN^2/MIN.
.012
.011
.010
.008
.006
.004
.002
0
0
1
2
3
4
5
6
7
8
9
10
11
APPLIED EFFECTIVE PRESSURE - kg/cm^2 (T/ft^2)

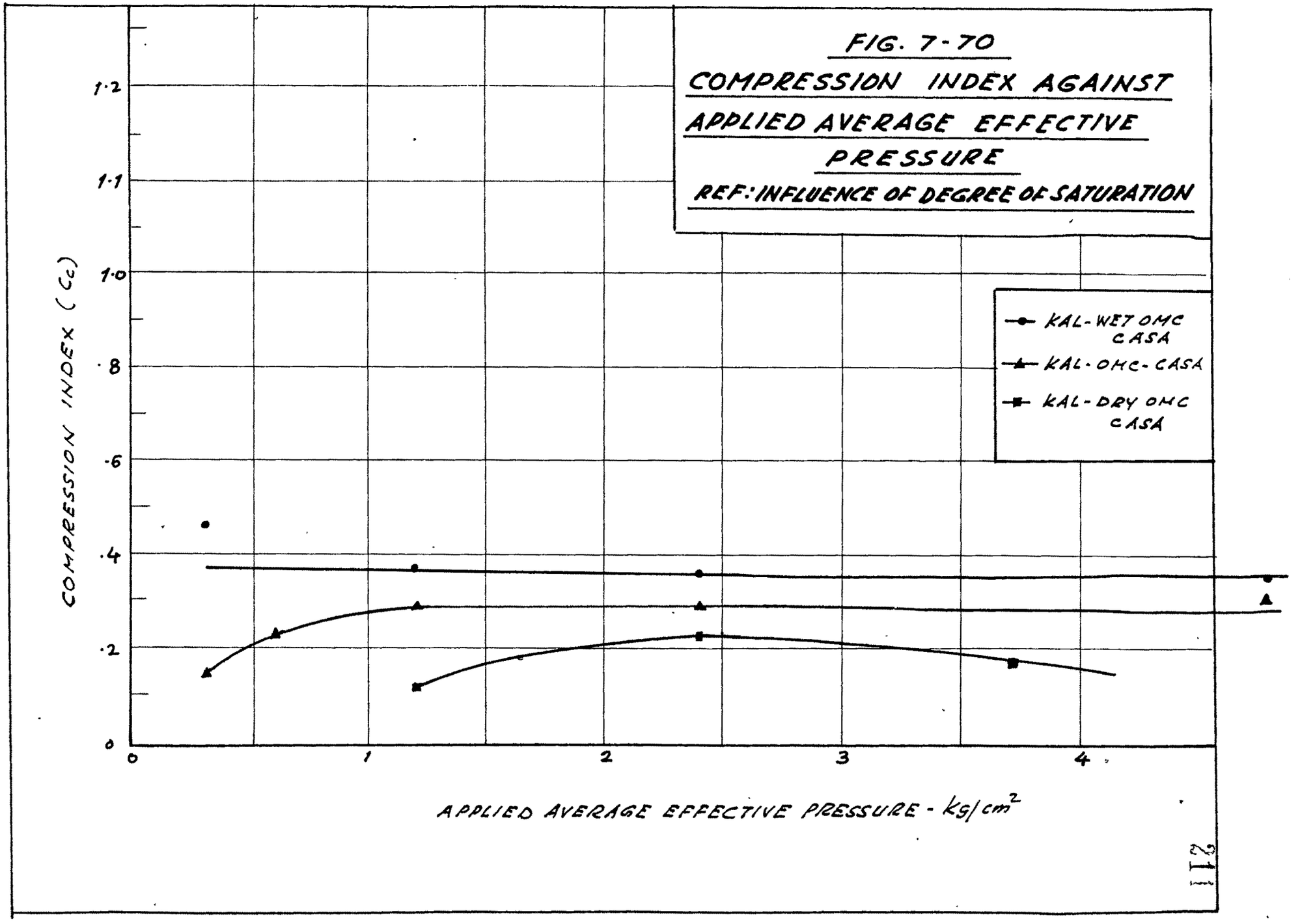
FIG. 7-70
COMPRESSION INDEX AGAINST APPLIED AVERAGE EFFECTIVE PRESSURE
REF: INFLUENCE OF DEGREE OF SATURATION
KAL-WET OMC CASA
KAL-OMC-CASA
KAL-DRY OMC CASA
COMPRESSION INDEX (C_c)
1·2
1·1
1·0
·8
·6
·4
·2
0
0
1
2
3
4
APPLIED AVERAGE EFFECTIVE PRESSURE - kg/cm²

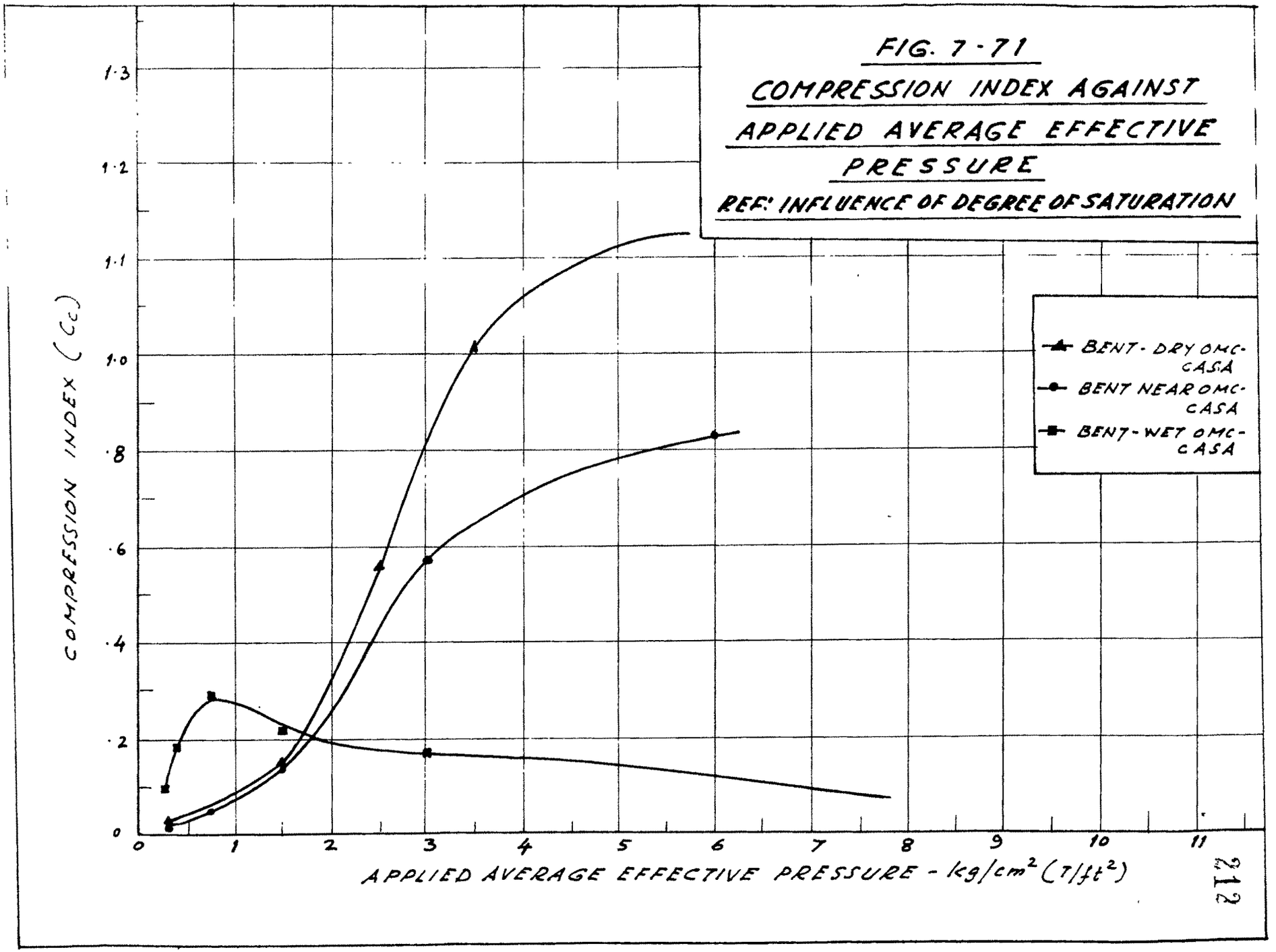
FIG. 7·71
COMPRESSION INDEX AGAINST APPLIED AVERAGE EFFECTIVE PRESSURE
REF: INFLUENCE OF DEGREE OF SATURATION
BENT - DRY OMC - CASA
BENT NEAR OMC - CASA
BENT - WET OMC - CASA
COMPRESSION INDEX (C_c)
1·3
1·2
1·1
1·0
·8
·6
·4
·2
0
0 1 2 3 4 5 6 7 8 9 10 11
APPLIED AVERAGE EFFECTIVE PRESSURE - kg/cm² (T/ft²)

constant compression index.

(iv) Degree of secondary compression against applied effective pressure.
(Figure 7.72 and 7.73).

General tendencies of curves indicate decrease of secondary compression with the increase of pressure in both the clays. In kaolinite and Bentonite samples compacted dry side of OMC show more secondary compression than in the other two cases. In kaolinite the secondary compression shows the following ascending order : sample at wet of OMC side, near OMC, and dry of OMC side, while in Bentonite, secondary compression for near OMC sample and wet side OMC sample shows more or less the same amount of secondary compression.

(v) Parameter 'P' versus applied effective pressure.
(Figure 7.74 and Figures 7.75 to 7.80)

Sample at dry side of OMC and samples at near OMC and wet side of OMC lie on opposite side of the Terzaghi curve in both the clays. Kaolinite at dry side of OMC, wet of OMC and at near OMC show 1.9%, 1.5% and 5.25% deviation from Terzaghi theory. Wet of OMC kaolinite sample fits nearer to the Terzaghi curve than the sample at OMC and the sample at dry of OMC side. Bentonite sample falls comparatively away from Terzaghi than kaolinite. Bentonite clay samples at OMC, wet side of OMC and dry side of OMC show 5%, 2.5% and 3% deviations.

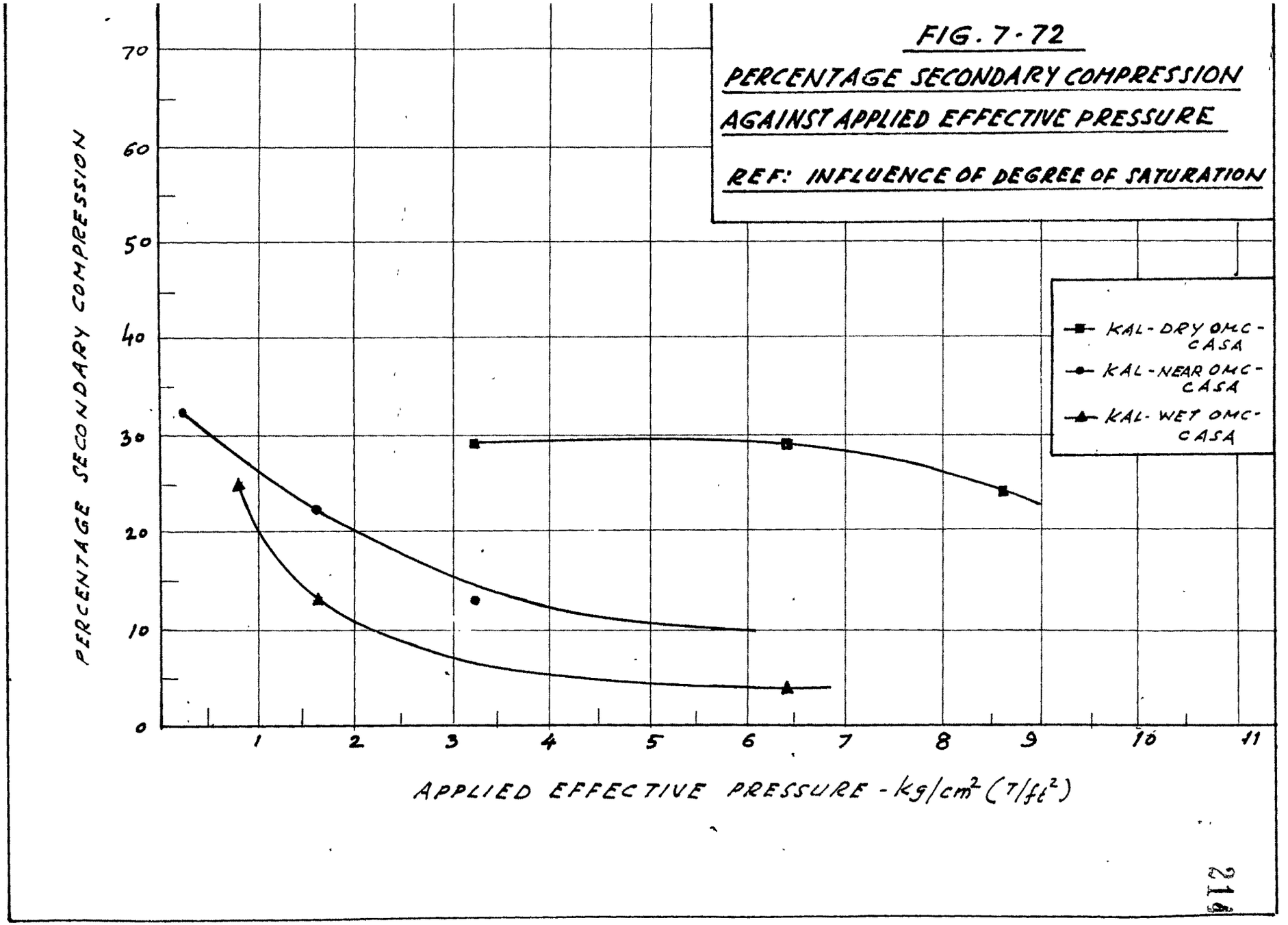
FIG. 7·72
PERCENTAGE SECONDARY COMPRESSION AGAINST APPLIED EFFECTIVE PRESSURE
REF: INFLUENCE OF DEGREE OF SATURATION
KAL - DRY OMC - CASA
KAL - NEAR OMC - CASA
KAL - WET OMC - CASA
PERCENTAGE SECONDARY COMPRESSION
0
10
20
30
40
50
60
70
1
2
3
4
5
6
7
8
9
10
11
APPLIED EFFECTIVE PRESSURE - kg/cm² (T/ft²)

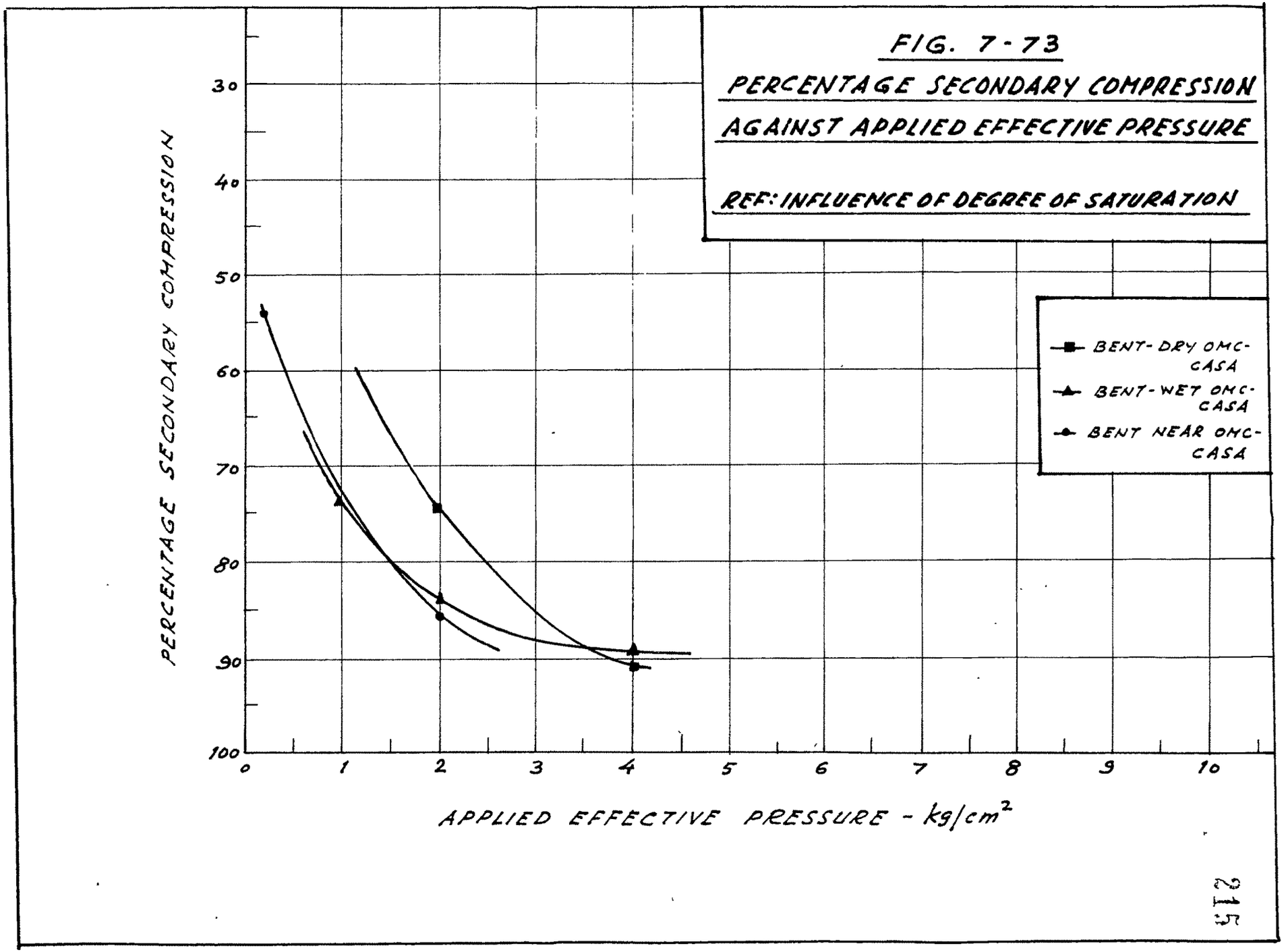
FIG. 7-73
PERCENTAGE SECONDARY COMPRESSION AGAINST APPLIED EFFECTIVE PRESSURE
REF: INFLUENCE OF DEGREE OF SATURATION
BENT- DRY OMC- CASA
BENT- WET OMC- CASA
BENT NEAR OMC- CASA
PERCENTAGE SECONDARY COMPRESSION
30
40
50
60
70
80
90
100
0
1
2
3
4
5
6
7
8
9
10
APPLIED EFFECTIVE PRESSURE - kg/cm²

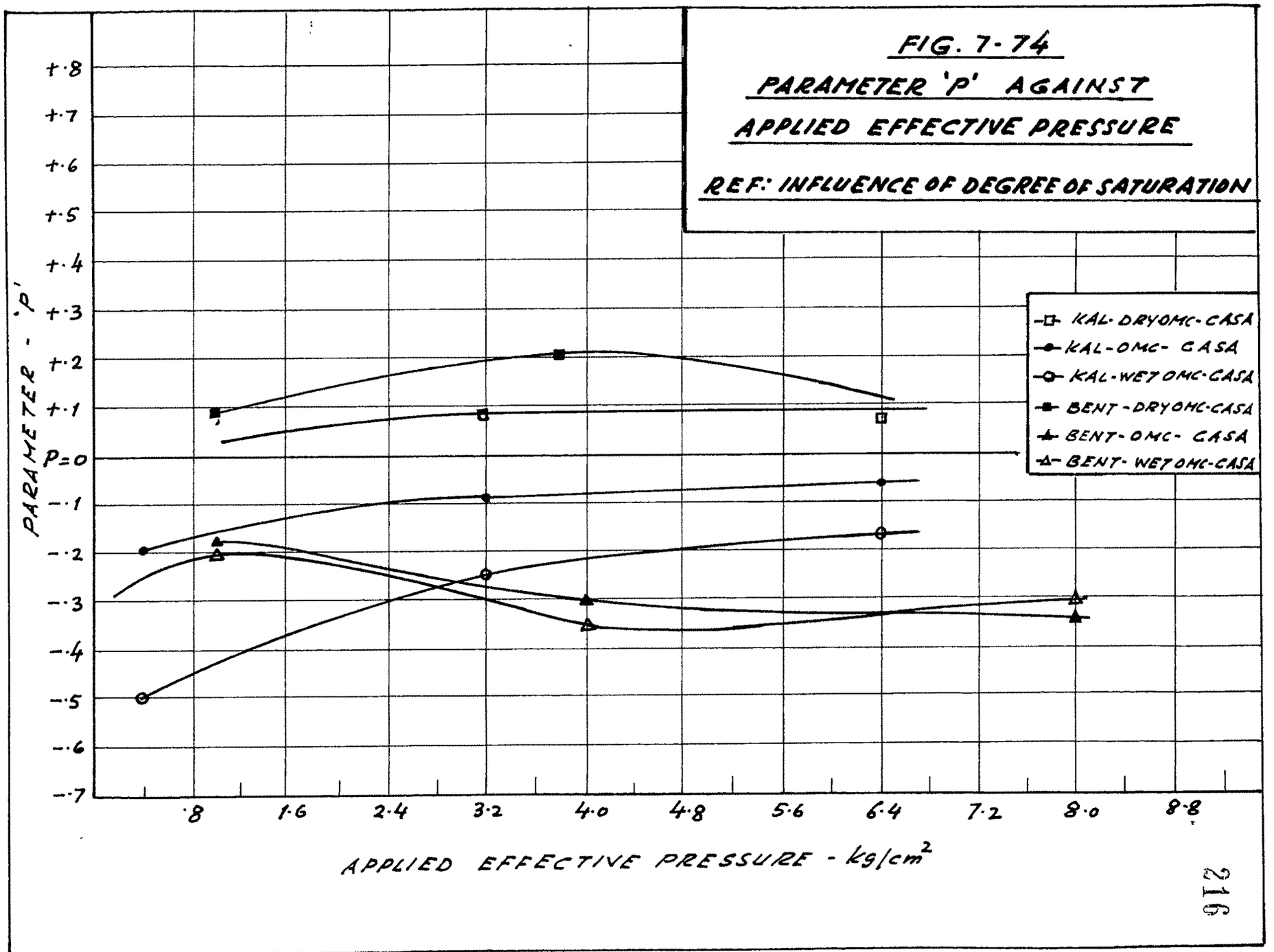
FIG. 7-74
PARAMETER 'P' AGAINST
APPLIED EFFECTIVE PRESSURE
REF: INFLUENCE OF DEGREE OF SATURATION
KAL-DRYOMC-CASA
KAL-OMC-CASA
KAL-WETOMC-CASA
BENT-DRYOMC-CASA
BENT-OMC-CASA
BENT-WETOMC-CASA
PARAMETER - 'P'
+·8
+·7
+·6
+·5
+·4
+·3
+·2
+·1
P=0
-·1
-·2
-·3
-·4
-·5
-·6
-·7
·8
1·6
2·4
3·2
4·0
4·8
5·6
6·4
7·2
8·0
8·8
APPLIED EFFECTIVE PRESSURE - kg/cm²
216

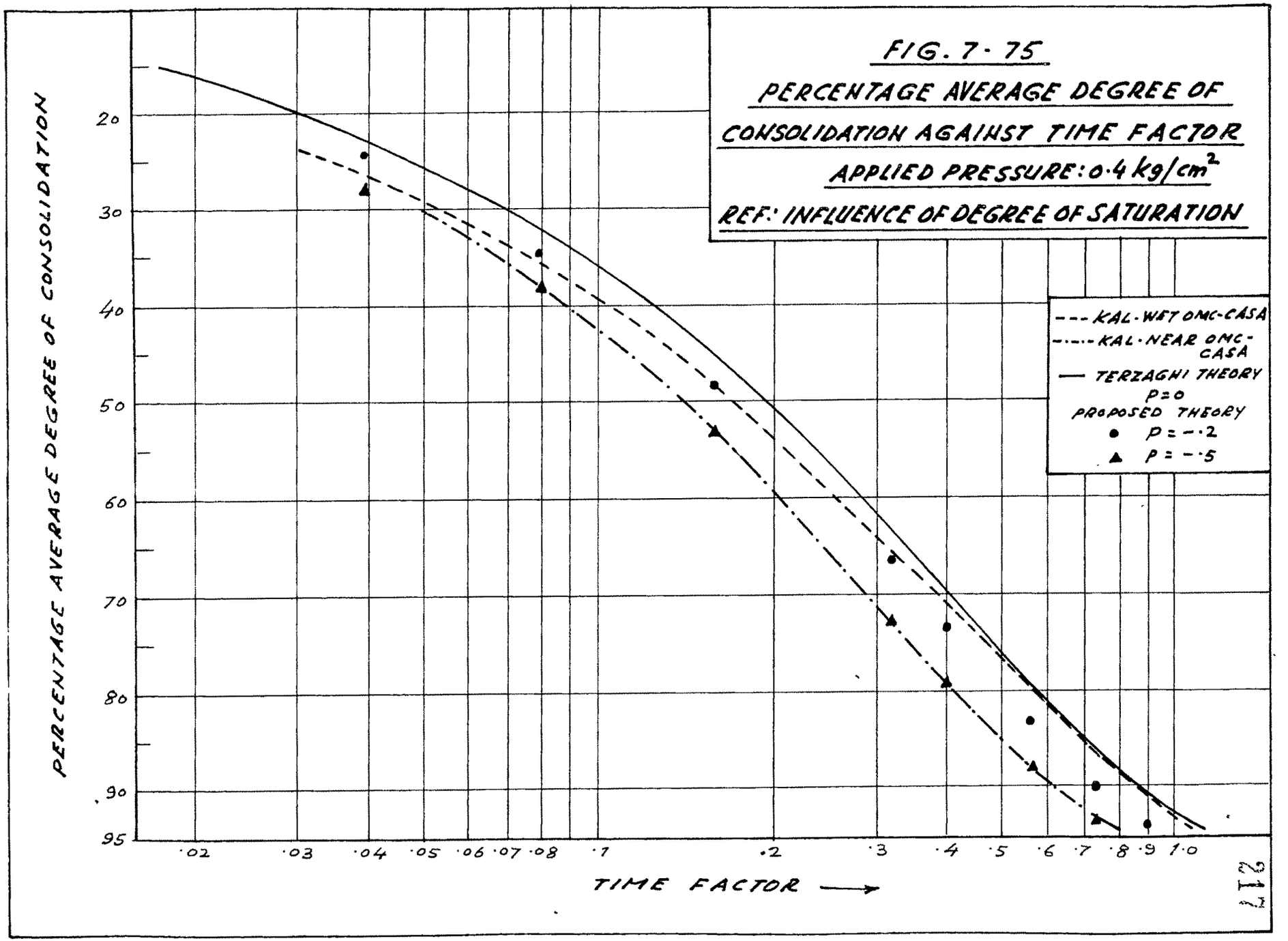
FIG. 7·75
PERCENTAGE AVERAGE DEGREE OF CONSOLIDATION AGAINST TIME FACTOR
APPLIED PRESSURE: 0·4 kg/cm²
REF: INFLUENCE OF DEGREE OF SATURATION
KAL·WET OMC-CASA
KAL·NEAR OMC-CASA
TERZAGHI THEORY
P=0
PROPOSED THEORY
P = −·2
P = −·5
PERCENTAGE AVERAGE DEGREE OF CONSOLIDATION
20
30
40
50
60
70
80
90
95
·02
·03
·04
·05
·06
·07
·08
·1
·2
·3
·4
·5
·6
·7
·8
·9
1·0
TIME FACTOR
212

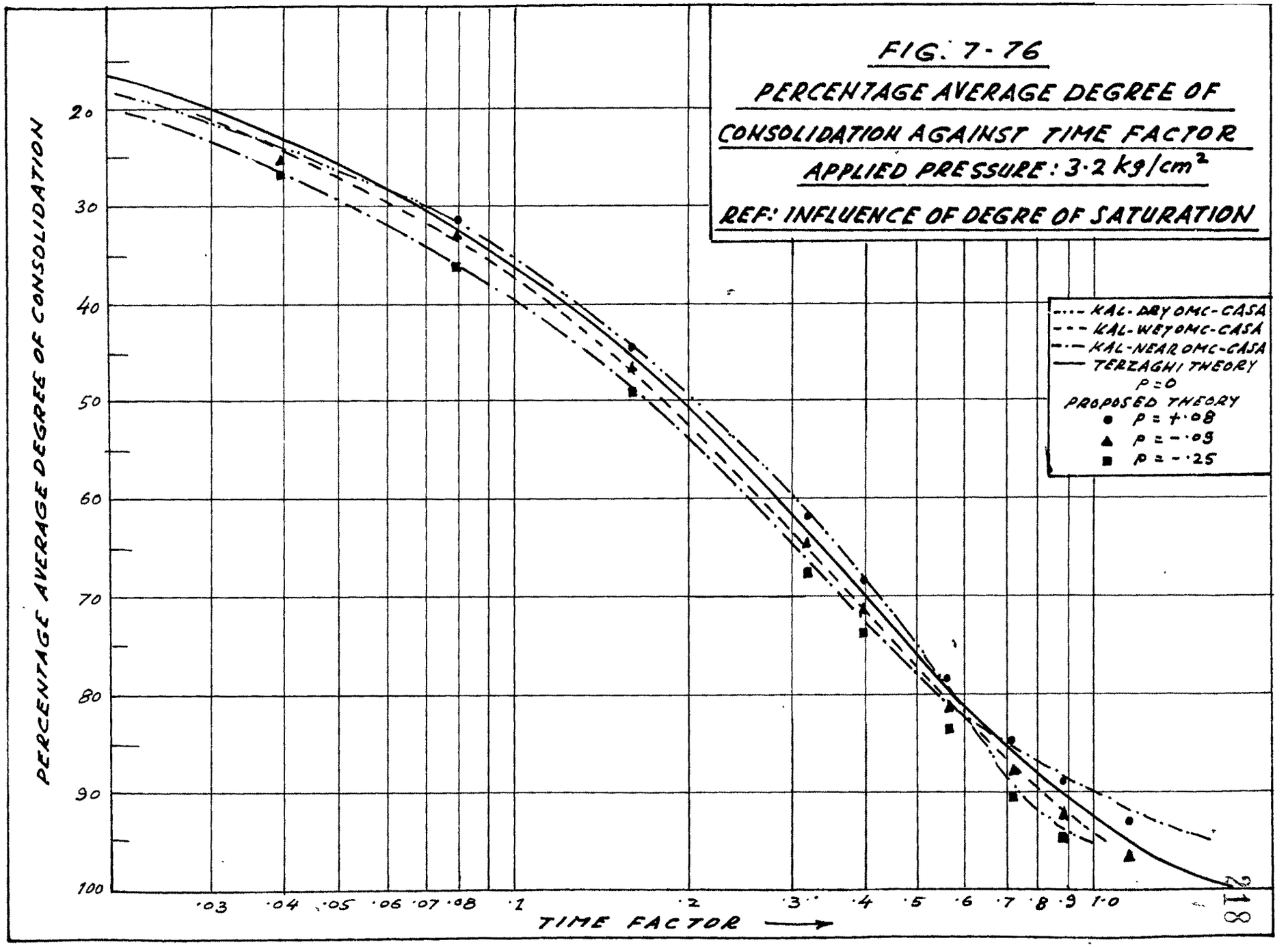
FIG. 7-76
PERCENTAGE AVERAGE DEGREE OF CONSOLIDATION AGAINST TIME FACTOR
APPLIED PRESSURE: 3·2 kg/cm²
REF: INFLUENCE OF DEGRE OF SATURATION
KAL-DRY OMC-CASA
KAL-WET OMC-CASA
KAL-NEAR OMC-CASA
TERZAGHI THEORY
P=0
PROPOSED THEORY
P = +·08
P = -·09
P = -·25
PERCENTAGE AVERAGE DEGREE OF CONSOLIDATION
20
30
40
50
60
70
80
90
100
·03 ·04 ·05 ·06 ·07 ·08 ·1 ·2 ·3 ·4 ·5 ·6 ·7 ·8 ·9 1·0
TIME FACTOR

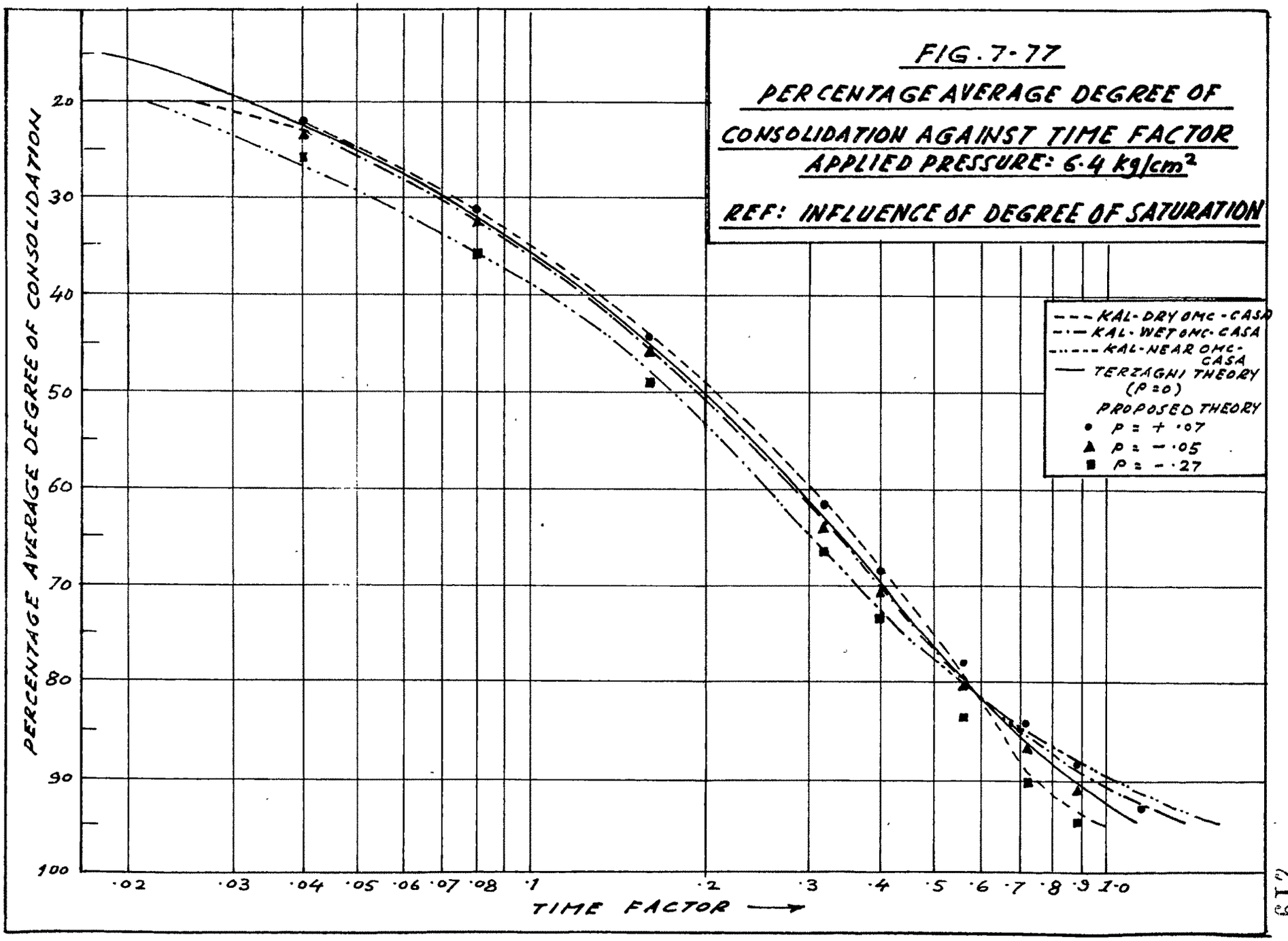
FIG. 7·77
PERCENTAGE AVERAGE DEGREE OF CONSOLIDATION AGAINST TIME FACTOR
APPLIED PRESSURE: 6·4 kg/cm²
REF: INFLUENCE OF DEGREE OF SATURATION
KAL-DRY OMC-CASA
KAL-WET OMC-CASA
KAL-NEAR OMC-CASA
TERZAGHI THEORY (P=0)
PROPOSED THEORY
P = +·07
P = −·05
P = −·27
PERCENTAGE AVERAGE DEGREE OF CONSOLIDATION
20
30
40
50
60
70
80
90
100
·02
·03
·04
·05
·06
·07
·08
·1
·2
·3
·4
·5
·6
·7
·8
·9
1·0
TIME FACTOR →

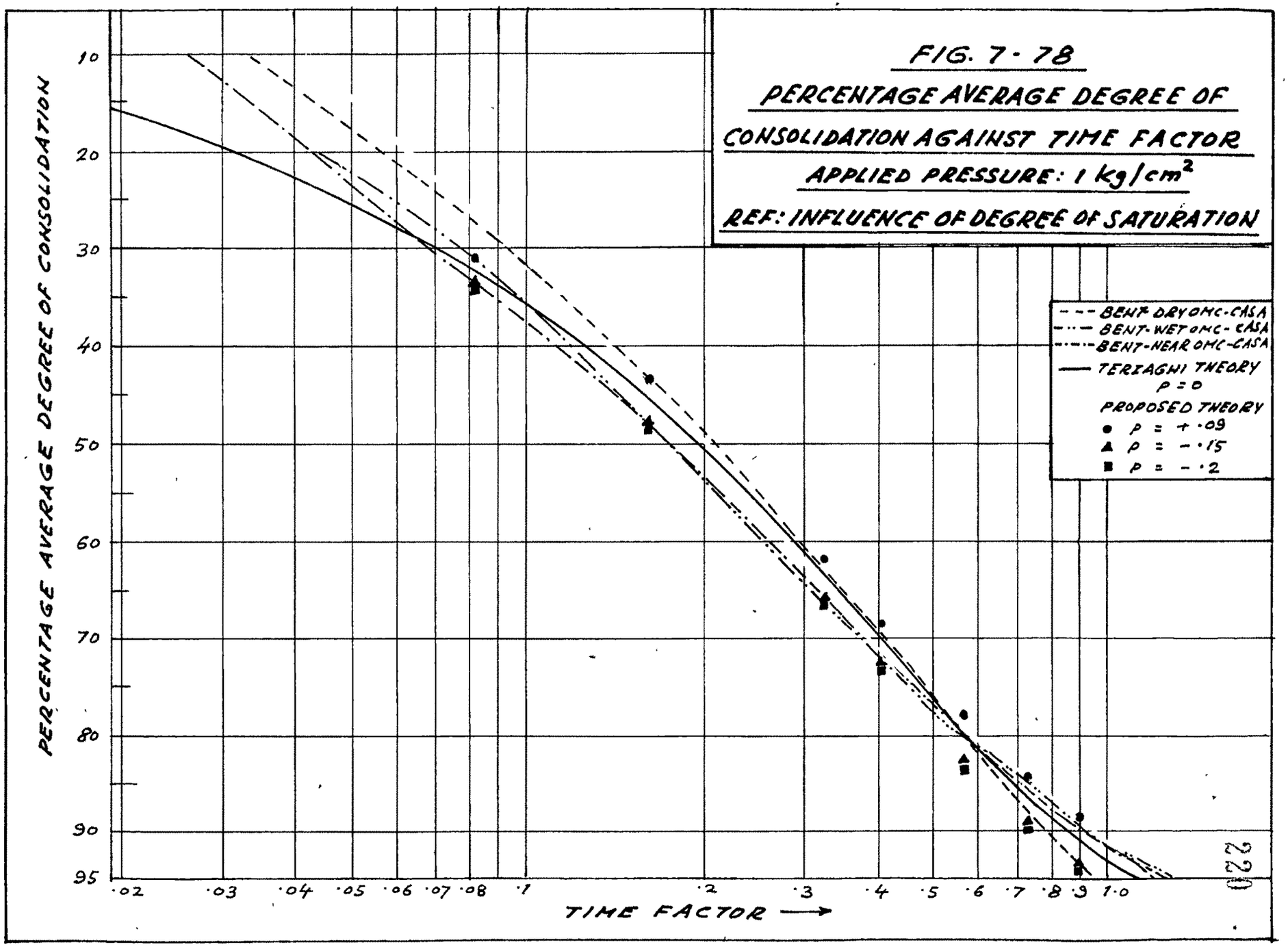
FIG. 7·78
PERCENTAGE AVERAGE DEGREE OF CONSOLIDATION AGAINST TIME FACTOR
APPLIED PRESSURE: 1 kg/cm²
REF: INFLUENCE OF DEGREE OF SATURATION
BENT. DRY OMC-CASA
BENT-WET OMC-CASA
BENT-NEAR OMC-CASA
TERZAGHI THEORY P=0
PROPOSED THEORY
P = +·09
P = −·15
P = −·2
PERCENTAGE AVERAGE DEGREE OF CONSOLIDATION
10
20
30
40
50
60
70
80
90
95
·02 ·03 ·04 ·05 ·06 ·07 ·08 ·1 ·2 ·3 ·4 ·5 ·6 ·7 ·8 ·9 1·0
TIME FACTOR →
223

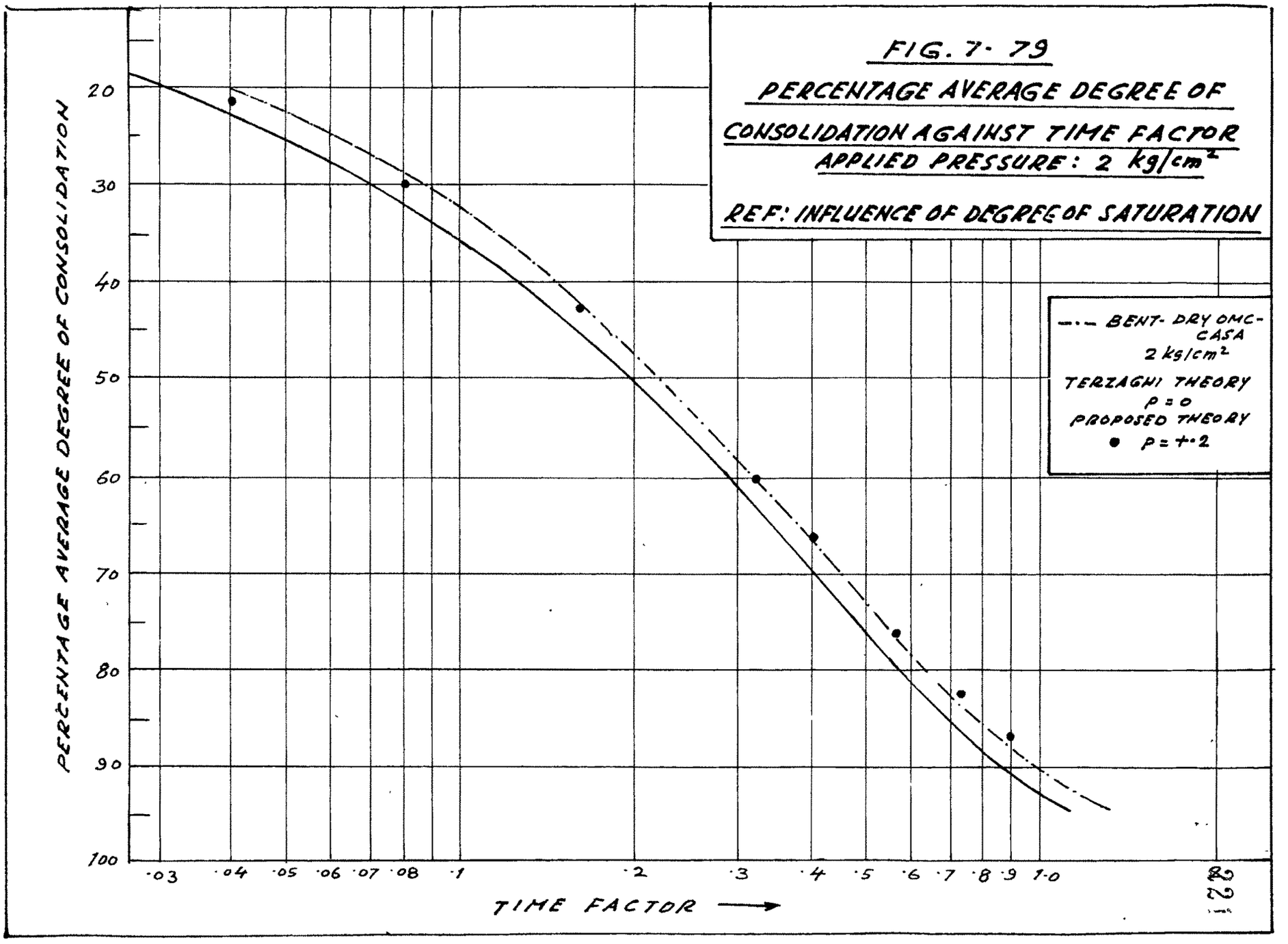
FIG. 7·79
PERCENTAGE AVERAGE DEGREE OF CONSOLIDATION AGAINST TIME FACTOR
APPLIED PRESSURE : 2 kg/cm²
REF: INFLUENCE OF DEGREE OF SATURATION
BENT- DRY OMC- CASA 2 kg/cm²
TERZAGHI THEORY p = 0
PROPOSED THEORY p = +·2
PERCENTAGE AVERAGE DEGREE OF CONSOLIDATION
20
30
40
50
60
70
80
90
100
·03 ·04 ·05 ·06 ·07 ·08 ·1 ·2 ·3 ·4 ·5 ·6 ·7 ·8 ·9 1·0
TIME FACTOR

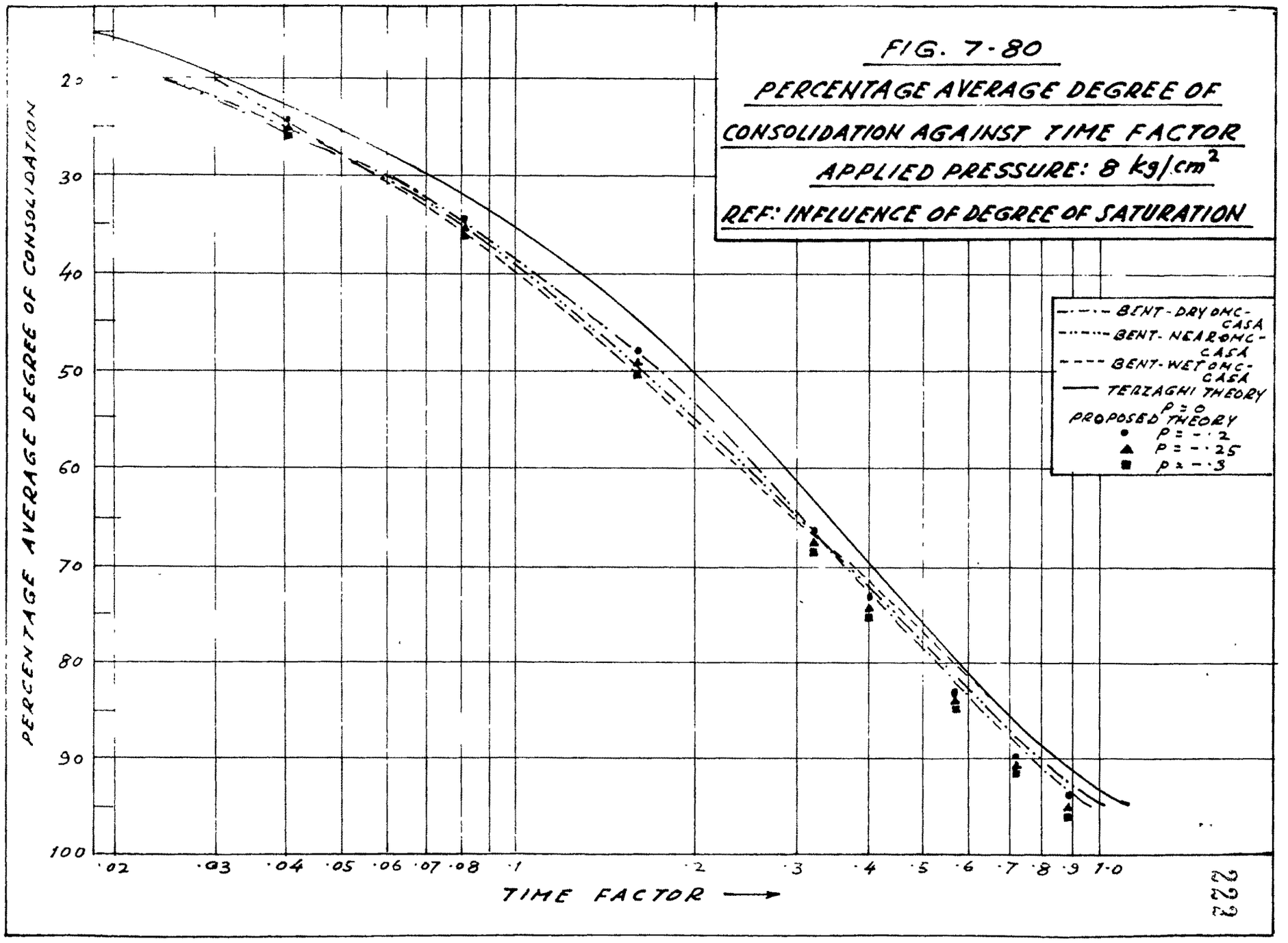
FIG. 7-80
PERCENTAGE AVERAGE DEGREE OF CONSOLIDATION AGAINST TIME FACTOR
APPLIED PRESSURE: 8 kg/cm²
REF: INFLUENCE OF DEGREE OF SATURATION
BENT-DRY OMC-CASA
BENT-NEAR OMC-CASA
BENT-WET OMC-CASA
TERZAGHI THEORY
PROPOSED THEORY P=0
P=·2
P=·25
P=·3
PERCENTAGE AVERAGE DEGREE OF CONSOLIDATION
20
30
40
50
60
70
80
90
100
·02 ·03 ·04 ·05 ·06 ·07 ·08 ·1 ·2 ·3 ·4 ·5 ·6 ·7 ·8 ·9 1·0
TIME FACTOR ⟶

Discussion :

The consolidation characteristics of clays compacted at various degrees of saturation can be discussed from considerations of the extent of air and water phase influencing the structural matrix.

At dry of optimum moisture content there prevails a thurst for water generating negative pore water pressures. The tendency of expansion of clay while making up the water deficiency to reach an equilibrium water content is resisted by the residual pore water tension inducing a 'compressive prestress' in the clay sample. Further, as a consequence of less amount of available water, a high concentration of electrolyte results due to which the diffused layer of ions surrounding the clay particle remains in a depressed state. It leads to low interparticle repulsion creating a flocculated arrangement of particles. In such air water environment, initially the consolidation process consists merely of relief of compressive prestress and breaking up of some flocculation link bonds without virtually causing any out flow of water.

On the other hand at wet of optimum moisture content the air gets occluded because of which it ceases to be continuous over a distance as water seals thin necks of air voids. The occluded air bubbles cling to the clay colloid remaining thereby out of the general flow channels. Because of no water deficiency

there is no environment for the generation of pore water tension and prestress in the clay skeleton. Also reduction of electrolyte concentration causes expansion in the double layer thereby increasing the repulsive forces between particles. This tends to produce a dispersed arrangement of particles. Under this conditions dissipation of free water pressure occurs during the consolidation process. While reaching the optimum moisture content, the air is forced out to the maximum degree corresponding to a particular compactive effort, so that no further flow of air can occur at this state. Under these conditions the consolidation pressure is resisted by the air bubbles trapped in the strongest structural arrangement and the air and water both get expelled only after the collapse of the resisting structure.

In the above physical background it can be argued that the samples of kaolinite or Bentonite compacted at dry of OMC would show at lighter loads initial resistance to compressive prestress and to the flocculated structure. Comparatively more resistance is observed in Bentonite because of its swelling potential besides the higher magnitude of usual combating forces. These forces are overcome at higher loads thereby indicating normal consolidation behaviour. At or near OMC the behaviour is similar as environmental conditions almost remain same. The observation of higher rate

of consolidation with increase of pressure in case of samples compacted at wet of OMC indicates easy dissipation of free pore water through soil skeleton which is more or less dispersed with no compressive prestressed and higher occlusion in the soil. Higher order of flocculation in Bentonite at dry side and wet side of OMC produces a steep compression curve compared to that in kaolinite. The increasing order of secondary compression with the increase in moulding water content is clearly evident from the fact that with it there is an increase in the orientation of particles and decrease in the pore water tensions. Obviously therefore while the wet side samples would show a near Terzaghi behaviour, deviation is marked as the moulding water content decreases.

7.3.4. Stress History

Refer Figures 7.81 to 7.113 which are reproduced from the original plots of Figures H 156 to H 212 reported in Appendix H pf Volume II.

A : Influence of Loading and Unloading :

Analysis :

(i) Coefficient of consolidation against percentage consolidation.
(Figures 7.81 to 7.84).

Only during the first cycle loading, the c_v value shows

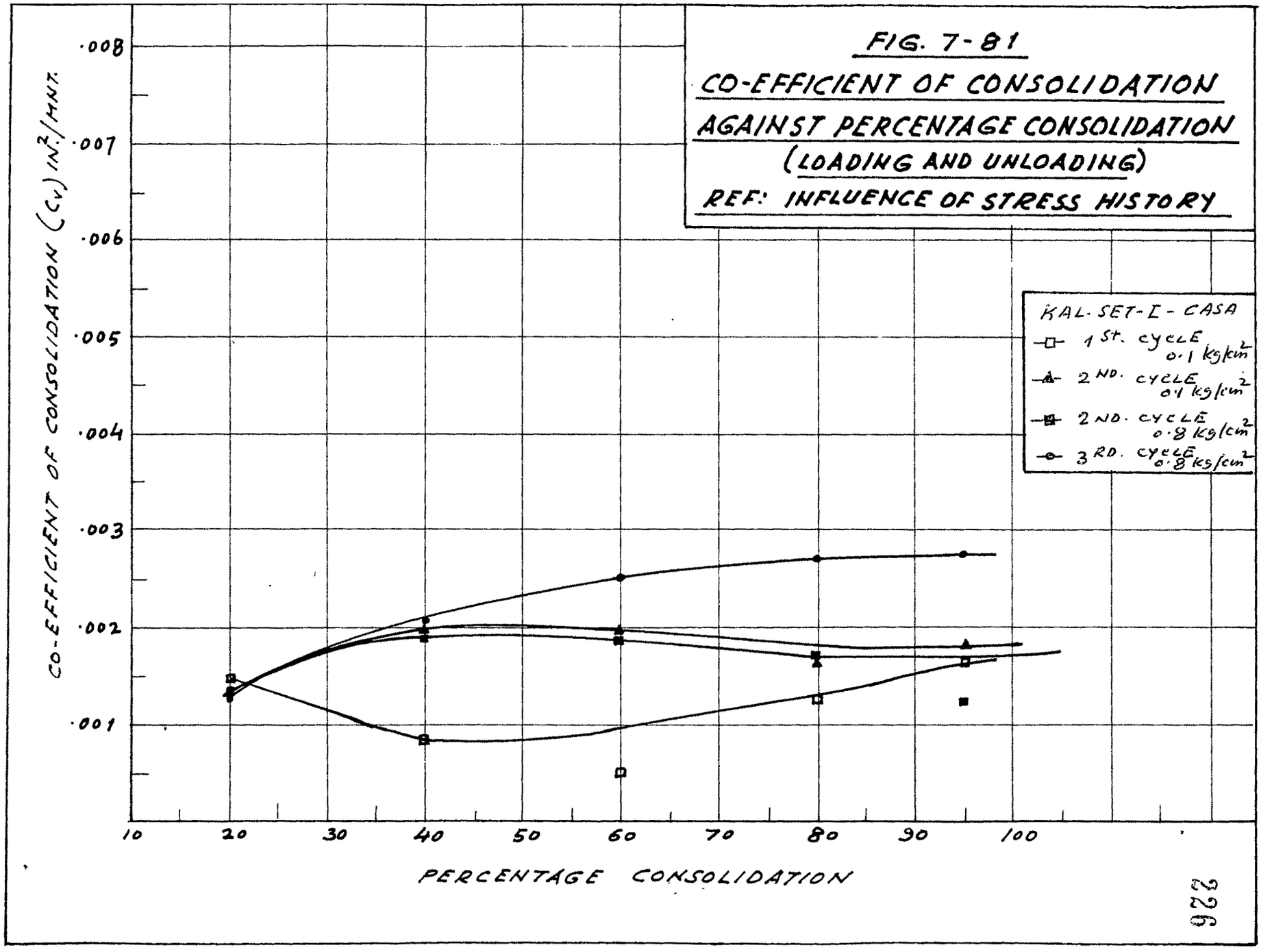
FIG. 7-81
CO-EFFICIENT OF CONSOLIDATION
AGAINST PERCENTAGE CONSOLIDATION
(LOADING AND UNLOADING)
REF: INFLUENCE OF STRESS HISTORY
KAL. SET-I - CASA
1 St. cycle 0·1 kg/cm²
2 ND. cycle 0·4 kg/cm²
2 ND. cycle 0·8 kg/cm²
3 RD. cycle 0·8 kg/cm²
CO-EFFICIENT OF CONSOLIDATION (Cv) IN.²/MNT.
·008
·007
·006
·005
·004
·003
·002
·001
10
20
30
40
50
60
70
80
90
100
PERCENTAGE CONSOLIDATION
922

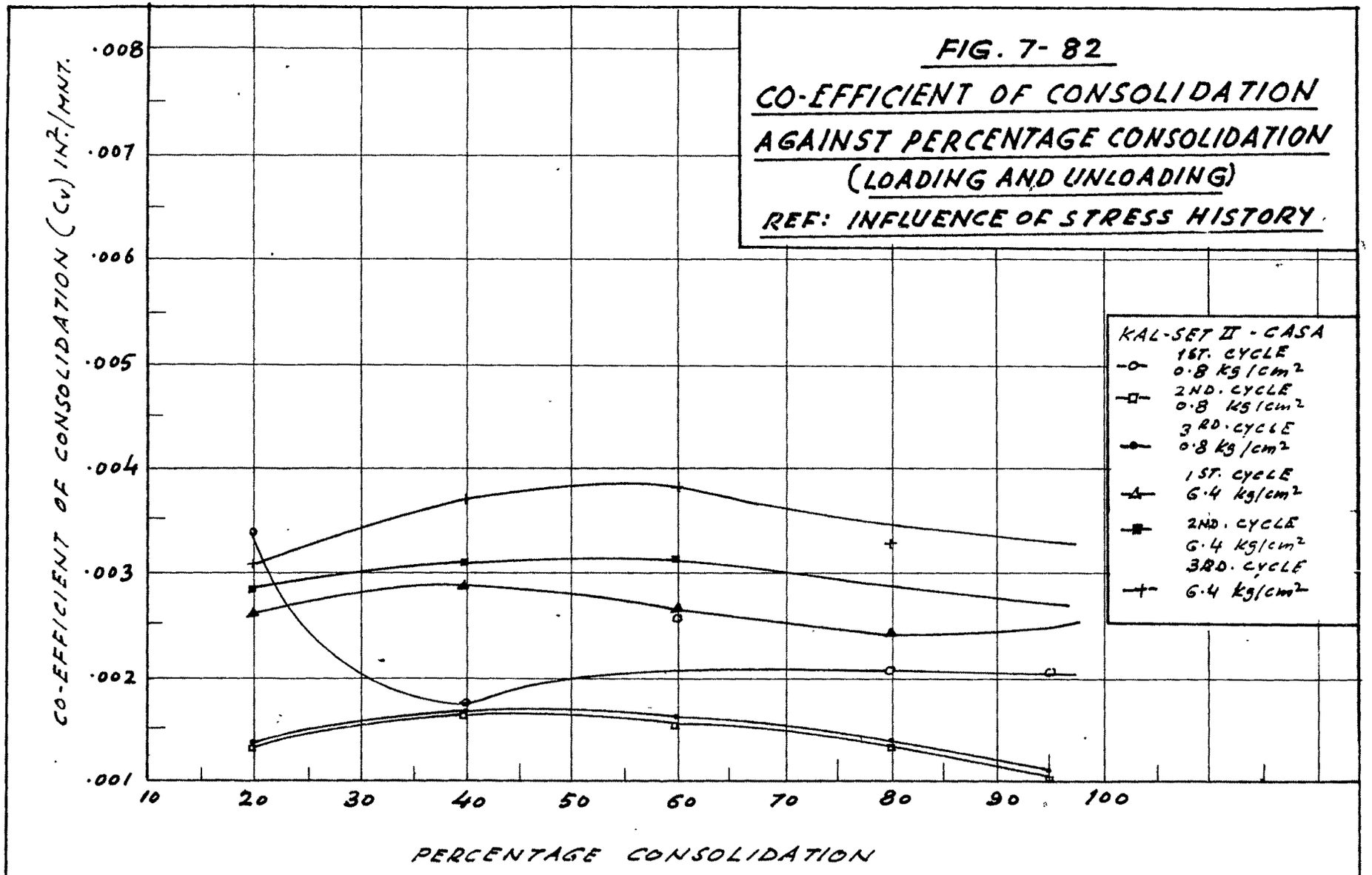
FIG. 7-82
CO-EFFICIENT OF CONSOLIDATION AGAINST PERCENTAGE CONSOLIDATION (LOADING AND UNLOADING)
REF: INFLUENCE OF STRESS HISTORY.
KAL-SET II - CASA
1ST. CYCLE 0·8 kg/cm²
2ND. CYCLE 0·8 kg/cm²
3RD. CYCLE 0·8 kg/cm²
1ST. CYCLE 6·4 kg/cm²
2ND. CYCLE 6·4 kg/cm²
3RD. CYCLE 6·4 kg/cm²
CO-EFFICIENT OF CONSOLIDATION (Cv) IN².MNT.
·008
·007
·006
·005
·004
·003
·002
·001
10
20
30
40
50
60
70
80
90
100
PERCENTAGE CONSOLIDATION

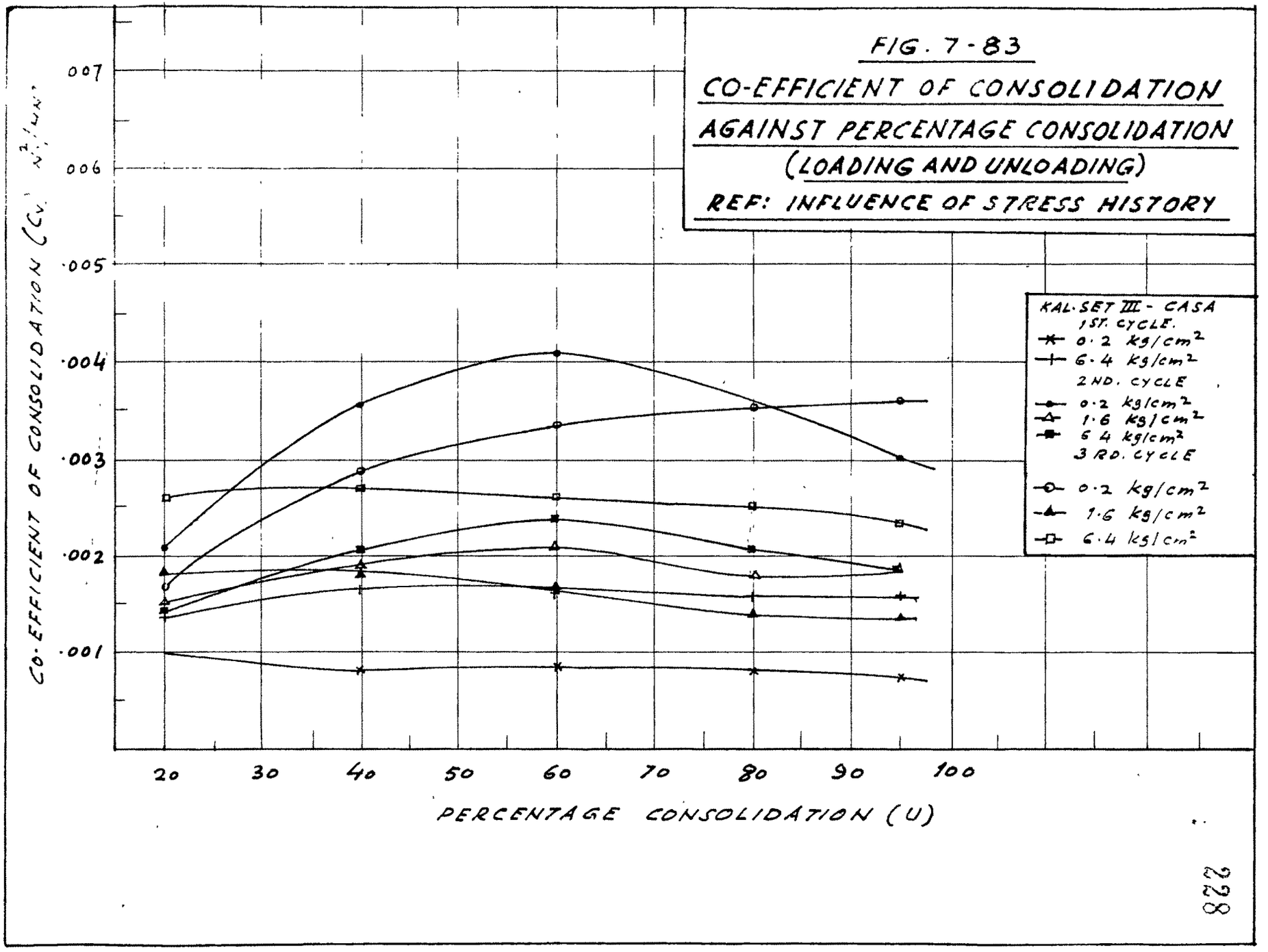
FIG. 7-83
CO-EFFICIENT OF CONSOLIDATION
AGAINST PERCENTAGE CONSOLIDATION
(LOADING AND UNLOADING)
REF: INFLUENCE OF STRESS HISTORY
KAL-SET III - CASA
1ST. CYCLE.
0·2 kg/cm²
6·4 kg/cm²
2ND. CYCLE
0·2 kg/cm²
1·6 kg/cm²
6·4 kg/cm²
3RD. CYCLE
0·2 kg/cm²
1·6 kg/cm²
6·4 kg/cm²
CO-EFFICIENT OF CONSOLIDATION (Cv) N²/MIN
·007
·006
·005
·004
·003
·002
·001
20
30
40
50
60
70
80
90
100
PERCENTAGE CONSOLIDATION (U)
228

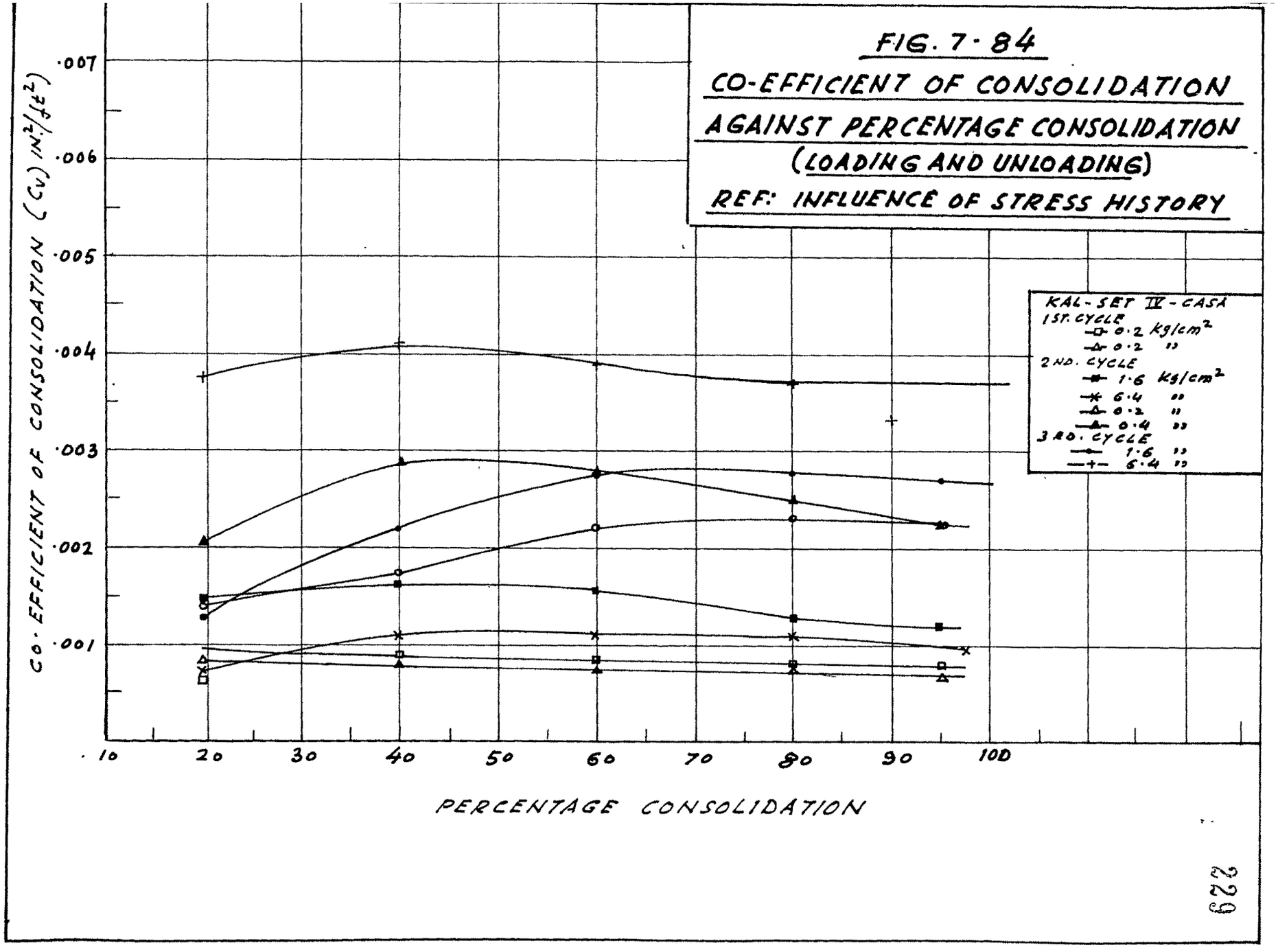
FIG. 7·84
CO-EFFICIENT OF CONSOLIDATION
AGAINST PERCENTAGE CONSOLIDATION
(LOADING AND UNLOADING)
REF: INFLUENCE OF STRESS HISTORY
KAL-SET IV-CASA
1ST. CYCLE
0·2 kg/cm²
0·2 "
2ND. CYCLE
1·6 kg/cm²
6·4 "
0·2 "
0·4 "
3RD. CYCLE
1·6 "
6·4 "
CO-EFFICIENT OF CONSOLIDATION (Cv) in²/ft²
·007
·006
·005
·004
·003
·002
·001
10
20
30
40
50
60
70
80
90
100
PERCENTAGE CONSOLIDATION

variation initially similar to that observed in case of saturated kaolinite. For other cycles of loading, it shows a slight increase initially under lighter loads which tends to gradually become constant. For any cycles of loading the value is comparatively higher during lighter loads.

(ii) Coefficient of consolidation against applied effective pressure.
(Figures 7.85 to 7.88).

The value of c_v is seen to increase with the number of loading and unloading cycles for the same load intensity irrespective of any set. General trend of the curves during any cycles of loading and unloading indicates a decrease in c_v during light loading. C_v therefore increases reaching a constant value for any set. Initial decrease in C_v during the first cycle in any set is comparatively little more than during further cycles of loading and unloading.

(iii) Void-ratio versus applied effective pressure and compression index against average effective pressure.
(Figures H 211 and H 212, Figures 7.91 to 7.94).

In general, void ratio against effective stress curve shows that initial load produces an irreversible deformation and exhibits very little elastic recovery in all the sets. Hysteresis loops formed by decompression and recompression are almost parallel among themselves for a particular set of samples. The modulus of elasticity (hysteresis modulus) can

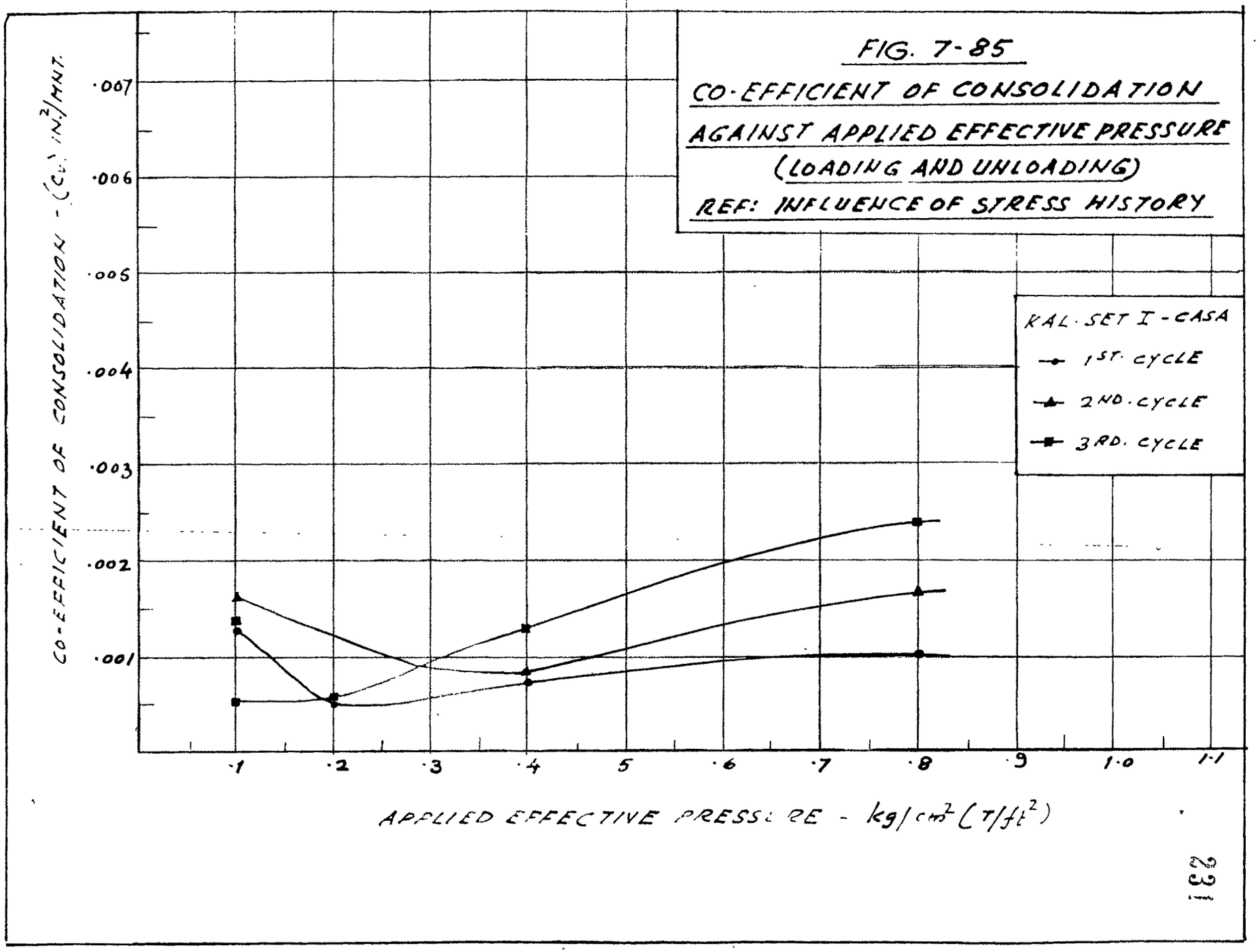
FIG. 7-85
CO-EFFICIENT OF CONSOLIDATION
AGAINST APPLIED EFFECTIVE PRESSURE
(LOADING AND UNLOADING)
REF: INFLUENCE OF STRESS HISTORY
KAL. SET I - CASA
1ST. CYCLE
2ND. CYCLE
3RD. CYCLE
CO-EFFICIENT OF CONSOLIDATION - (cv) IN.²/MNT.
·007
·006
·005
·004
·003
·002
·001
·1
·2
·3
·4
5
·6
·7
·8
·9
1·0
1·1
APPLIED EFFECTIVE PRESSURE - kg/cm² (T/ft²)

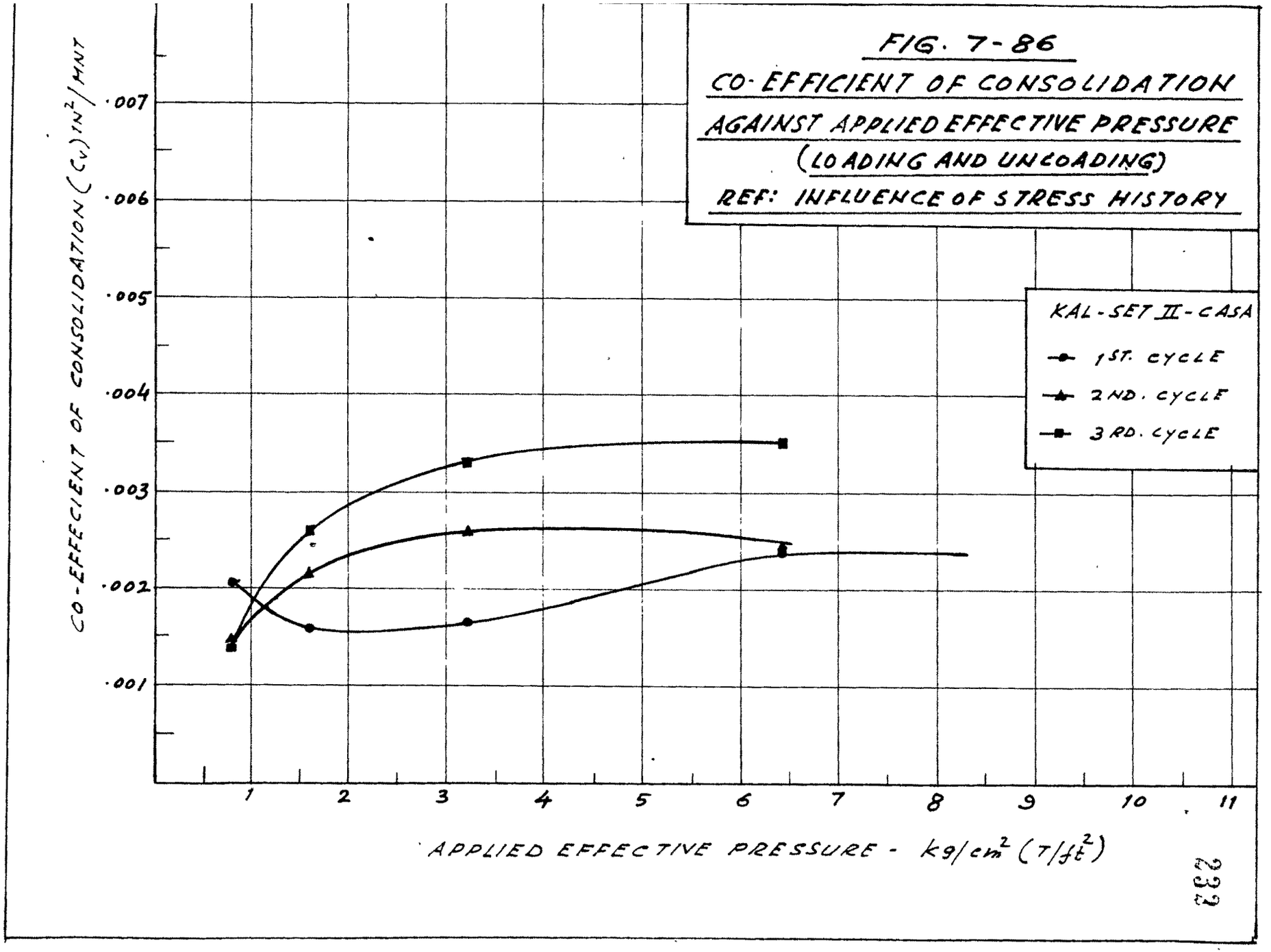
FIG. 7-86
CO-EFFICIENT OF CONSOLIDATION
AGAINST APPLIED EFFECTIVE PRESSURE
(LOADING AND UNLOADING)
REF: INFLUENCE OF STRESS HISTORY
KAL-SET II-CASA
1ST. CYCLE
2ND. CYCLE
3RD. CYCLE
CO-EFFECIENT OF CONSOLIDATION (C_v) IN^2/MNT
.007
.006
.005
.004
.003
.002
.001
1
2
3
4
5
6
7
8
9
10
11
APPLIED EFFECTIVE PRESSURE - kg/cm^2 (T/ft^2)

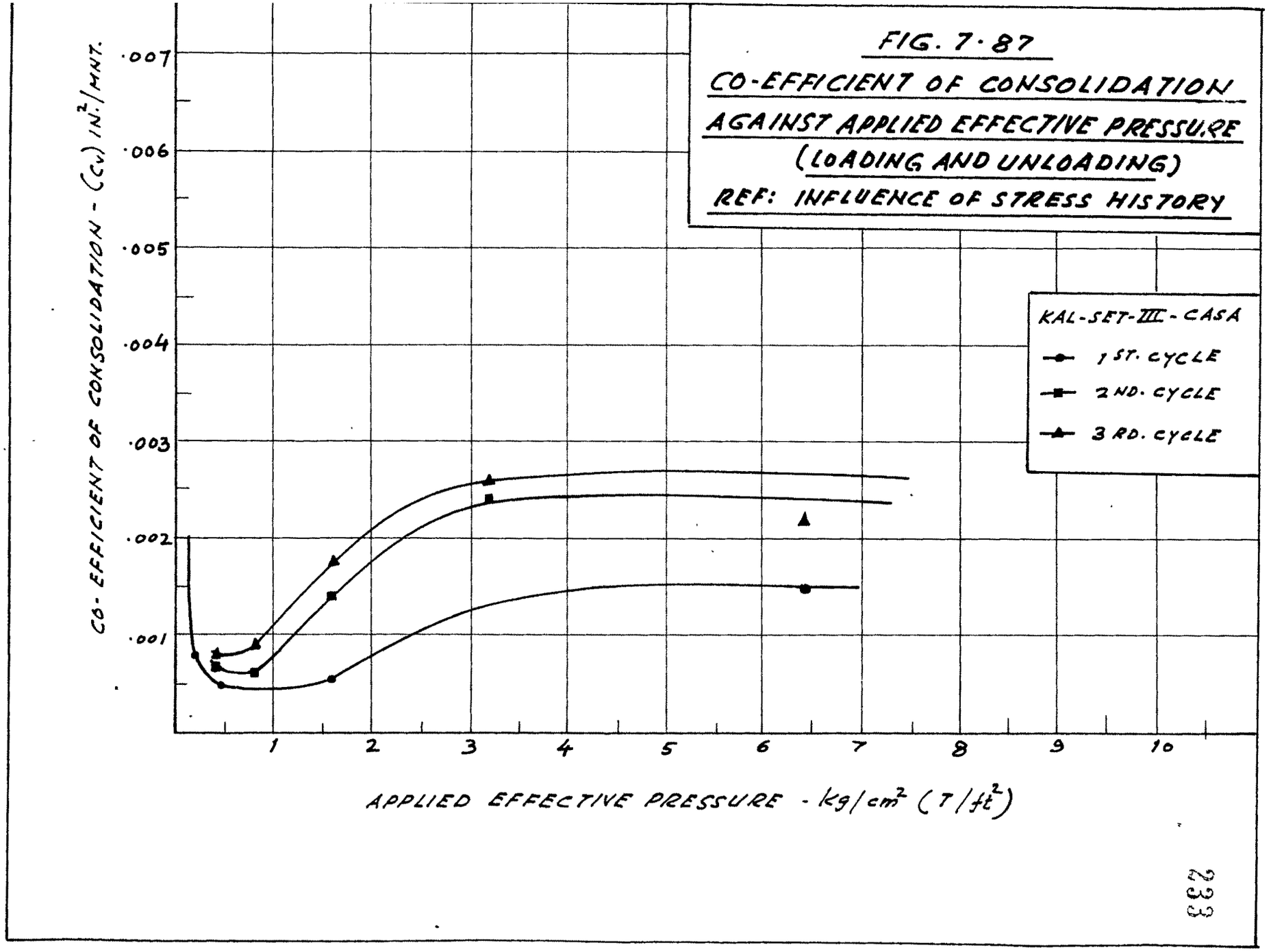
FIG. 7·87
CO-EFFICIENT OF CONSOLIDATION AGAINST APPLIED EFFECTIVE PRESSURE (LOADING AND UNLOADING)
REF: INFLUENCE OF STRESS HISTORY
KAL-SET-III - CASA
1 ST. CYCLE
2 ND. CYCLE
3 RD. CYCLE
CO-EFFICIENT OF CONSOLIDATION - (Cv) IN.²/MNT.
·007
·006
·005
·004
·003
·002
·001
1
2
3
4
5
6
7
8
9
10
APPLIED EFFECTIVE PRESSURE - kg/cm² (T/ft²)

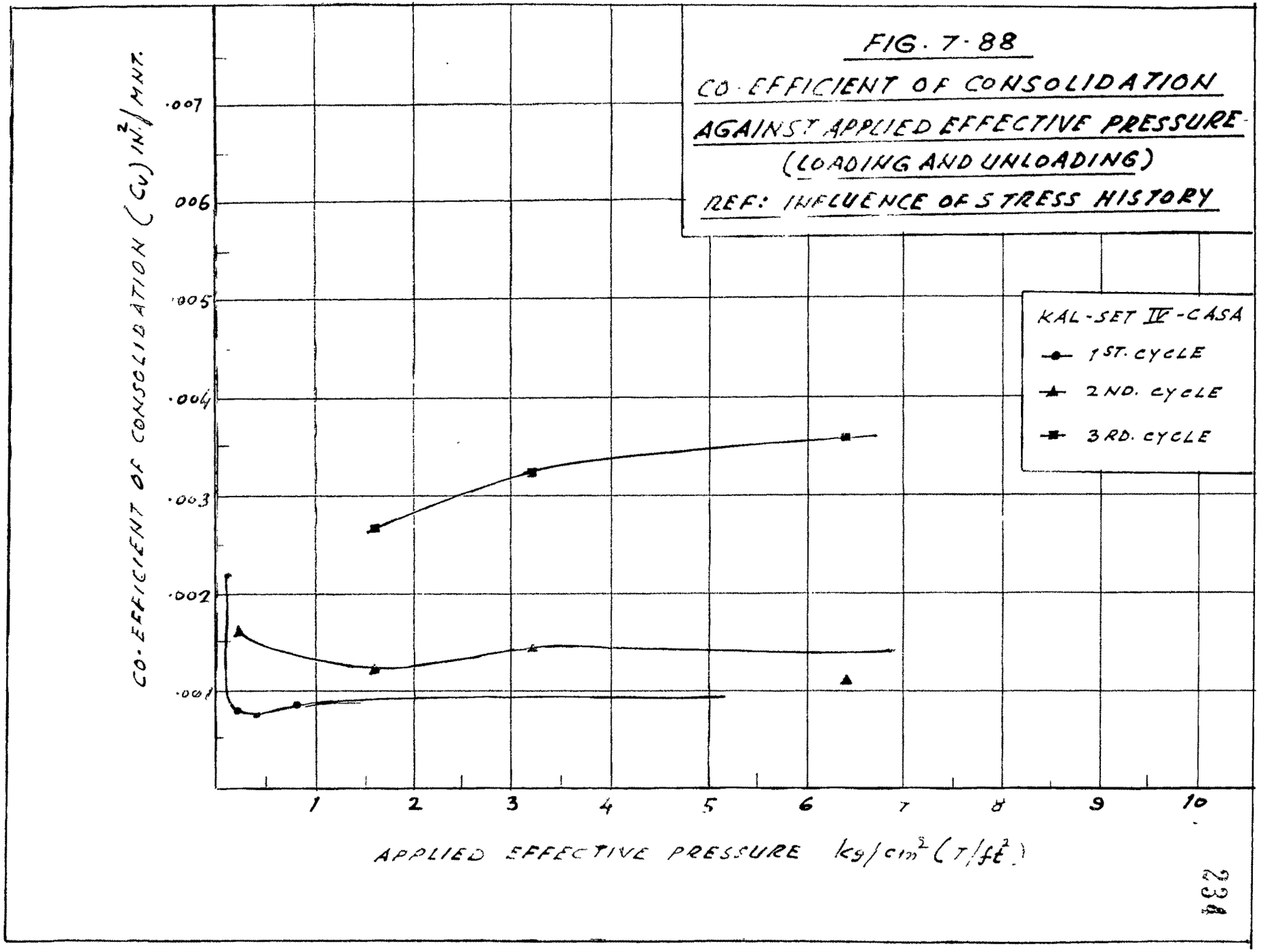
FIG. 7·88
CO-EFFICIENT OF CONSOLIDATION
AGAINST APPLIED EFFECTIVE PRESSURE
(LOADING AND UNLOADING)
REF: INFLUENCE OF STRESS HISTORY
KAL-SET IV-CASA
1ST. CYCLE
2ND. CYCLE
3RD. CYCLE
CO-EFFICIENT OF CONSOLIDATION (Cv) IN.²/MNT.
.007
.006
.005
.004
.003
.002
.001
1
2
3
4
5
6
7
8
9
10
APPLIED EFFECTIVE PRESSURE kg/cm² (T/ft²)
238

FIG. 7-89

VOID RATIO AGAINST LOG EFFECTIVE PRESSURE - kg/cm²
(LOADING AND UNLOADING)

REF: INFLUENCE OF STRESS HISTORY

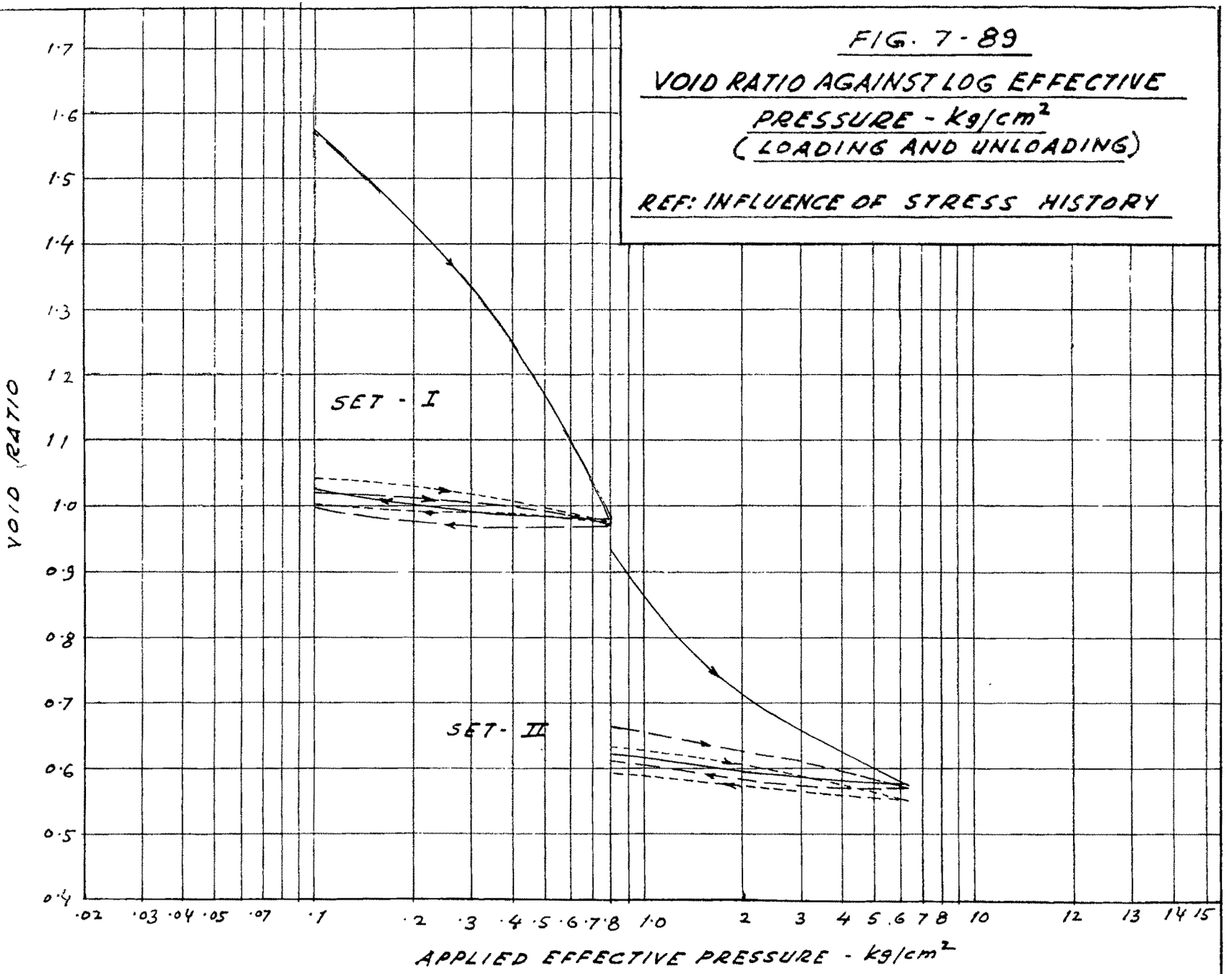

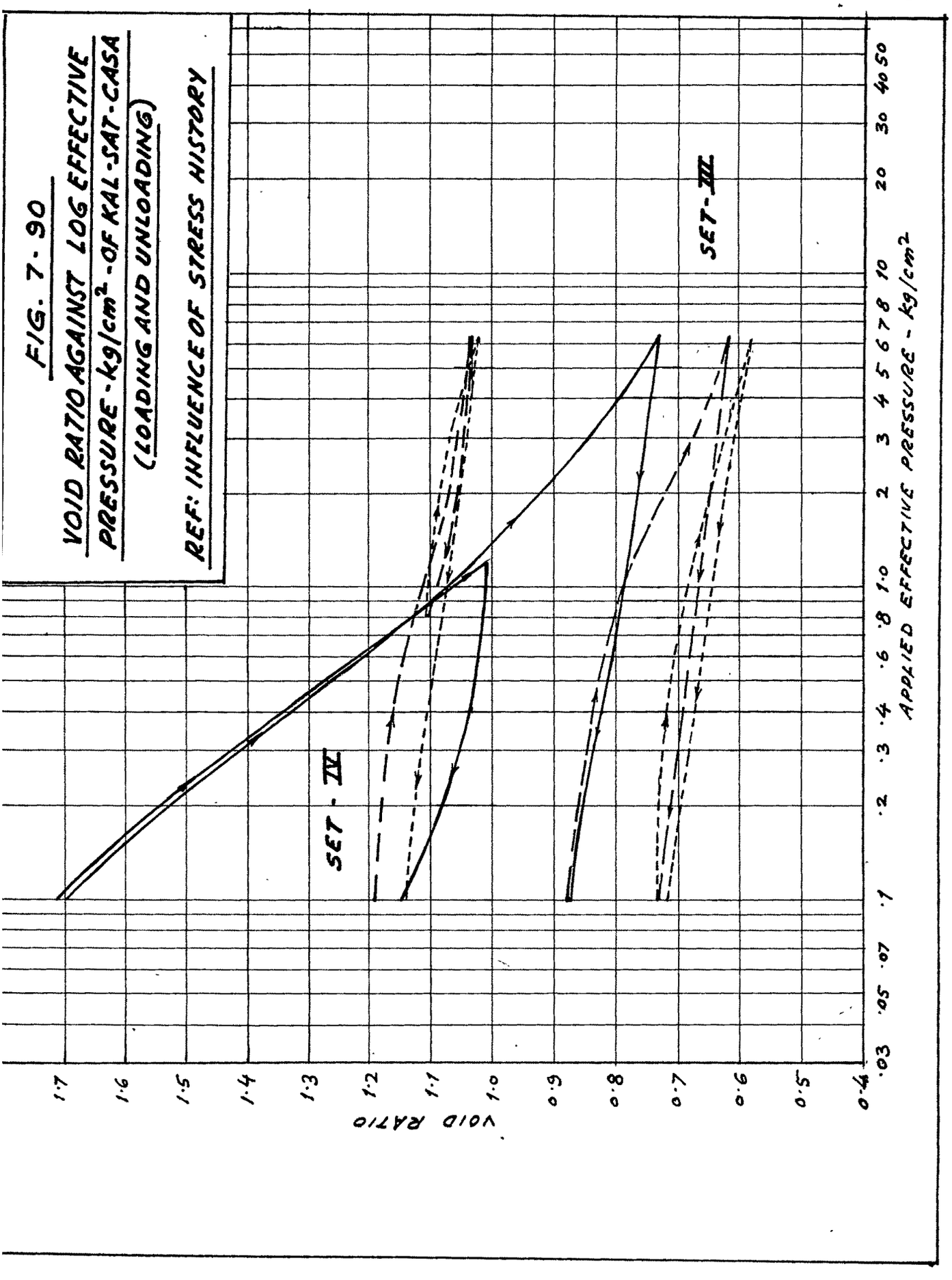
FIG. 7·90
VOID RATIO AGAINST LOG EFFECTIVE PRESSURE - kg/cm² - OF KAL-SAT-CASA (LOADING AND UNLOADING)
REF: INFLUENCE OF STRESS HISTORY
SET - IV
SET - III
VOID RATIO
APPLIED EFFECTIVE PRESSURE - kg/cm²
1·7
1·6
1·5
1·4
1·3
1·2
1·1
1·0
0·9
0·8
0·7
0·6
0·5
0·4
·03
·05
·07
·1
·2
·3
·4
·6
·8
1·0
2
3
4
5
6
7
8
10
20
30
40
50

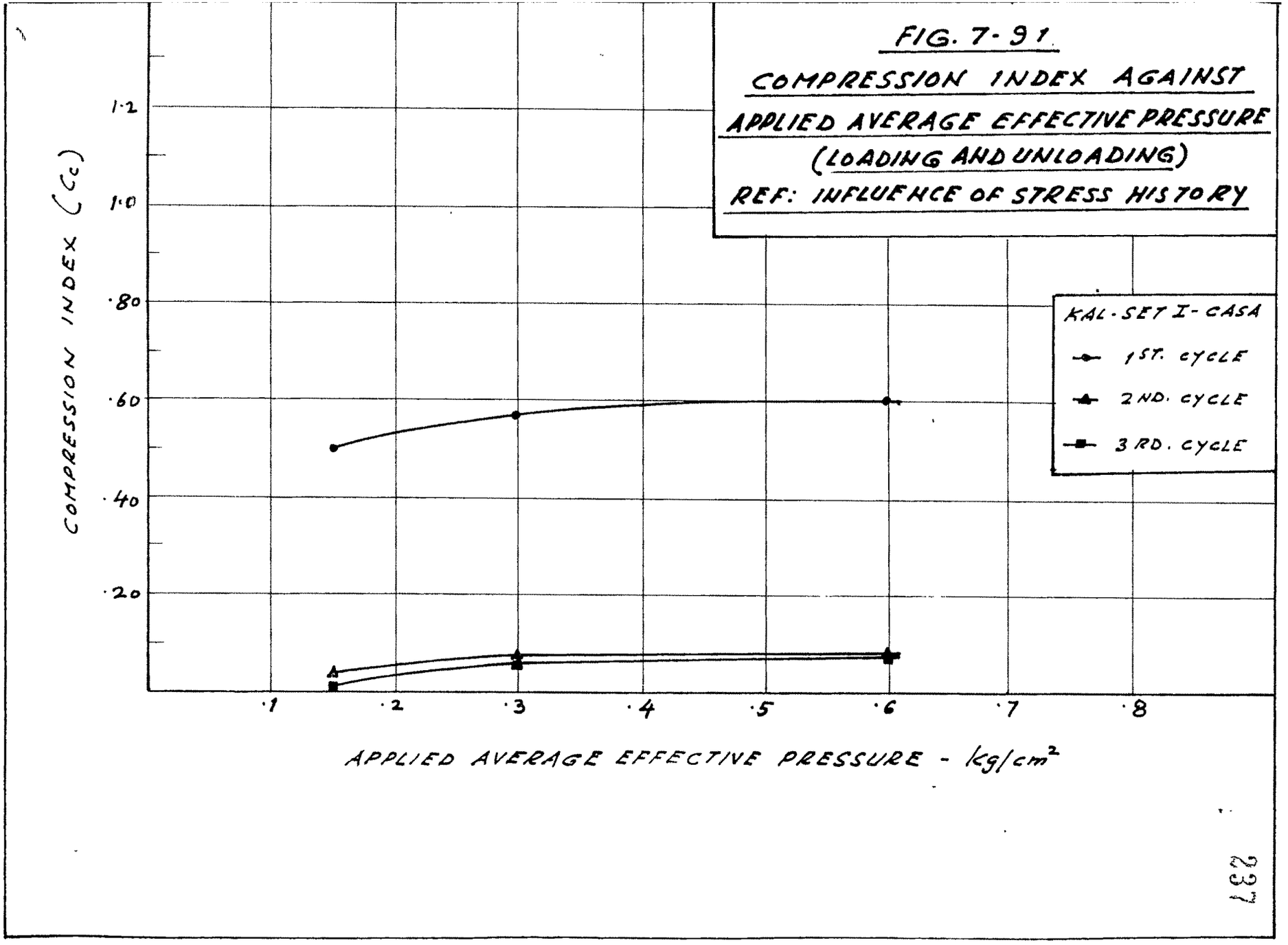
FIG. 7-91
COMPRESSION INDEX AGAINST APPLIED AVERAGE EFFECTIVE PRESSURE (LOADING AND UNLOADING)
REF: INFLUENCE OF STRESS HISTORY
KAL-SET I-CASA
1ST. CYCLE
2ND. CYCLE
3RD. CYCLE
COMPRESSION INDEX (Cc)
1·2
1·0
·80
·60
·40
·20
·1
·2
·3
·4
·5
·6
·7
·8
APPLIED AVERAGE EFFECTIVE PRESSURE - kg/cm²

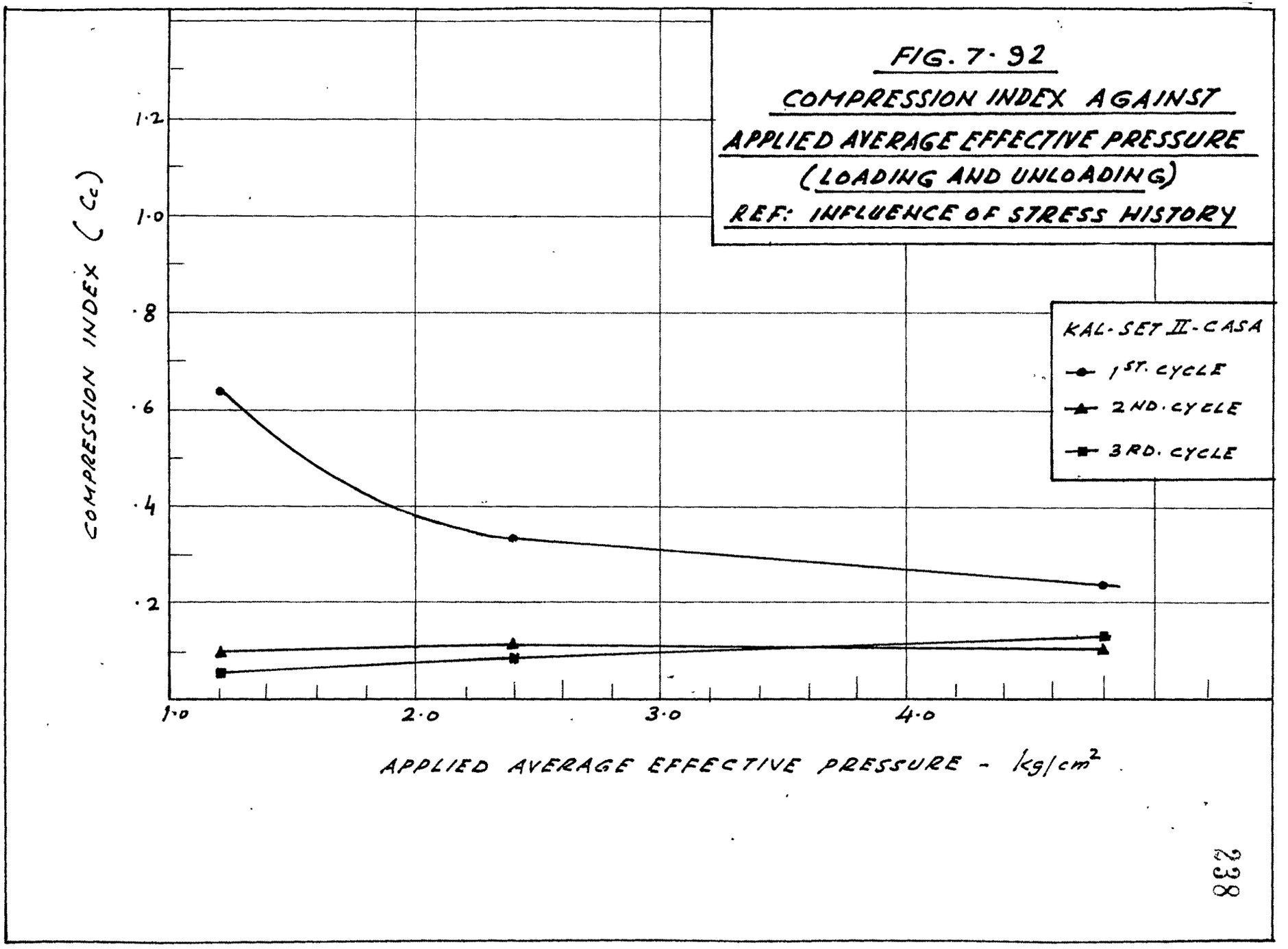
FIG. 7·92
COMPRESSION INDEX AGAINST
APPLIED AVERAGE EFFECTIVE PRESSURE
(LOADING AND UNLOADING)
REF: INFLUENCE OF STRESS HISTORY
KAL-SET II-CASA
1ST. CYCLE
2ND. CYCLE
3RD. CYCLE
COMPRESSION INDEX (Cc)
1·2
1·0
·8
·6
·4
·2
1·0
2·0
3·0
4·0
APPLIED AVERAGE EFFECTIVE PRESSURE - kg/cm²

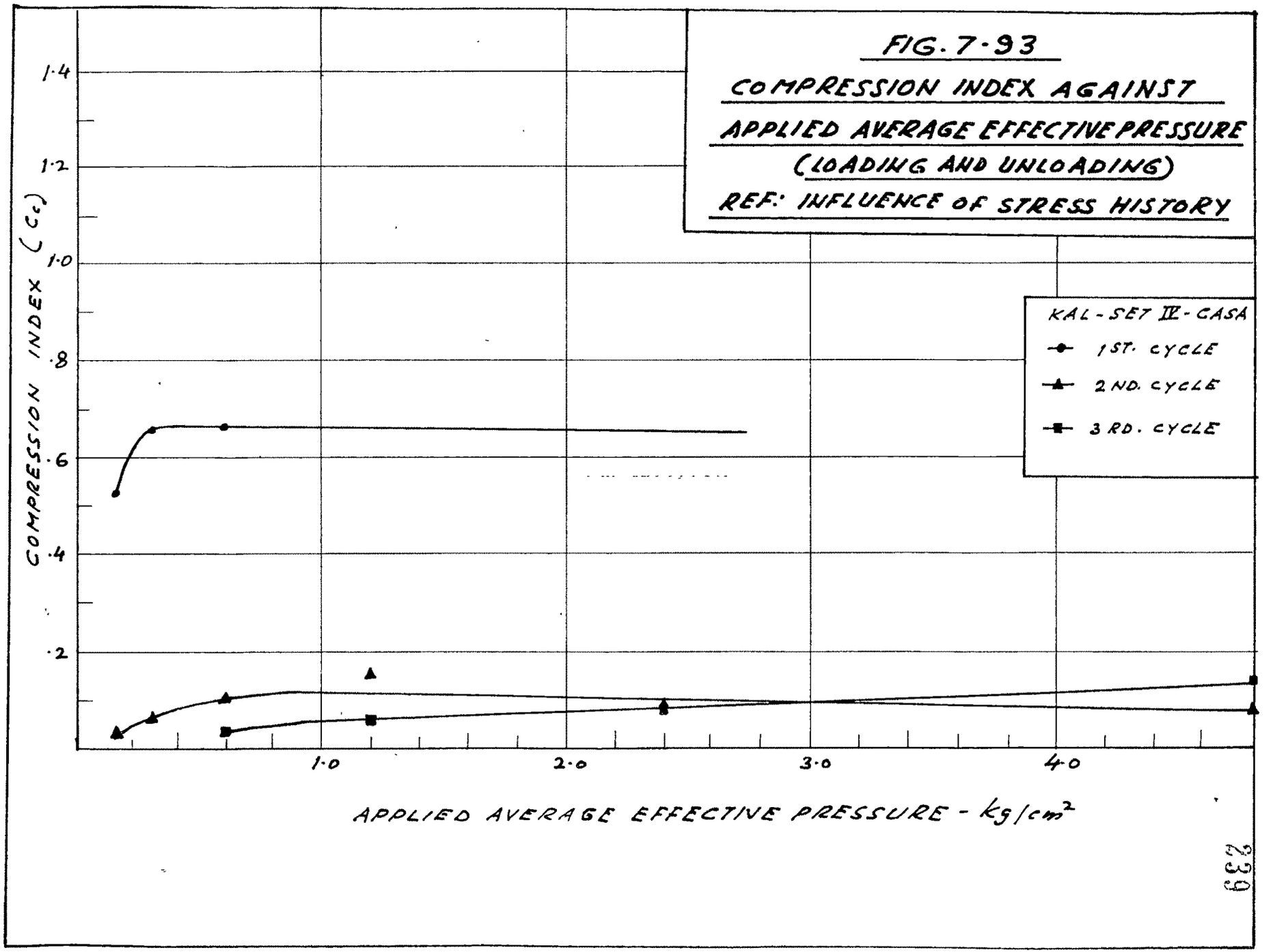
FIG. 7·93
COMPRESSION INDEX AGAINST
APPLIED AVERAGE EFFECTIVE PRESSURE
(LOADING AND UNLOADING)
REF: INFLUENCE OF STRESS HISTORY
KAL - SET III - CASA
1ST. CYCLE
2ND. CYCLE
3RD. CYCLE
COMPRESSION INDEX (Cc)
1·4
1·2
1·0
·8
·6
·4
·2
1·0
2·0
3·0
4·0
APPLIED AVERAGE EFFECTIVE PRESSURE - kg/cm²

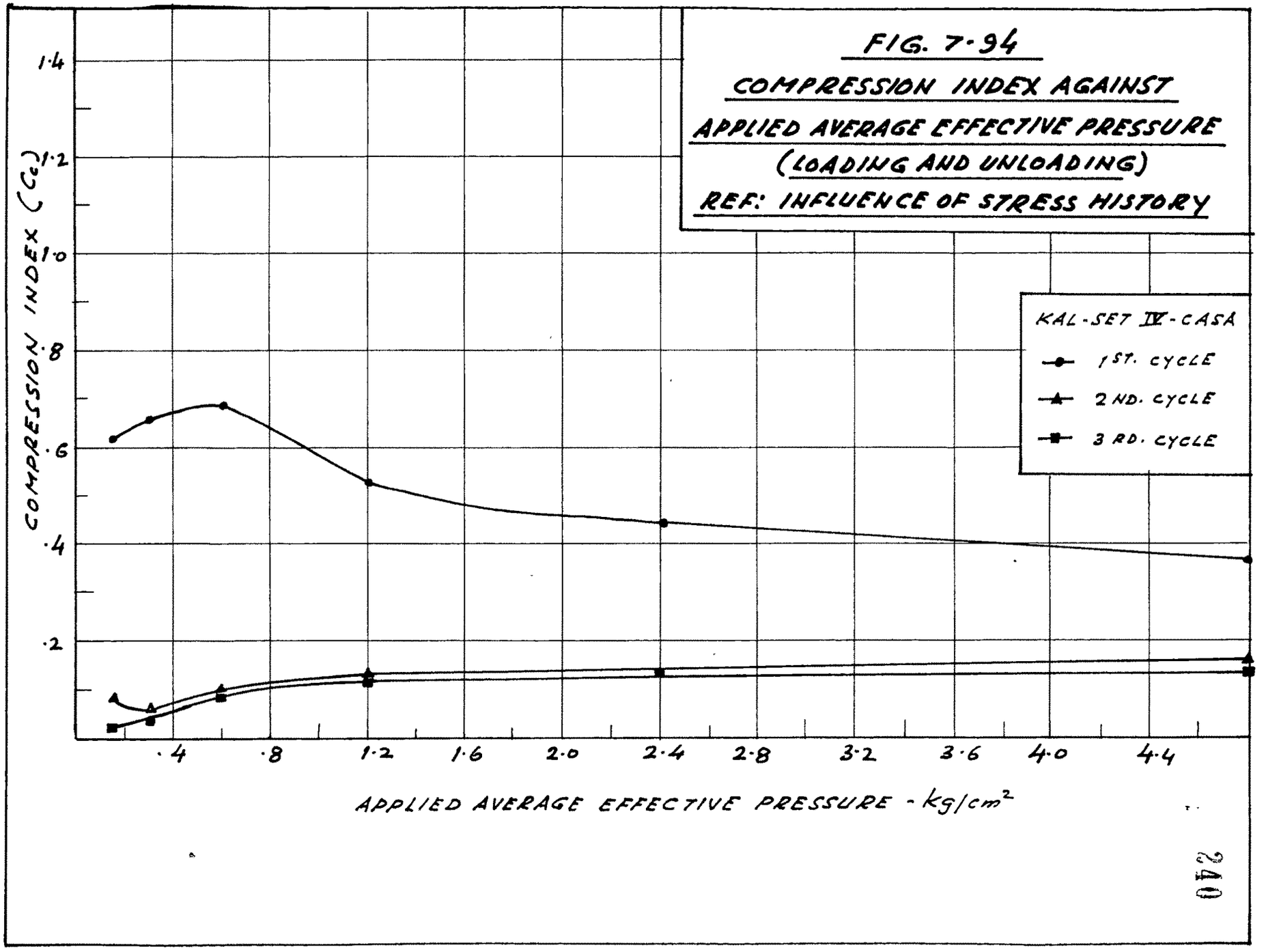
FIG. 7·94
COMPRESSION INDEX AGAINST
APPLIED AVERAGE EFFECTIVE PRESSURE
(LOADING AND UNLOADING)
REF: INFLUENCE OF STRESS HISTORY
KAL-SET IV-CASA
1ST. CYCLE
2ND. CYCLE
3RD. CYCLE
COMPRESSION INDEX (Cc)
1·4
1·2
1·0
·8
·6
·4
·2
·4
·8
1·2
1·6
2·0
2·4
2·8
3·2
3·6
4·0
4·4
APPLIED AVERAGE EFFECTIVE PRESSURE - kg/cm²

thus be considered as constant. From the curves, it is also seen that the area of the hysteresis loop is progressively decreasing with further loading and unloading cycles. These decrease is small in the first set of sample where loading and unloading cycles remain in the lighter load region. The values of initial tangent modulus and secant modulus measured for various sets shows that these values increase slightly with each set. Trend of compression index with average applied pressure is similar in nature to that observed for saturated kaolinite with further cycles of loading and unloading it tends to remain constant for all average pressures.

(iv) Percentage secondary compression against effective applied pressure.
(Figures 7.95 to 7.98).

General nature of relationship during the first cycle in all the sets of samples remains same. In the light loading region it shows a steep rise and then becomes almost flat. During the second and third cycles of loading and unloading the degree of secondary compression remains constant.

(v) Parameter P against effective applied pressure.
(Figures 7.99 to 7.102 to 103 to 7.119).

Experimental curves of the first cycle in all the sets of sample fit closer to the Terzaghi theoretical curve. Deviations observed in the first set from Terzaghi theory are 2.25%, 3% and 3.8% respectively for first, second and the third cycle.

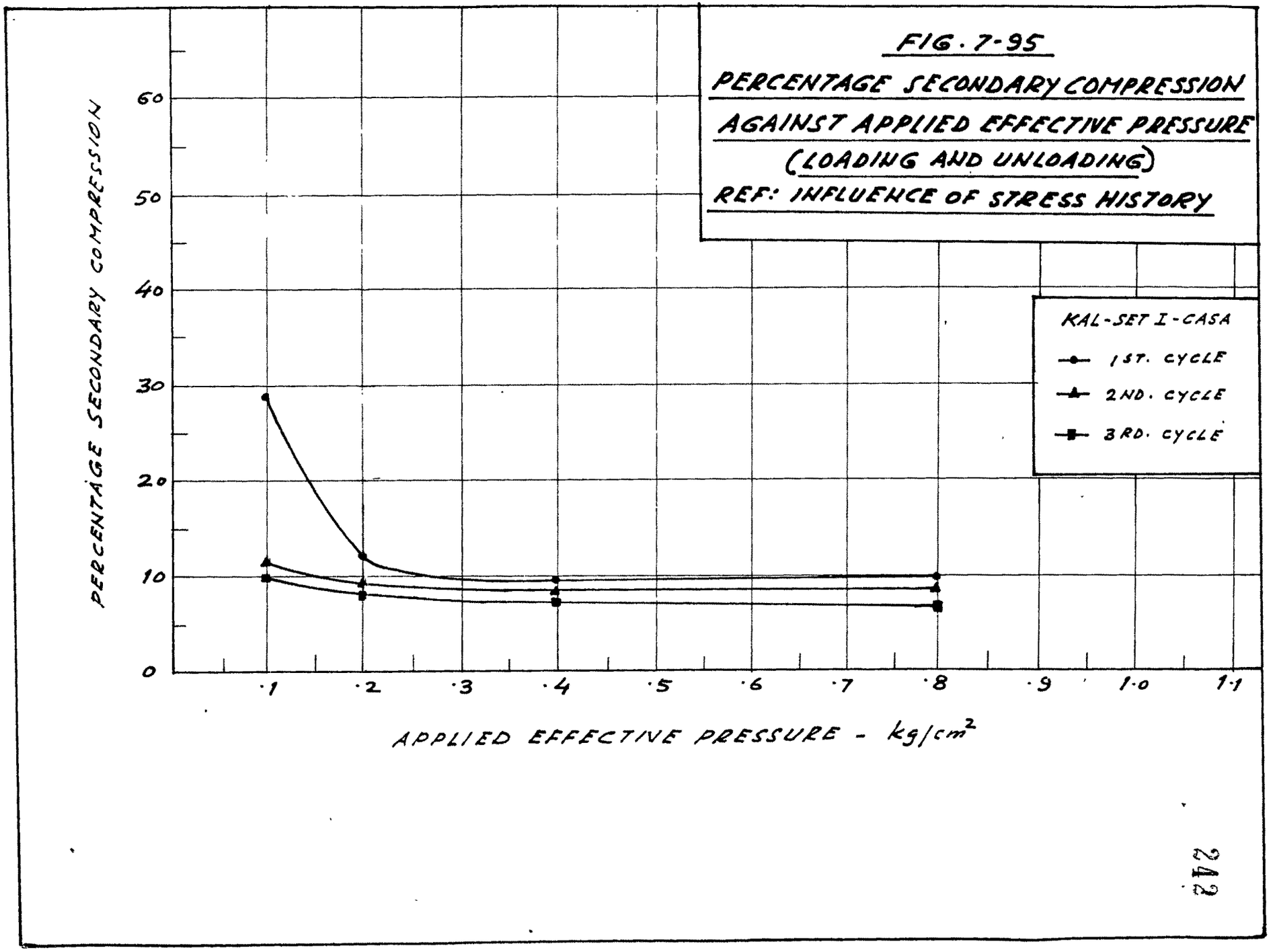
FIG. 7-95
PERCENTAGE SECONDARY COMPRESSION AGAINST APPLIED EFFECTIVE PRESSURE (LOADING AND UNLOADING)
REF: INFLUENCE OF STRESS HISTORY
KAL-SET I-CASA
1ST. CYCLE
2ND. CYCLE
3RD. CYCLE
PERCENTAGE SECONDARY COMPRESSION
0
10
20
30
40
50
60
·1
·2
·3
·4
·5
·6
·7
·8
·9
1·0
1·1
APPLIED EFFECTIVE PRESSURE - kg/cm²

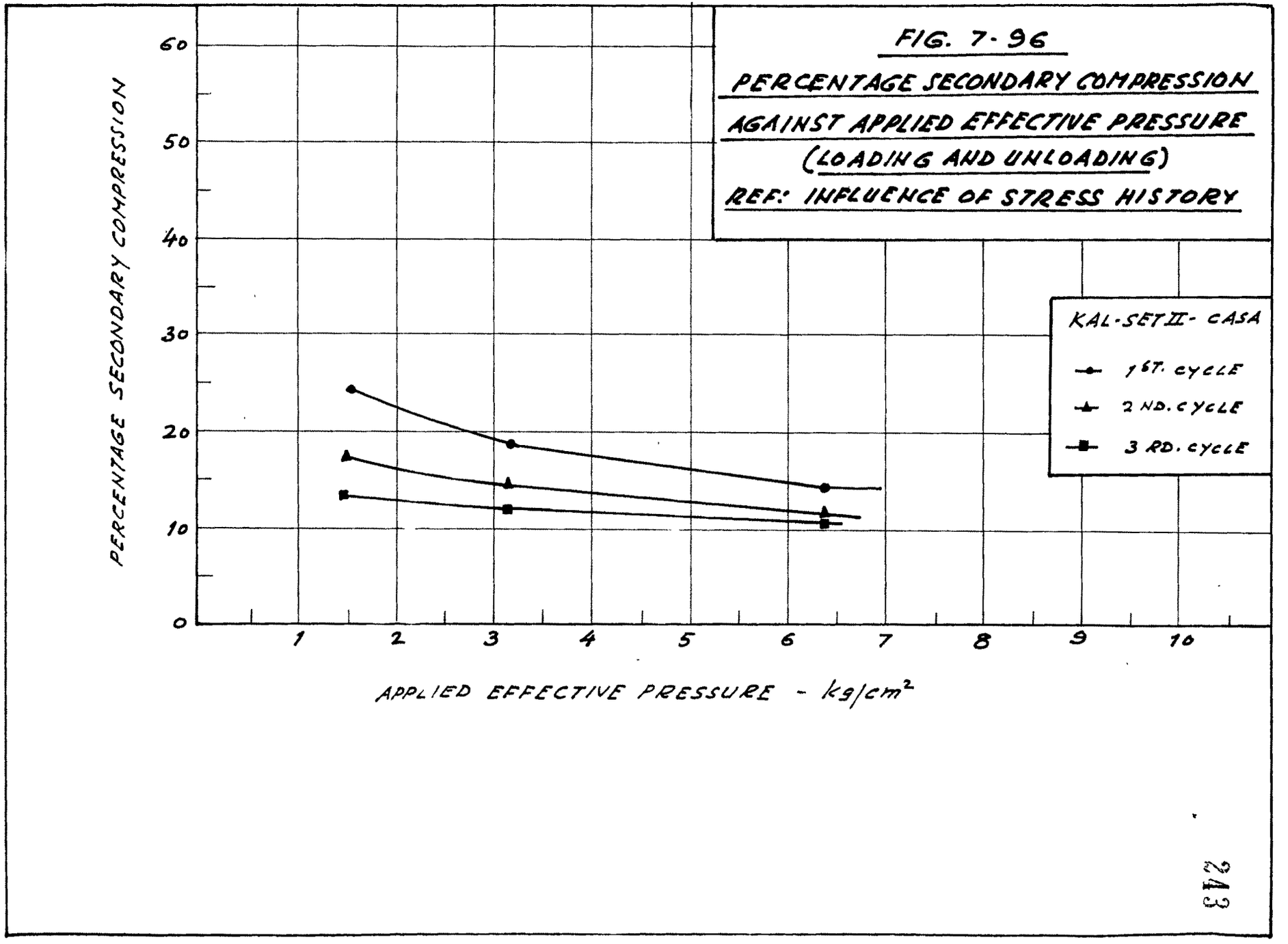
FIG. 7-96
PERCENTAGE SECONDARY COMPRESSION AGAINST APPLIED EFFECTIVE PRESSURE (LOADING AND UNLOADING)
REF: INFLUENCE OF STRESS HISTORY
KAL-SET II- CASA
1 ST. CYCLE
2 ND. CYCLE
3 RD. CYCLE
PERCENTAGE SECONDARY COMPRESSION
0
10
20
30
40
50
60
1
2
3
4
5
6
7
8
9
10
APPLIED EFFECTIVE PRESSURE - kg/cm²

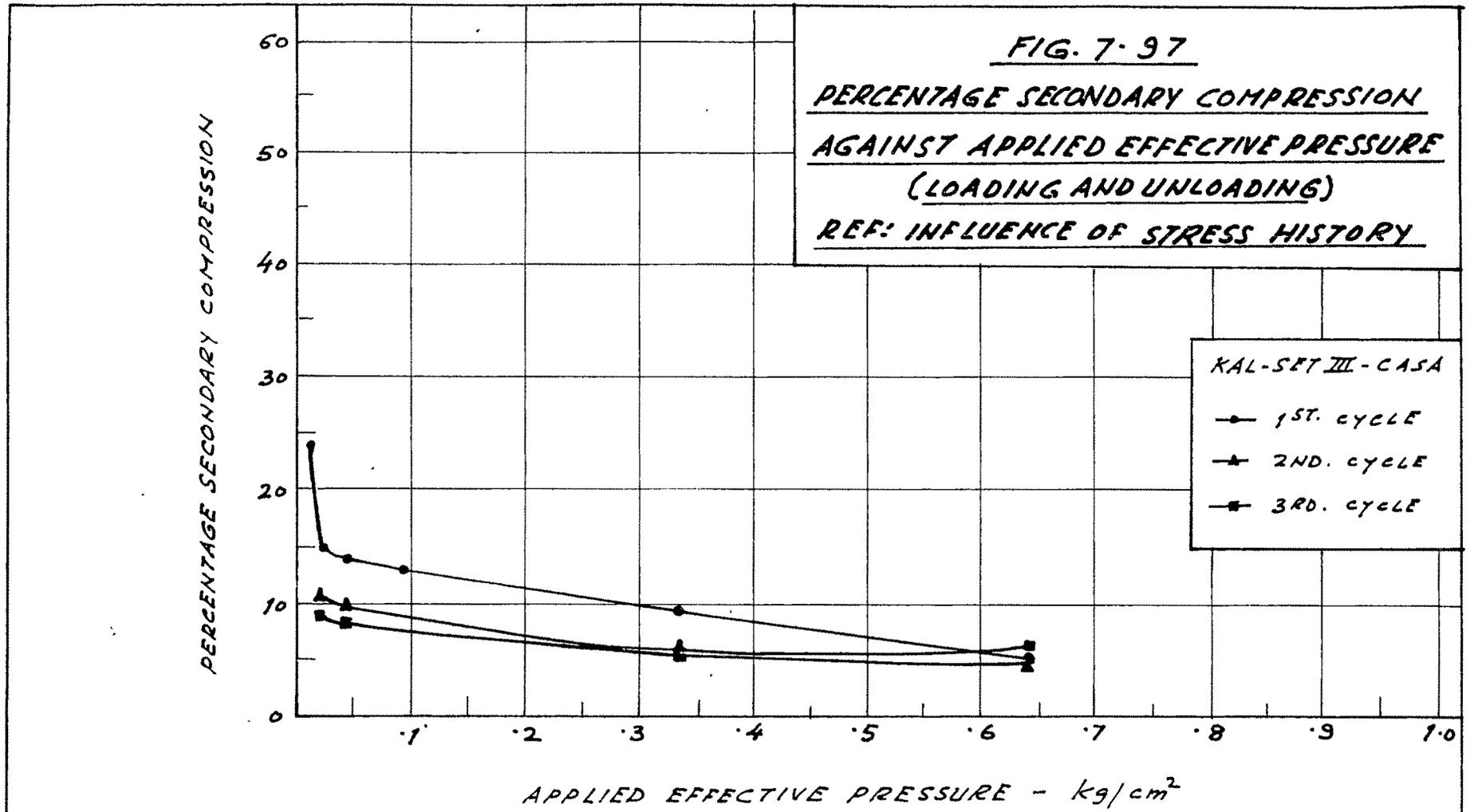
FIG. 7·97
PERCENTAGE SECONDARY COMPRESSION AGAINST APPLIED EFFECTIVE PRESSURE (LOADING AND UNLOADING)
REF: INFLUENCE OF STRESS HISTORY
KAL-SET III - CASA
1ST. CYCLE
2ND. CYCLE
3RD. CYCLE
PERCENTAGE SECONDARY COMPRESSION
60
50
40
30
20
10
0
·1
·2
·3
·4
·5
·6
·7
·8
·9
1·0
APPLIED EFFECTIVE PRESSURE - kg/cm²

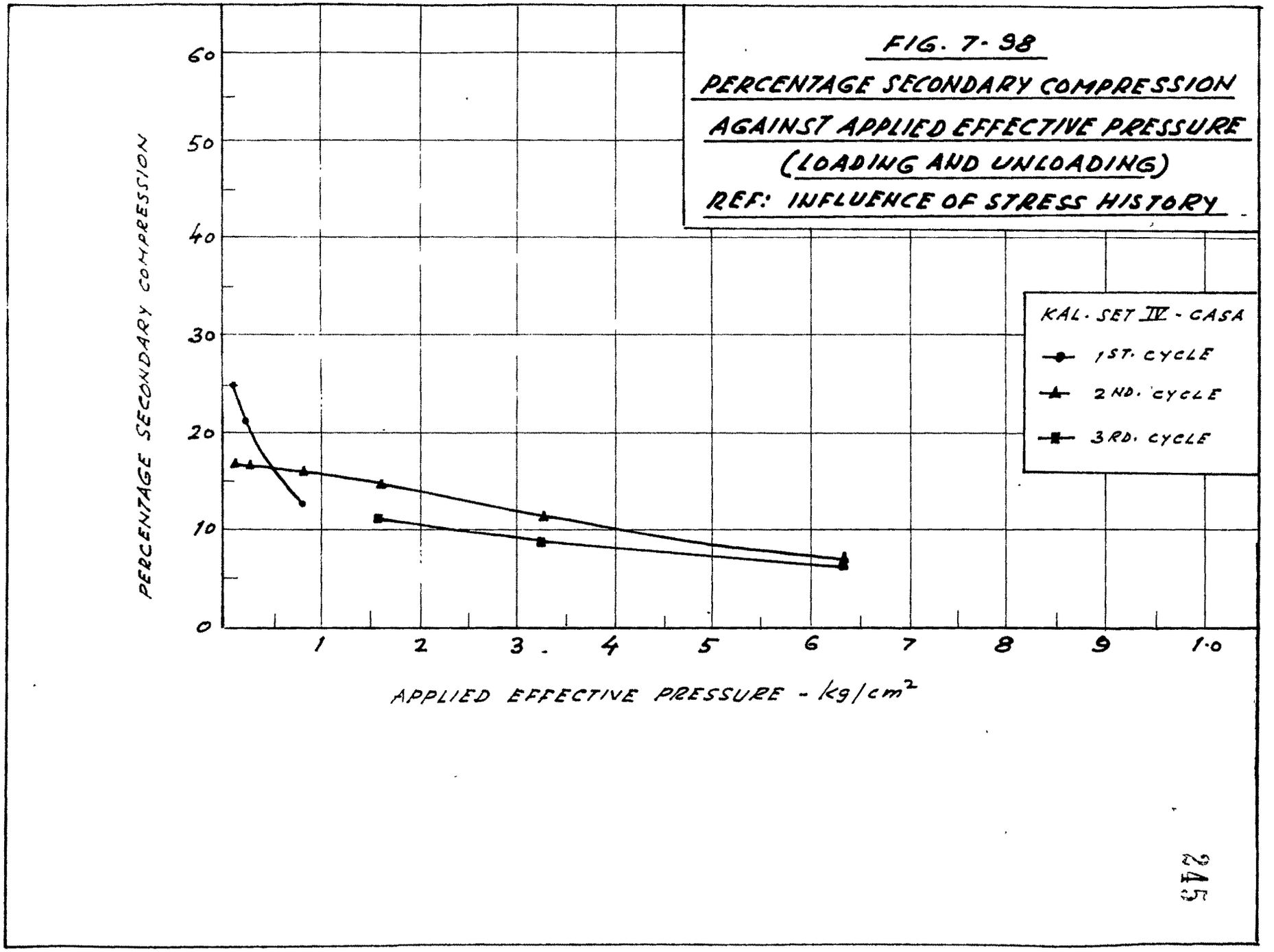
FIG. 7-98
PERCENTAGE SECONDARY COMPRESSION AGAINST APPLIED EFFECTIVE PRESSURE (LOADING AND UNLOADING)
REF: INFLUENCE OF STRESS HISTORY
KAL. SET IV - CASA
1ST. CYCLE
2ND. CYCLE
3RD. CYCLE
PERCENTAGE SECONDARY COMPRESSION
0
10
20
30
40
50
60
1
2
3
4
5
6
7
8
9
1·0
APPLIED EFFECTIVE PRESSURE - kg/cm²

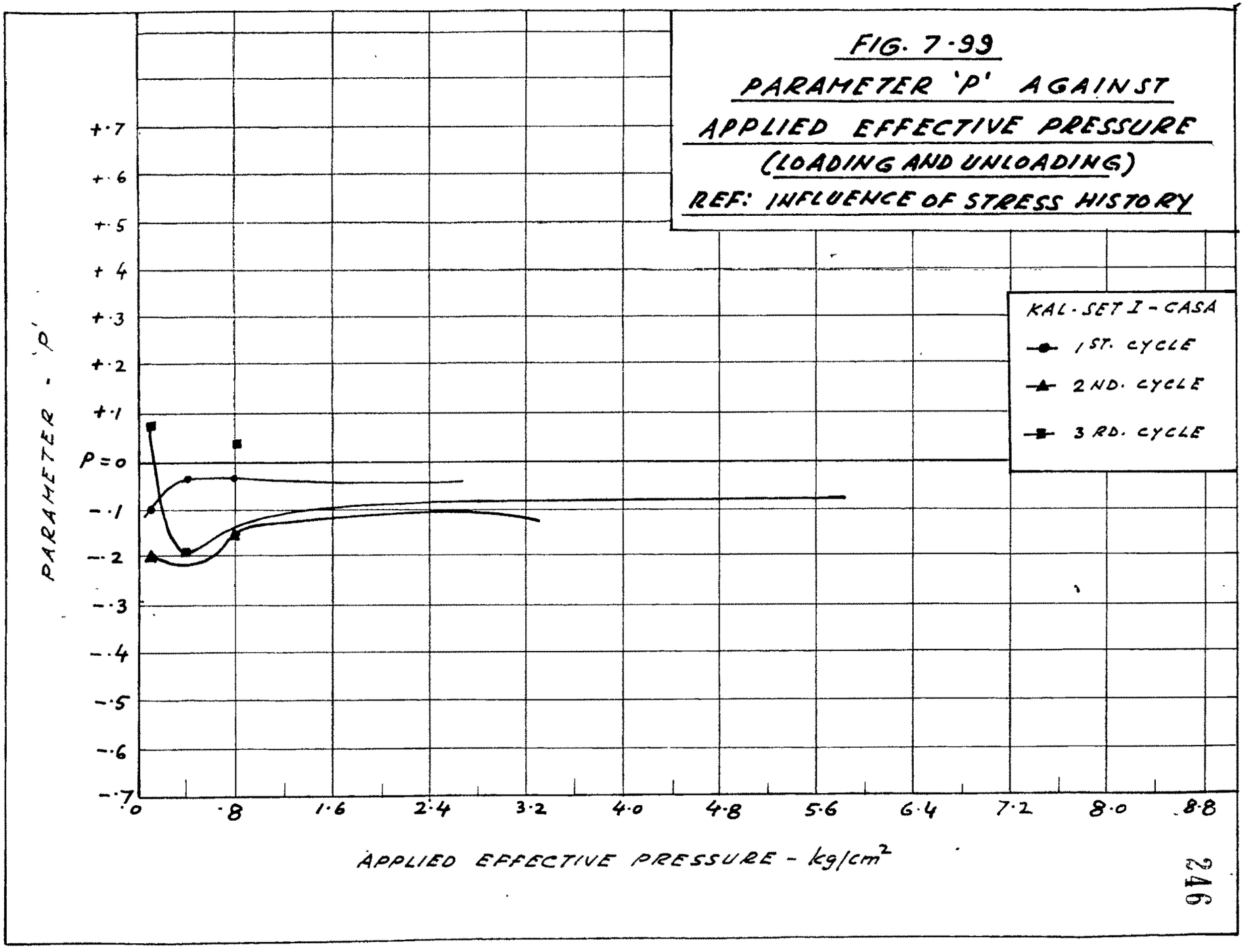
FIG. 7·99
PARAMETER 'P' AGAINST
APPLIED EFFECTIVE PRESSURE
(LOADING AND UNLOADING)
REF: INFLUENCE OF STRESS HISTORY
KAL - SET I - CASA
1ST. CYCLE
2ND. CYCLE
3RD. CYCLE
PARAMETER - 'P'
+·7
+·6
+·5
+ 4
+·3
+·2
+·1
P = 0
-·1
-·2
-·3
-·4
-·5
-·6
-·7
·0
·8
1·6
2·4
3·2
4·0
4·8
5·6
6·4
7·2
8·0
8·8
APPLIED EFFECTIVE PRESSURE - kg/cm²

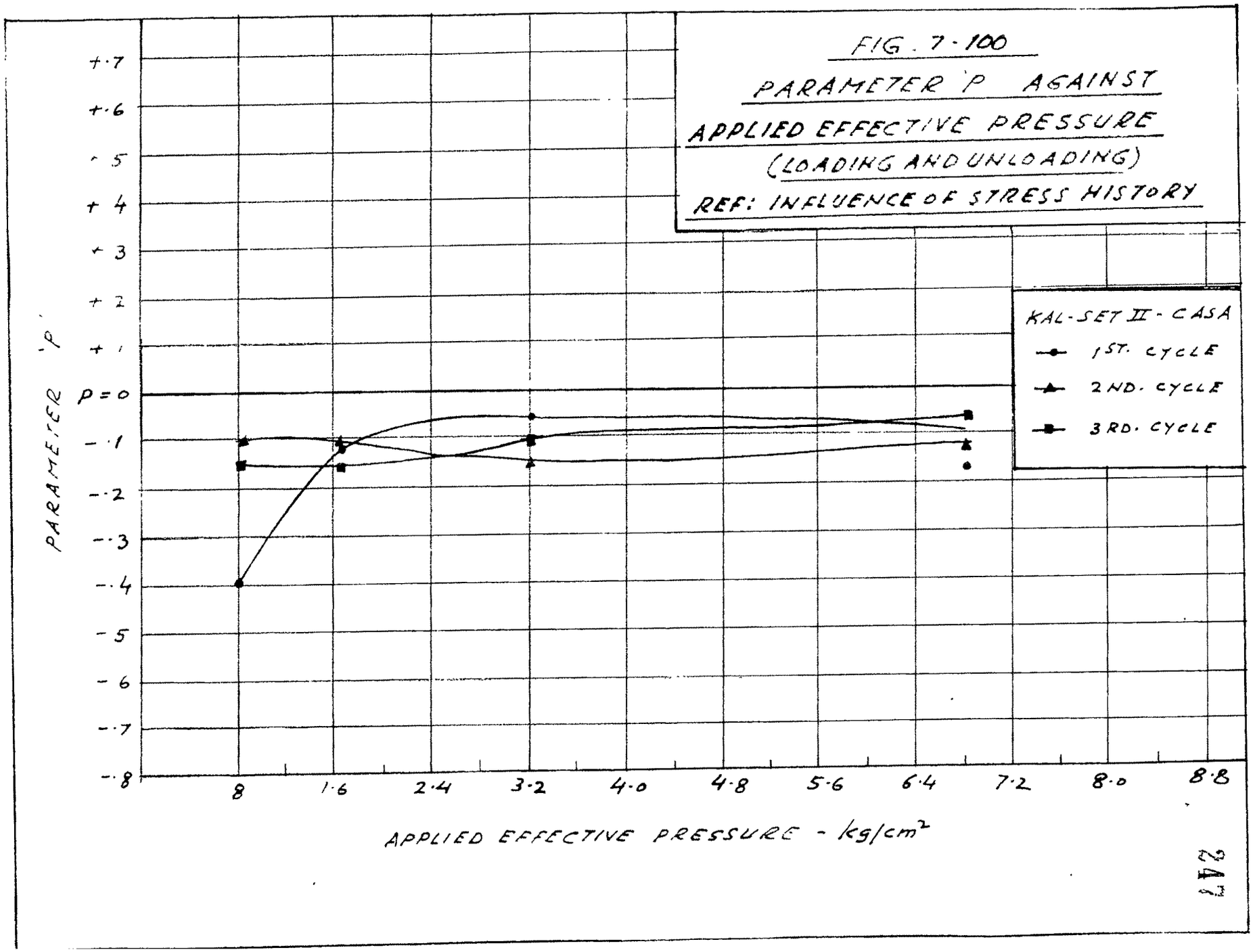
FIG. 7·100
PARAMETER 'P' AGAINST
APPLIED EFFECTIVE PRESSURE
(LOADING AND UNLOADING)
REF: INFLUENCE OF STRESS HISTORY
KAL-SET II - CASA
1ST. CYCLE
2ND. CYCLE
3RD. CYCLE
PARAMETER 'P'
+·7
+·6
+·5
+·4
+·3
+·2
+·1
P=0
-·1
-·2
-·3
-·4
-·5
-·6
-·7
-·8
·8
1·6
2·4
3·2
4·0
4·8
5·6
6·4
7·2
8·0
8·8
APPLIED EFFECTIVE PRESSURE - kg/cm²

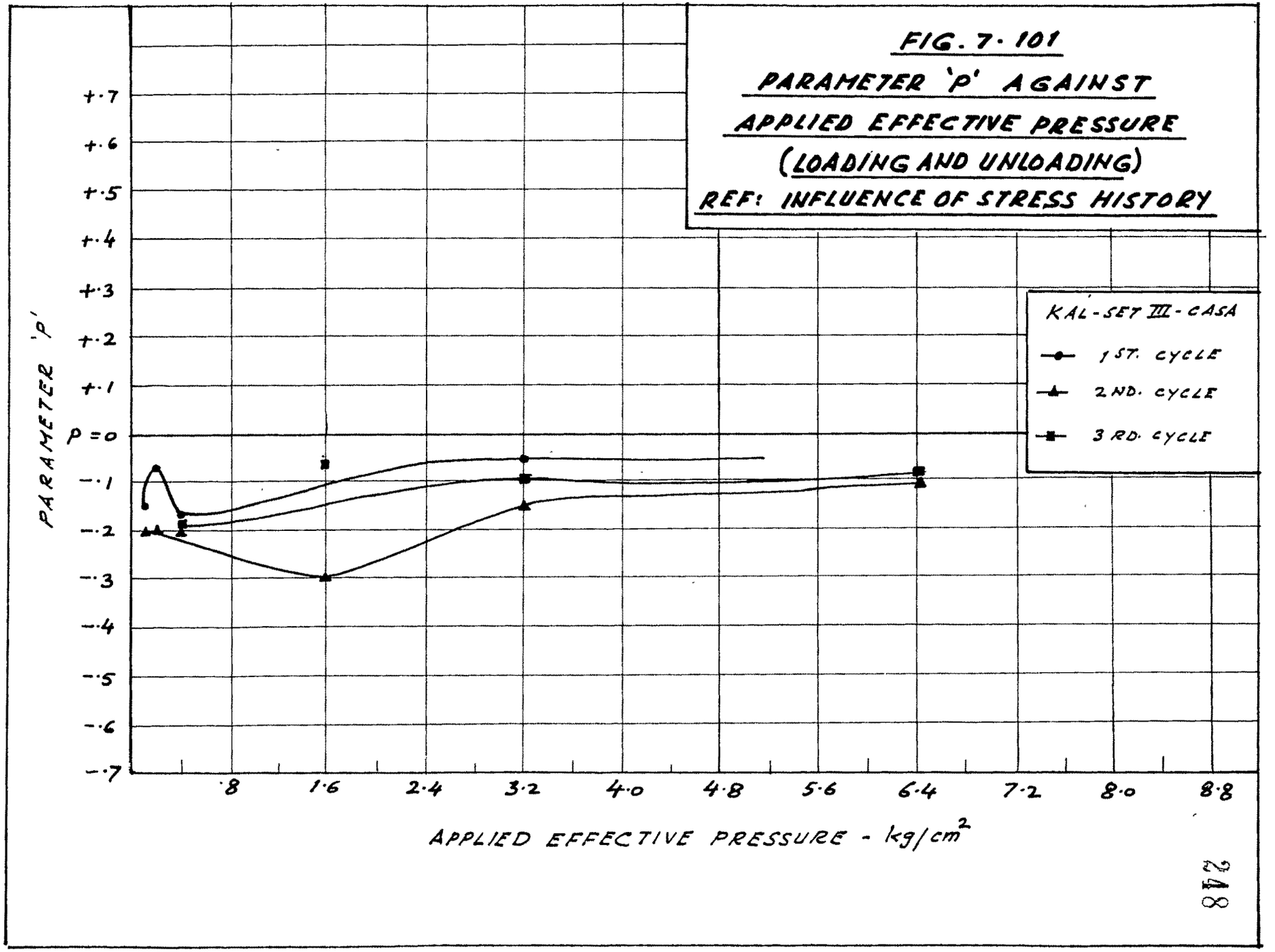
FIG. 7·101
PARAMETER 'P' AGAINST
APPLIED EFFECTIVE PRESSURE
(LOADING AND UNLOADING)
REF: INFLUENCE OF STRESS HISTORY
KAL-SET III - CASA
1ST. CYCLE
2ND. CYCLE
3 RD. CYCLE
PARAMETER 'P'
+·7
+·6
+·5
+·4
+·3
+·2
+·1
P = 0
−·1
−·2
−·3
−·4
−·5
−·6
−·7
·8
1·6
2·4
3·2
4·0
4·8
5·6
6·4
7·2
8·0
8·8
APPLIED EFFECTIVE PRESSURE - kg/cm²

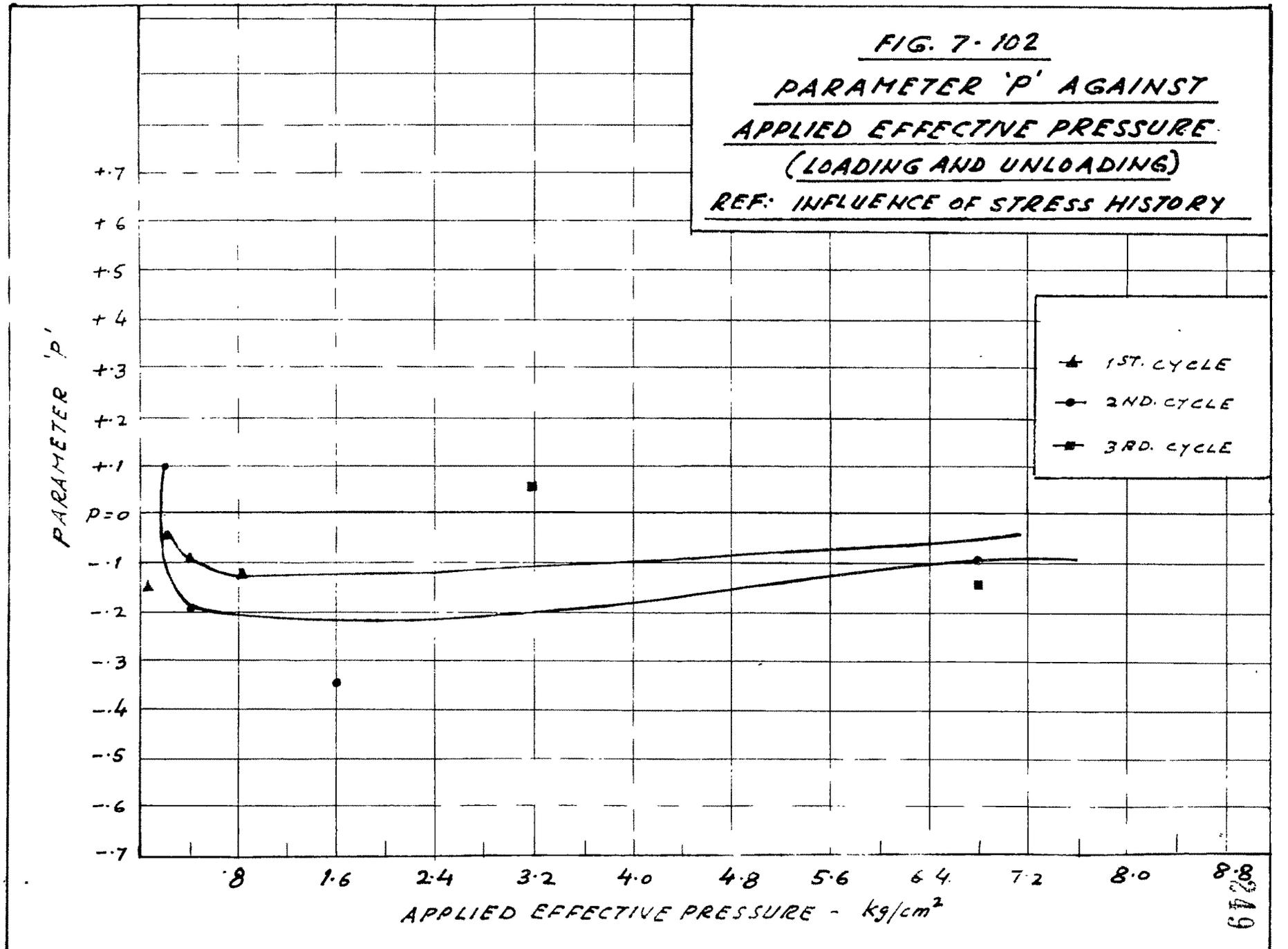
FIG. 7·102
PARAMETER 'P' AGAINST
APPLIED EFFECTIVE PRESSURE
(LOADING AND UNLOADING)
REF: INFLUENCE OF STRESS HISTORY
1ST. CYCLE
2ND. CYCLE
3RD. CYCLE
PARAMETER 'P'
+·7
+ 6
+·5
+ 4
+·3
+·2
+·1
P=0
-·1
-·2
-·3
-·4
-·5
-·6
-·7
·8
1·6
2·4
3·2
4·0
4·8
5·6
6 4
7·2
8·0
8·8
APPLIED EFFECTIVE PRESSURE - kg/cm²
67249

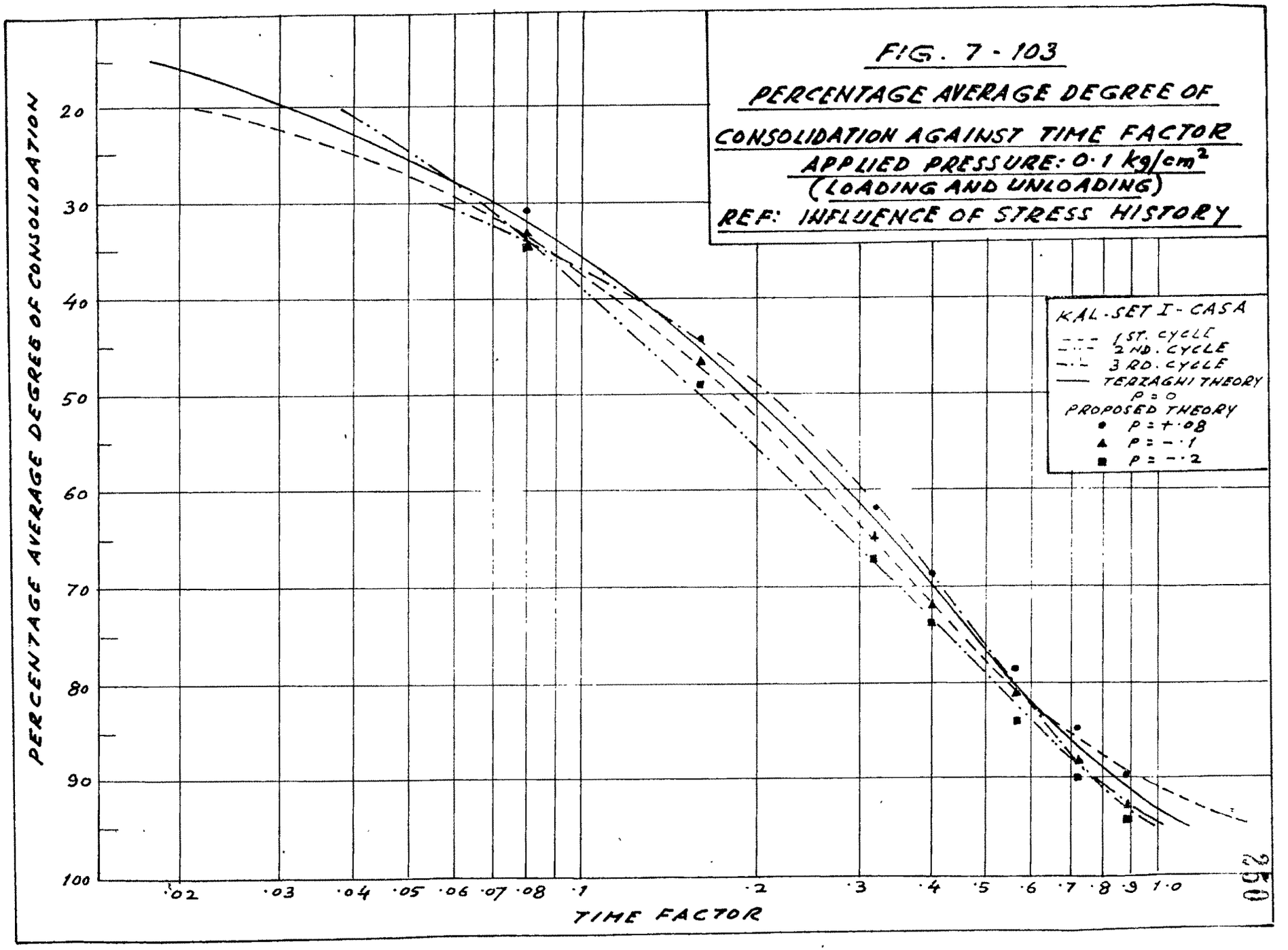
FIG. 7 - 103
PERCENTAGE AVERAGE DEGREE OF CONSOLIDATION AGAINST TIME FACTOR
APPLIED PRESSURE: 0·1 kg/cm²
(LOADING AND UNLOADING)
REF: INFLUENCE OF STRESS HISTORY
KAL-SET I - CASA
1ST. CYCLE
2ND. CYCLE
3RD. CYCLE
TERZAGHI THEORY
p = 0
PROPOSED THEORY
p = +·08
p = −·1
p = −·2
PERCENTAGE AVERAGE DEGREE OF CONSOLIDATION
20
30
40
50
60
70
80
90
100
·02
·03
·04
·05
·06
·07
·08
·1
·2
·3
·4
·5
·6
·7
·8
·9
1·0
TIME FACTOR
092

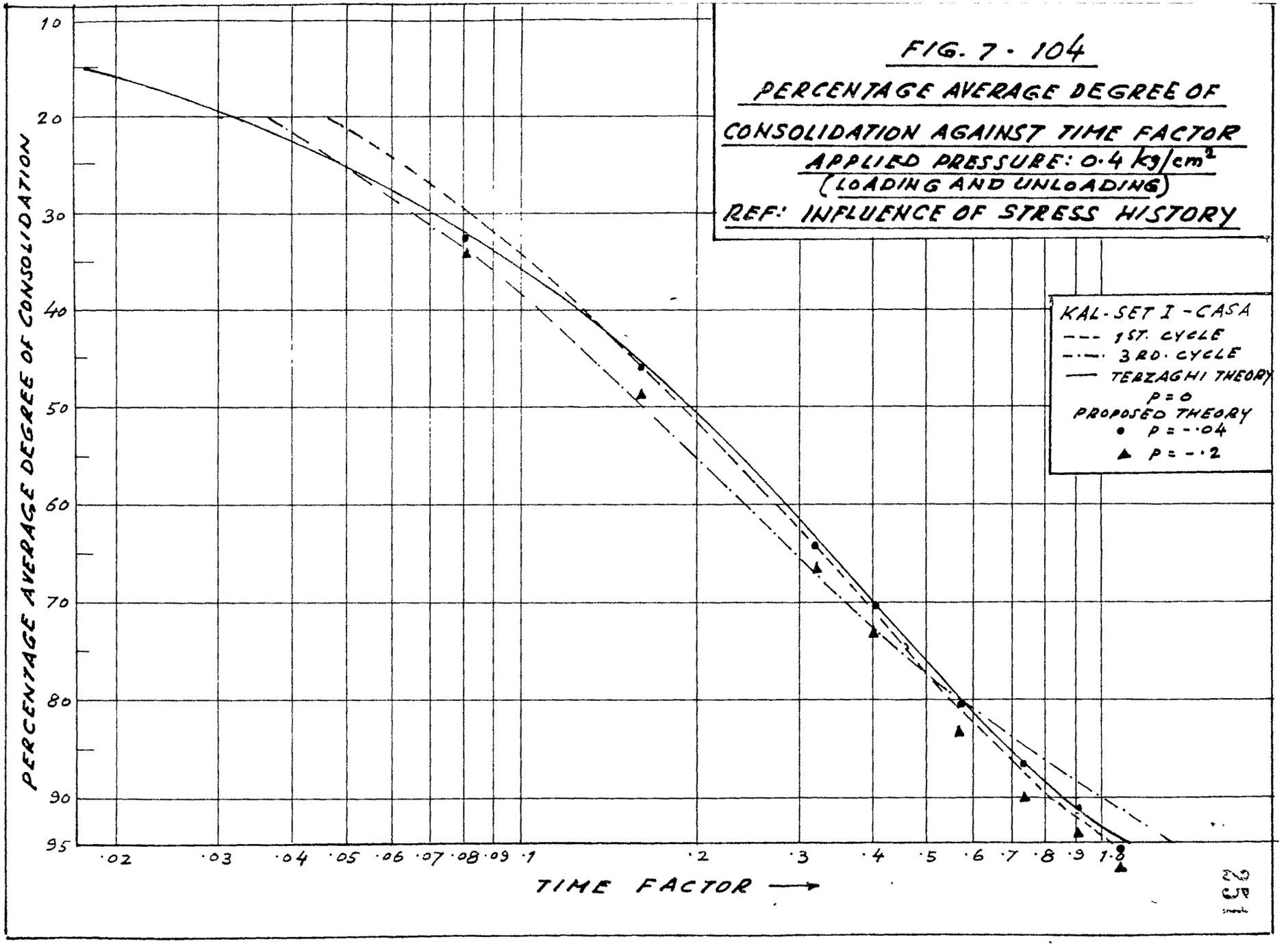
FIG. 7 · 104
PERCENTAGE AVERAGE DEGREE OF CONSOLIDATION AGAINST TIME FACTOR
APPLIED PRESSURE: 0·4 kg/cm²
(LOADING AND UNLOADING)
REF: INFLUENCE OF STRESS HISTORY
KAL-SET I - CASA
--- 1ST. CYCLE
-·-·- 3RD. CYCLE
—— TERZAGHI THEORY
P = 0
PROPOSED THEORY
● P = ·04
▲ P = ·2
PERCENTAGE AVERAGE DEGREE OF CONSOLIDATION
10
20
30
40
50
60
70
80
90
95
·02 ·03 ·04 ·05 ·06 ·07 ·08 ·09 ·1 ·2 ·3 ·4 ·5 ·6 ·7 ·8 ·9 1·0
TIME FACTOR →

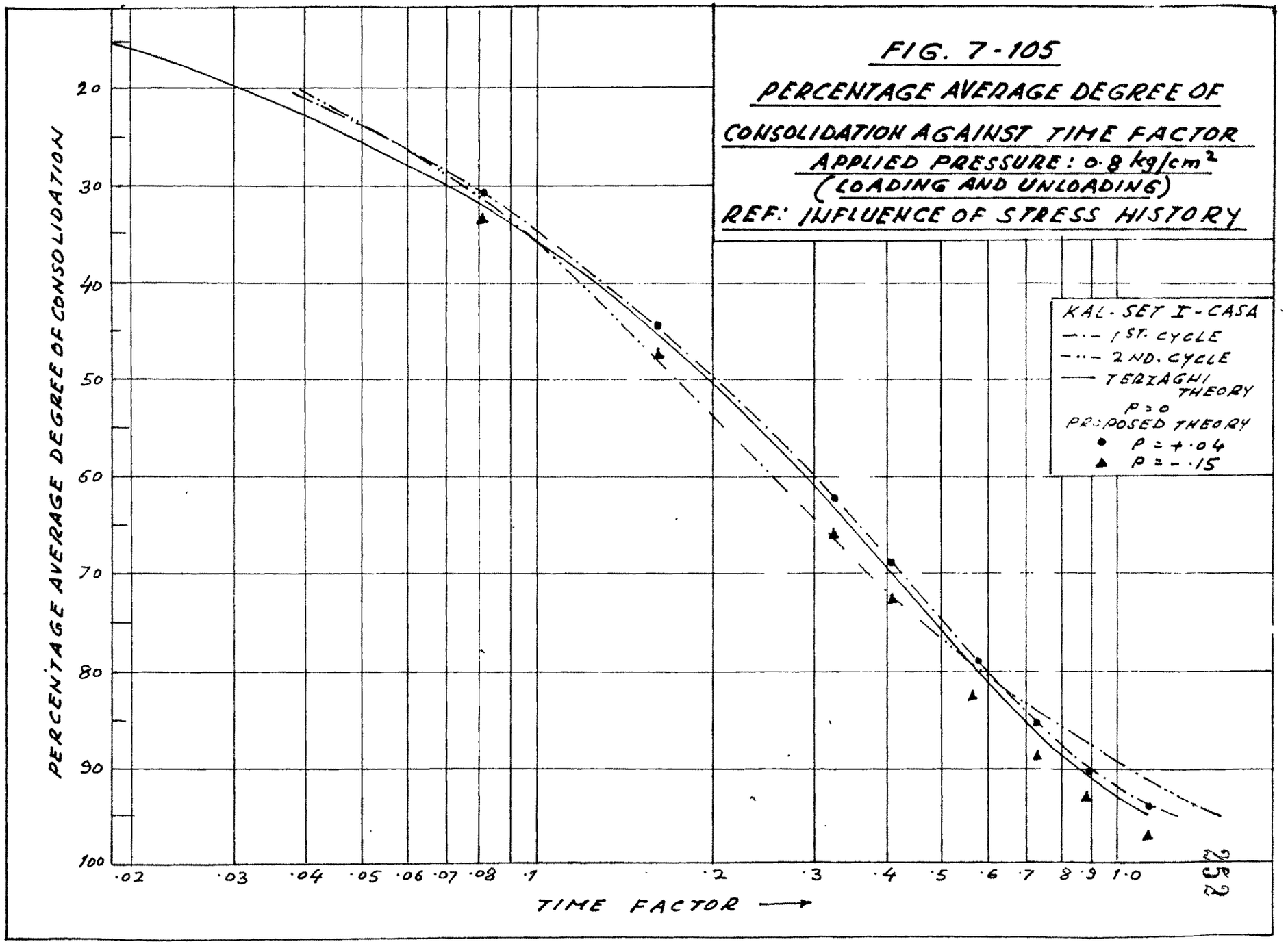
FIG. 7-105
PERCENTAGE AVERAGE DEGREE OF CONSOLIDATION AGAINST TIME FACTOR
APPLIED PRESSURE : 0·8 kg/cm²
(LOADING AND UNLOADING)
REF: INFLUENCE OF STRESS HISTORY
KAL - SET I - CASA
1 ST. CYCLE
2 ND. CYCLE
TERZAGHI THEORY
PROPOSED THEORY
P = 0
P = +·04
P = −·15
PERCENTAGE AVERAGE DEGREE OF CONSOLIDATION
20
30
40
50
60
70
80
90
100
·02
·03
·04
·05
·06
·07
·08
·1
·2
·3
·4
·5
·6
·7
·8
·9
1·0
TIME FACTOR
252

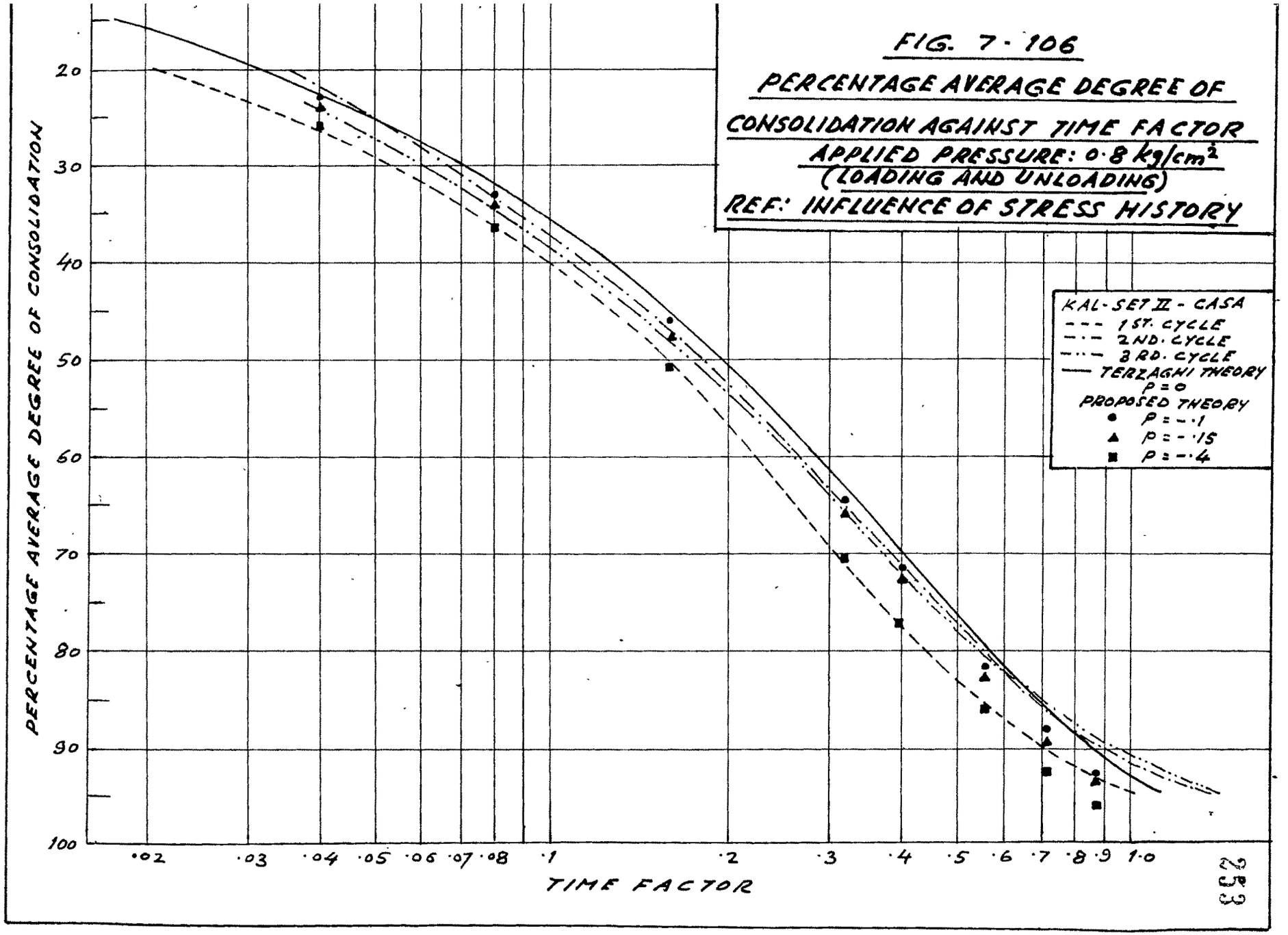
FIG. 7·106
PERCENTAGE AVERAGE DEGREE OF CONSOLIDATION AGAINST TIME FACTOR
APPLIED PRESSURE: 0·8 kg/cm²
(LOADING AND UNLOADING)
REF: INFLUENCE OF STRESS HISTORY
KAL-SET II - CASA
1ST. CYCLE
2ND. CYCLE
3RD. CYCLE
TERZAGHI THEORY
PROPOSED THEORY
p = 0
p = -·1
p = -·15
p = -·4
PERCENTAGE AVERAGE DEGREE OF CONSOLIDATION
20
30
40
50
60
70
80
90
100
·02
·03
·04
·05
·06
·07
·08
·1
·2
·3
·4
·5
·6
·7
·8
·9
1·0
TIME FACTOR

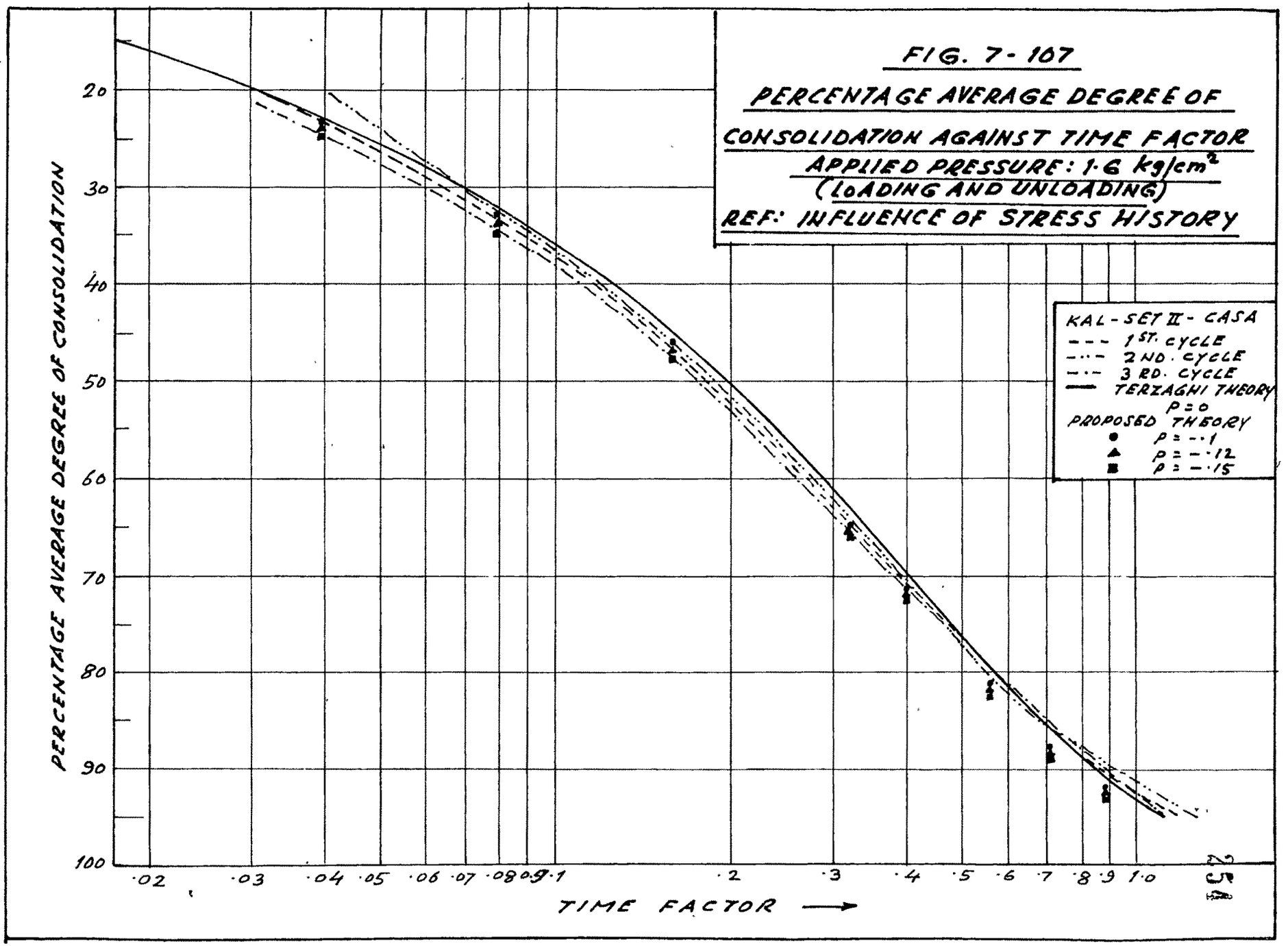
FIG. 7-107
PERCENTAGE AVERAGE DEGREE OF CONSOLIDATION AGAINST TIME FACTOR
APPLIED PRESSURE: 1·6 kg/cm²
(LOADING AND UNLOADING)
REF: INFLUENCE OF STRESS HISTORY
KAL-SET II - CASA
1ST. CYCLE
2ND. CYCLE
3RD. CYCLE
TERZAGHI THEORY
P=0
PROPOSED THEORY
P=-·1
P=-·12
P=-·15
PERCENTAGE AVERAGE DEGREE OF CONSOLIDATION
20
30
40
50
60
70
80
90
100
·02
·03
·04
·05
·06
·07
·08
·09
·1
·2
·3
·4
·5
·6
·7
·8
·9
1·0
TIME FACTOR

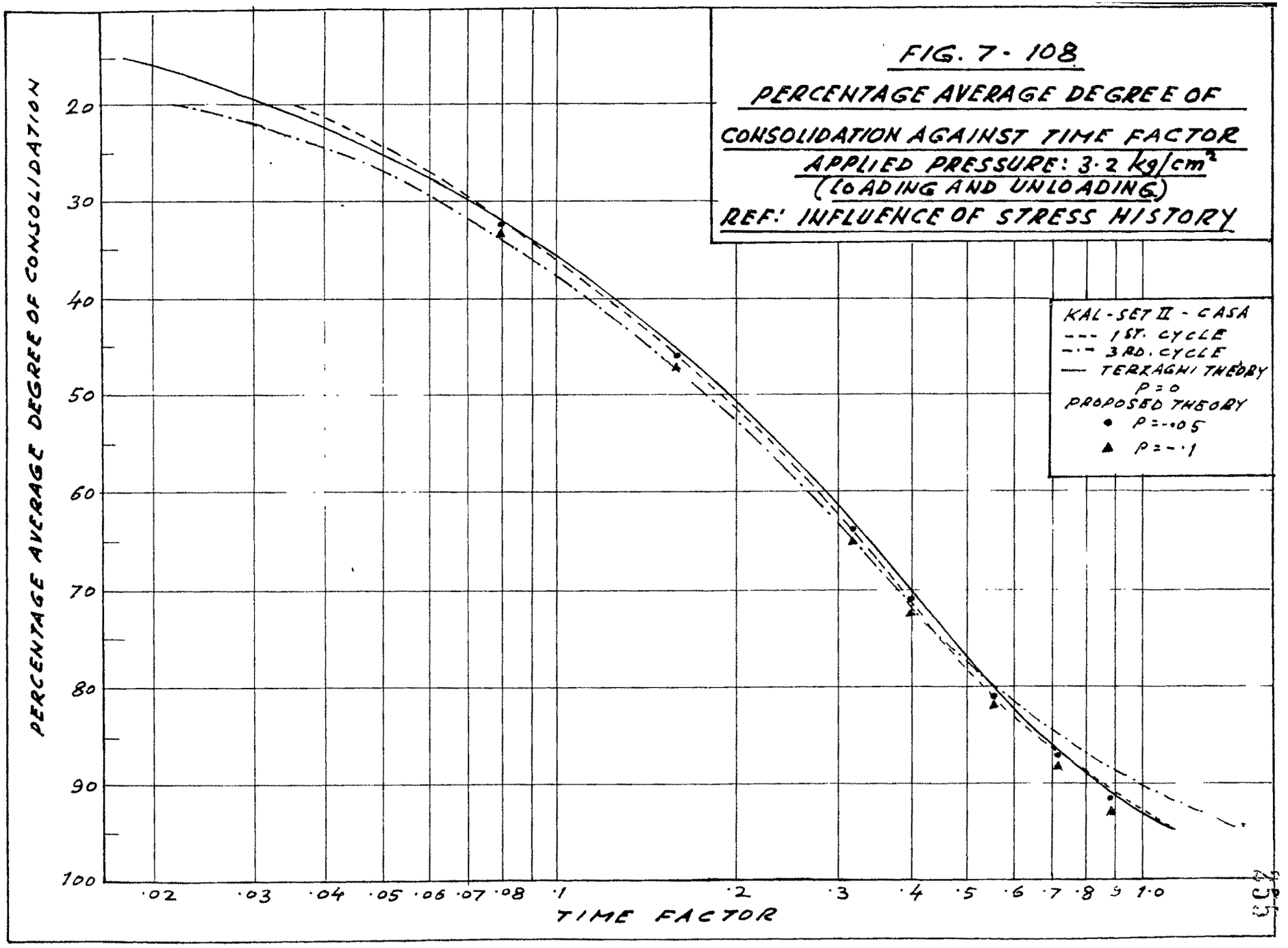
FIG. 7 - 108
PERCENTAGE AVERAGE DEGREE OF CONSOLIDATION AGAINST TIME FACTOR
APPLIED PRESSURE: 3·2 kg/cm²
(LOADING AND UNLOADING)
REF: INFLUENCE OF STRESS HISTORY
KAL - SET II - CASA
--- 1ST. CYCLE
-·- 3RD. CYCLE
— TERZAGHI THEORY
PROPOSED THEORY
P = 0
● P = -·05
▲ P = -·1
PERCENTAGE AVERAGE DEGREE OF CONSOLIDATION
20
30
40
50
60
70
80
90
100
·02
·03
·04
·05
·06
·07
·08
·1
·2
·3
·4
·5
·6
·7
·8
·9
1·0
TIME FACTOR

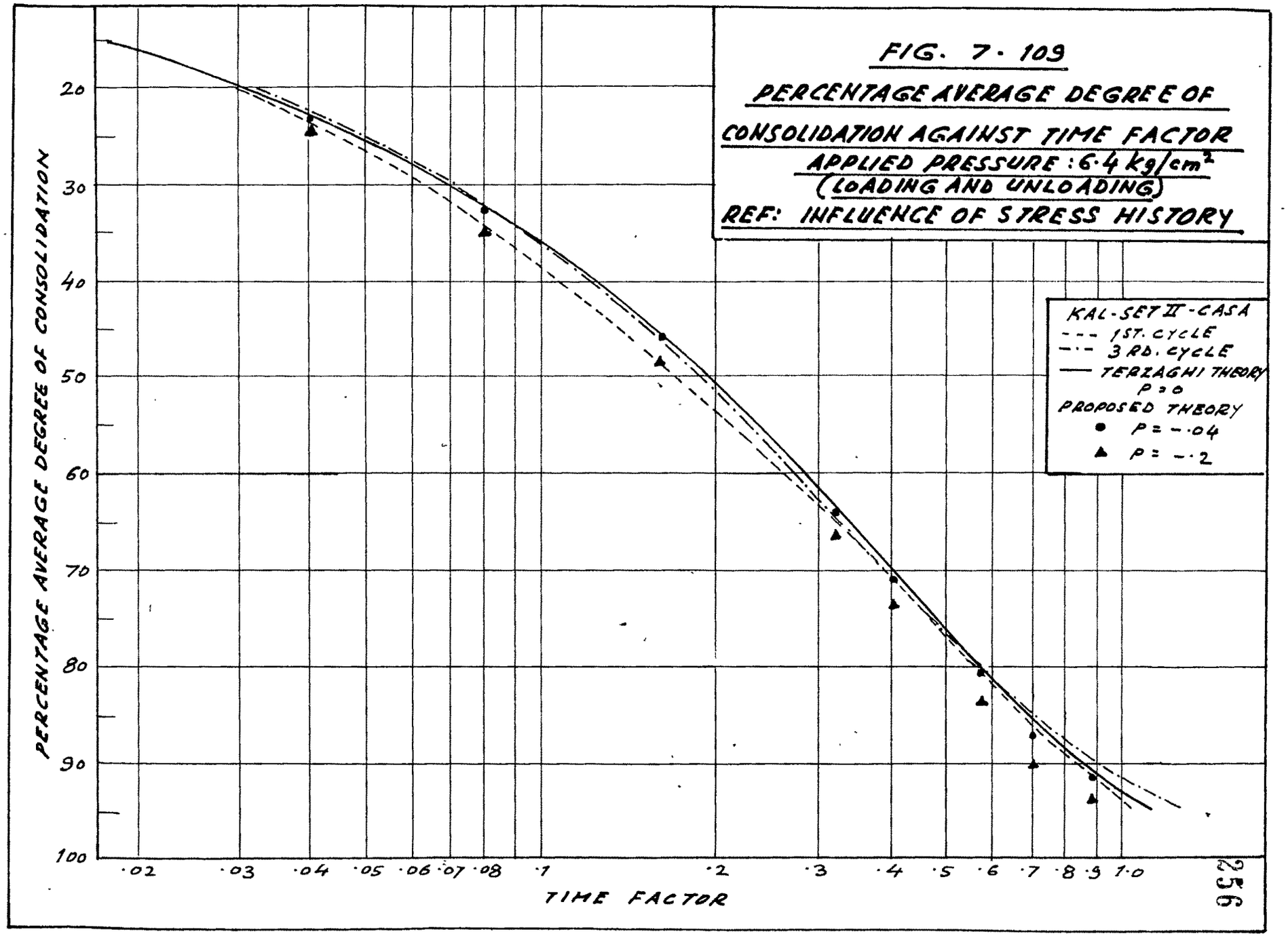
FIG. 7·109
PERCENTAGE AVERAGE DEGREE OF CONSOLIDATION AGAINST TIME FACTOR
APPLIED PRESSURE : 6·4 kg/cm²
(LOADING AND UNLOADING)
REF: INFLUENCE OF STRESS HISTORY
KAL-SET II-CASA
--- 1ST. CYCLE
-·- 3 RD. CYCLE
—— TERZAGHI THEORY P=0
PROPOSED THEORY
● P = -·04
▲ P = -·2
PERCENTAGE AVERAGE DEGREE OF CONSOLIDATION
20
30
40
50
60
70
80
90
100
·02
·03
·04
·05
·06
·07
·08
·1
·2
·3
·4
·5
·6
·7
·8
·9
1·0
TIME FACTOR
952

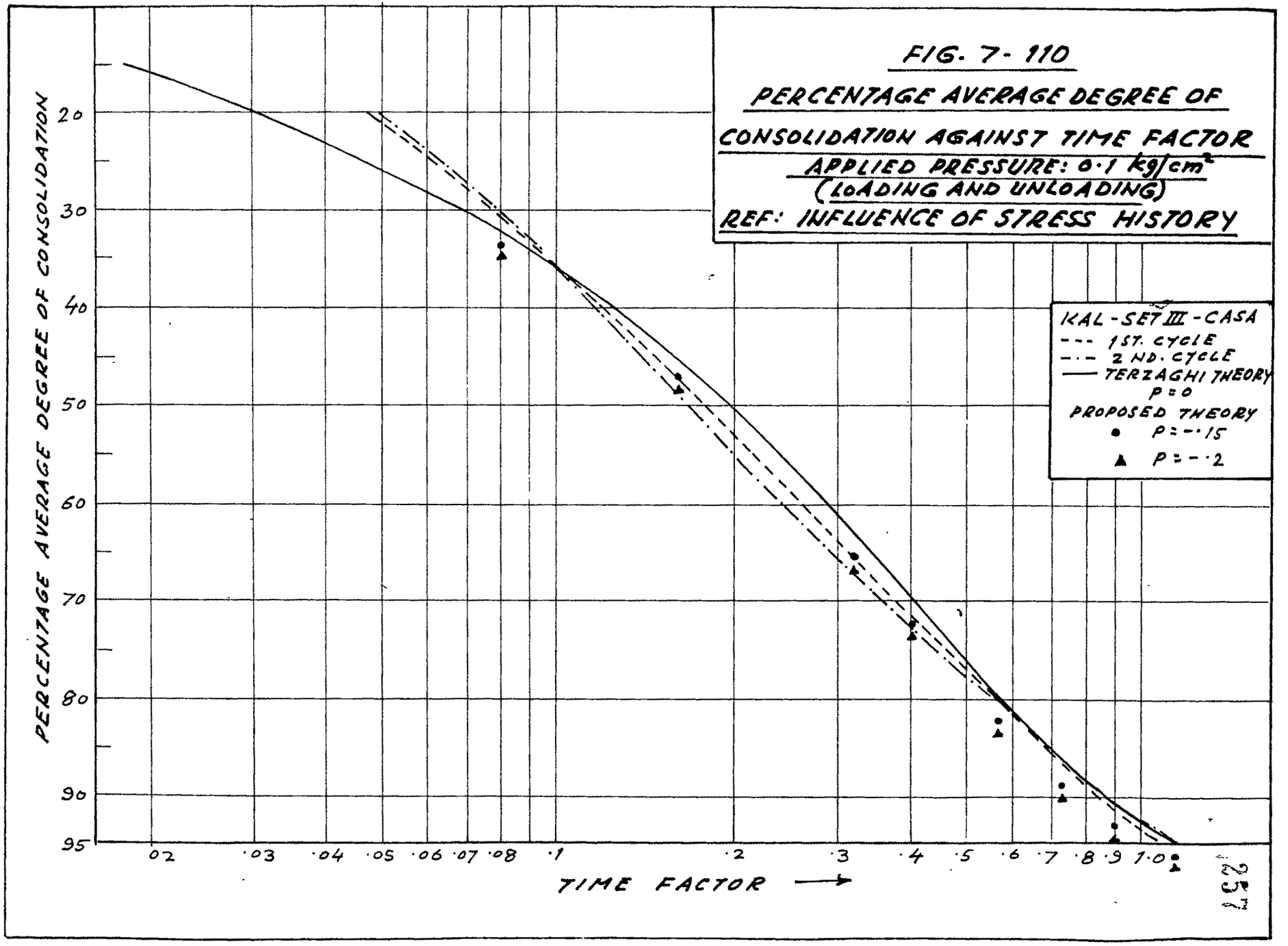
FIG. 7-110
PERCENTAGE AVERAGE DEGREE OF CONSOLIDATION AGAINST TIME FACTOR
APPLIED PRESSURE: 0·1 kg/cm²
(LOADING AND UNLOADING)
REF: INFLUENCE OF STRESS HISTORY
IKAL-SET III-CASA
--- 1ST. CYCLE
-·- 2 ND. CYCLE
—— TERZAGHI THEORY P=0
PROPOSED THEORY
● P=-·15
▲ P=-·2
PERCENTAGE AVERAGE DEGREE OF CONSOLIDATION
20
30
40
50
60
70
80
90
95
·02
·03
·04
·05
·06
·07
·08
·1
·2
·3
·4
·5
·6
·7
·8
·9
1·0
TIME FACTOR →
4.32

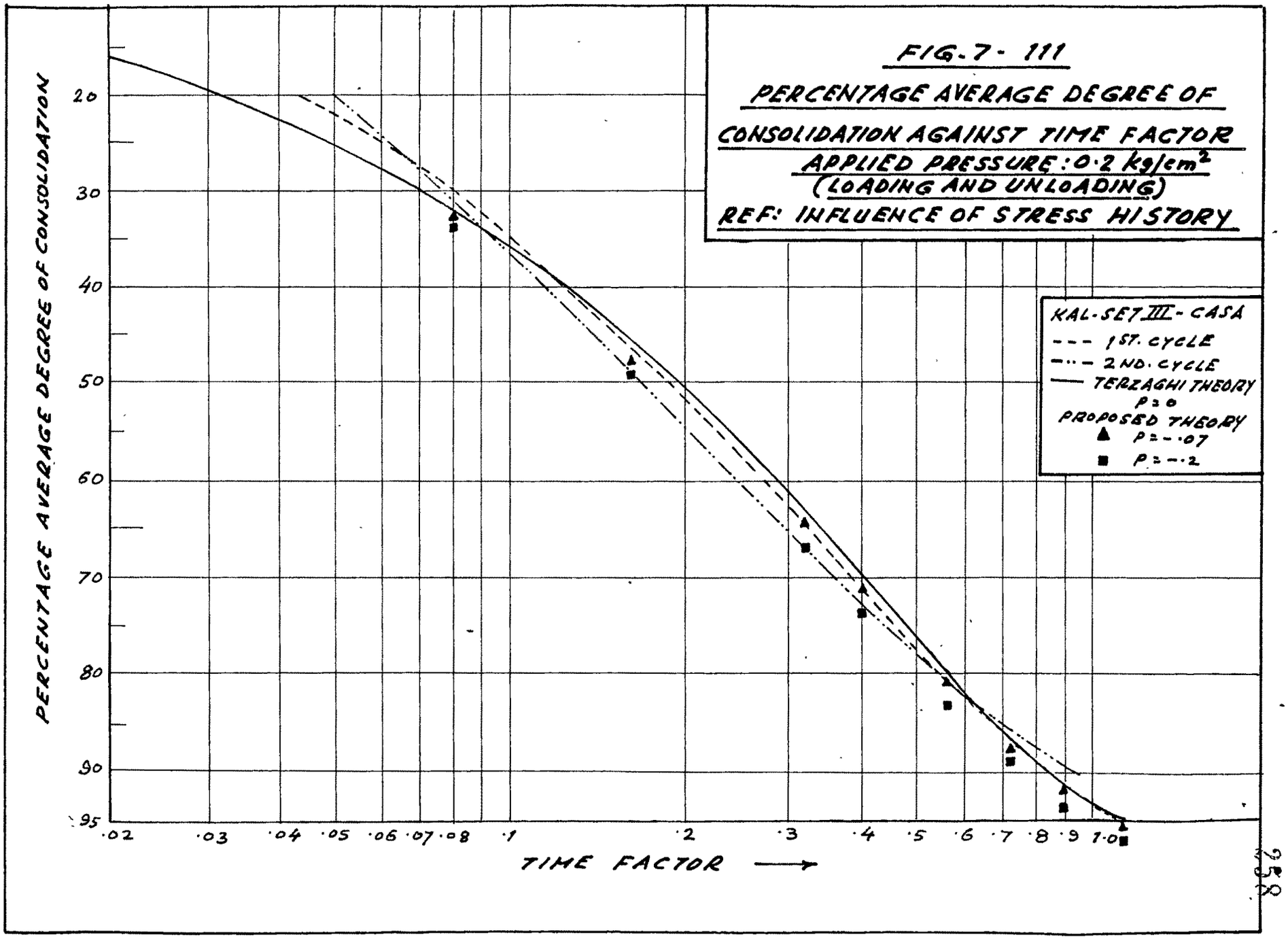
FIG. 7 - 111
PERCENTAGE AVERAGE DEGREE OF CONSOLIDATION AGAINST TIME FACTOR
APPLIED PRESSURE : 0·2 kg/cm²
(LOADING AND UNLOADING)
REF: INFLUENCE OF STRESS HISTORY
KAL-SET III - CASA
--- 1ST. CYCLE
-·-· 2ND. CYCLE
—— TERZAGHI THEORY P = 0
PROPOSED THEORY
▲ P = -·07
■ P = -·2
PERCENTAGE AVERAGE DEGREE OF CONSOLIDATION
20
30
40
50
60
70
80
90
95
·02
·03
·04
·05
·06
·07
·08
·1
·2
·3
·4
·5
·6
·7
·8
·9
1·0
TIME FACTOR ⟶

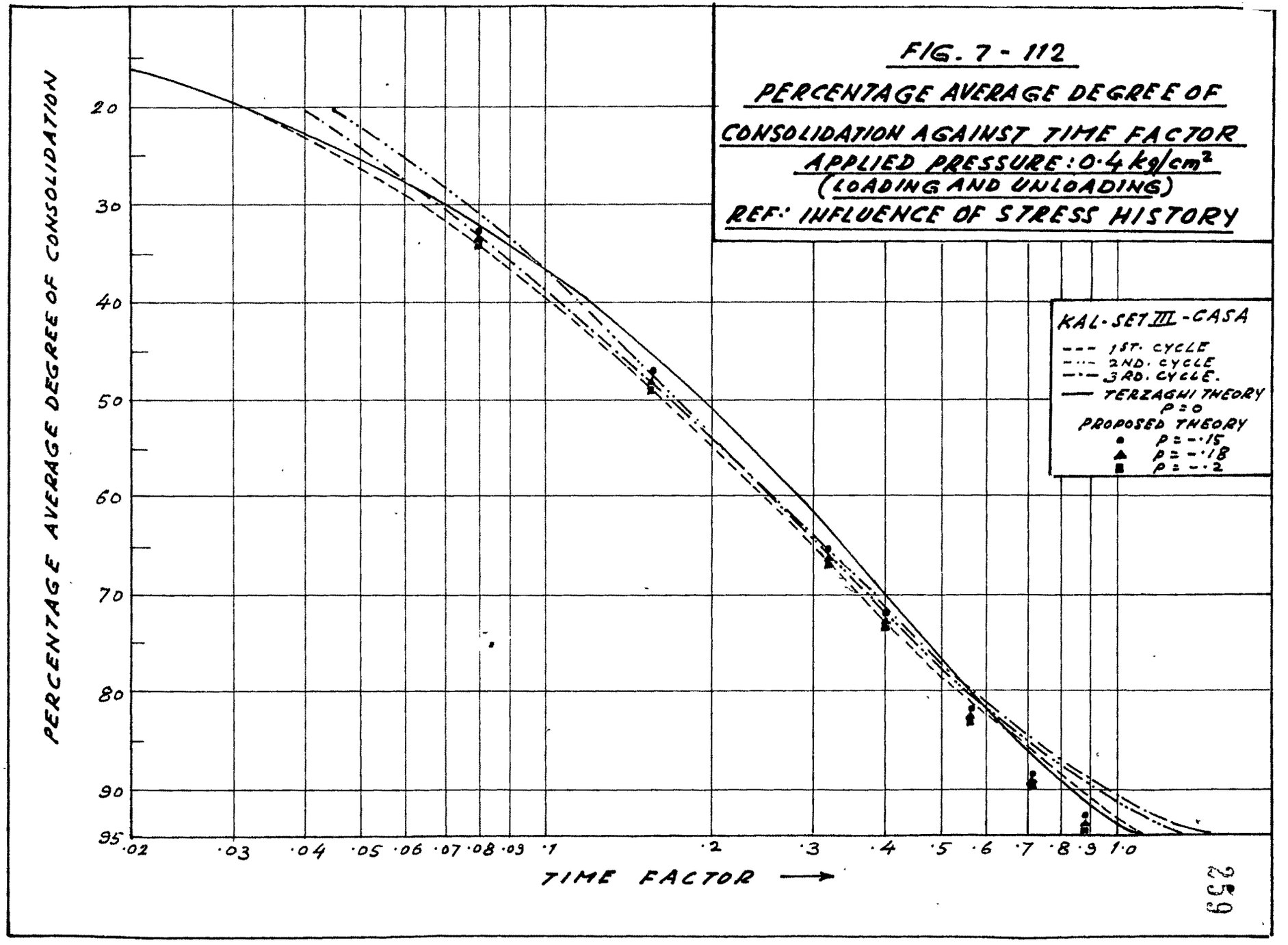
FIG. 7 - 112
PERCENTAGE AVERAGE DEGREE OF CONSOLIDATION AGAINST TIME FACTOR
APPLIED PRESSURE : 0·4 kg/cm²
(LOADING AND UNLOADING)
REF: INFLUENCE OF STRESS HISTORY
KAL-SET III - CASA
--- 1ST. CYCLE
-·-·- 2ND. CYCLE
-··-··- 3RD. CYCLE.
—— TERZAGHI THEORY P=0
PROPOSED THEORY
● P = -·15
▲ P = -·18
■ P = -·2
PERCENTAGE AVERAGE DEGREE OF CONSOLIDATION
20
30
40
50
60
70
80
90
95
·02 ·03 ·04 ·05 ·06 ·07 ·08 ·09 ·1 ·2 ·3 ·4 ·5 ·6 ·7 ·8 ·9 1·0
TIME FACTOR →

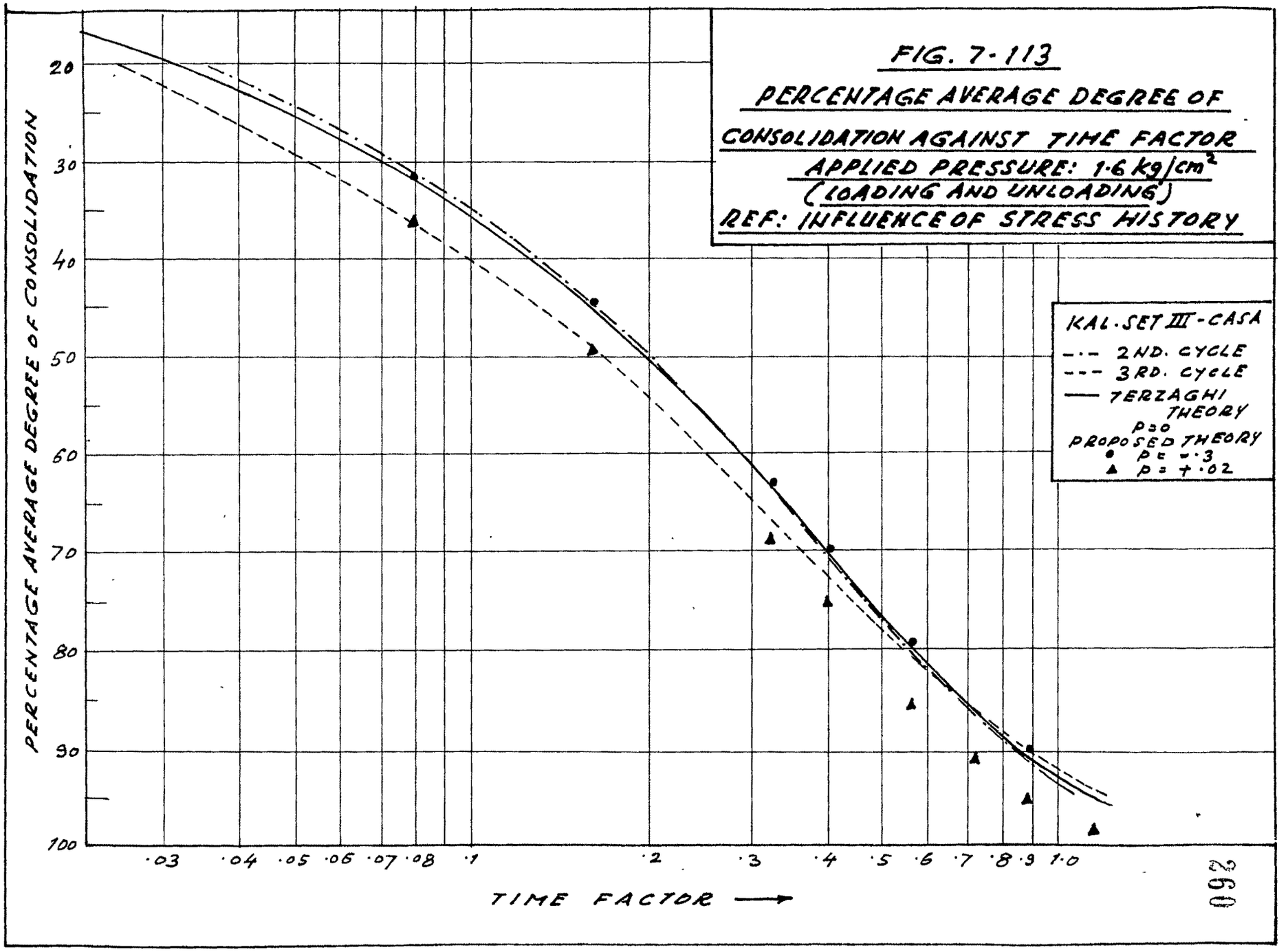
FIG. 7-113
PERCENTAGE AVERAGE DEGREE OF CONSOLIDATION AGAINST TIME FACTOR
APPLIED PRESSURE: 1·6 kg/cm²
(LOADING AND UNLOADING)
REF: INFLUENCE OF STRESS HISTORY
KAL. SET III - CASA
2ND. CYCLE
3RD. CYCLE
TERZAGHI THEORY
P=0
PROPOSED THEORY
P = -·3
P = +·02
PERCENTAGE AVERAGE DEGREE OF CONSOLIDATION
20
30
40
50
60
70
80
90
100
·03 ·04 ·05 ·06 ·07 ·08 ·1 ·2 ·3 ·4 ·5 ·6 ·7 ·8 ·9 1·0
TIME FACTOR
092

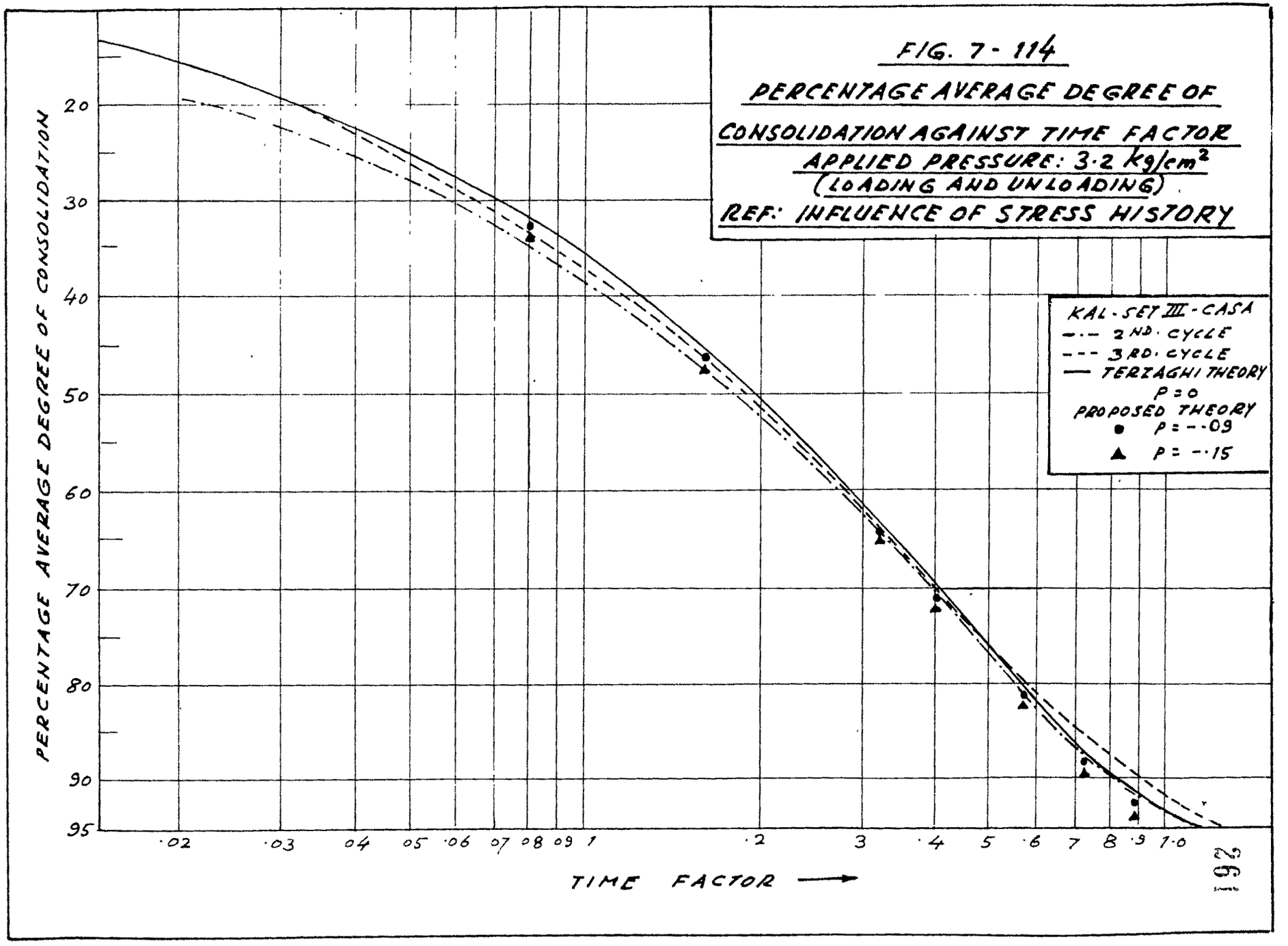
FIG. 7-114
PERCENTAGE AVERAGE DEGREE OF CONSOLIDATION AGAINST TIME FACTOR
APPLIED PRESSURE: 3·2 kg/cm²
(LOADING AND UNLOADING)
REF: INFLUENCE OF STRESS HISTORY
KAL-SET III-CASA
2ND. CYCLE
3RD. CYCLE
TERZAGHI THEORY
P=0
PROPOSED THEORY
P=-·09
P=-·15
PERCENTAGE AVERAGE DEGREE OF CONSOLIDATION
20
30
40
50
60
70
80
90
95
·02
·03
04
05
·06
07
08
09
1
·2
3
·4
5
·6
7
8
·9
1·0
TIME FACTOR
192

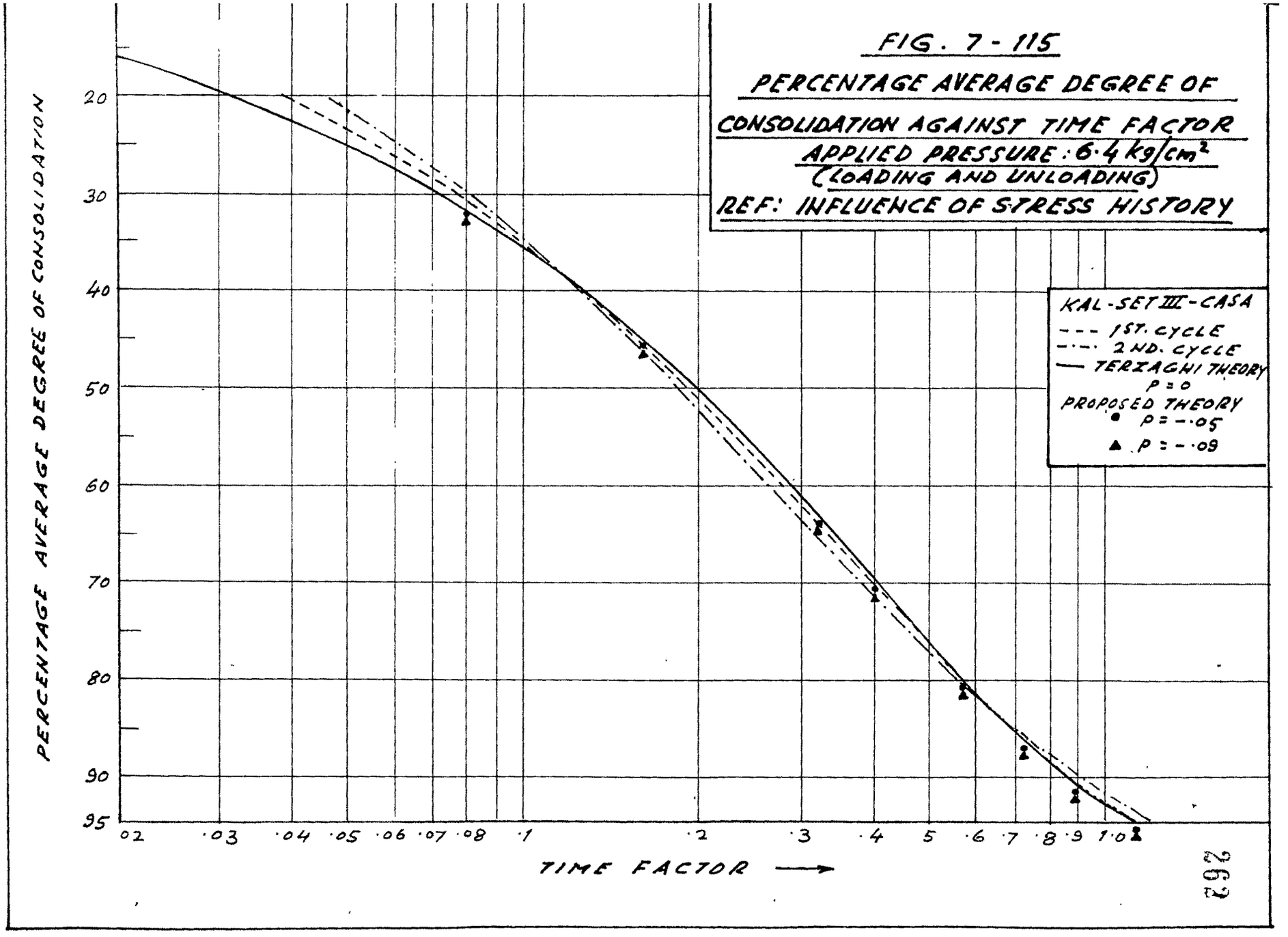
FIG. 7-115
PERCENTAGE AVERAGE DEGREE OF CONSOLIDATION AGAINST TIME FACTOR
APPLIED PRESSURE : 6·4 kg/cm²
(LOADING AND UNLOADING)
REF: INFLUENCE OF STRESS HISTORY
KAL-SET III-CASA
--- 1ST. CYCLE
-·-·- 2ND. CYCLE
— TERZAGHI THEORY P = 0
PROPOSED THEORY
● P = -·05
▲ P = -·09
PERCENTAGE AVERAGE DEGREE OF CONSOLIDATION
20
30
40
50
60
70
80
90
95
02
·03
·04
·05
·06
·07
·08
·1
·2
·3
·4
5
·6
·7
·8
·9
1·0
TIME FACTOR ⟶
292

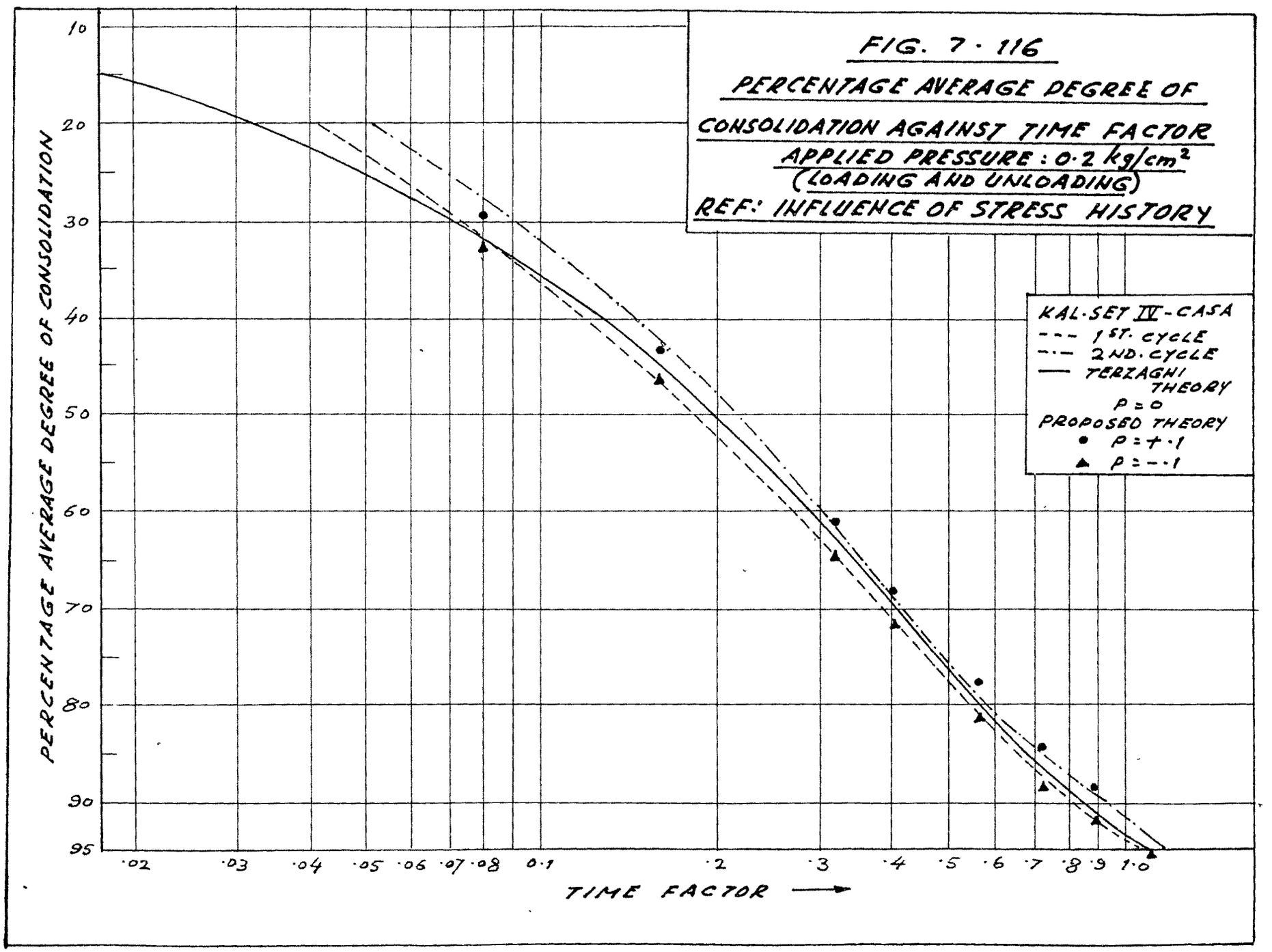
FIG. 7·116
PERCENTAGE AVERAGE DEGREE OF CONSOLIDATION AGAINST TIME FACTOR
APPLIED PRESSURE : 0·2 kg/cm²
(LOADING AND UNLOADING)
REF: INFLUENCE OF STRESS HISTORY
KAL·SET IV - CASA
--- 1ST. CYCLE
-·- 2ND. CYCLE
— TERZAGHI THEORY
P = 0
PROPOSED THEORY
● P = +·1
▲ P = -·1
PERCENTAGE AVERAGE DEGREE OF CONSOLIDATION
10
20
30
40
50
60
70
80
90
95
·02 ·03 ·04 ·05 ·06 ·07 ·08 0·1 ·2 ·3 ·4 ·5 ·6 ·7 ·8 ·9 1·0
TIME FACTOR ⟶

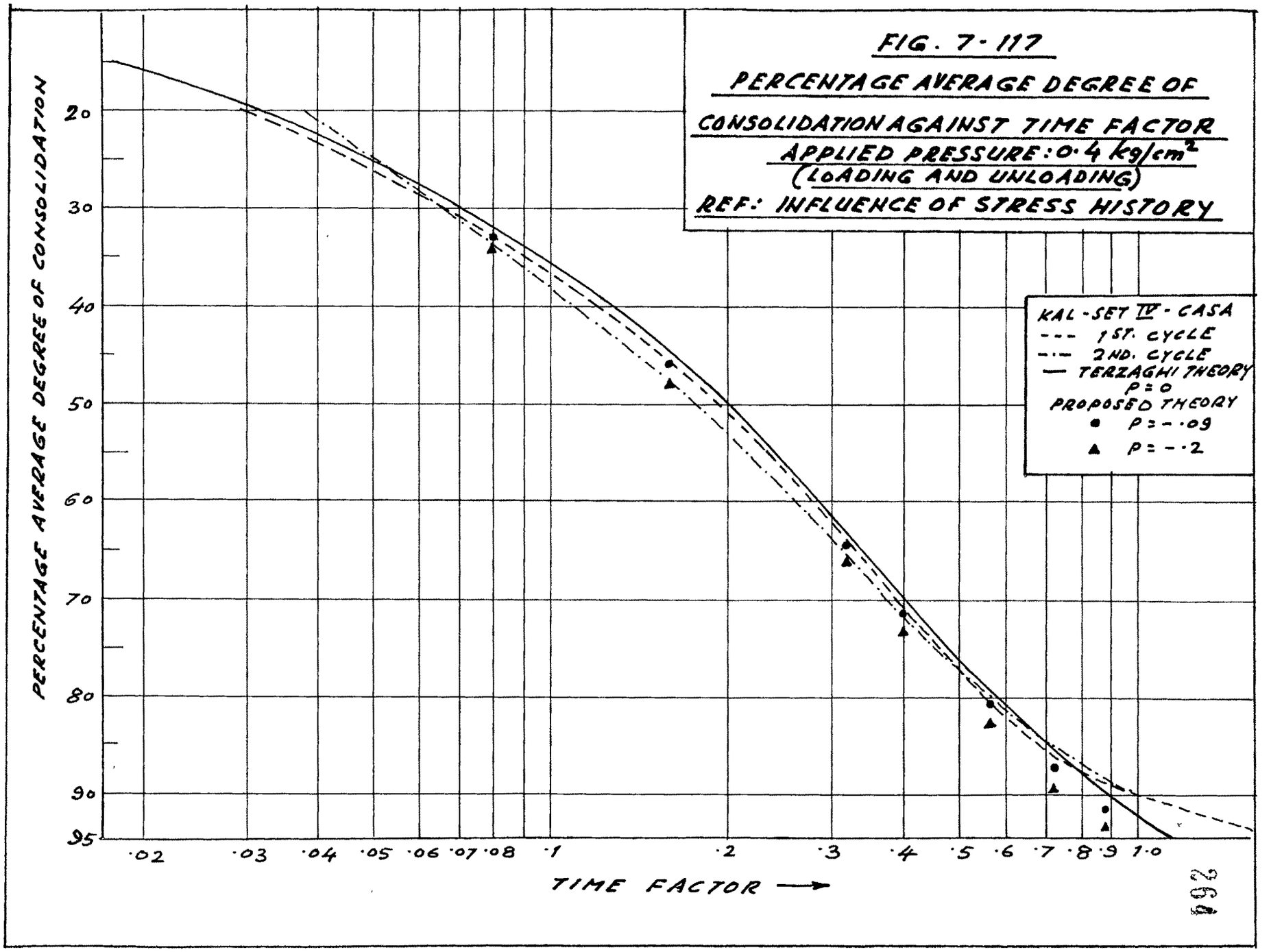
FIG. 7·117
PERCENTAGE AVERAGE DEGREE OF CONSOLIDATION AGAINST TIME FACTOR
APPLIED PRESSURE: 0·4 kg/cm²
(LOADING AND UNLOADING)
REF: INFLUENCE OF STRESS HISTORY
KAL-SET IV - CASA
--- 1ST. CYCLE
-·- 2ND. CYCLE
— TERZAGHI THEORY P=0
PROPOSED THEORY
● P=-·09
▲ P=-·2
PERCENTAGE AVERAGE DEGREE OF CONSOLIDATION
20
30
40
50
60
70
80
90
95
·02 ·03 ·04 ·05 ·06 ·07 ·08 ·1 ·2 ·3 ·4 ·5 ·6 ·7 ·8 ·9 1·0
TIME FACTOR →
992

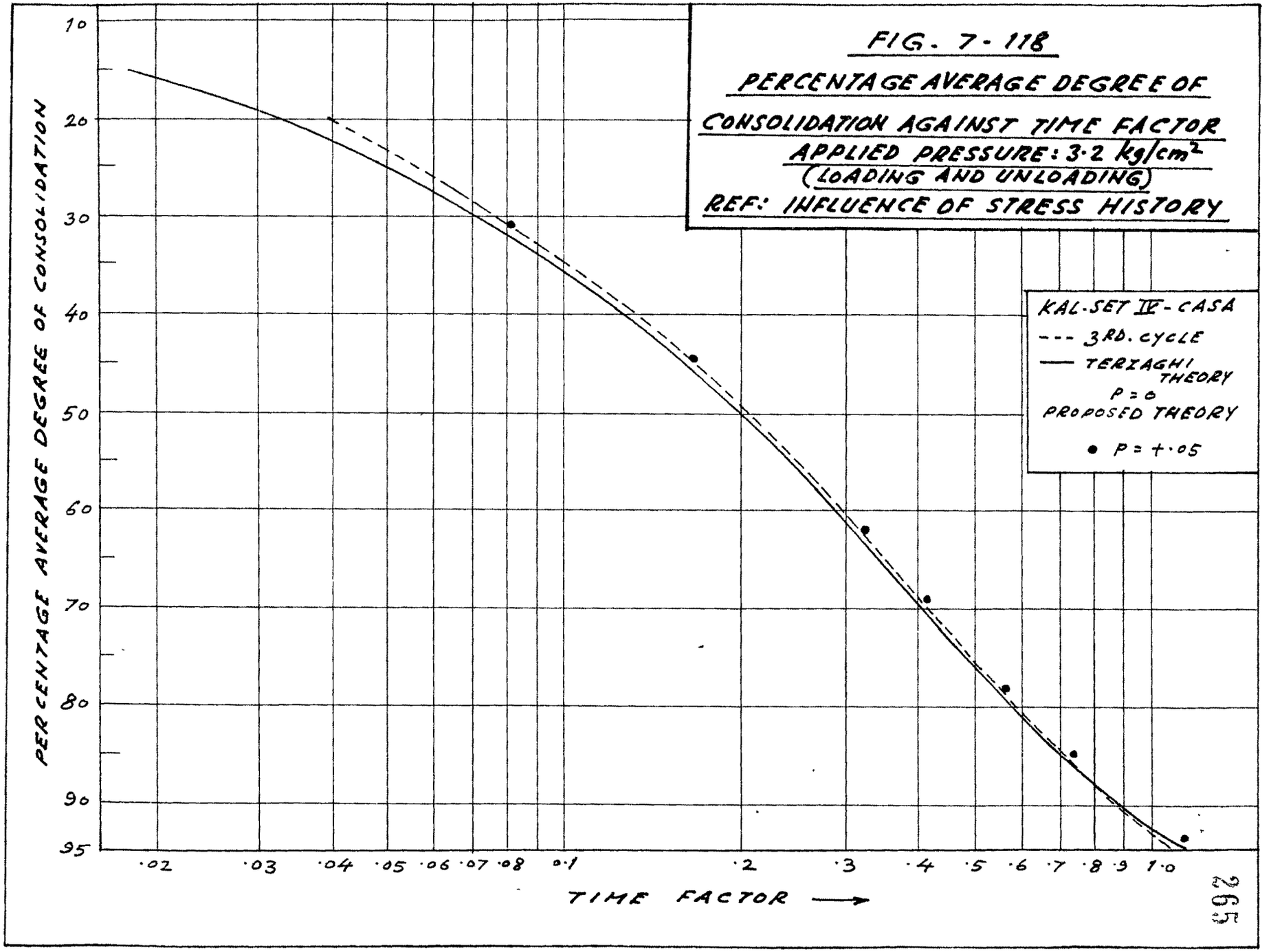
FIG. 7-118
PERCENTAGE AVERAGE DEGREE OF CONSOLIDATION AGAINST TIME FACTOR
APPLIED PRESSURE: 3·2 kg/cm²
(LOADING AND UNLOADING)
REF: INFLUENCE OF STRESS HISTORY
KAL-SET IV - CASA
--- 3RD. CYCLE
— TERZAGHI THEORY
P = 0
PROPOSED THEORY
● P = +·05
PERCENTAGE AVERAGE DEGREE OF CONSOLIDATION
10
20
30
40
50
60
70
80
90
95
·02 ·03 ·04 ·05 ·06 ·07 ·08 0·1 ·2 ·3 ·4 ·5 ·6 ·7 ·8 ·9 1·0
TIME FACTOR →

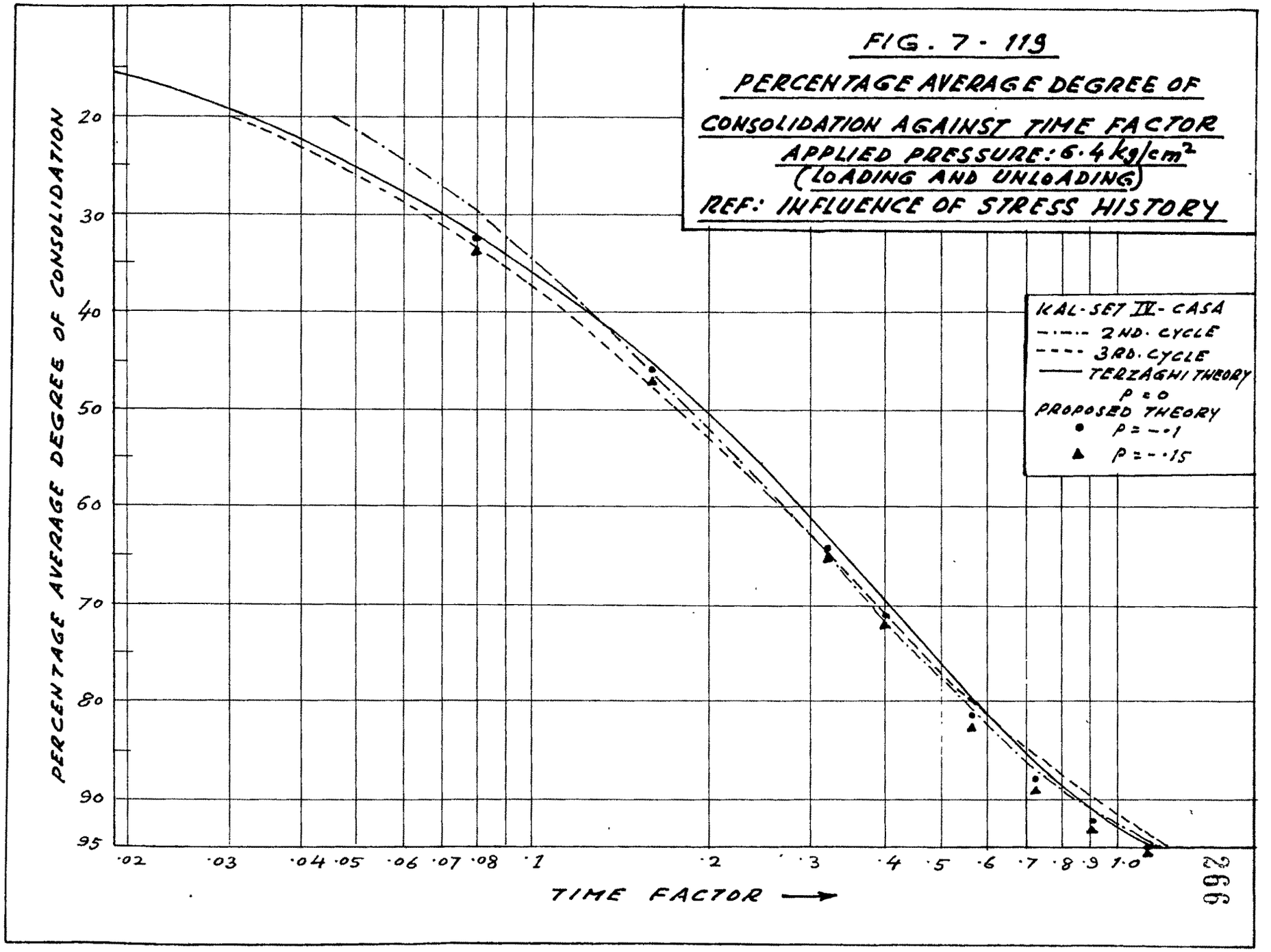
FIG. 7 · 119
PERCENTAGE AVERAGE DEGREE OF CONSOLIDATION AGAINST TIME FACTOR
APPLIED PRESSURE: 6·4 kg/cm²
(LOADING AND UNLOADING)
REF: INFLUENCE OF STRESS HISTORY
KAL-SET IV - CASA
2ND. CYCLE
3RD. CYCLE
TERZAGHI THEORY
P = 0
PROPOSED THEORY
P = -·1
P = -·15
PERCENTAGE AVERAGE DEGREE OF CONSOLIDATION
20
30
40
50
60
70
80
90
95
·02
·03
·04
·05
·06
·07
·08
·1
·2
·3
·4
·5
·6
·7
·8
·9
1·0
TIME FACTOR
9962

In the second set the deviation during the first cycle, though large initially, is reduced to 1.6% during higher loads. In the second and the third cycles, the deviations are found to be 2.25% and 3% respectively. In the third set, deviations of 2.5%, 4.5% and 3.0% are observed for the first, second and third cycles respectively. In the fourth set, experimental curves deviate by 1.6%, 3.8%, 1.0% for the first, second and third cycles.

Discussion :

The compression of saturated clay resulting from an increase in pressure can be visualised to occur primarily due to reorientation of particles and to a certain extent as a result of decrease in size of colloid micelle which causes structural adjustment. In other words, the work done over the saturated sample has to overcome the internal friction during the process and the Zeta potential energy of colloid micelle. Internal frictional resistance is partly due to the displacement of plate shaped clay particles along each other and partly due to the internal frictional resistance(viscosity) of pore water. On loading initially 'edge to face' or 'edge to edge' domains representing higher energy level tend to compress to 'face to face' domains depending on the magnitude and mode of loading. Under each successive loading and unloading there may

develope Lower Zeta potential energy on one hand; on the other hand the particles having reached their optimum structural positions, the loss of energy on displacement may decrease.

The experimental observations more or less support the above hypothesis. Under the first compression and decompression a fixed path for the movement of particle is established and consequently during further cycles of loading practically only a little bond resistance remains to be overcome. It is because of this lower resistance that the experimental observation of second and third cycles of loading and unloading shows initially an increase in C_v . An initial decrease in C_v value in case of the first cycle in the second set can be attributed to the mode of application of load. Since light loads may not be able to overcome the resistance of internal friction and potential energy of colloid micelle the C_v value is seen to decrease at initial loads but with increasing loads its value gradually increases and later tends to almost unchanged.

The void ratio-effective pressure relationship of kaolinite sample under first loading indicates establishment of parallel alignment of particles in the very first cycle. The exhibition of a slight elastic recovery is due to the imperfectness of adsorbed water in micelle. With increase of cycles of loading and unloading, interfacial grip progressively breaks up giving less and less hysteresis loop area. The initial

variation as seen in the tangent and secant modulus is due to the mode of load application. The Cc value varies only at lighter loads under the first loading but subsequently in all the cycles it remains constant. The change in the swelling index goes on decreasing with the cycles of loading as elastic recovery vanishes. As a result of breakdown of physico-chemical forces, the decrease in secondary compression can be expected at each successive loading and unloading cycle. After the first cycles of compression practically there is no hydrodynamic lag, and consequently not much variation in secondary compression is observed during the second and third cycles of compression. The compliance of Terzaghi primary theory with experimental observation of first cycle is evident.

B : Influence of Load Intensity

Analysis :

(i) Coefficient of consolidation against degree of consolidation.
(Figures 7.120 to 7.123).

Under stress incremental ratios of four and eight, kaolinite sample shows a rapid decrease at an initial light load of .01 kg/cm^2. With subsequent loads at increment stress ratios of two and four C_v tends to be constant while for increment stress ratios of eight, rapid increase in the value of C_v is seen upto about 70% consolidation after which it almost remains constant. Bentonite under an incremental ratio of one, shows a slight

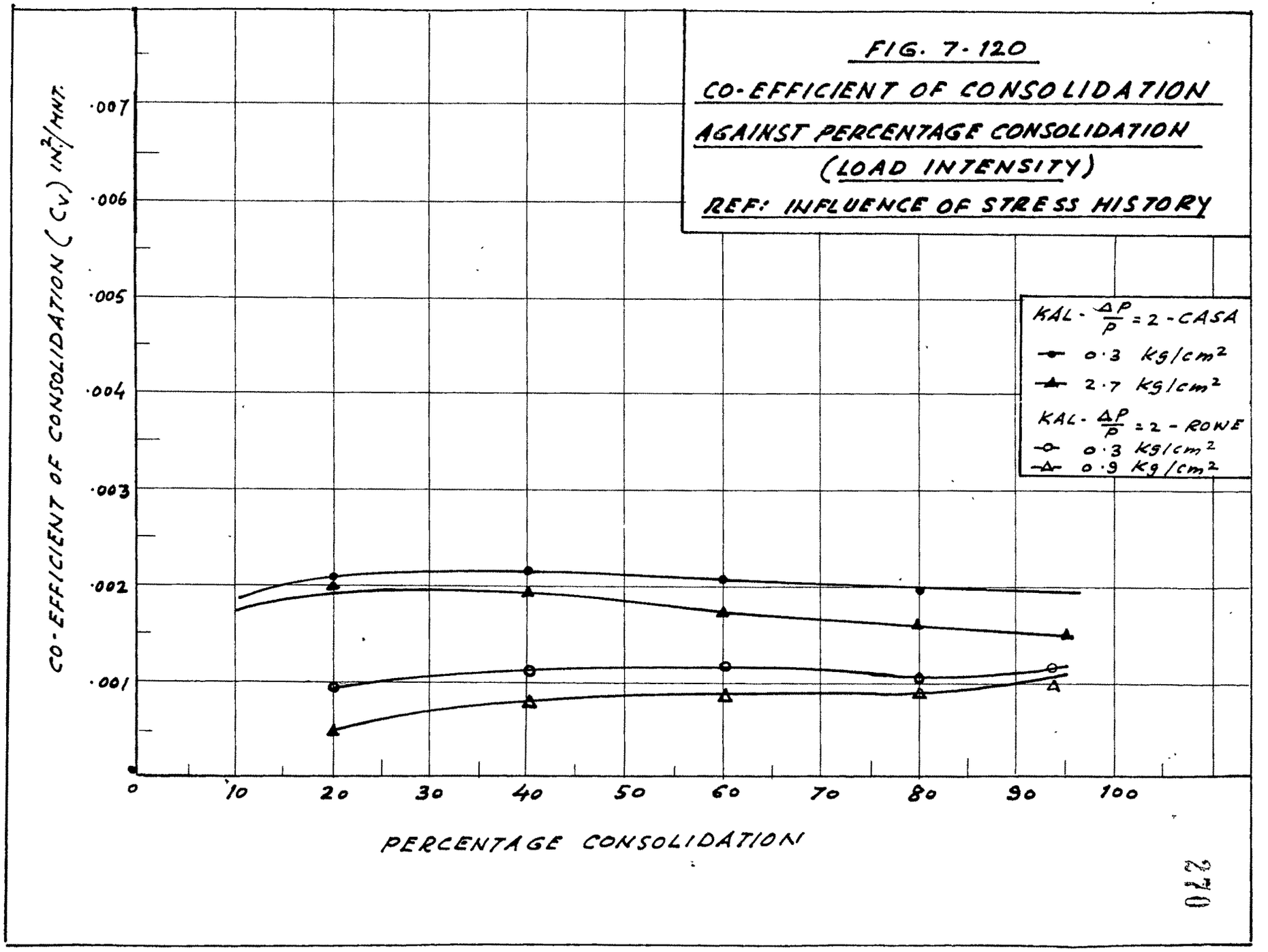
FIG. 7-120
CO-EFFICIENT OF CONSOLIDATION
AGAINST PERCENTAGE CONSOLIDATION
(LOAD INTENSITY)
REF: INFLUENCE OF STRESS HISTORY
KAL - ΔP/P = 2 - CASA
0·3 kg/cm²
2·7 kg/cm²
KAL - ΔP/P = 2 - ROWE
0·3 kg/cm²
0·9 kg/cm²
CO-EFFICIENT OF CONSOLIDATION (Cv) IN.²/MNT.
·007
·006
·005
·004
·003
·002
·001
0
10
20
30
40
50
60
70
80
90
100
PERCENTAGE CONSOLIDATION

012

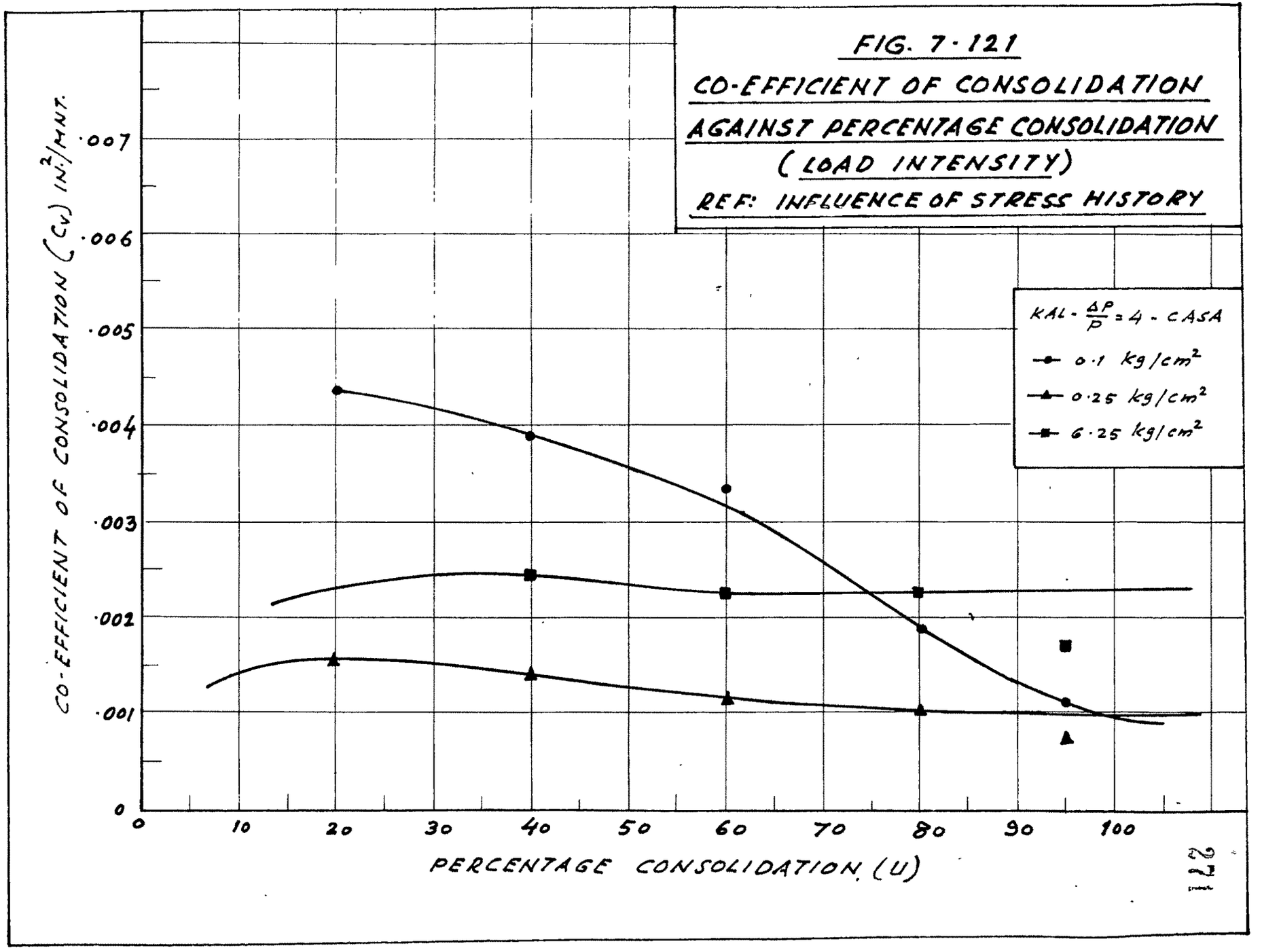
FIG. 7·121
CO-EFFICIENT OF CONSOLIDATION
AGAINST PERCENTAGE CONSOLIDATION
(LOAD INTENSITY)
REF: INFLUENCE OF STRESS HISTORY
KAL - ΔP/P = 4 - CASA
0·1 kg/cm²
0·25 kg/cm²
6·25 kg/cm²
CO-EFFICIENT OF CONSOLIDATION (Cv) IN.²/MNT.
·007
·006
·005
·004
·003
·002
·001
0
0
10
20
30
40
50
60
70
80
90
100
PERCENTAGE CONSOLIDATION (U)

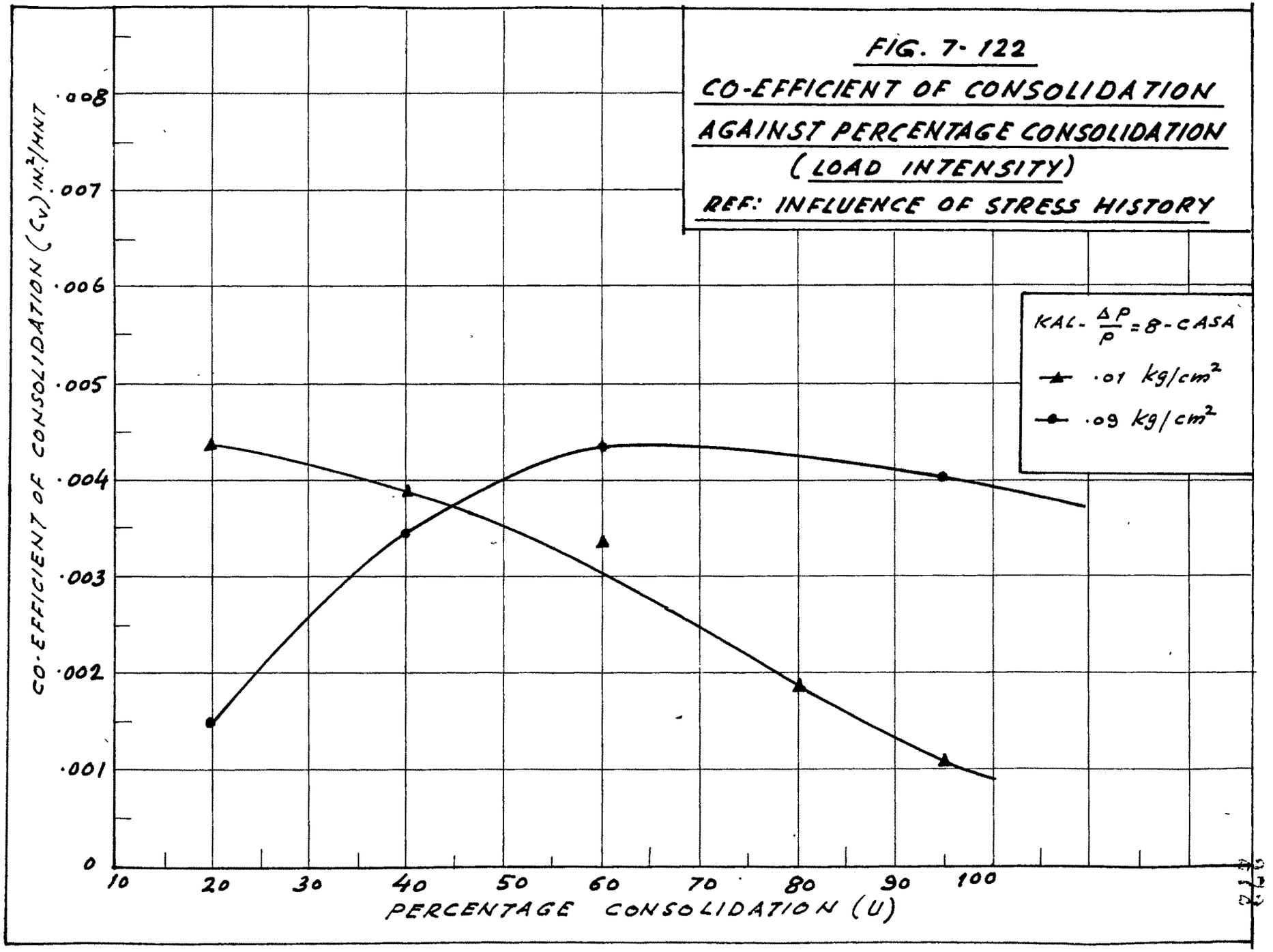
FIG. 7-122
CO-EFFICIENT OF CONSOLIDATION
AGAINST PERCENTAGE CONSOLIDATION
(LOAD INTENSITY)
REF: INFLUENCE OF STRESS HISTORY
KAL- $\frac{\Delta P}{P}$ = 8-CASA
·01 kg/cm²
·09 kg/cm²
CO-EFFICIENT OF CONSOLIDATION (C_v) IN.²/HNT
·008
·007
·006
·005
·004
·003
·002
·001
0
10
20
30
40
50
60
70
80
90
100
PERCENTAGE CONSOLIDATION (U)

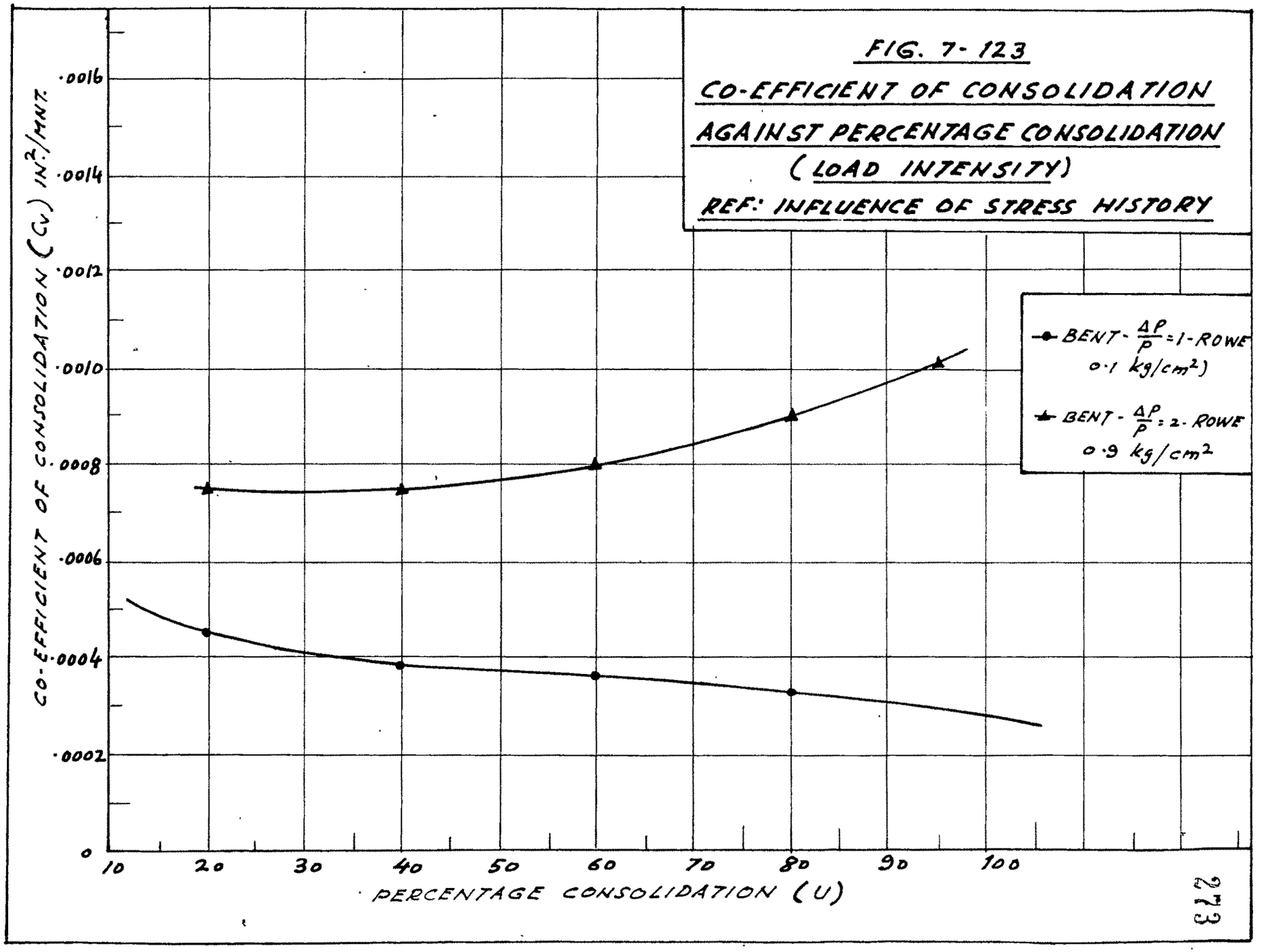
FIG. 7-123
CO-EFFICIENT OF CONSOLIDATION
AGAINST PERCENTAGE CONSOLIDATION
(LOAD INTENSITY)
REF: INFLUENCE OF STRESS HISTORY
BENT - ΔP/P = 1 - ROWE
0·1 kg/cm²)
BENT - ΔP/P = 2 - ROWE
0·9 kg/cm²
CO-EFFICIENT OF CONSOLIDATION (Cv) IN²/MNT.
·0016
·0014
·0012
·0010
·0008
·0006
·0004
·0002
0
10
20
30
40
50
60
70
80
90
100
PERCENTAGE CONSOLIDATION (U)
213

increase in the value of C_v while at increment stress ratio of two a slight decrease is seen.

(ii) Coefficient of consolidation against applied effective pressure.
(Figure 7.124).

Under the stress increment ratios of two and four there is a decrease in the value of C_v at lighter loads but with higher loads it increases and then tends to become constant. But at stress increment ratio of eight there is a rapid rise of C_v value.

(iii) Compression index against average applied effective pressure.
(Figure 7.125).

General nature represents a same family showing an initial hump which becomes narrower as incremental stress ratio increases. The compression index tends to attain a constant value earlier with the decrease in the incremental stress ratios from eight to four, two and one.

(iv) Percentage secondary compression against effective applied pressure.
(Figure 7.126).

The general nature of curves indicates that percentage secondary compression increases with the increase in the load. For incremental stress ratio four and eight the rate with which the secondary compression decreases is however more rapid.

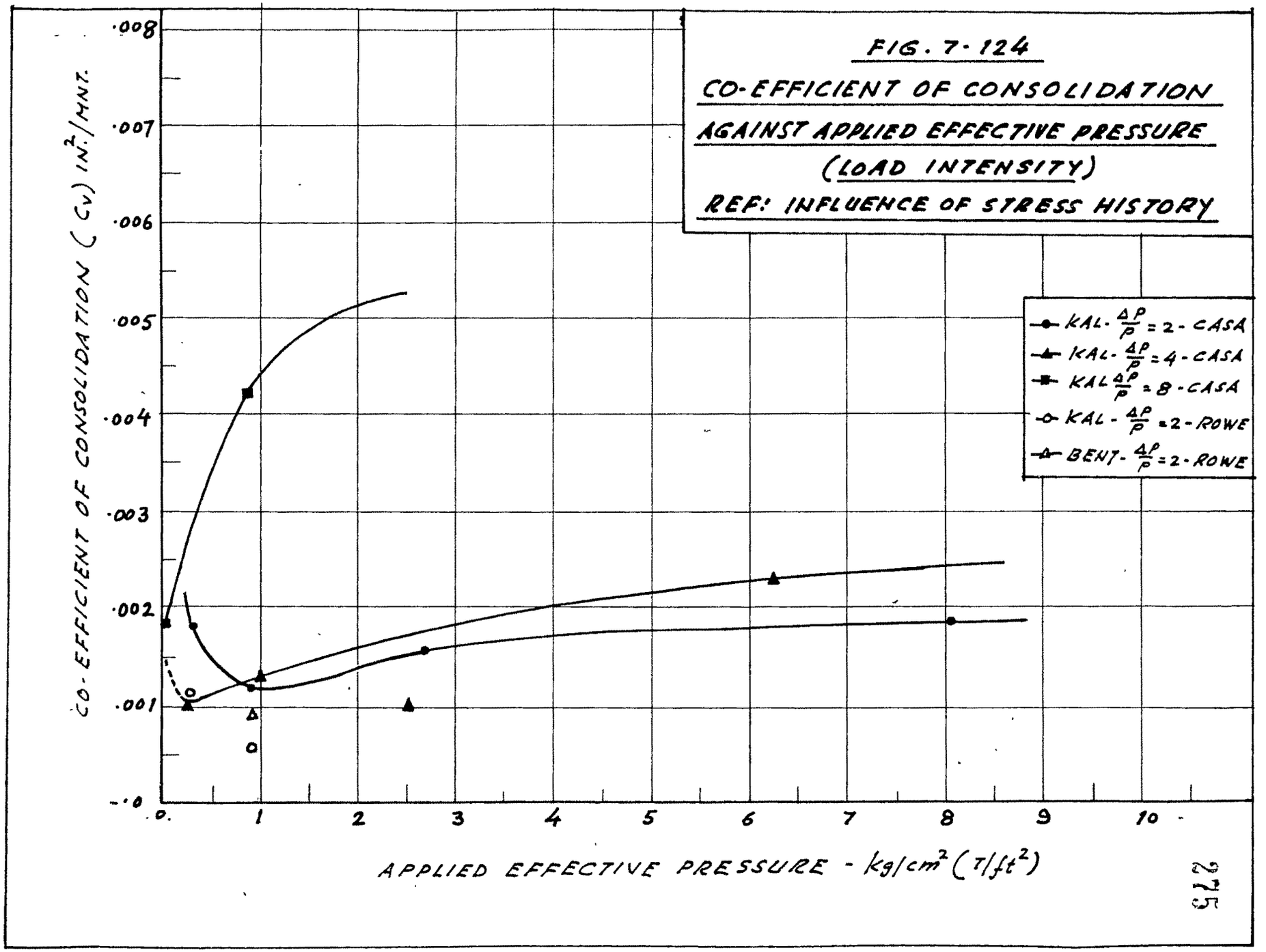
FIG. 7·124
CO-EFFICIENT OF CONSOLIDATION
AGAINST APPLIED EFFECTIVE PRESSURE
(LOAD INTENSITY)
REF: INFLUENCE OF STRESS HISTORY
KAL - Δp/p = 2 - CASA
KAL - Δp/p = 4 - CASA
KAL Δp/p = 8 - CASA
KAL - Δp/p = 2 - ROWE
BENT - Δp/p = 2 - ROWE
CO-EFFICIENT OF CONSOLIDATION (Cv) IN.²/MNT.
·008
·007
·006
·005
·004
·003
·002
·001
·0
0.
1
2
3
4
5
6
7
8
9
10
APPLIED EFFECTIVE PRESSURE - kg/cm² (T/ft²)

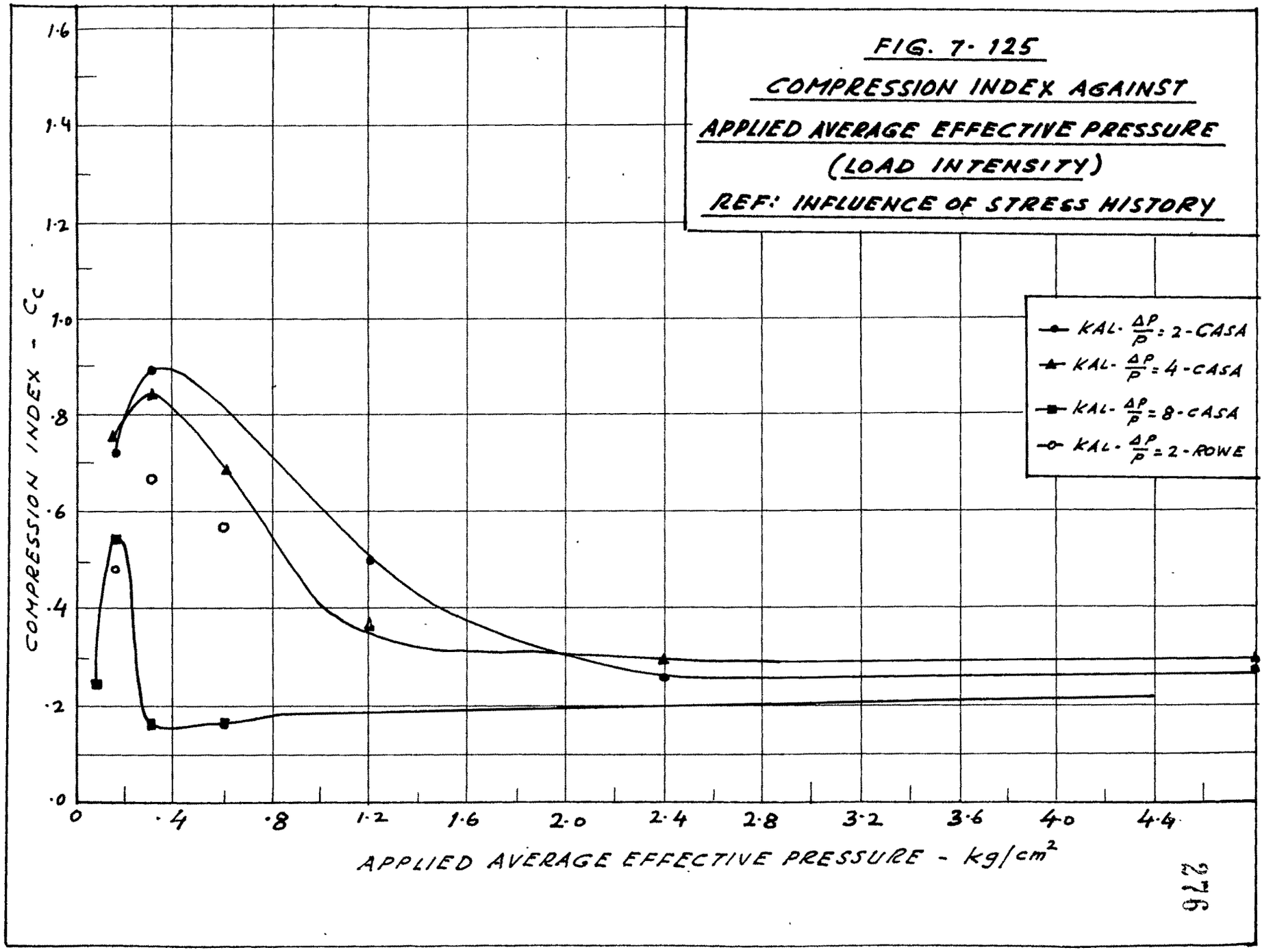
FIG. 7·125
COMPRESSION INDEX AGAINST
APPLIED AVERAGE EFFECTIVE PRESSURE
(LOAD INTENSITY)
REF: INFLUENCE OF STRESS HISTORY
KAL· ΔP/P = 2 - CASA
KAL· ΔP/P = 4 - CASA
KAL· ΔP/P = 8 - CASA
KAL· ΔP/P = 2 - POWE
COMPRESSION INDEX - Cc
APPLIED AVERAGE EFFECTIVE PRESSURE - kg/cm²
1·6
1·4
1·2
1·0
·8
·6
·4
·2
·0
0
·4
·8
1·2
1·6
2·0
2·4
2·8
3·2
3·6
4·0
4·4

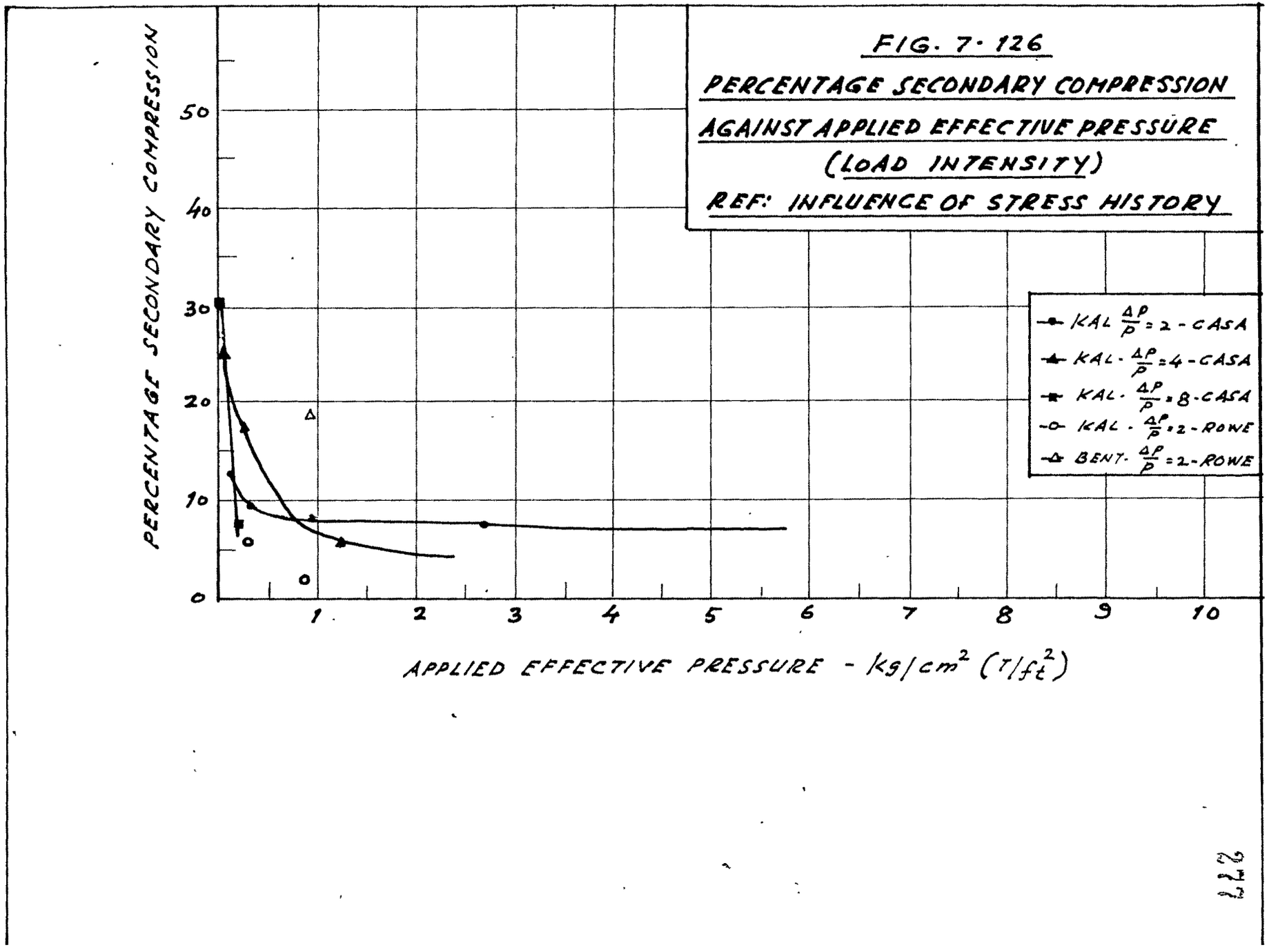
FIG. 7·126
PERCENTAGE SECONDARY COMPRESSION AGAINST APPLIED EFFECTIVE PRESSURE (LOAD INTENSITY)
REF: INFLUENCE OF STRESS HISTORY
PERCENTAGE OF SECONDARY COMPRESSION
0
10
20
30
40
50
1
2
3
4
5
6
7
8
9
10
APPLIED EFFECTIVE PRESSURE - kg/cm² (T/ft²)
KAL Δp/p = 2 - CASA
KAL - Δp/p = 4 - CASA
KAL - Δp/p = 8 - CASA
KAL - Δp/p = 2 - ROWE
BENT - Δp/p = 2 - ROWE

(v) Parameter 'P' against effective applied pressure. (Figures 7.127 and Figures 7.128 to 7.134).

At very light loads the curve with increment stress ratios of two fits closer to the Terzaghi curve. Deviations observed are 3% and 5.5% in experimental curves at increment stress ratios of two and four respectively.

Discussion :

The influence of the load intensity on the consolidation characteristics can be explained in terms of structural variations of the clay configuration. The resultant deformation is dependent on the bond resistance and the ability of individual particle to take position of equilibrium. Under lower load intensity the resultant compression will be small as readjustment of particles to new positions of equilibrium is achieved with minimum displacement and without generation of large pore pressures. On the other hand if the load intensity is high, initially the particles cannot easily readjust to position of equilibrium since the rate of application is sufficiently more than the rate at which the pore pressure can dissipate. It is only when there occurs a complete collapse of the bonds that the displacement of particles takes place producing dissipation of pore pressures.

The first light load is resisted by physico-chemical bond strength at various contact points is time dependent show a reduction in c_v value during consolidation process. Under

FIG. 7·127

PARAMETER 'P' AGAINST APPLIED EFFECTIVE PRESSURE (LOAD INTENSITY)

REF: INFLUENCE OF STRESS HISTORY

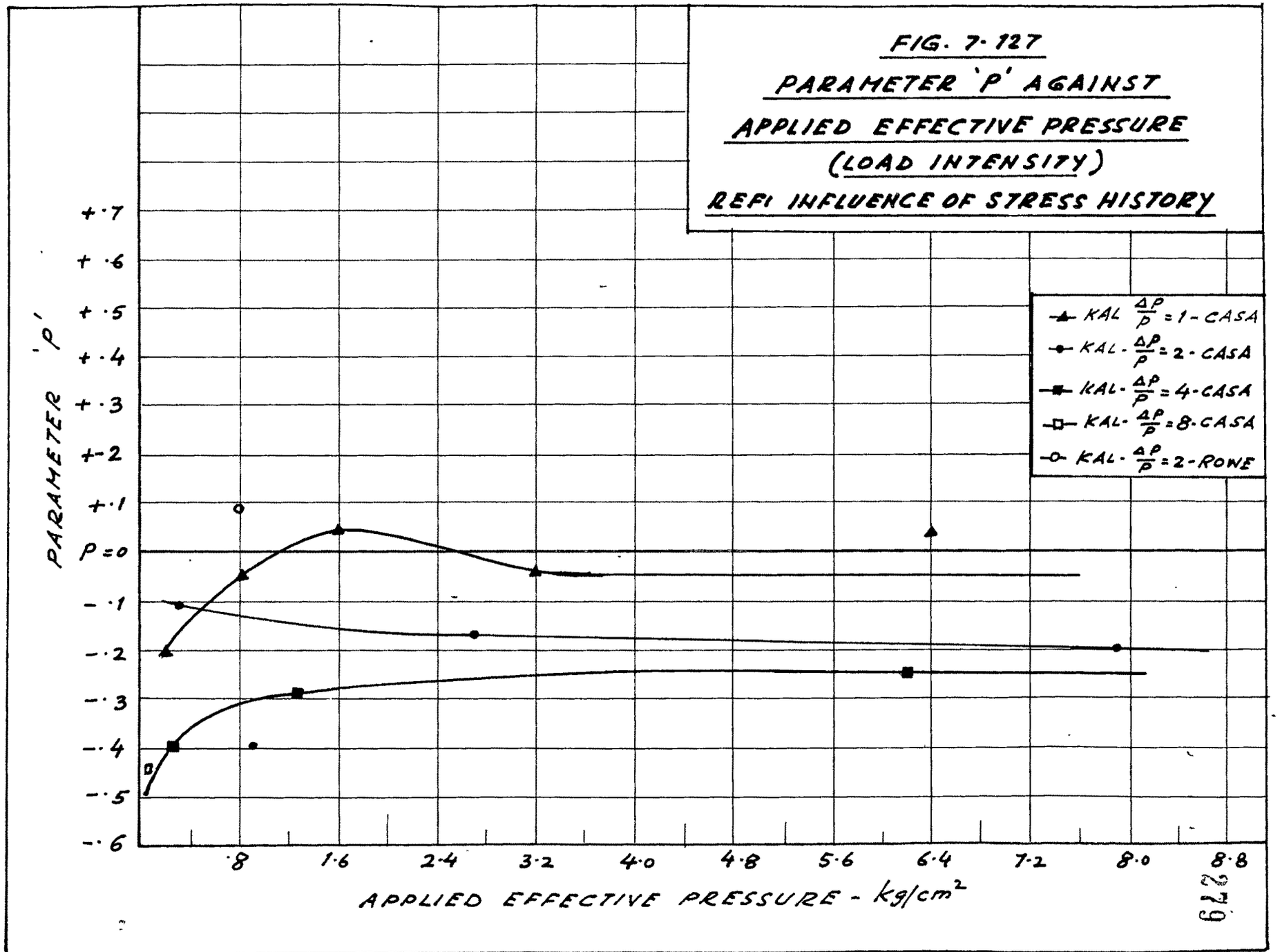

6279

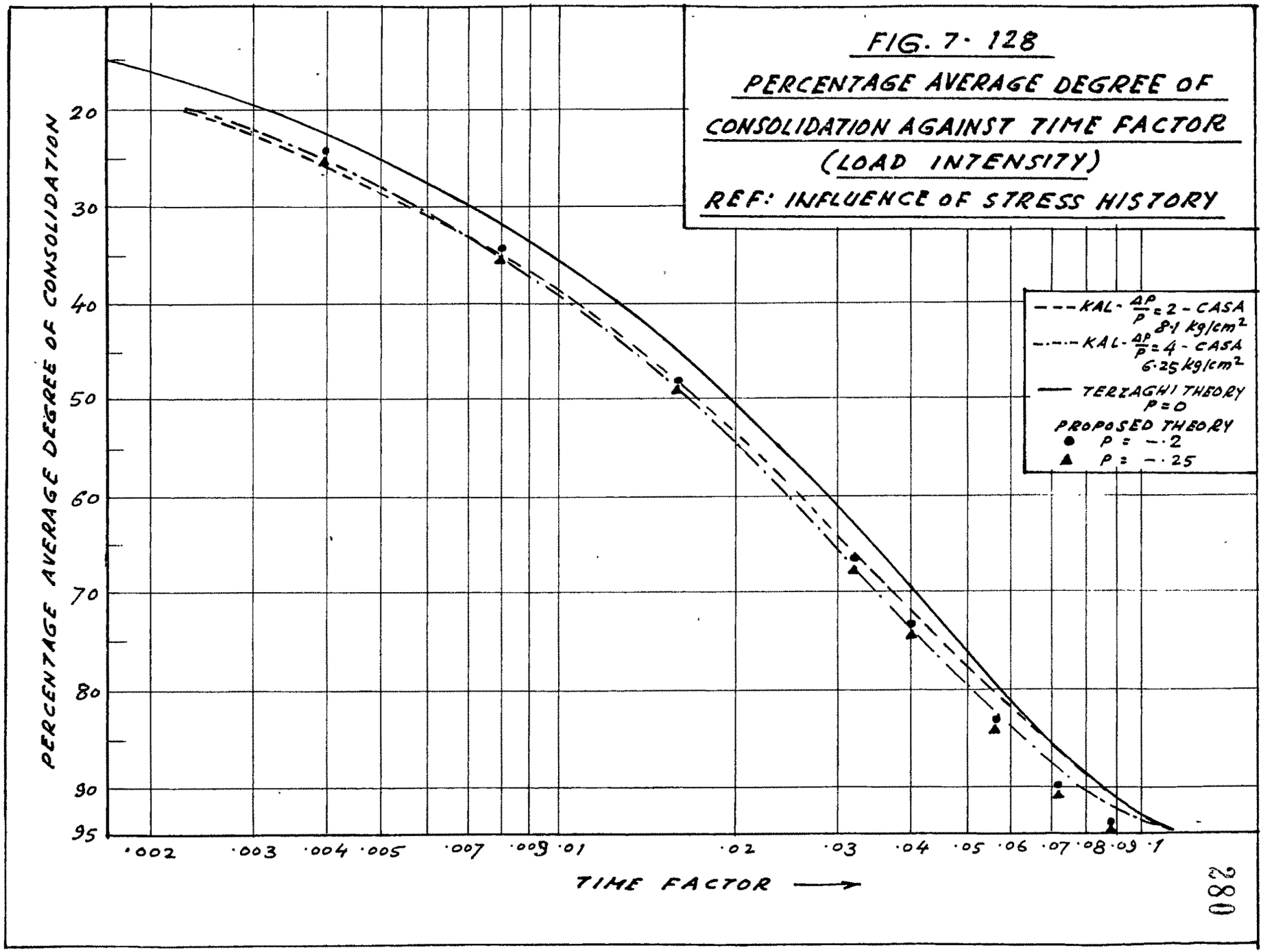
FIG. 7·128
PERCENTAGE AVERAGE DEGREE OF CONSOLIDATION AGAINST TIME FACTOR (LOAD INTENSITY)
REF: INFLUENCE OF STRESS HISTORY
KAL - ΔP/P = 2 - CASA 8·1 kg/cm²
KAL - ΔP/P = 4 - CASA 6·25 kg/cm²
TERZAGHI THEORY P = 0
PROPOSED THEORY
P = −·2
P = −·25
PERCENTAGE AVERAGE DEGREE OF CONSOLIDATION
20
30
40
50
60
70
80
90
95
·002
·003
·004
·005
·007
·009
·01
·02
·03
·04
·05
·06
·07
·08
·09
·1
TIME FACTOR ⟶
0822

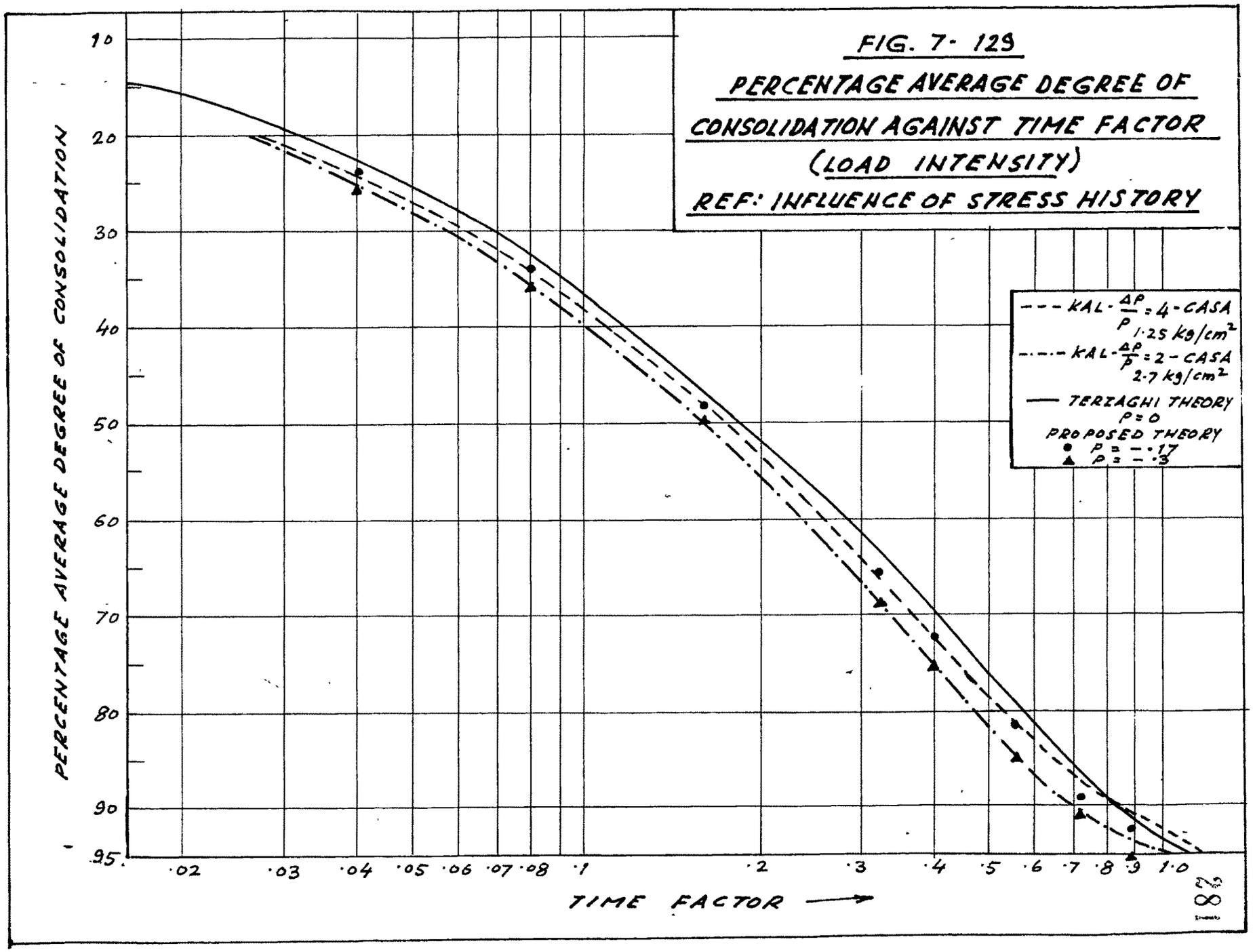
FIG. 7- 129
PERCENTAGE AVERAGE DEGREE OF CONSOLIDATION AGAINST TIME FACTOR (LOAD INTENSITY)
REF: INFLUENCE OF STRESS HISTORY
PERCENTAGE AVERAGE DEGREE OF CONSOLIDATION
10
20
30
40
50
60
70
80
90
95
.02
.03
.04
.05
.06
.07
.08
.1
.2
.3
.4
.5
.6
.7
.8
.9
1.0
TIME FACTOR
KAL - ΔP/P = 4 - CASA 1·25 kg/cm²
KAL - ΔP/P = 2 - CASA 2·7 kg/cm²
TERZAGHI THEORY P=0
PROPOSED THEORY
P = -·17
P = -·3
82

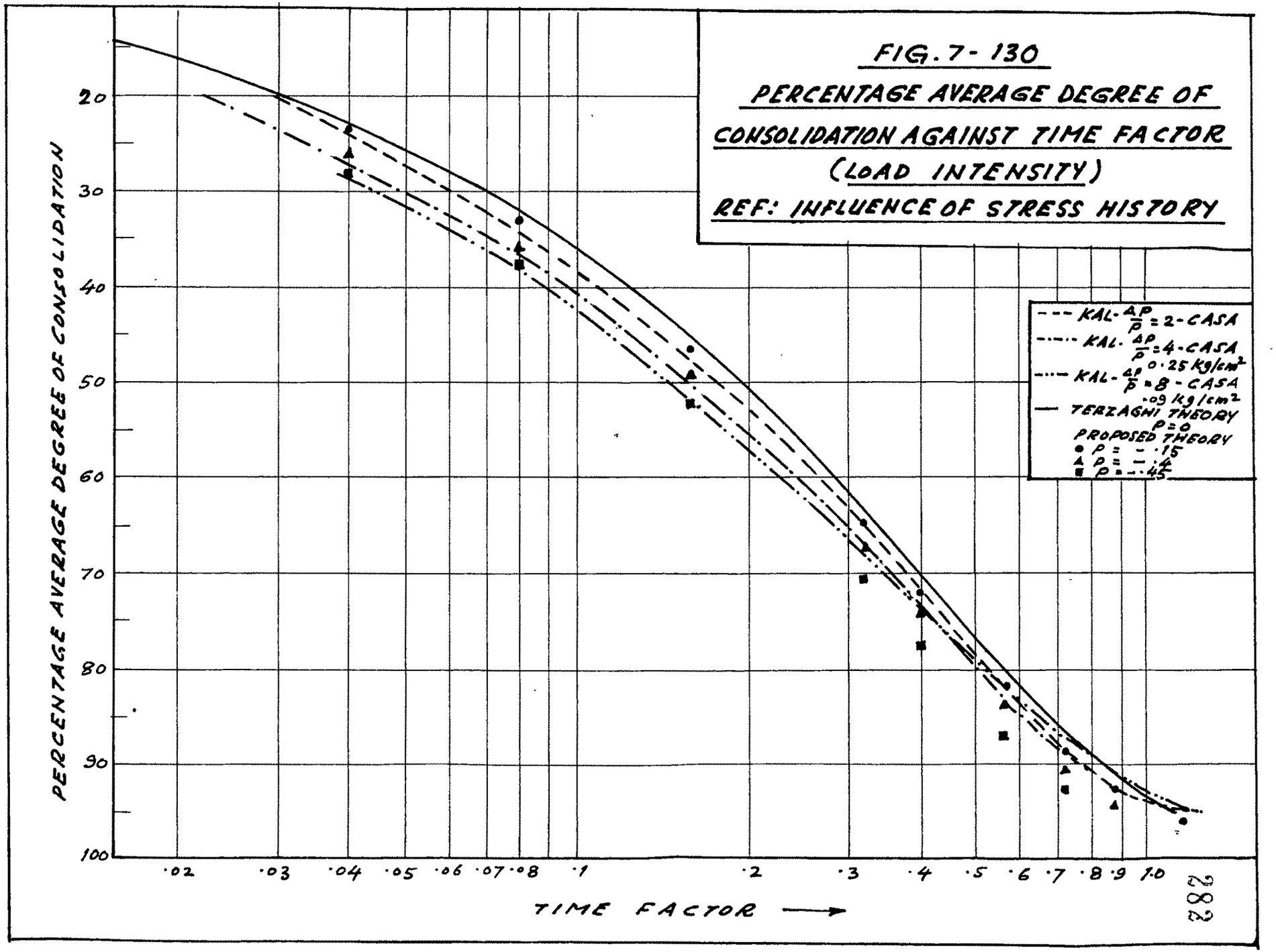
FIG. 7-130
PERCENTAGE AVERAGE DEGREE OF CONSOLIDATION AGAINST TIME FACTOR (LOAD INTENSITY)
REF: INFLUENCE OF STRESS HISTORY
KAL- Δp/p = 2 - CASA
KAL- Δp/p = 4 - CASA
KAL- Δp/p = 8 - CASA
0·25 kg/cm²
·09 kg/cm²
TERZAGHI THEORY
p = 0
PROPOSED THEORY
p = -·15
p = -·4
p = -·45
PERCENTAGE AVERAGE DEGREE OF CONSOLIDATION
20
30
40
50
60
70
80
90
100
·02
·03
·04
·05
·06
·07
·08
·1
·2
·3
·4
·5
·6
·7
·8
·9
1·0
TIME FACTOR

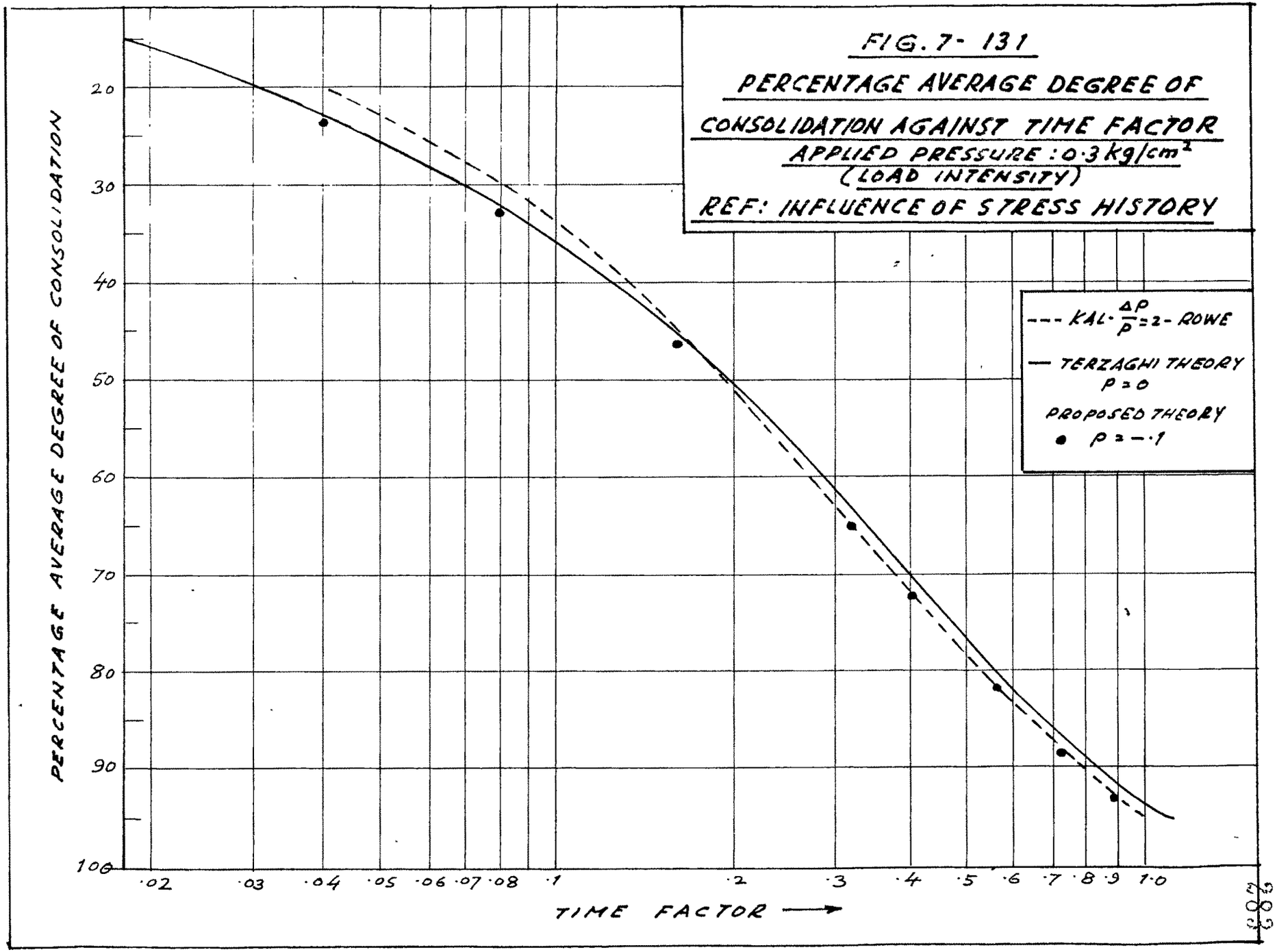
FIG. 7- 131
PERCENTAGE AVERAGE DEGREE OF CONSOLIDATION AGAINST TIME FACTOR
APPLIED PRESSURE : 0·3 kg/cm²
(LOAD INTENSITY)
REF: INFLUENCE OF STRESS HISTORY
--- KAL· $\frac{\Delta P}{P}$ = 2 - ROWE
— TERZAGHI THEORY P = 0
PROPOSED THEORY
● P = −·1
PERCENTAGE AVERAGE DEGREE OF CONSOLIDATION
20
30
40
50
60
70
80
90
100
·02 ·03 ·04 ·05 ·06 ·07 ·08 ·1 ·2 ·3 ·4 ·5 ·6 ·7 ·8 ·9 1·0
TIME FACTOR ⟶

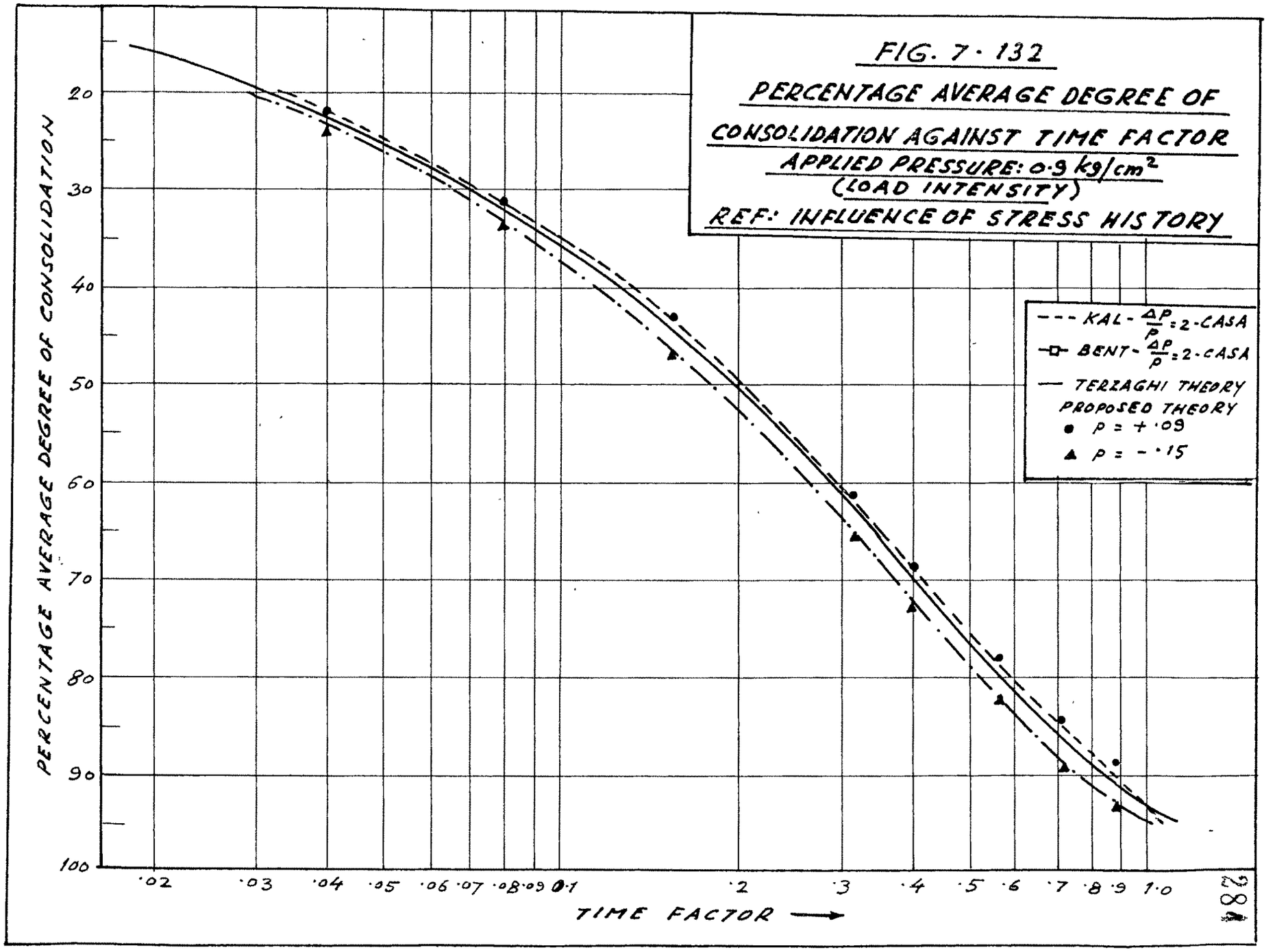
FIG. 7·132
PERCENTAGE AVERAGE DEGREE OF CONSOLIDATION AGAINST TIME FACTOR
APPLIED PRESSURE: 0·9 kg/cm²
(LOAD INTENSITY)
REF: INFLUENCE OF STRESS HISTORY
KAL - ΔP/P = 2 - CASA
BENT - ΔP/P = 2 - CASA
TERZAGHI THEORY
PROPOSED THEORY
p = + ·09
p = - ·15
PERCENTAGE AVERAGE DEGREE OF CONSOLIDATION
20
30
40
50
60
70
80
90
100
·02 ·03 ·04 ·05 ·06 ·07 ·08 ·09 0·1 ·2 ·3 ·4 ·5 ·6 ·7 ·8 ·9 1·0
TIME FACTOR

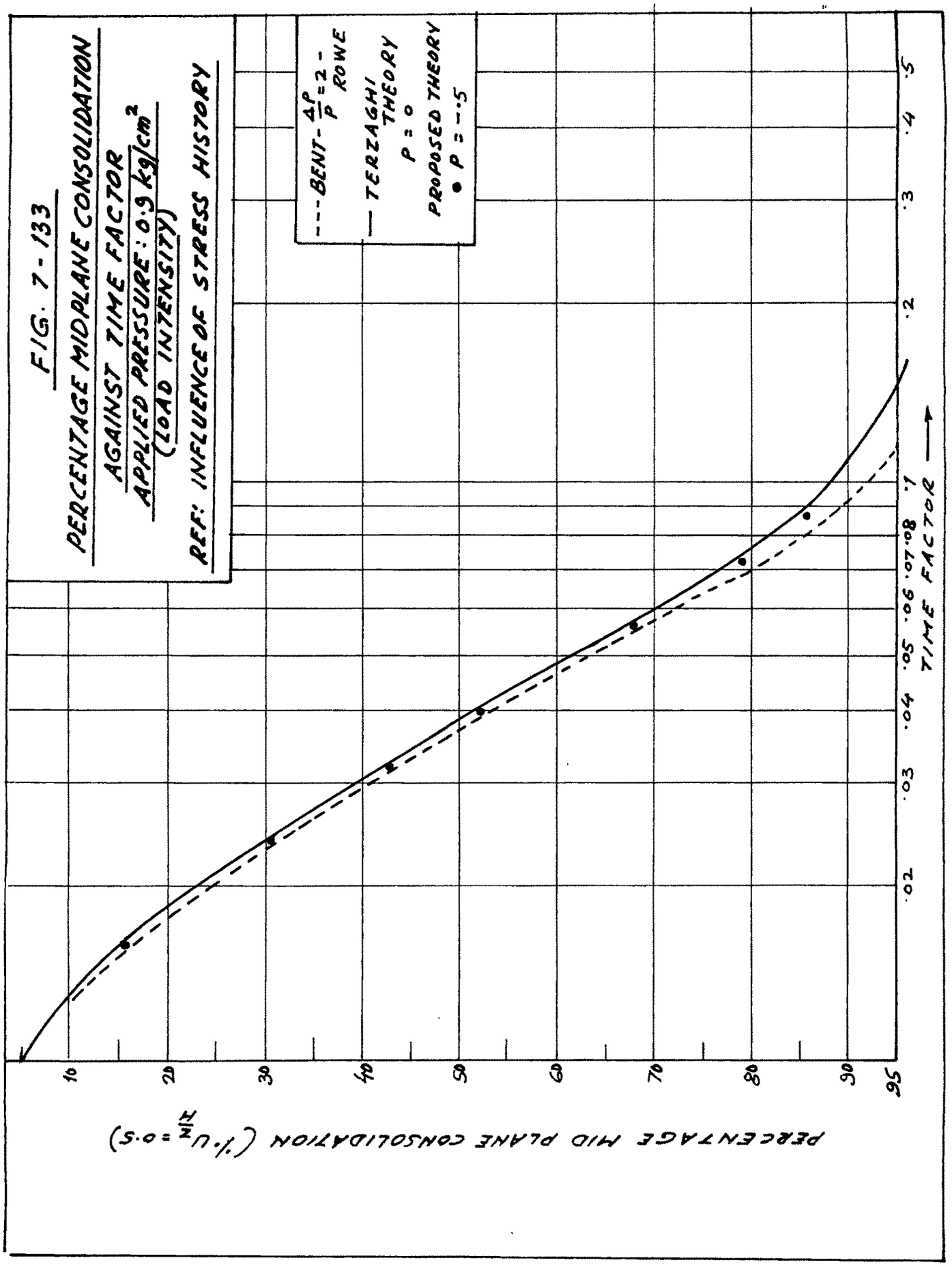
FIG. 7-133
PERCENTAGE MIDPLANE CONSOLIDATION
AGAINST TIME FACTOR
APPLIED PRESSURE: 0.9 kg/cm²
(LOAD INTENSITY)
REF: INFLUENCE OF STRESS HISTORY
--- BENT- ΔP/P = 2 - ROWE
— TERZAGHI THEORY
P = 0
PROPOSED THEORY
• P = -.5
PERCENTAGE MID PLANE CONSOLIDATION (% U_H = 0.5)
10
20
30
40
50
60
70
80
90
95
.02
.03
.04
.05
.06
.07
.08
.1
.2
.3
.4
.5
TIME FACTOR

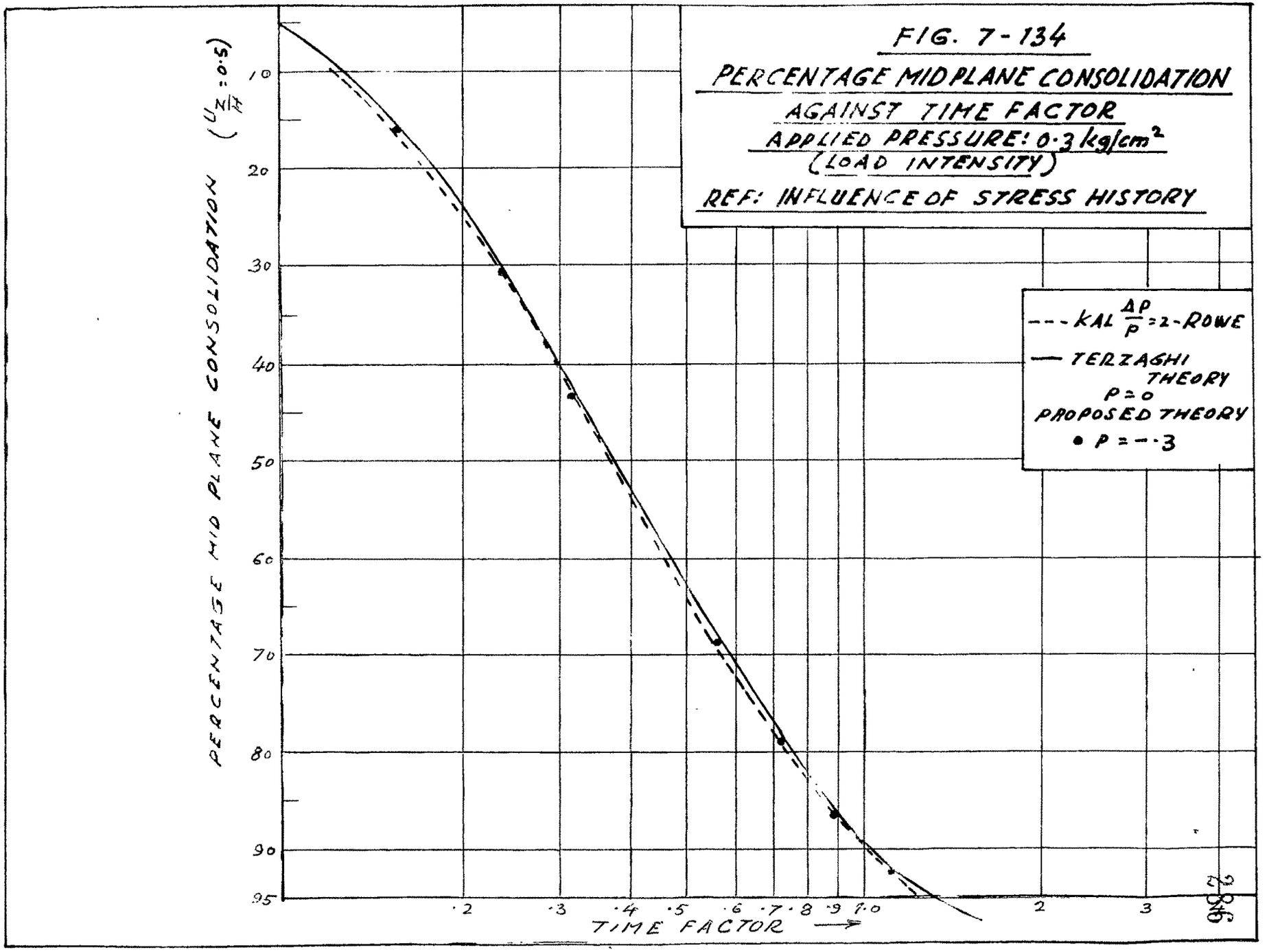
FIG. 7-134
PERCENTAGE MIDPLANE CONSOLIDATION
AGAINST TIME FACTOR
APPLIED PRESSURE: 0·3 kg/cm²
(LOAD INTENSITY)
REF: INFLUENCE OF STRESS HISTORY
--- KAL ΔP/P = 2 - ROWE
— TERZAGHI THEORY
P = 0
PROPOSED THEORY
• P = -·3
PERCENTAGE MID PLANE CONSOLIDATION ($U_{N/H}$: 0·5)
10
20
30
40
50
60
70
80
90
95
·2
·3
·4
·5
·6
·7
·8
·9
1·0
2
3
TIME FACTOR →
2946

moderate incremental stress ratio when the resistance is minimum a slight increase in C_v value tending to a constancy is possible, but at very high incremental stress ratios the rapid increase in C_v value is due to total collapse of bonds leading to complete displacement of particles during the consolidation process. It can be also argued that during lighter loads the structural viscosity of clay water system dominates the effect of stress ratio showing the decrease in the value of C_v . At high increment stress ratios, physico-chemical effect is completely destroyed which is evident from the nature of the plot of compression index against applied average pressure. The explanation for decrease in the secondary compression with higher incremental stress ratios is due to the dormancy of the physico-chemical forces.

7.3.5. Drainage Path

Refer Figures 7.135 to 7.159 which are reproduced from the original plots of Figures H 142 to H 157 and H.257 to H.285 reported in Appendix H of Volume II.

A : Orientation of Drainage Path

Analysis :

(i) Coefficient of consolidation against percentage consolidation.
(Figures 7.135 to 7.137).

The samples taken in the vertical, horizontal and inclined directions do not show much variation in the C_v value during the

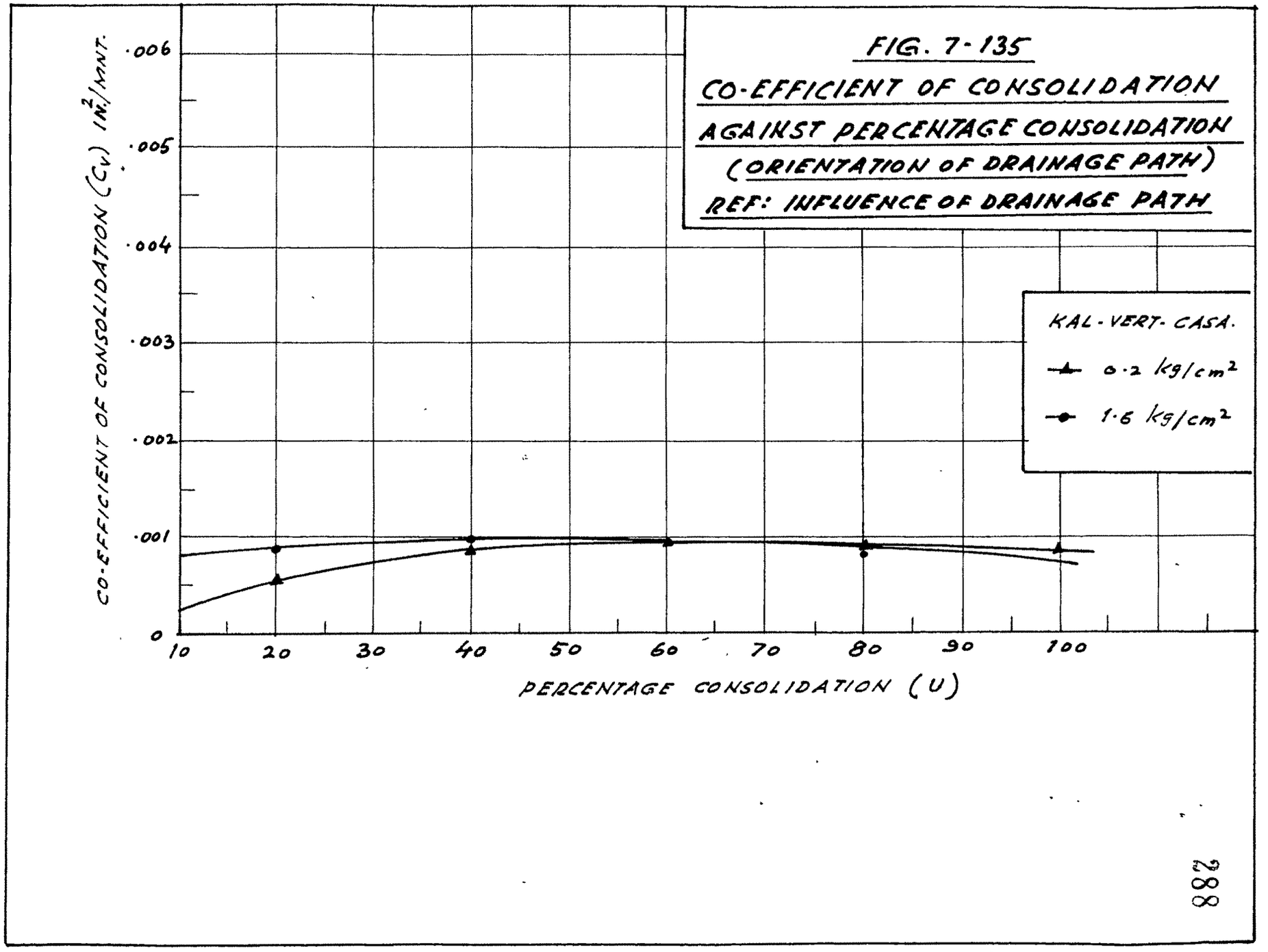
FIG. 7-135
CO-EFFICIENT OF CONSOLIDATION
AGAINST PERCENTAGE CONSOLIDATION
(ORIENTATION OF DRAINAGE PATH)
REF: INFLUENCE OF DRAINAGE PATH
KAL-VERT-CASA.
0·2 kg/cm²
1·6 kg/cm²
CO-EFFICIENT OF CONSOLIDATION (Cv) IN²/MNT.
·006
·005
·004
·003
·002
·001
0
10
20
30
40
50
60
70
80
90
100
PERCENTAGE CONSOLIDATION (U)

FIG. 7·136

CO-EFFICIENT OF CONSOLIDATION AGAINST PERCENTAGE CONSOLIDATION (ORIENTATION OF DRAINAGE PATH)

REF: INFLUENCE OF DRAINAGE PATH

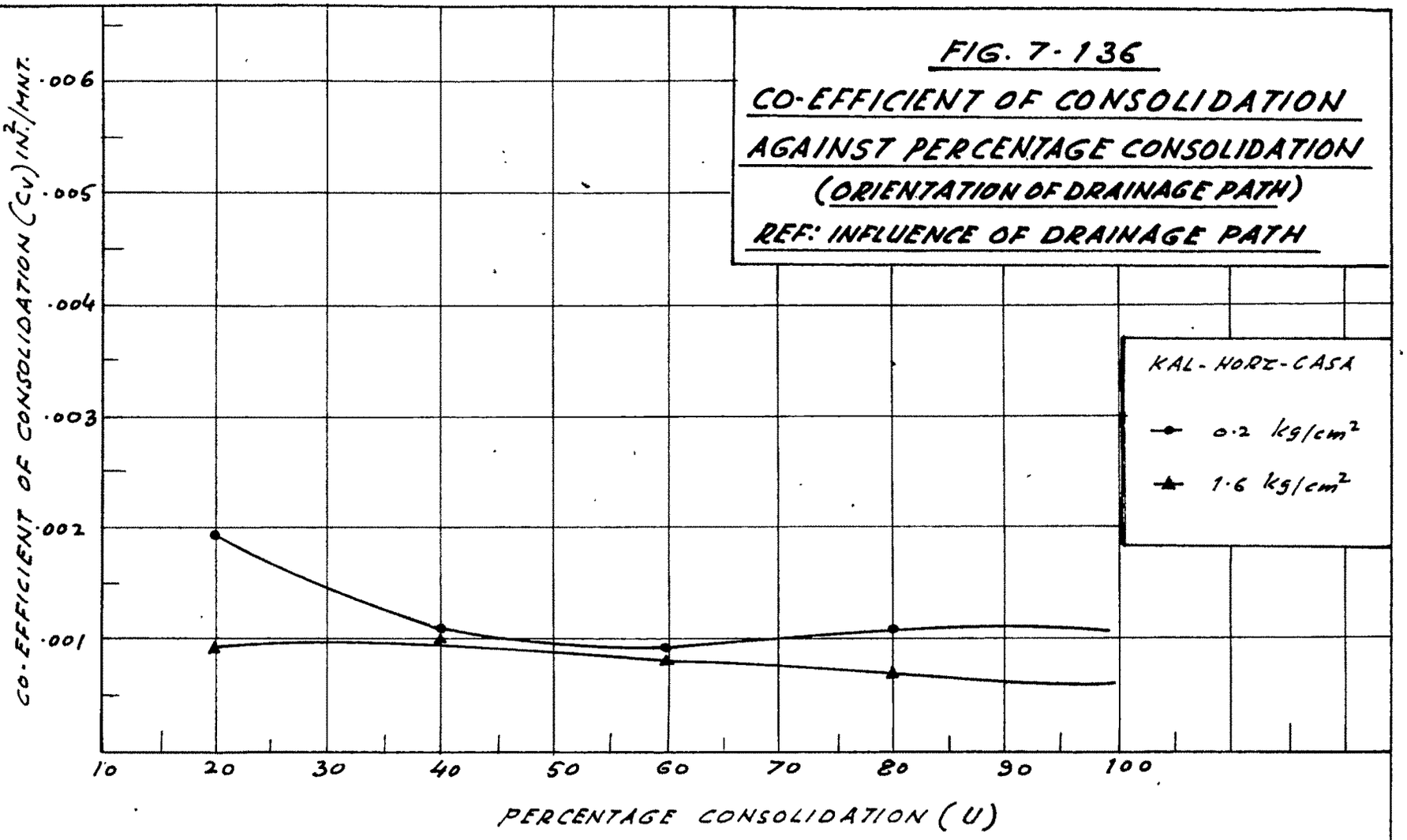

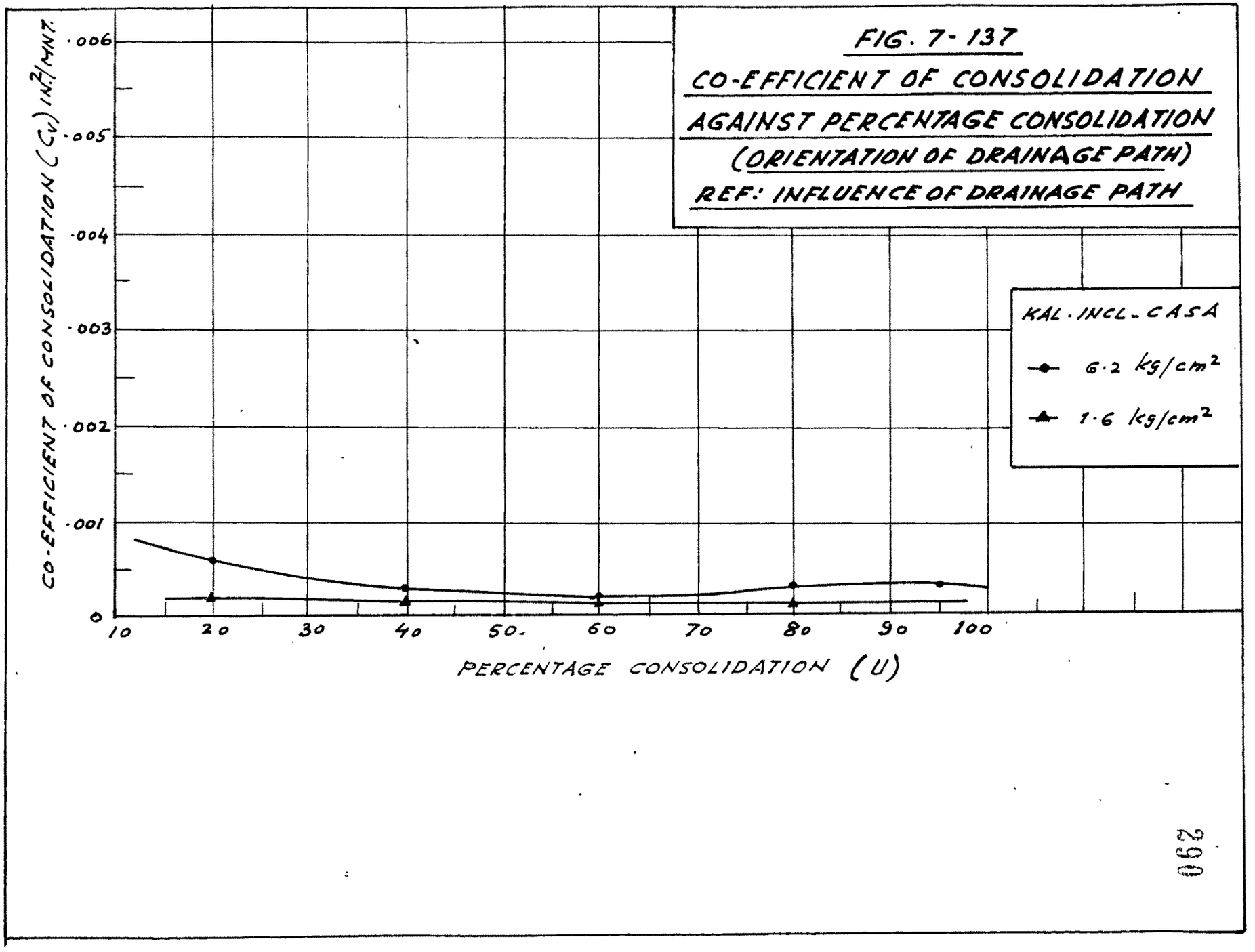
FIG. 7-137
CO-EFFICIENT OF CONSOLIDATION
AGAINST PERCENTAGE CONSOLIDATION
(ORIENTATION OF DRAINAGE PATH)
REF: INFLUENCE OF DRAINAGE PATH
KAL. INCL. CASA
6·2 kg/cm²
1·6 kg/cm²
CO-EFFICIENT OF CONSOLIDATION (Cv) IN.²/MNT.
·006
·005
·004
·003
·002
·001
0
10
20
30
40
50
60
70
80
90
100
PERCENTAGE CONSOLIDATION (U)

062

process of consolidation. At light loads while the horizontal sample shows a decrease initially, the verticle sample shows slight increase in the initial stages of consolidation.

(ii) Coefficient of consolidation against applied effective pressure.
(Figure 7.138).

At light loads the C_v value decreases rather rapidly but after about 1 kg/cm^2 a slight increase is noticeable. The decrease is comparatively more rapid in case of horizontal samples, but at higher loads the magnitude of C_v is almost the same.

(iii) Compression index against applied average effective pressure.
(Figure 7.139).

The general characteristics of all the samples are more or less similar showing a humpy curve. Horizontal sample gives a larger hump while the vertical sample shows a low or no hump in the initial portion of the curve. The inclined sample exhibits intermediate characteristics.

(iv) Percentage secondary compression against applied effective pressure.
(Figure 7.140).

It seems from the experimental curves that the degree of secondary compression is not much affected. With increase in load the secondary compression decreases as usual.

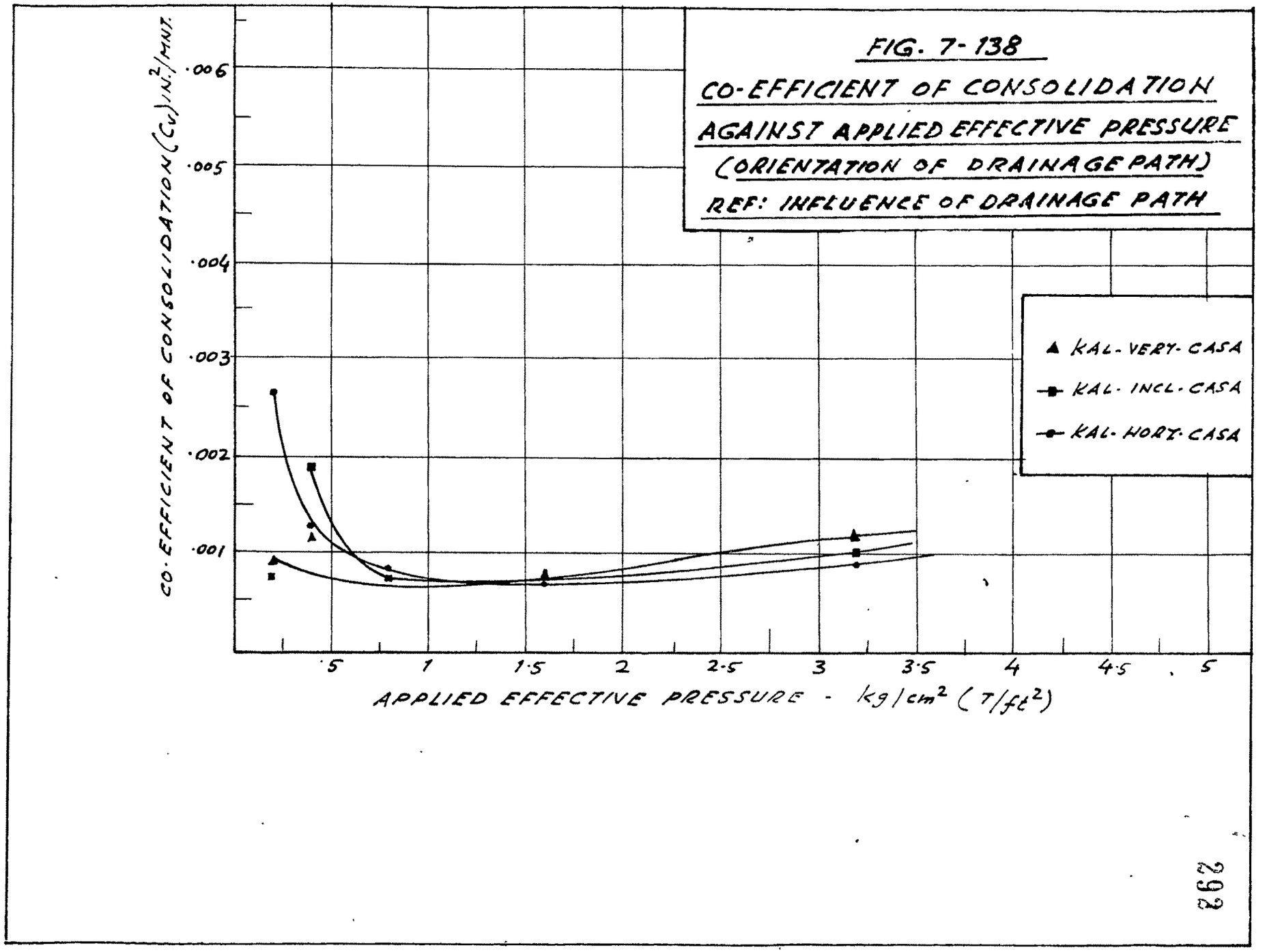
FIG. 7-138
CO-EFFICIENT OF CONSOLIDATION AGAINST APPLIED EFFECTIVE PRESSURE (ORIENTATION OF DRAINAGE PATH)
REF: INFLUENCE OF DRAINAGE PATH
KAL-VERY-CASA
KAL-INCL-CASA
KAL-HORT-CASA
CO-EFFICIENT OF CONSOLIDATION (Cv) IN.²/MNT.
.006
.005
.004
.003
.002
.001
.5
1
1·5
2
2·5
3
3·5
4
4·5
5
APPLIED EFFECTIVE PRESSURE - kg/cm² (T/ft²)

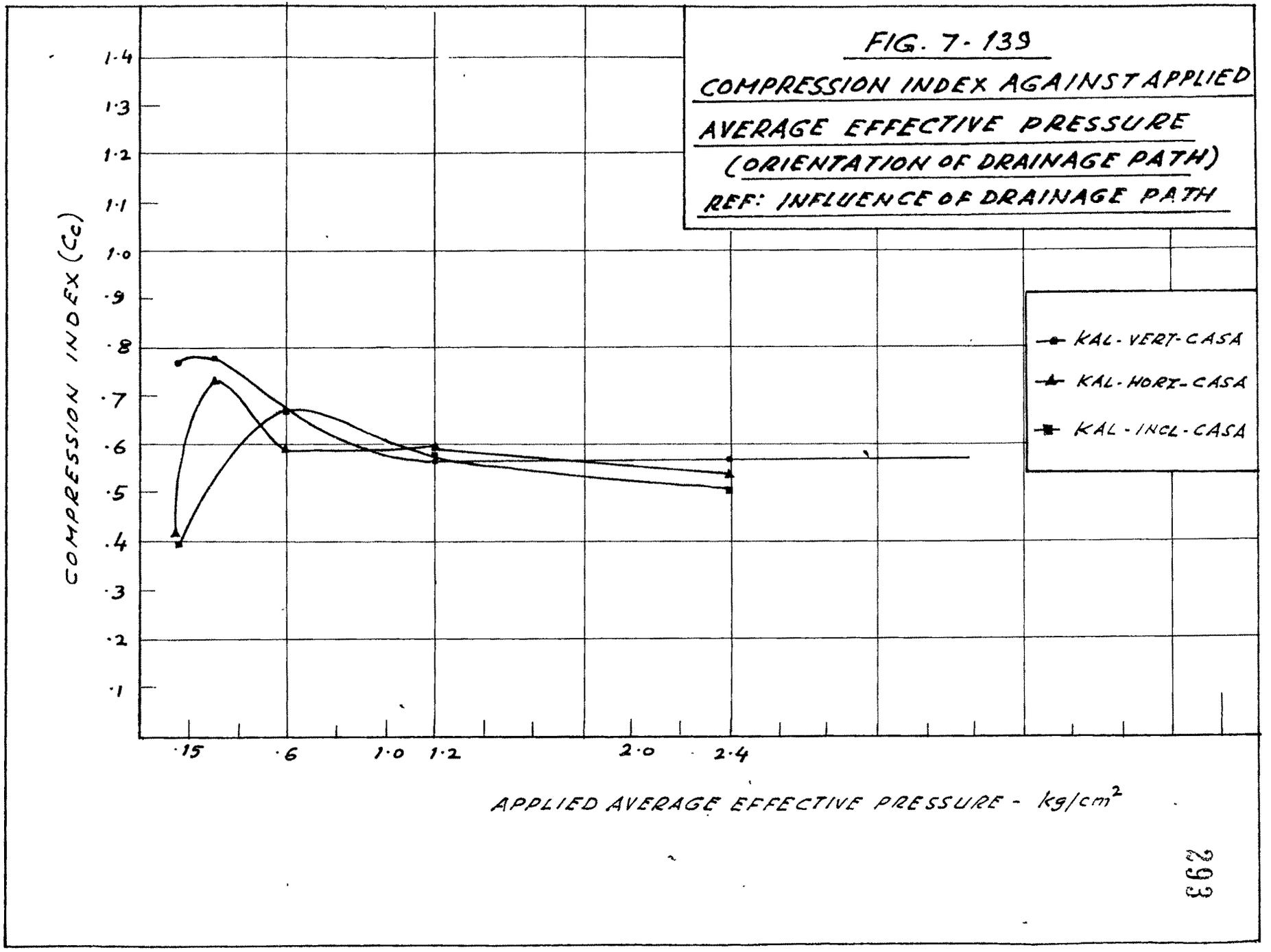
FIG. 7·139
COMPRESSION INDEX AGAINST APPLIED AVERAGE EFFECTIVE PRESSURE
(ORIENTATION OF DRAINAGE PATH)
REF: INFLUENCE OF DRAINAGE PATH
KAL-VERT-CASA
KAL-HORI-CASA
KAL-INCL-CASA
COMPRESSION INDEX (Cc)
1·4
1·3
1·2
1·1
1·0
·9
·8
·7
·6
·5
·4
·3
·2
·1
·15
·6
1·0
1·2
2·0
2·4
APPLIED AVERAGE EFFECTIVE PRESSURE - kg/cm²

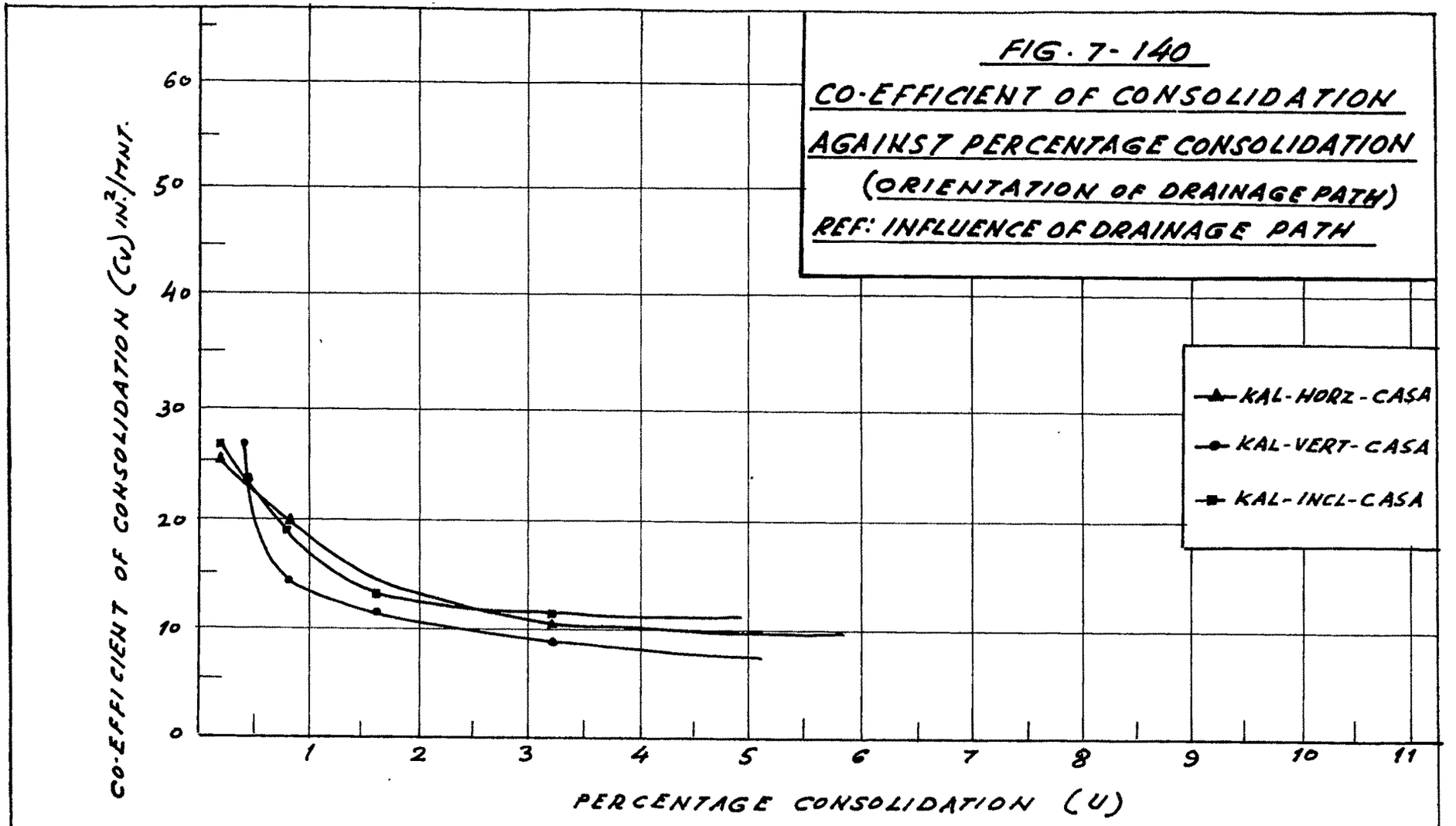
FIG. 7-140
CO-EFFICIENT OF CONSOLIDATION
AGAINST PERCENTAGE CONSOLIDATION
(ORIENTATION OF DRAINAGE PATH)
REF: INFLUENCE OF DRAINAGE PATH
KAL-HORZ-CASA
KAL-VERT-CASA
KAL-INCL-CASA
CO-EFFICIENT OF CONSOLIDATION (Cv) IN.²/MNT.
0
10
20
30
40
50
60
1
2
3
4
5
6
7
8
9
10
11
PERCENTAGE CONSOLIDATION (U)

(v) Parameter P against applied effective pressure. (Figures 7.141 and 7.145).

Vertically oriented sample fits nearer to the Terzaghi. Horizontal sample deviates most at light loads. All the sample show little deviations at higher loads. Vertical sample shows about 1% average deviation under practically all loads. Horizontal and inclined samples show 0.5% and 3.9% deviation under light loads respectively, and 1.5% deviation under higher loads.

Discussion :

The initial structure of a soil sample of inactive clay like kaolinite prepared at liquid limit under a light precompression load will be approximately of a semi-oriented nature with the majority of particles aligned parallel to the bed. Orienting the initial structure at vertical, inclined and horizontal direction it can be visualised that the majority of particles will array in parallel, random and vertical direction. Explanation for the consolidation behaviour can be derived from the consideration of turtuosity (effective flow path in relation to thickness of sample) and interfacial grips. When pressure is applied along the length of the plate shaped particle i.e. on one hand the sample at horizontal direction, has to orient particles in parallel position overcoming interfacial grip but on the other hand the water has to pass through a shorter flow path. However, when the load

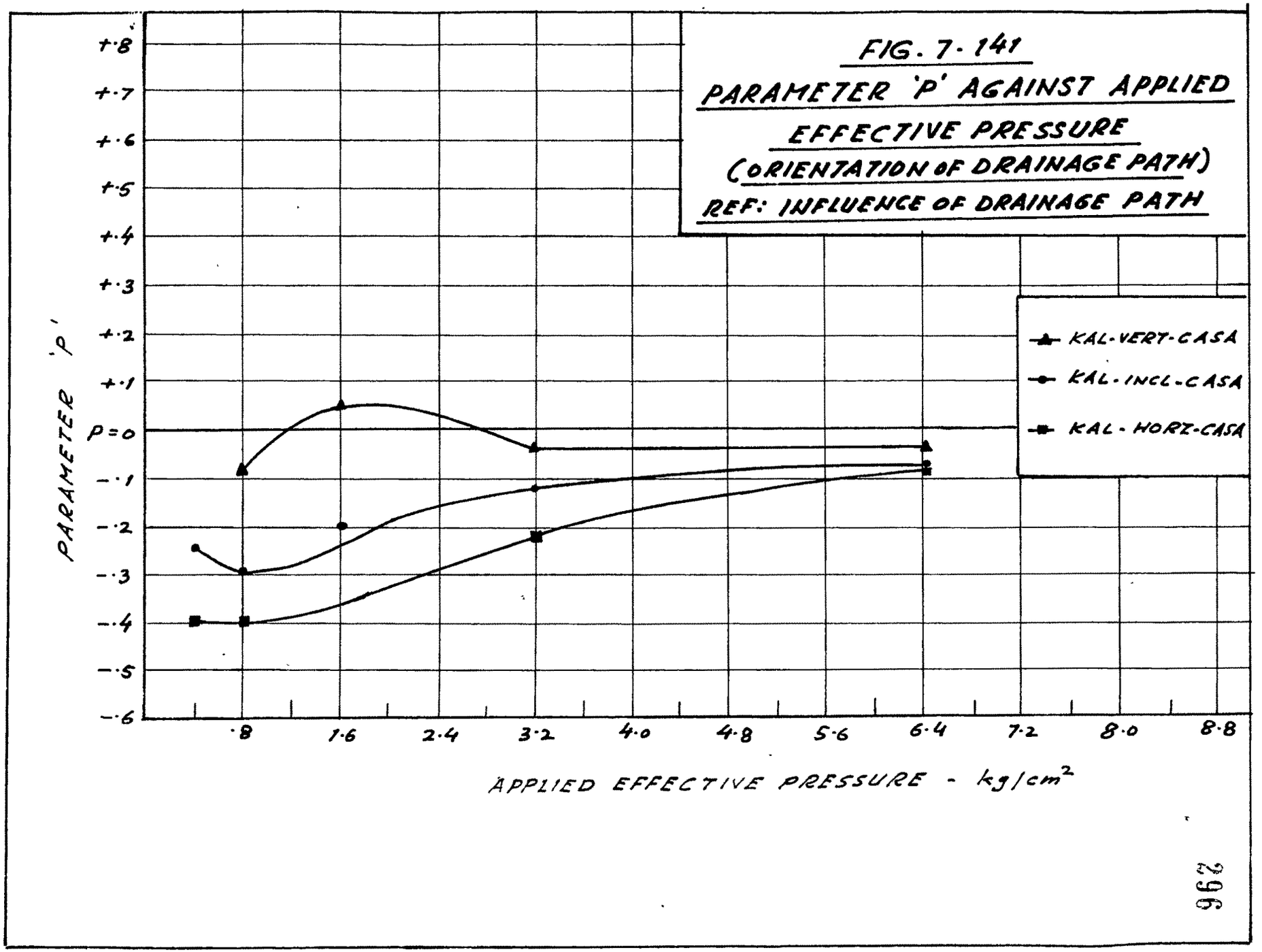
FIG. 7·141
PARAMETER 'P' AGAINST APPLIED EFFECTIVE PRESSURE
(ORIENTATION OF DRAINAGE PATH)
REF: INFLUENCE OF DRAINAGE PATH
KAL-VERT-CASA
KAL-INCL-CASA
KAL-HORZ-CASA
PARAMETER 'P'
+·8
+·7
+·6
+·5
+·4
+·3
+·2
+·1
P=0
−·1
−·2
−·3
−·4
−·5
−·6
·8
1·6
2·4
3·2
4·0
4·8
5·6
6·4
7·2
8·0
8·8
APPLIED EFFECTIVE PRESSURE - kg/cm²
962

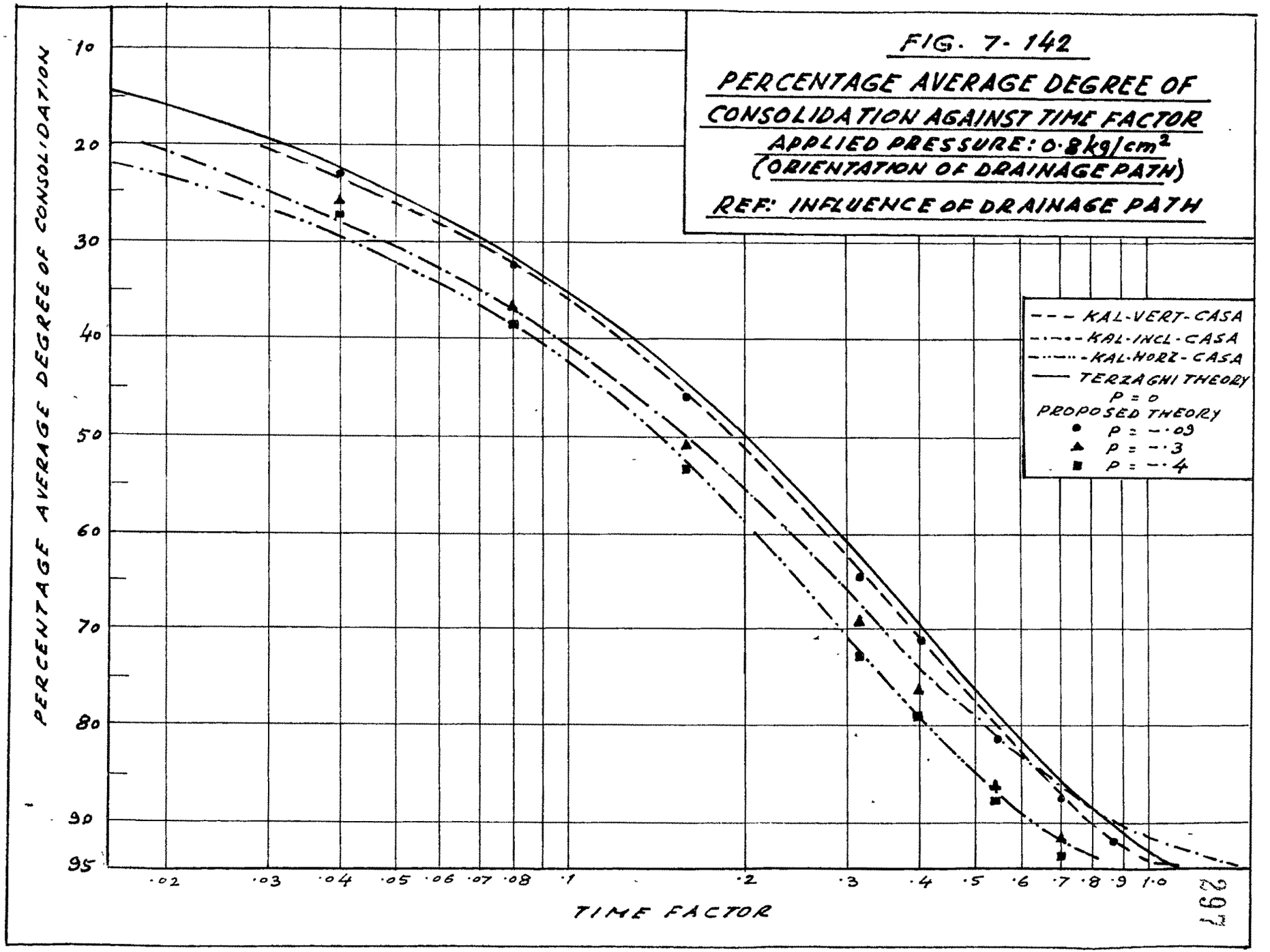
FIG. 7-142
PERCENTAGE AVERAGE DEGREE OF CONSOLIDATION AGAINST TIME FACTOR
APPLIED PRESSURE: 0·8 kg/cm²
(ORIENTATION OF DRAINAGE PATH)
REF: INFLUENCE OF DRAINAGE PATH
KAL-VERT-CASA
KAL-INCL-CASA
KAL-HORZ-CASA
TERZAGHI THEORY
P = 0
PROPOSED THEORY
P = -·09
P = -·3
P = -·4
PERCENTAGE AVERAGE DEGREE OF CONSOLIDATION
10
20
30
40
50
60
70
80
90
95
·02
·03
·04
·05
·06
·07
·08
·1
·2
·3
·4
·5
·6
·7
·8
·9
1·0
TIME FACTOR

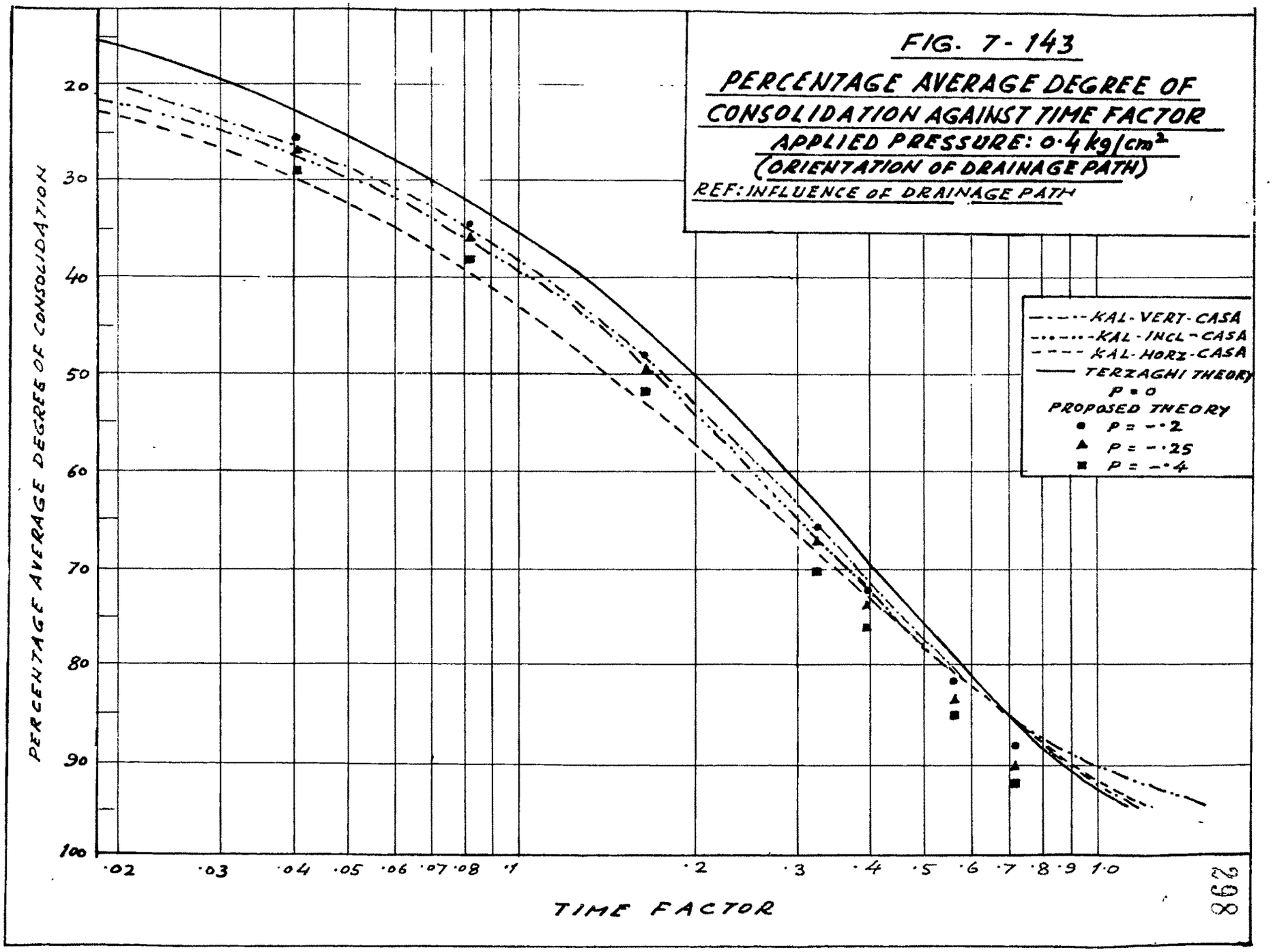
FIG. 7-143
PERCENTAGE AVERAGE DEGREE OF CONSOLIDATION AGAINST TIME FACTOR
APPLIED PRESSURE: 0·4 kg/cm²
(ORIENTATION OF DRAINAGE PATH)
REF: INFLUENCE OF DRAINAGE PATH
KAL-VERT-CASA
KAL-INCL-CASA
KAL-HORZ-CASA
TERZAGHI THEORY
P = 0
PROPOSED THEORY
P = -·2
P = -·25
P = -·4
PERCENTAGE AVERAGE DEGREE OF CONSOLIDATION
20
30
40
50
60
70
80
90
100
·02
·03
·04
·05
·06
·07
·08
·1
·2
·3
·4
·5
·6
·7
·8
·9
1·0
TIME FACTOR
8662

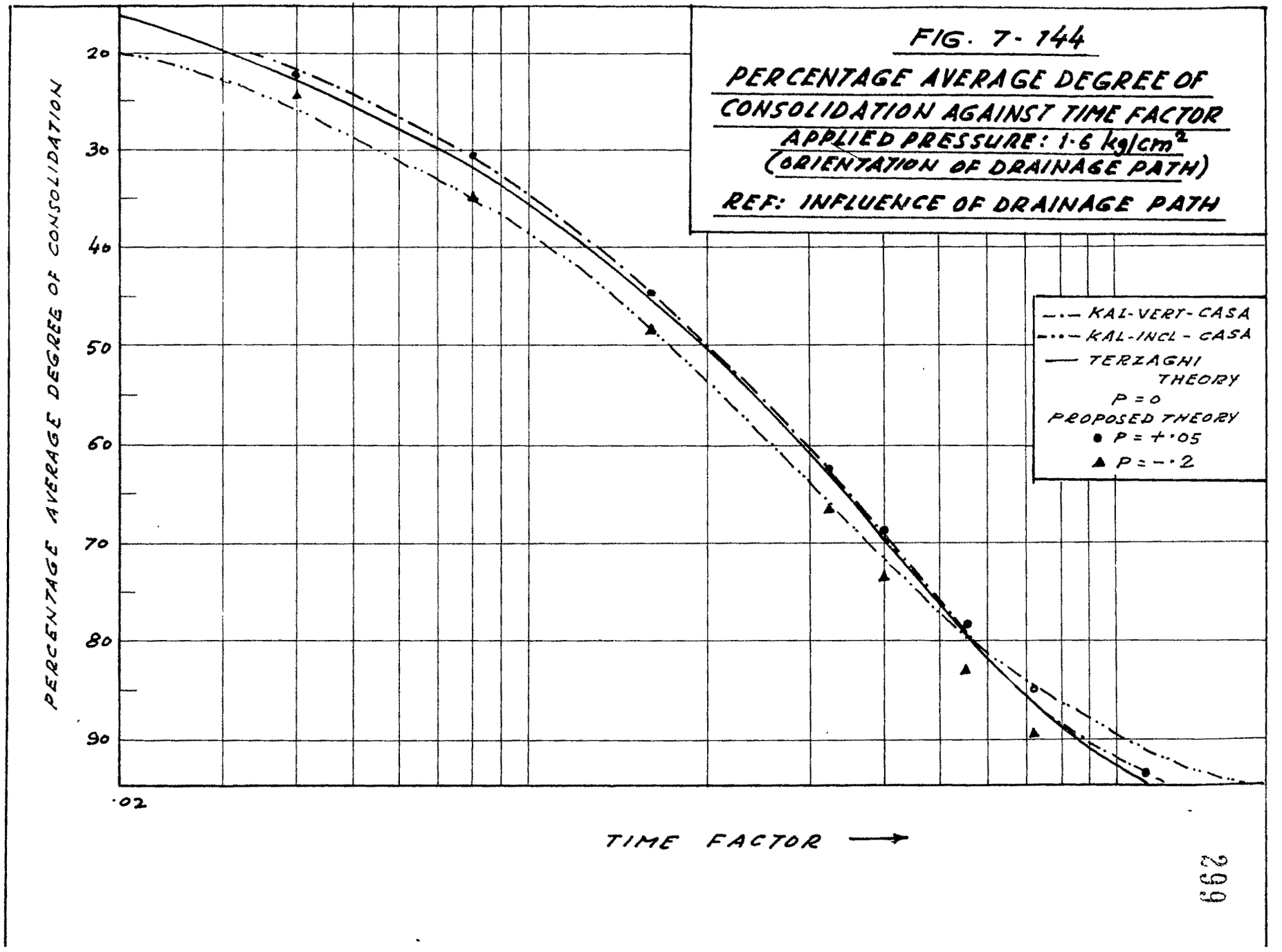
FIG. 7-144
PERCENTAGE AVERAGE DEGREE OF CONSOLIDATION AGAINST TIME FACTOR
APPLIED PRESSURE: 1·6 kg/cm²
(ORIENTATION OF DRAINAGE PATH)
REF: INFLUENCE OF DRAINAGE PATH
PERCENTAGE AVERAGE DEGREE OF CONSOLIDATION
20
30
40
50
60
70
80
90
·02
TIME FACTOR
KAL-VERT-CASA
KAL-INCL-CASA
TERZAGHI THEORY
P = 0
PROPOSED THEORY
P = +·05
P = −·2

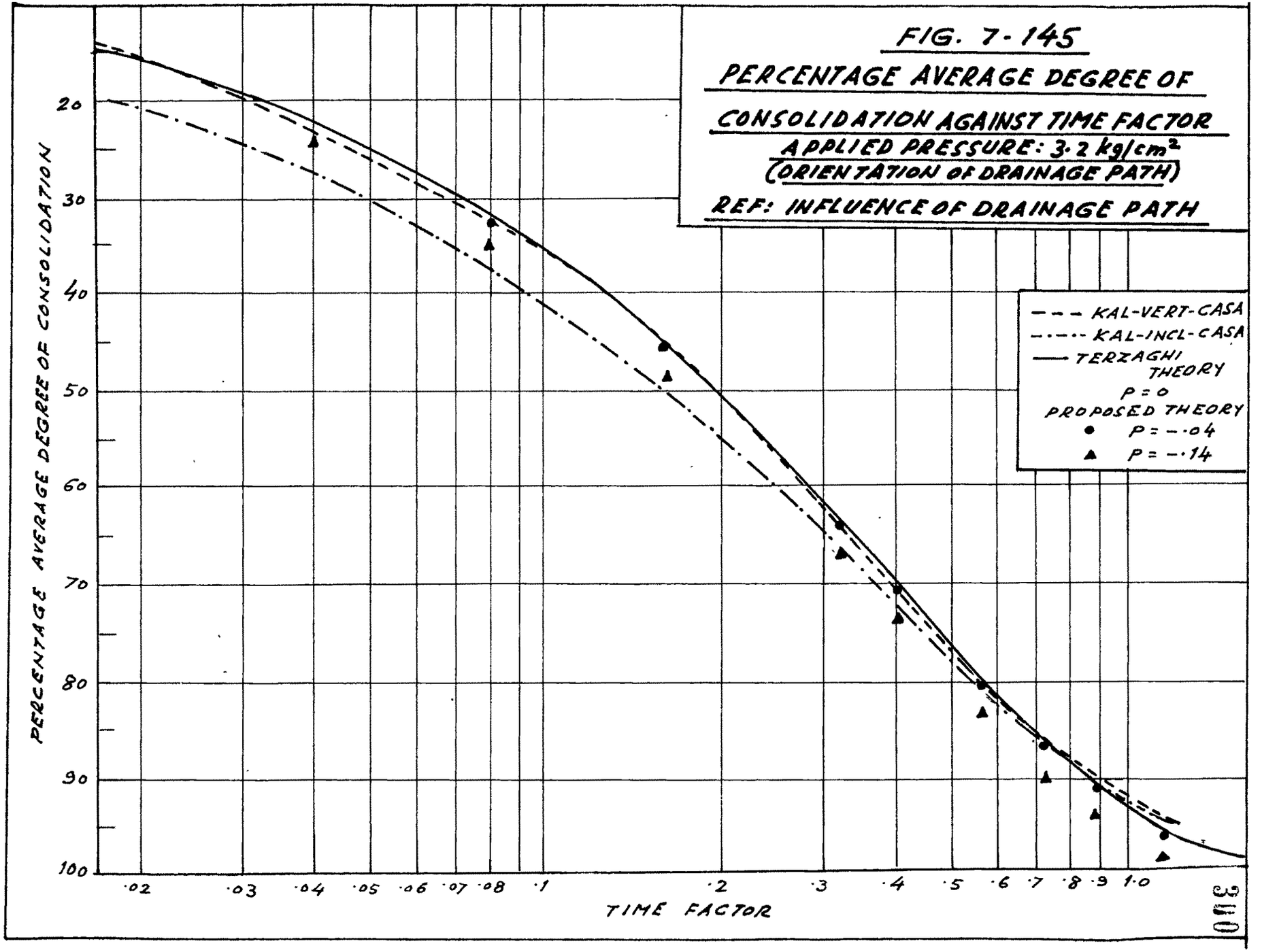
FIG. 7-145
PERCENTAGE AVERAGE DEGREE OF CONSOLIDATION AGAINST TIME FACTOR
APPLIED PRESSURE: 3·2 kg/cm²
(ORIENTATION OF DRAINAGE PATH)
REF: INFLUENCE OF DRAINAGE PATH
KAL-VERT-CASA
KAL-INCL-CASA
TERZAGHI THEORY
P = 0
PROPOSED THEORY
P = -·04
P = -·14
PERCENTAGE AVERAGE DEGREE OF CONSOLIDATION
20
30
40
50
60
70
80
90
100
·02
·03
·04
·05
·06
·07
·08
·1
·2
·3
·4
·5
·6
·7
·8
·9
1·0
TIME FACTOR
0138

is acting across the length of plate shaped particles there is little resistance from interfacial grip but a longer flow path has to be covered by water. Situation in samples taken in the inclined direction can be considered intermediate. Therefore, it can be argued that under lighter loads when interfacial resistance is predominant, horizontal sample shows comparatively higher resistance indicated by large reduction in c_v and humpy compression characteristics. Under higher consolidating pressure the load potential dominates the above described resistance causing a complete structural breakdown, and the characteristics become almost similar. The same degree of secondary compression suggests that for any orientation of particles the physico-chemical environment does not change, once the particles are alligned in parallel arrays. The analysis by P parameter also supports the above arguments.

B : Length of Drainage Path

(i) Coefficient of consolidation against percentage consolidation.
(Figures 7.146 to 7.149).

In case of samples thinner than conventional samples, the value of c_v increases initially eventually becoming constant at higher pressures. In the case of samples thicker than the conventional samples the value remains almost the same throughout the process at lighter loads.

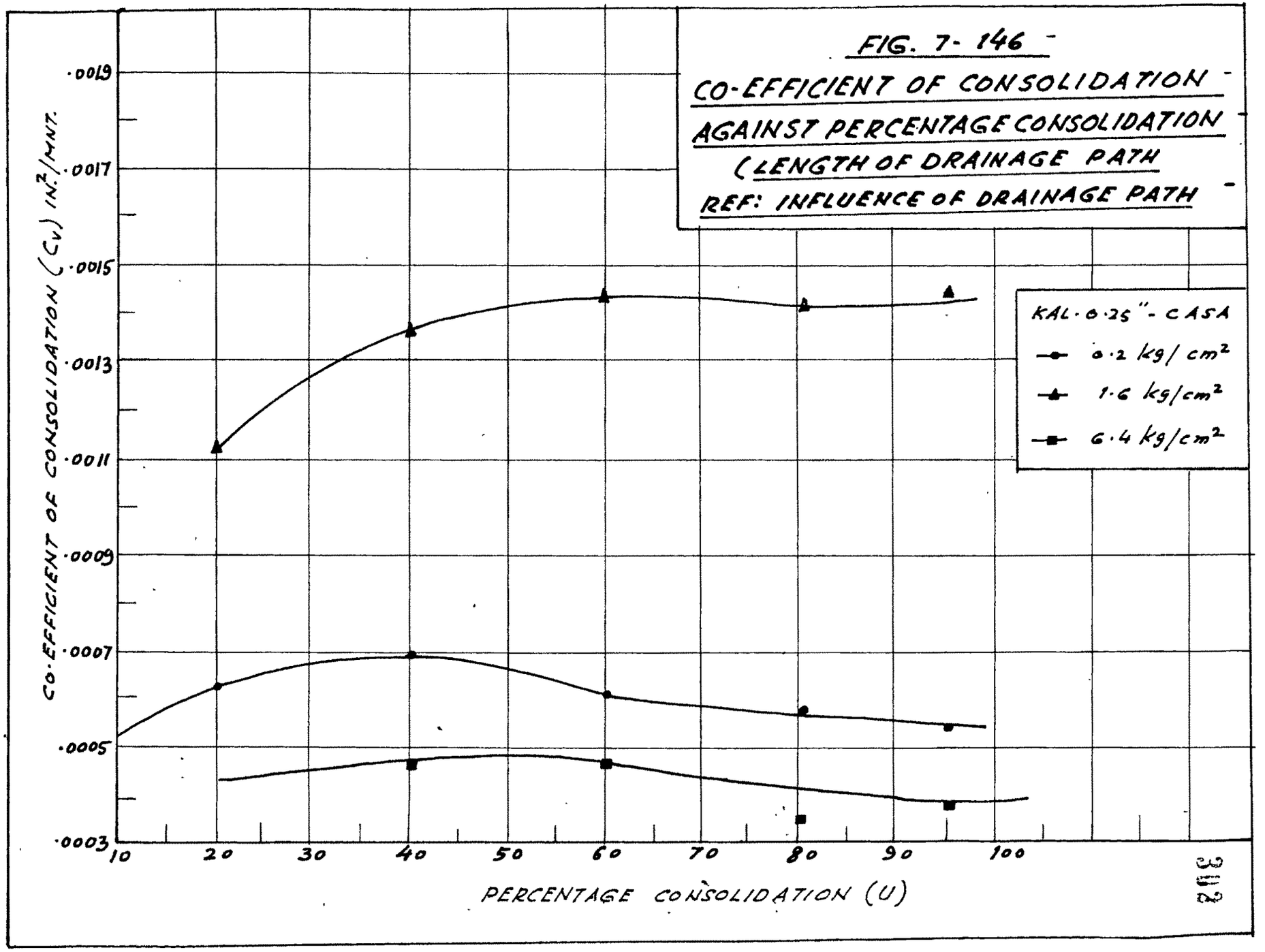
FIG. 7-146
CO-EFFICIENT OF CONSOLIDATION AGAINST PERCENTAGE CONSOLIDATION (LENGTH OF DRAINAGE PATH
REF: INFLUENCE OF DRAINAGE PATH
KAL-0·25"-CASA
0·2 kg/cm²
1·6 kg/cm²
6·4 kg/cm²
CO-EFFICIENT OF CONSOLIDATION (Cv) IN.²/MNT.
·0019
·0017
·0015
·0013
·0011
·0009
·0007
·0005
·0003
10
20
30
40
50
60
70
80
90
100
PERCENTAGE CONSOLIDATION (U)

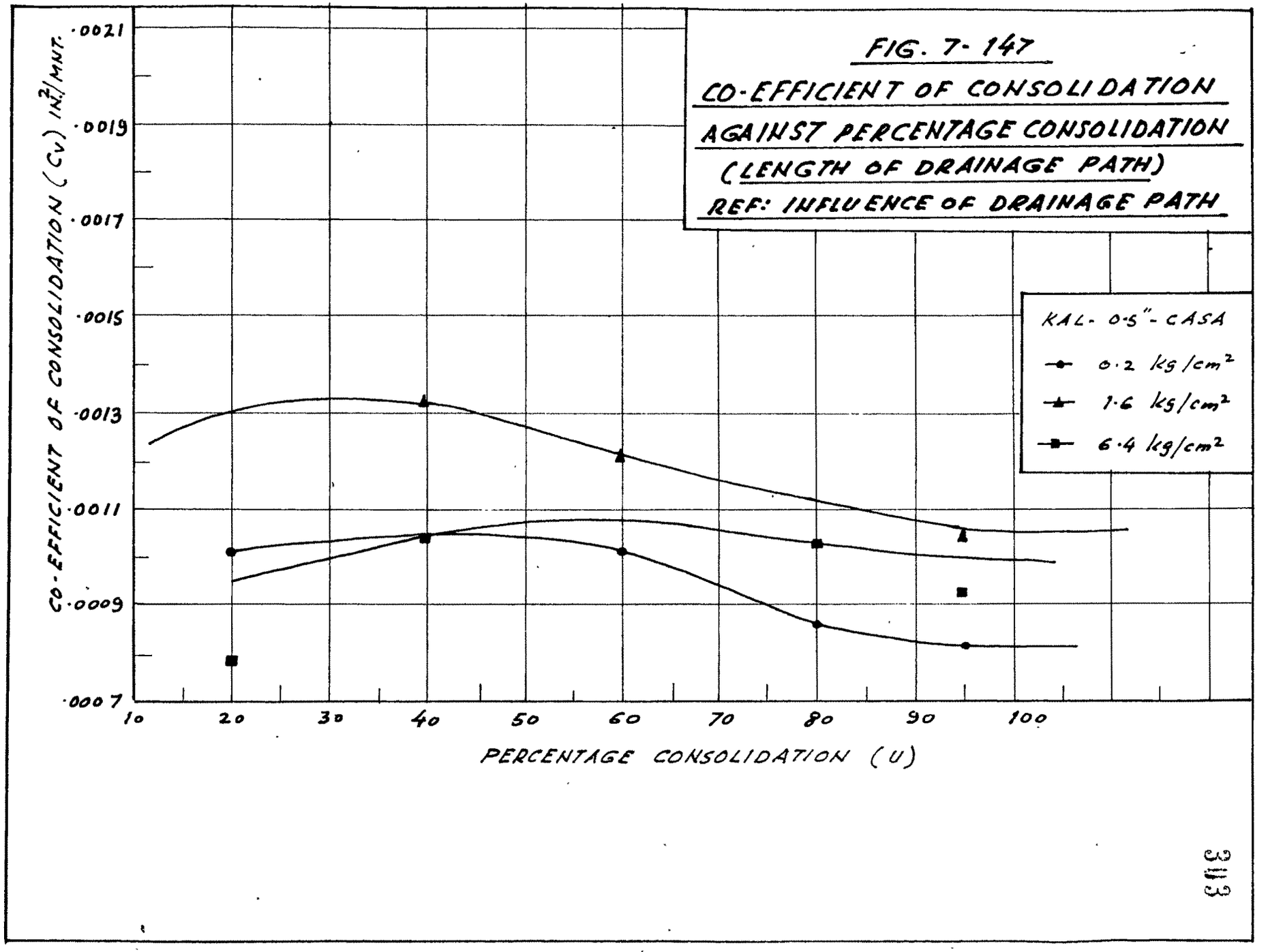
FIG. 7-147
CO-EFFICIENT OF CONSOLIDATION
AGAINST PERCENTAGE CONSOLIDATION
(LENGTH OF DRAINAGE PATH)
REF: INFLUENCE OF DRAINAGE PATH
KAL-0·5"-CASA
0·2 kg/cm²
1·6 kg/cm²
6·4 kg/cm²
CO-EFFICIENT OF CONSOLIDATION (Cv) IN²/MNT.
·0021
·0019
·0017
·0015
·0013
·0011
·0009
·0007
10
20
30
40
50
60
70
80
90
100
PERCENTAGE CONSOLIDATION (U)

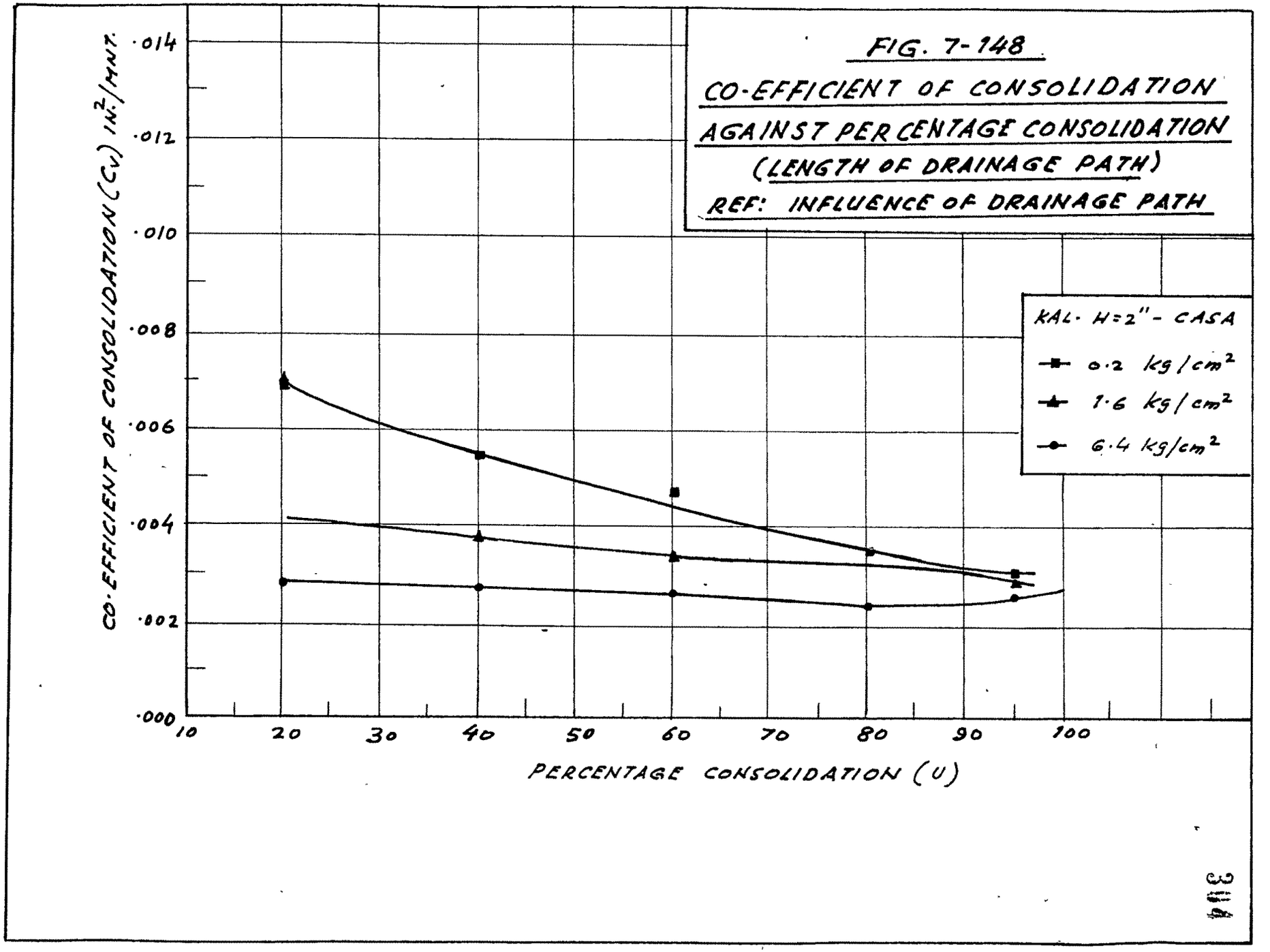
FIG. 7-148
CO-EFFICIENT OF CONSOLIDATION
AGAINST PER CENTAGE CONSOLIDATION
(LENGTH OF DRAINAGE PATH)
REF: INFLUENCE OF DRAINAGE PATH
KAL. H=2" - CASA
0.2 kg/cm²
1.6 kg/cm²
6.4 kg/cm²
CO-EFFICIENT OF CONSOLIDATION (Cv) in.²/MNT.
.014
.012
.010
.008
.006
.004
.002
.000
10
20
30
40
50
60
70
80
90
100
PERCENTAGE CONSOLIDATION (U)

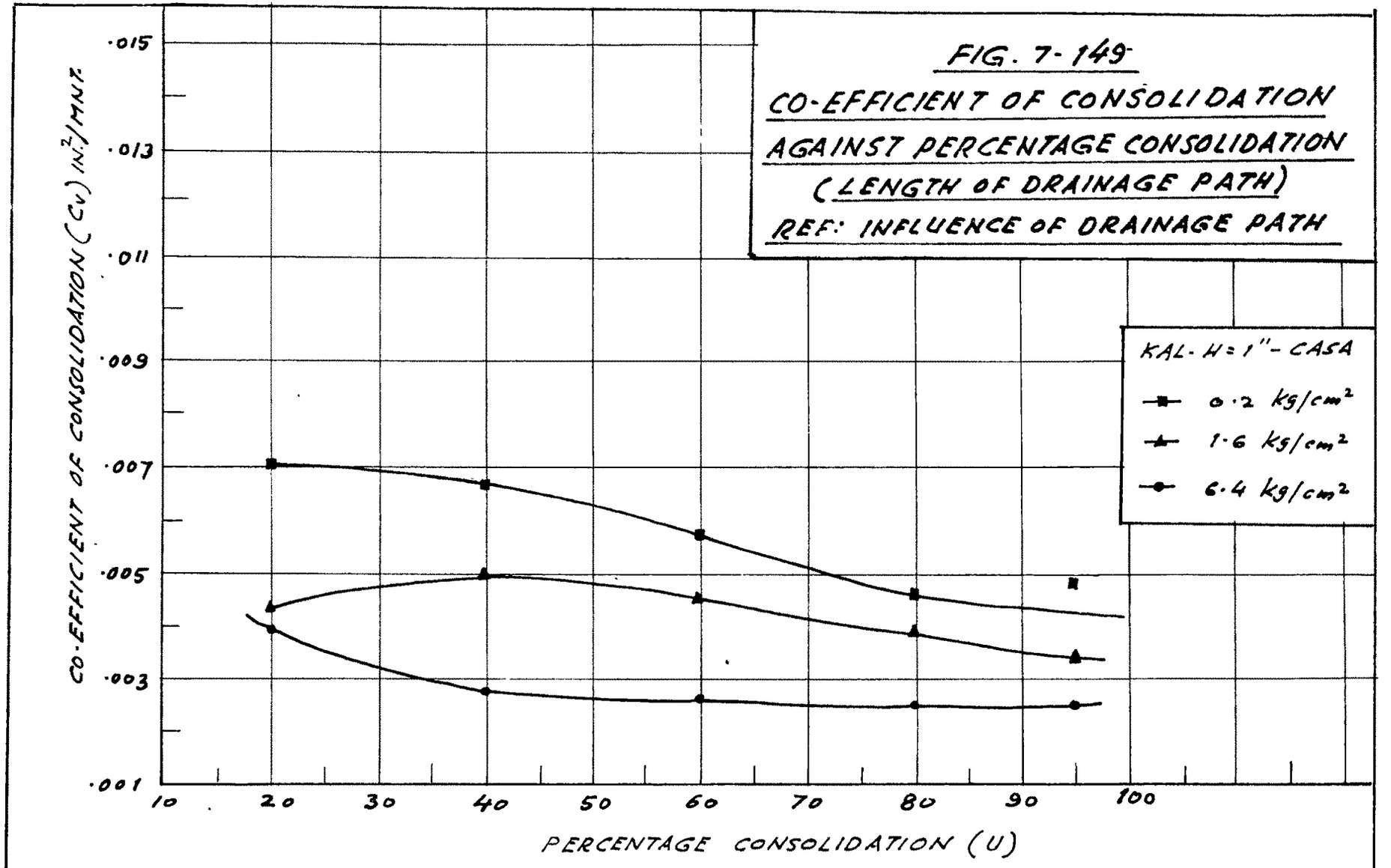
FIG. 7-149
CO-EFFICIENT OF CONSOLIDATION
AGAINST PERCENTAGE CONSOLIDATION
(LENGTH OF DRAINAGE PATH)
REF: INFLUENCE OF DRAINAGE PATH
KAL-H=1"-CASA
0·2 kg/cm²
1·6 kg/cm²
6·4 kg/cm²
CO-EFFICIENT OF CONSOLIDATION (Cv) in²/MNT.
·015
·013
·011
·009
·007
·005
·003
·001
10
20
30
40
50
60
70
80
90
100
PERCENTAGE CONSOLIDATION (U)

(ii) Coefficient of consolidation against applied effective pressure.
(Figure 7.150).

General nature of the relationship is of a similar type showing a decrease in c_v at lighter loads and an increase with higher loads. At very high loads the c_v value tends to remain constant. Thicker sample exhibits higher values of c_v compared to thinner ones.

(iii) Compression index against applied average effective pressure.
(Figure 7.151).

General trend of curves is similar for the thick and the thin samples except in the initial portion of the curves. Thick samples show an initial hump unlike the thin samples.

(iv) Percentage secondary compression against effective applied pressure.
(Figure 7.152).

Thicker samples exhibit a lesser degree of secondary compression than the thin samples. Under higher consolidating loads the degree of secondary compression is more or less same in both the thick and thin samples.

(v) Parameter 'P' against applied effective pressure.
(Figure 7.153 and 7.154 to 7.159).

At higher consolidating loads the thick as well as the thin samples fit closer to the Terzaghi. Practically under all loads the thick sample fit nearer to the Terzaghi curve.

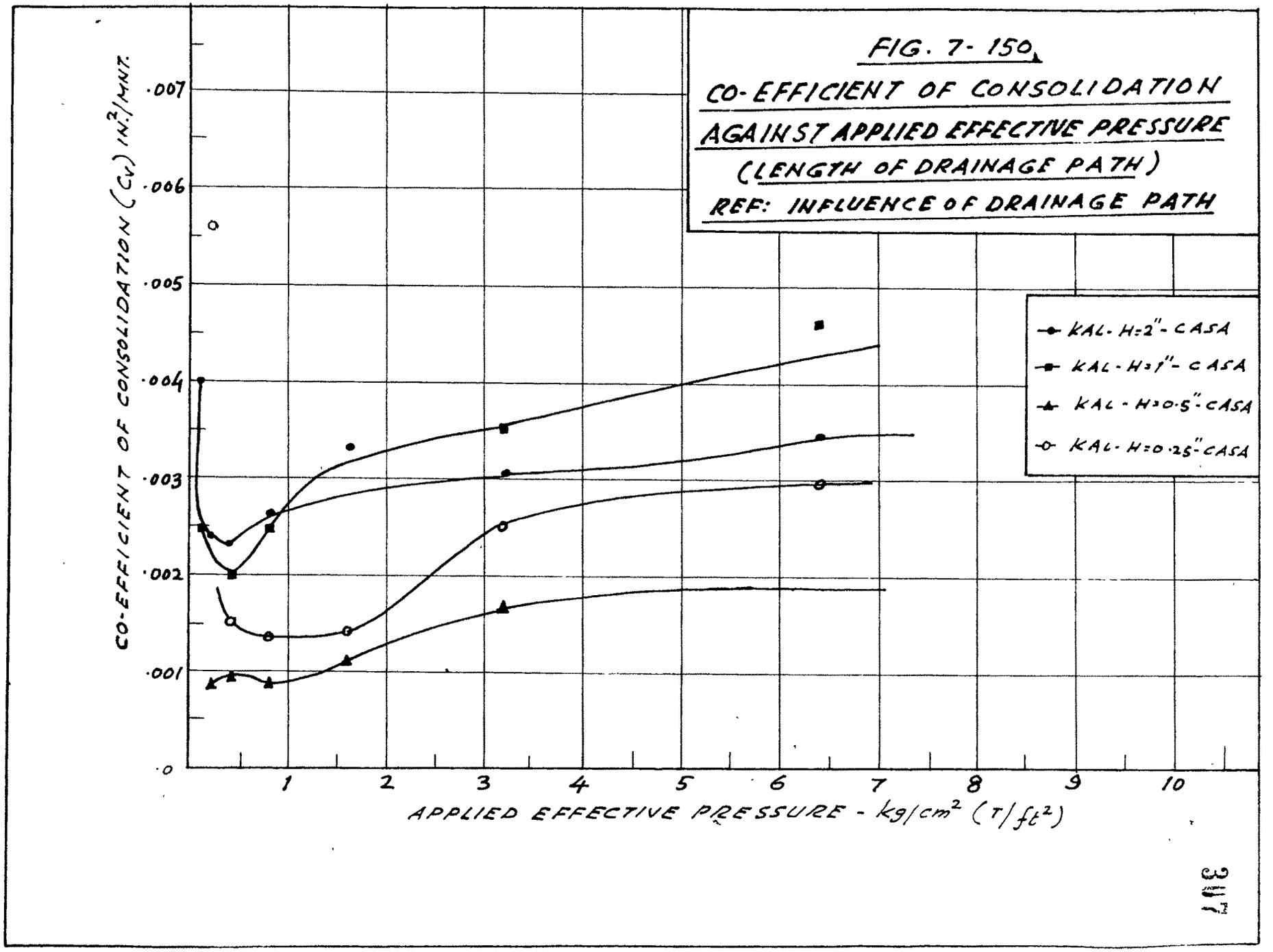
FIG. 7-150
CO-EFFICIENT OF CONSOLIDATION
AGAINST APPLIED EFFECTIVE PRESSURE
(LENGTH OF DRAINAGE PATH)
REF: INFLUENCE OF DRAINAGE PATH
KAL - H=2" - CASA
KAL - H=1" - CASA
KAL - H=0·5" - CASA
KAL - H=0·25" - CASA
CO-EFFICIENT OF CONSOLIDATION (C_v) IN.²/MNT.
·007
·006
·005
·004
·003
·002
·001
·0
1
2
3
4
5
6
7
8
9
10
APPLIED EFFECTIVE PRESSURE - kg/cm² (T/ft²)

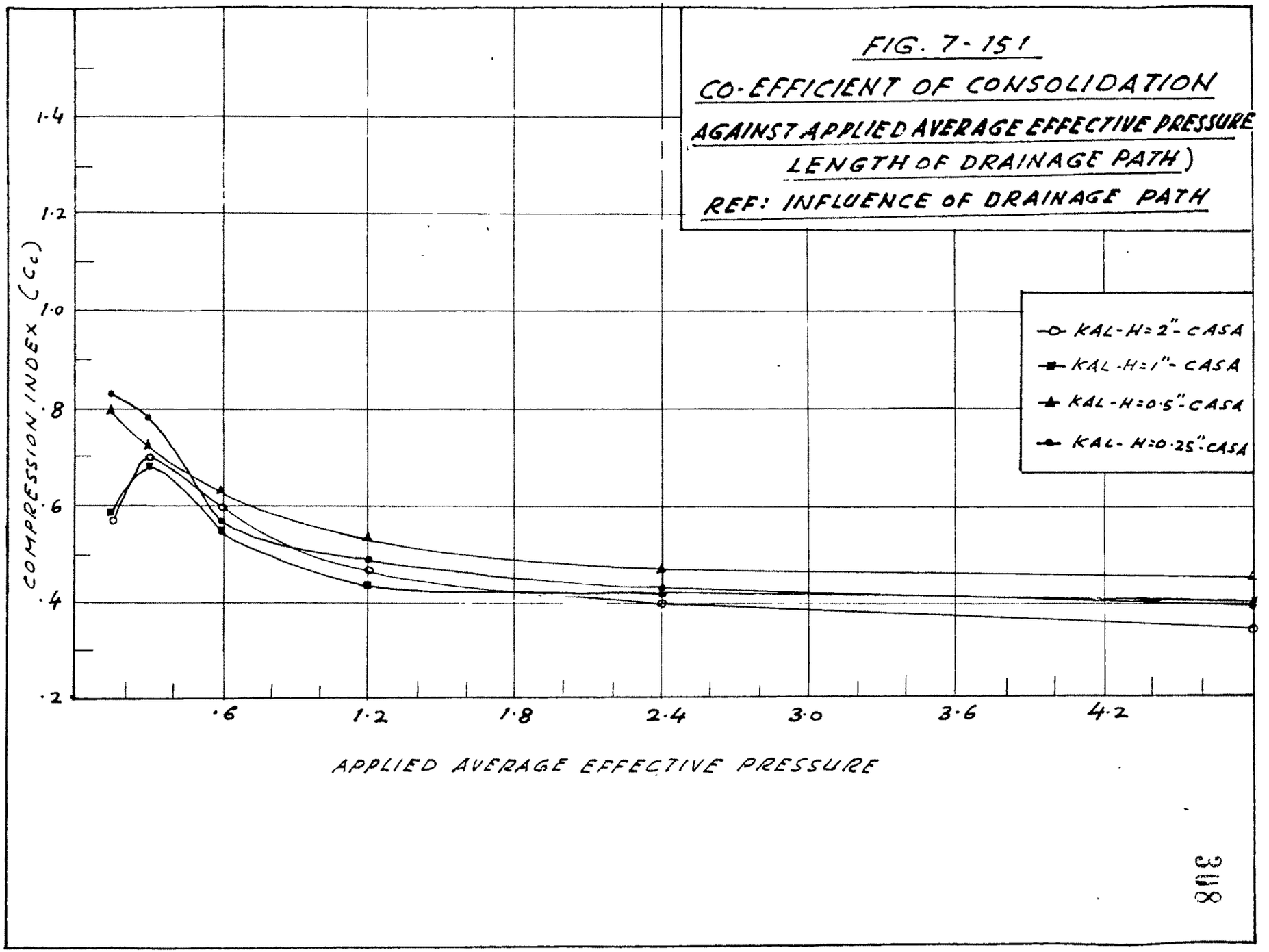
FIG. 7-151
CO-EFFICIENT OF CONSOLIDATION
AGAINST APPLIED AVERAGE EFFECTIVE PRESSURE
LENGTH OF DRAINAGE PATH)
REF: INFLUENCE OF DRAINAGE PATH
KAL-H=2"-CASA
KAL-H=1"-CASA
KAL-H=0.5"-CASA
KAL-H=0.25"-CASA
COMPRESSION INDEX (Cc)
1.4
1.2
1.0
.8
.6
.4
.2
.6
1.2
1.8
2.4
3.0
3.6
4.2
APPLIED AVERAGE EFFECTIVE PRESSURE

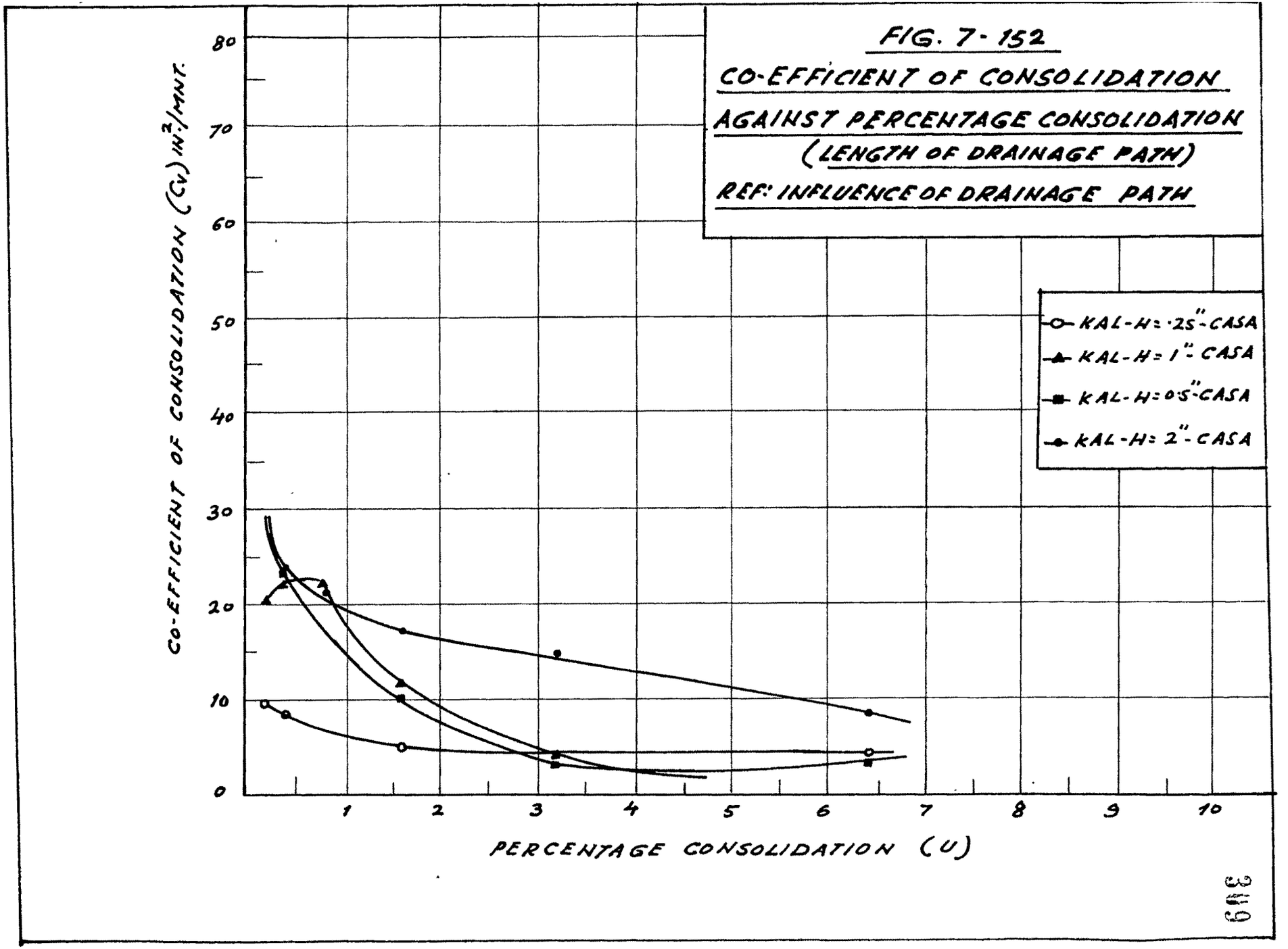
FIG. 7-152
CO-EFFICIENT OF CONSOLIDATION
AGAINST PERCENTAGE CONSOLIDATION
(LENGTH OF DRAINAGE PATH)
REF: INFLUENCE OF DRAINAGE PATH
KAL-H=·25"-CASA
KAL-H=1"-CASA
KAL-H=0·5"-CASA
KAL-H=2"-CASA
CO-EFFICIENT OF CONSOLIDATION (Cv) IN²/MNT.
PERCENTAGE CONSOLIDATION (U)
0
10
20
30
40
50
60
70
80
1
2
3
4
5
6
7
8
9
10

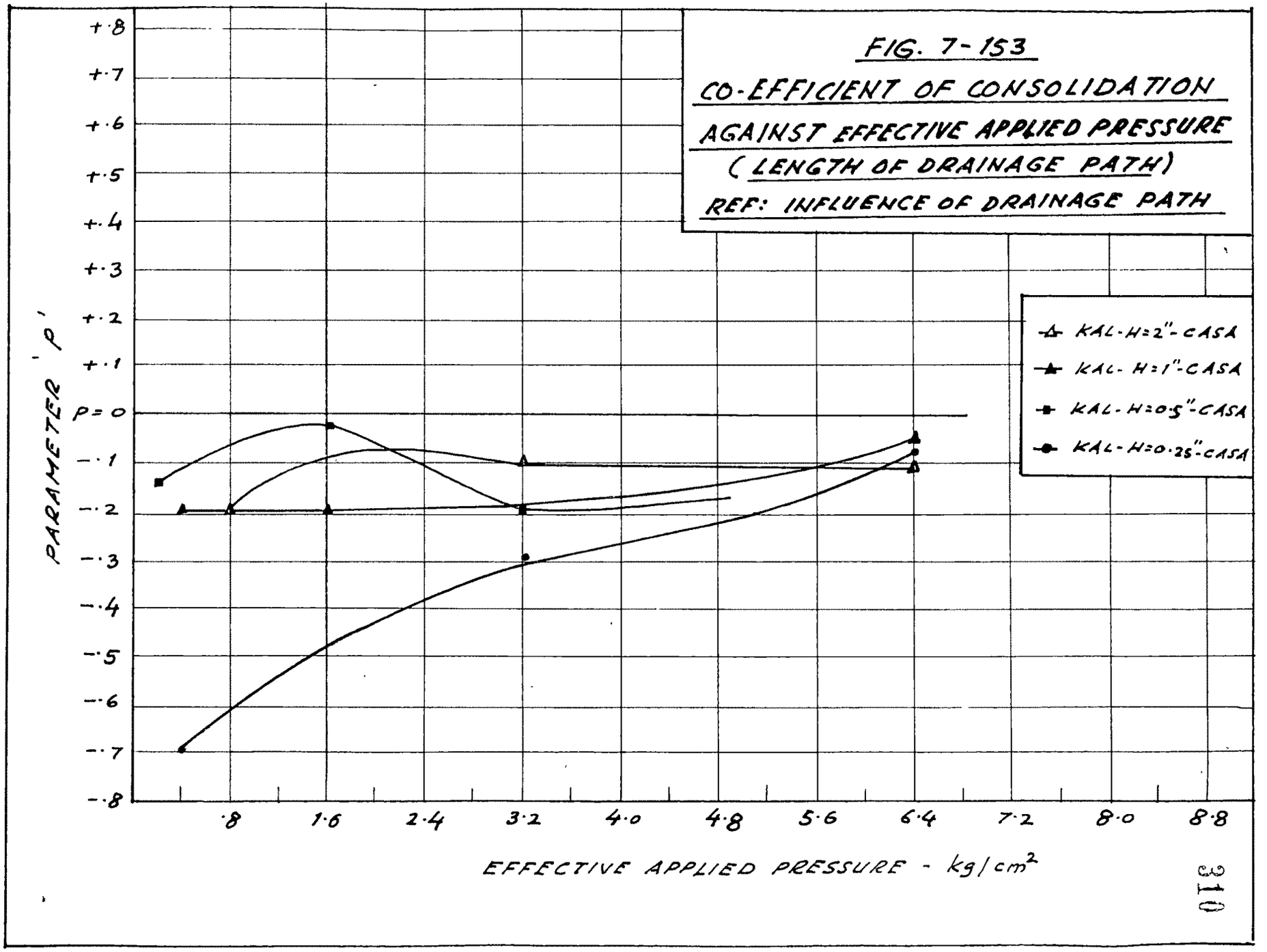
FIG. 7-153
CO-EFFICIENT OF CONSOLIDATION
AGAINST EFFECTIVE APPLIED PRESSURE
(LENGTH OF DRAINAGE PATH)
REF: INFLUENCE OF DRAINAGE PATH
KAL-H=2"-CASA
KAL-H=1"-CASA
KAL-H=0.5"-CASA
KAL-H=0.25"-CASA
PARAMETER 'P'
+.8
+.7
+.6
+.5
+.4
+.3
+.2
+.1
P=0
-.1
-.2
-.3
-.4
-.5
-.6
-.7
-.8
.8
1.6
2.4
3.2
4.0
4.8
5.6
6.4
7.2
8.0
8.8
EFFECTIVE APPLIED PRESSURE - kg/cm²
310

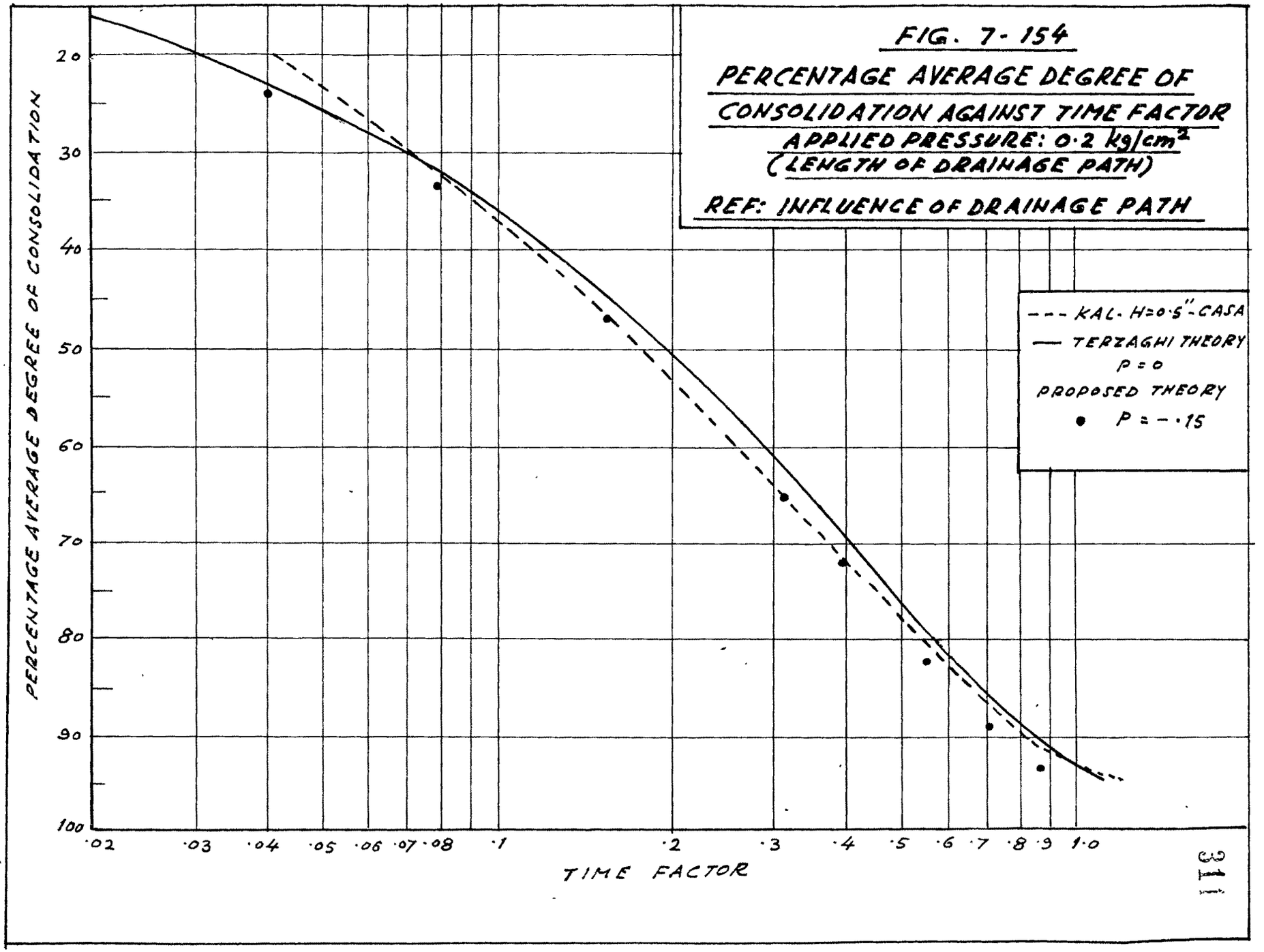
FIG. 7-154
PERCENTAGE AVERAGE DEGREE OF CONSOLIDATION AGAINST TIME FACTOR
APPLIED PRESSURE: 0·2 kg/cm²
(LENGTH OF DRAINAGE PATH)
REF: INFLUENCE OF DRAINAGE PATH
--- KAL. H=0·5"-CASA
— TERZAGHI THEORY P=0
PROPOSED THEORY
● P=-·15
PERCENTAGE AVERAGE DEGREE OF CONSOLIDATION
20
30
40
50
60
70
80
90
100
·02
·03
·04
·05
·06
·07
·08
·1
·2
·3
·4
·5
·6
·7
·8
·9
1·0
TIME FACTOR

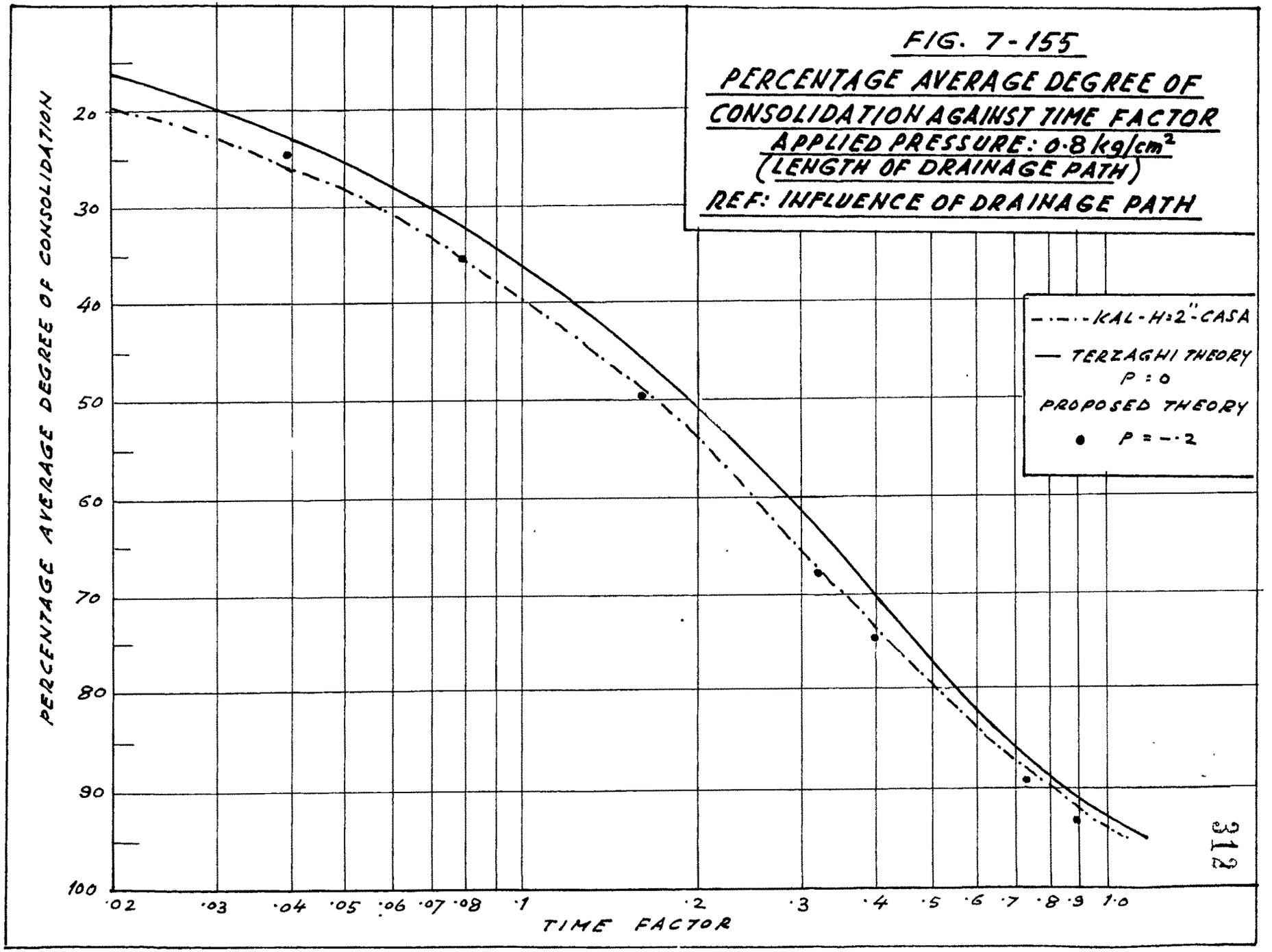
FIG. 7-155
PERCENTAGE AVERAGE DEGREE OF CONSOLIDATION AGAINST TIME FACTOR
APPLIED PRESSURE: 0·8 kg/cm²
(LENGTH OF DRAINAGE PATH)
REF: INFLUENCE OF DRAINAGE PATH
KAL-H=2"-CASA
TERZAGHI THEORY P=0
PROPOSED THEORY P=-·2
PERCENTAGE AVERAGE DEGREE OF CONSOLIDATION
20
30
40
50
60
70
80
90
100
·02 ·03 ·04 ·05 ·06 ·07 ·08 ·1 ·2 ·3 ·4 ·5 ·6 ·7 ·8 ·9 1·0
TIME FACTOR

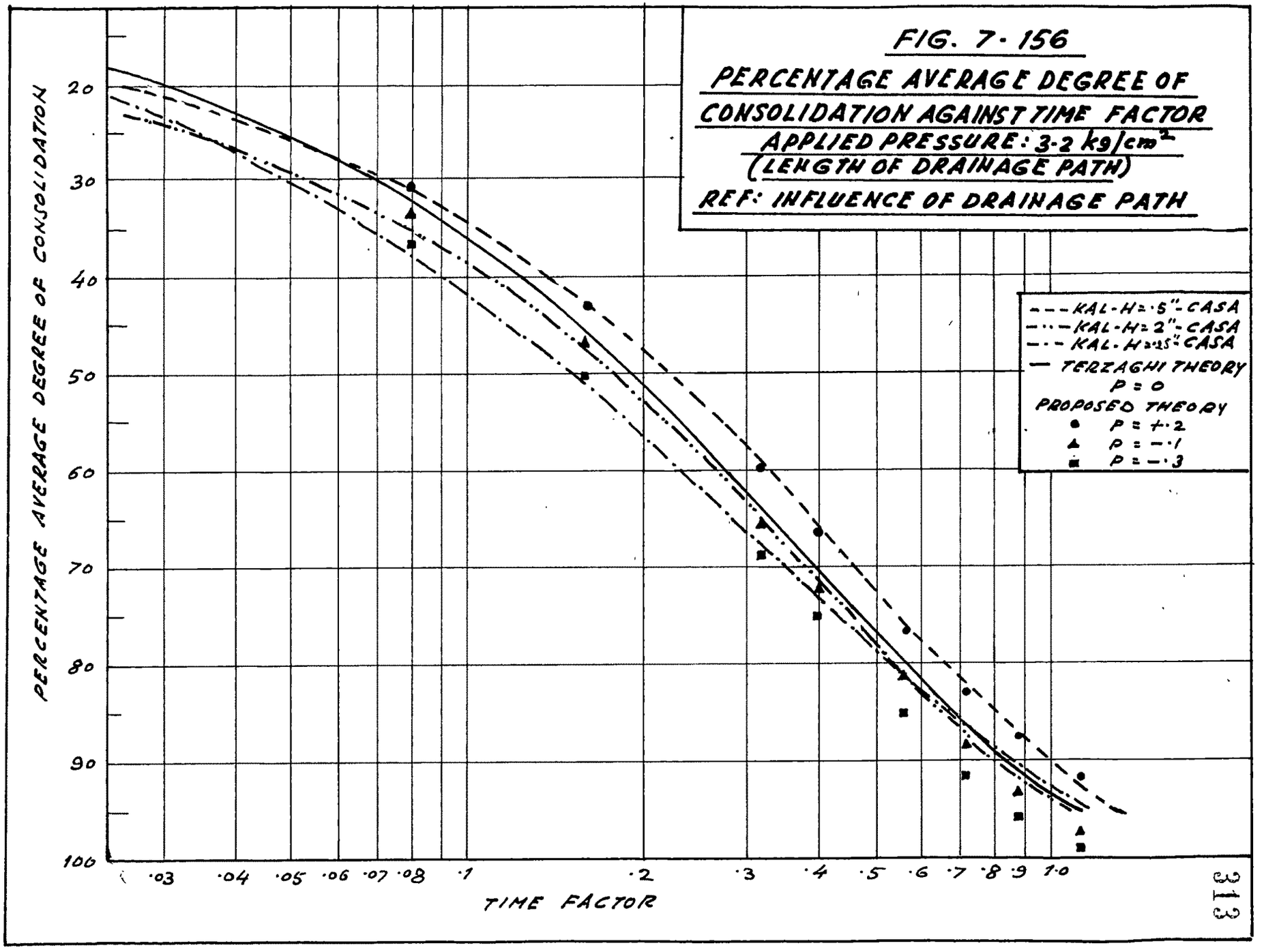
FIG. 7·156
PERCENTAGE AVERAGE DEGREE OF CONSOLIDATION AGAINST TIME FACTOR
APPLIED PRESSURE: 3·2 kg/cm²
(LENGTH OF DRAINAGE PATH)
REF: INFLUENCE OF DRAINAGE PATH
KAL-H=·5"-CASA
KAL-H=2"-CASA
KAL-H=1·5"-CASA
TERZAGHI THEORY
P=0
PROPOSED THEORY
P=+·2
P=−·1
P=−·3
PERCENTAGE AVERAGE DEGREE OF CONSOLIDATION
20
30
40
50
60
70
80
90
100
·03
·04
·05
·06
·07
·08
·1
·2
·3
·4
·5
·6
·7
·8
·9
1·0
TIME FACTOR
E3
E3

FIG. 7·157

PERCENTAGE AVERAGE DEGREE OF CONSOLIDATION AGAINST TIME FACTOR

APPLIED PRESSURE : 6·4 kg/cm²

(LENGTH OF DRAINAGE PATH)

REF: INFLUENCE OF DRAINAGE PATH

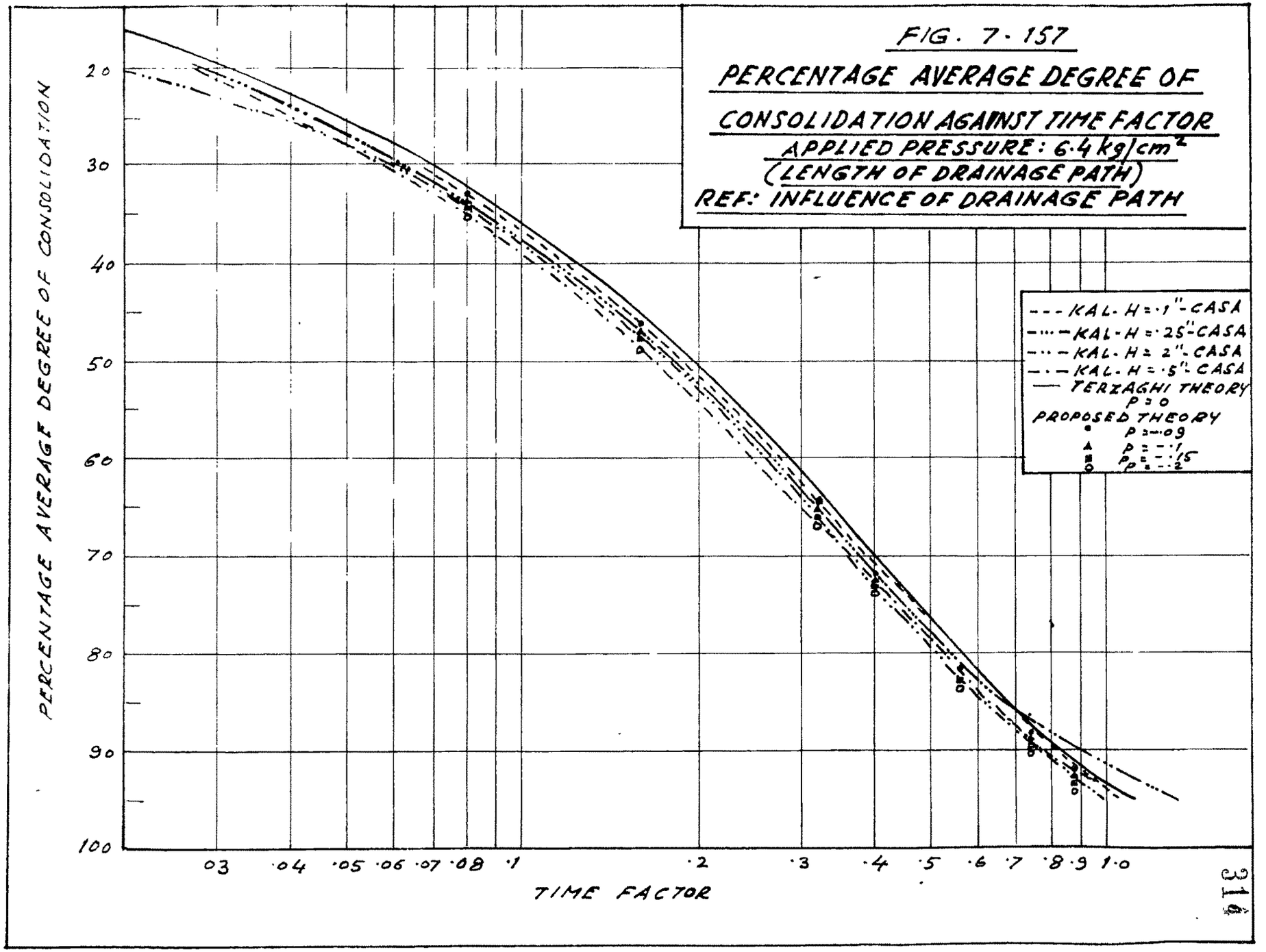

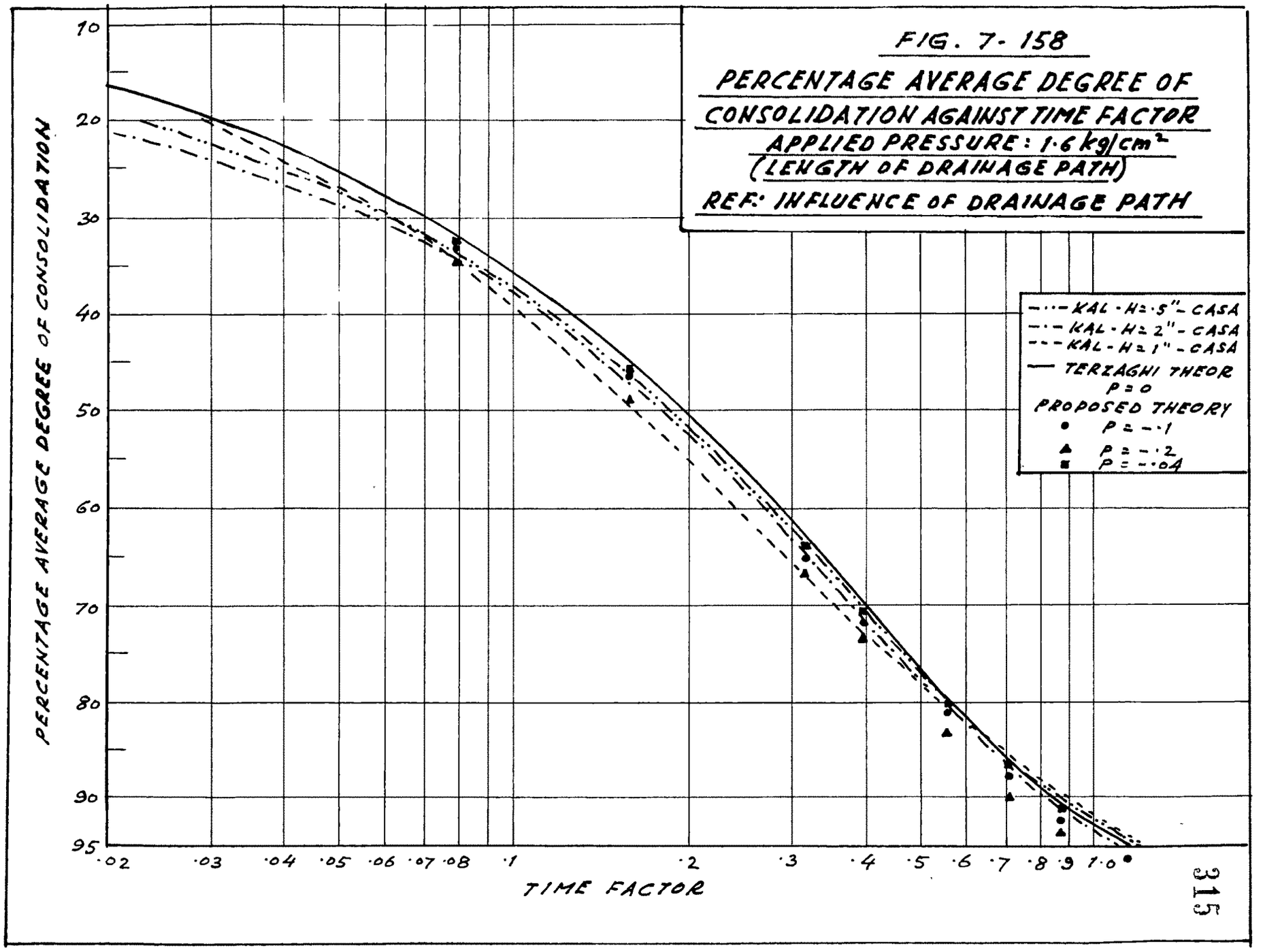
FIG. 7-158
PERCENTAGE AVERAGE DEGREE OF CONSOLIDATION AGAINST TIME FACTOR
APPLIED PRESSURE : 1·6 kg/cm²
(LENGTH OF DRAINAGE PATH)
REF: INFLUENCE OF DRAINAGE PATH
KAL - H = ·5" - CASA
KAL - H = 2" - CASA
KAL - H = 1" - CASA
TERZAGHI THEOR P = 0
PROPOSED THEORY
P = -·1
P = -·2
P = -·04
PERCENTAGE AVERAGE DEGREE OF CONSOLIDATION
10
20
30
40
50
60
70
80
90
95
·02
·03
·04
·05
·06
·07
·08
·1
·2
·3
·4
·5
·6
·7
·8
·9
1·0
TIME FACTOR

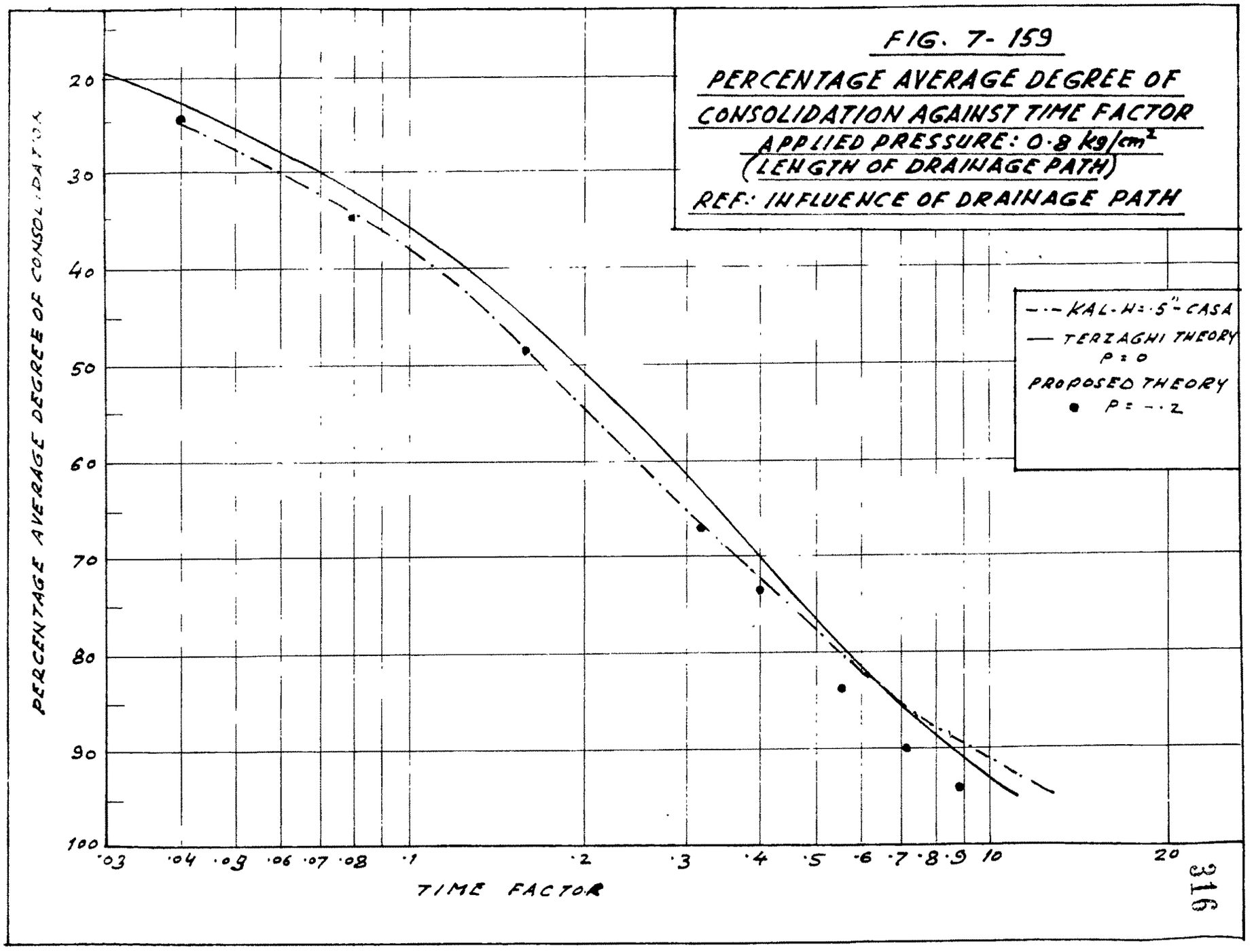
FIG. 7-159
PERCENTAGE AVERAGE DEGREE OF CONSOLIDATION AGAINST TIME FACTOR
APPLIED PRESSURE: 0·8 kg/cm²
(LENGTH OF DRAINAGE PATH)
REF: INFLUENCE OF DRAINAGE PATH
KAL-H=·5" CASA
TERZAGHI THEORY P=0
PROPOSED THEORY P=·2
PERCENTAGE AVERAGE DEGREE OF CONSOLIDATION
20
30
40
50
60
70
80
90
100
·03 ·04 ·05 ·06 ·07 ·08 ·1 ·2 ·3 ·4 ·5 ·6 ·7 ·8 ·9 10 20
TIME FACTOR

Discussion :

It is revealed from the previous discussion that the flow path is not much influenced by tortuosity in semioriented structure. The length of flow path may increase or decrease the time to reach 100% consolidation in soil for a particular load. Thick sample will require relatively more time to reach 100% consolidation under light loads. In thick samples under higher consolidating stress, the load potential dominates the effect of longer length of drainage path and the rate of consolidation increases. Therefore, with the increase in consolidating load the C_v value in thick samples increases while in thin sample after some increase in C_v value, it remains more or less constant. A small hump in thick sample at light loads in the compression index average pressure curve is attributed to the lag in dissipation of water from the longer drainage path with the physico-chemical environment. After attainment of the equilibrium conditions under the higher stress, the physico-chemical effect will be more or less the same both in the thin and the thick samples and therefore the degree of secondary compression will be also the same. As the hydrodynamic lag will be less at high loads the thick sample fits nearer to the Terzaghi curve.
